



**SCIENTIFIC COMMITTEE
EIGHTEENTH REGULAR SESSION
ELECTRONIC MEETING
10-18 August 2022**

Inputs to the Stock assessment of Southwest Pacific Shortfin mako shark

WCPFC-SC18-2022/SA-IP-13

Kath Large¹, Philipp Neubauer¹, Stephen Brouwer², Mikihiko Kai³

¹ Dragonfly Data Science

² Saggittus Consulting

³ Fisheries Resources Institutes, Japan Fisheries Research and Education Agency



Inputs to the stock assessment of Southwest Pacific Shortfin Mako shark

Authors:

Kath Large
Philipp Neubauer
Stephen Brouwer
Mikihiko Kai





Cover Notes

To be cited as:

Large, Kath; Neubauer, Philipp; Brouwer, Stephen; Kai, Mikihiko (2022). Inputs to the stock assessment of Southwest Pacific Shortfin Mako shark, 152 pages. WCPFC-SC18-2022/SA-IP-13. Report to the WCPFC Scientific Committee. Eighteenth Regular Session, 10–18 August 2022.

CONTENTS

EXECUTIVE SUMMARY	3
1 INTRODUCTION	4
2 METHODS	5
2.1 Description of datasets	5
2.2 Length frequency for assessments	7
2.3 Catch reconstruction	7
2.3.1 Prediction of catch rates from observed sets	7
2.3.2 Extrapolation of observed catch rates to WCPO - wide effort	9
2.3.3 Adjusting for discarding and condition at release	9
2.4 Logsheets CPUE standardisation	10
2.4.1 Adjusting CPUE for estimates of rates of cutting-free of shortfin mako	11
3 RESULTS	12
3.1 Length frequency data	12
3.2 Models of catch rates based on observer data	12
3.2.1 Observer data	12
3.2.2 Historical catch reconstructions	13
3.2.3 Estimates of discard fate	14
3.3 CPUE standardisation for logsheet CPUE data	14
3.3.1 New Zealand CPUE	14
3.3.2 Japanese low-latitude CPUE	15
3.3.3 Australian CPUE	16
3.3.4 Fijian and Combined Distant Water CPUE	16
3.3.5 Comparing CPUE series	17
4 DISCUSSION	17
5 REFERENCES	20
TABLES	22

FIGURES	24
A OBSERVER MODEL DIAGNOSTICS	48
B LOGSHEET CPUE STANDARDISATION DIAGNOSTICS	52
B.1 New Zealand fleet high latitude CPUE	52
B.2 Japan low latitude CPUE	66
B.3 Alternative CPUE standardisations	86
B.3.1 Japan high latitude CPUE	86
B.3.2 Australia low latitude CPUE	98
B.3.3 Australia high latitude CPUE	112
B.3.4 Fiji low latitude CPUE	125
B.3.5 Combined low latitude CPUE	139

EXECUTIVE SUMMARY

Shortfin mako (*Isurus oxyrinchus*) are large pelagic predators that are caught as bycatch in tuna and billfish fisheries worldwide. This report details data inputs for the southwestern Pacific stock assessment for shortfin mako, including length frequency information from regional observer programmes, reconstructed catch histories, and a number of alternative catch per unit effort (CPUE) series.

Observed biological data held by the Pacific Community (SPC) were relatively sparse for shortfin mako, leading to high spatial variability of samples, with few clear spatial trends. Despite the paucity of records, higher latitude fisheries appeared to capture juvenile (1–2 m) fish that do not appear as frequently in other fisheries. Based on the occurrence of age zero and juvenile sharks in these latitudes, we hypothesised that fleets in these latitudes form a separate fishery from those in lower latitudes. In addition, observer data suggests very low relative abundance between the equator and 15°South, therefore, we excluded these equatorial data. Fleets were therefore structured latitudinally, as combining data within latitudinal bands helped to overcome these data deficiencies.

Catch was reconstructed from observer data using Bayesian spatial GLMMs to extrapolate observed CPUE to unobserved effort. Due to the importance of extrapolation, we used blocked cross-validation by vessel-flag to weight models of varying complexity in terms of their prediction skills for data from different fleets. Model weighting using stacking of Bayesian posterior distributions, showed that no single model performed best across all fleets, and the most complex model was not usually the best one. We combined models by averaging weights across all holdout sets, producing a weighted ensemble prediction of catches. The model produced relatively high catches between the mid-1990s and early 2000s, with relatively strong reductions in catch since about 2010. Additionally, analysis of discarding rates suggested that across many fleets with consistent recent observer coverage, discarding rates have been high, with a large proportion of mako sharks being cut free and released alive in the most recent years.

Logsheets based CPUE series were attempted, using delta-lognormal and negative binomial GLM models, for a number of areas and fleets, including New Zealand, Australian, Japanese and topical south Pacific fleets. We found that there was little consistency in CPUE trends for Southwest Pacific mako, especially in latter years. Trends in the 1990s are relatively uncertain, due to poor observer coverage, and poor reporting of sharks in logsheet data. While early CPUE in the 1990s often showed a decline, recent CPUE in some fleets has been increasing, i.e., New Zealand, while CPUE in other areas has been relatively flat or even declining in recent years. We suggest that this discrepancy may be due to these indices measuring different components of the stock, as evidenced by latitudinal length frequencies.

We found that recent rates of cutting sharks free from lines may have resulted in lower recent CPUE in many fleets if cut-free sharks are not recorded in log-sheets and the possibility that they may not all be seen by observers. To adjust for this, we produced alternative CPUE time

series that included the rate of cutting free to provide a more realistic measure of encounter rate of mako sharks. Despite these adjustments we found relatively little consistency in fleet specific CPUE trends, which may hint at either regional abundance patterns, or problems with using logsheet CPUE to index shortfin mako abundance.

The following recommendations are made:

- Future assessments should spend increased effort to reconstruct spatio-temporal abundance patterns for shortfin mako, and develop a better understanding of how these patterns drive regional abundance indices.
- Providing more time, either as inter-sessional projects, or by extending time-frames for shark analyses will allow more thorough investigation of input data quality and trends, which shape assessment choices. In addition, this approach would allow input analyses to be completed in time to be presented to the March pre-assessment workshop prior to the stock assessment commencing. Moreover, this will provide more time for the assessments themselves allowing a more thorough investigation of alternative model structures or assessment approaches.
- Increased effort should be made to re-construct catch histories for sharks (and other bycatch species) from a range of sources. Our catch reconstruction models showed that model assumptions and formulation can have important implications for reconstructed catch. Additional data sources, such as log-sheet reported captures from reliably reporting vessels, may be incorporated into integrated catch-reconstruction models to fill gaps in observer coverage.

1. INTRODUCTION

South Pacific shortfin mako sharks (*Isurus oxyrinchus*) are wide ranging across the South Pacific Ocean and have not been recorded crossing the Equator into the North Pacific. Shortfin mako sharks are caught as bycatch in longline fisheries targeting tuna, billfish and blue sharks throughout the Western and Central Pacific Ocean (WCPO). Unlike blue shark, where some target fisheries exist in the South Pacific Ocean, no mako shark target fisheries exist (Williams and Ruaia 2021).

Historically, bycatch went unreported or were poorly reported on vessel logsheets, particularly for sharks that were finned and discarded (Brouwer and Harley 2015, Brouwer and Hamer 2020). Observer data exist for most longline fisheries in the WCPO. However, for many fleets the programmes are relatively new and observer effort is not representative of the fishing effort distribution (Williams et al. 2020). As a result, historic catch for sharks is ambiguous, and catch histories often need to be reconstructed rather than relying on reported or observed catch (Peatman et al. 2018, Neubauer et al. 2021a).

While it appears that there are a reasonable amount of observer and logsheet effort data available for undertaking catch reconstructions and catch per unit effort (CPUE)

standardisations, for the development of a South Pacific shortfin mako stock assessment, these analyses and those in the accompanying assessment (Large et al. 2022) highlight the deficiencies in both the quantity and quality of these data. The data are patchy in space and time and by fleets, and therefore any catch reconstruction is expected to have a high uncertainty (Brouwer et al. 2022). These authors also note that past management interventions may complicate the CPUE standardisation, along with: a) the impact of regulatory changes on fishery dependent data; b) generally low observer coverage in longline fleets particularly in the high seas; and, c) for most fleets after 2015, most shortfin mako sharks are released, with a high proportion of releases being alive and healthy at release.

Brouwer et al. (2022) report there are good biological data for shortfin mako sharks. (e.g. Clarke et al. 2015; Bishop et al. 2006; Campana et al. 2005 and Francis and Duffy 2005). Also, while there are length samples from the 1990s to present, these are not available for all fleets, and not recorded consistently through time. These data are limited mostly to the New Zealand fleet with a few samples from other fleets such as Australia, China, Chinese Taipei, Fiji and Japan, and are difficult to interpret due to changes in overall reporting and the time periods covered by the data from different flags (Brouwer et al. 2022). Due to the largest individuals likely to break free from the gear, length data are truncated and not likely useful as indicators of trends in biomass of mature shortfin mako or for assessing other temporal trends for most fleets, and their use is mostly restricting to assessing selectivity (Brouwer et al. 2022).

In order to overcome problematic shark reporting, WCPPO shark catch reconstruction has been undertaken to estimate shark catch using observed catch data (Lawson 2011, Rice 2012, Tremblay-Boyer and Takeuchi 2016, Peatman et al. 2018, Neubauer et al. 2021b) or fin trade information (Clarke 2009). In addition, a range of approaches were trialled to elucidate relative abundance indices that may be useful indicators of abundance in various regions across the South Pacific (Tremblay-Boyer and Takeuchi 2016). However, these indices were found to be variable among data sources, and potentially in conflict.

Here we build on previous analyses, particularly that used in the southwest Pacific blue shark assessment (Neubauer et al. 2021a), to reconstruct catch histories and develop standardised CPUE indices as inputs for the stock assessment.

2. METHODS

2.1 Description of datasets

We used a range of data-sources held by the Pacific community (SPC) who are the custodians of data supplied to the WCPFC by Members, Cooperating Non-Members and Participating Territories (CCMs). These datasets were extracted by SPC upon request, and analysed by the assessment team. In addition, scientists from Japan were contacted with the intention of working collaboratively to develop shortfin mako shark CPUE indices from their longline fleets. A summary of the Japanese longline fleets and the resulting CPUE analyses are provided below. For Japan, the assessment team supplied standardised scripts for CPUE to ensure that

analyses were comparable between datasets.

In summary, the following datasets were used for analysis:

- **L-BEST:** SPC's best (raised) estimates of longline catch and effort (in hooks) for fleets in the WCPFC Convention Area (WCPFC-CA), available at the $5^\circ \times$ month \times year \times flag \times fleet resolution for key species of tuna and billfish, and sharks in some years.
- **Observer programmes for the WCPO longline fleet:** The full observer dataset for the WCPFC longline fleet available to SPC was used for the analysis, including data from the SPC's Regional Observer Programme and national observer programmes. Records collected by longline observers that are relevant to this assessment are key fishing event attributes (including date and time, location), as well as information on gear and catch:
 - Gear/set characteristics (hooks between floats, total number of hooks fished);
 - species;
 - fate code of the catch (e.g., discarded or retained);
 - condition at capture and at release (if not retained); and
 - length and the sex of the individual.

The quality and coverage for most variables changes over time and between programmes.

- **Operational logsheet data:** Operational (logsheet) catch and effort data, by day, flag, Exclusive Economic Zone (EEZ), latitude and longitude, set type, catch and effort. Note that logsheet data is not a complete reflection of fishing effort (as estimated in L-BEST), and shark reporting is variable among vessels, fleets, and years (Brouwer and Hamer 2020).

Further detail on datasets and characteristics of the fisheries landing South Pacific shortfin mako sharks can be found in Brouwer and Hamer (2020).

Data preparation largely followed recent shark stock-assessment protocols (Tremblay-Boyer et al. 2019, Neubauer et al. 2021b). All datasets were filtered to retain records south of the equator within the WCPFC-CA only, over the period of the stock assessment from 1990 to 2020. For the longline observer datasets, when the number of hooks was missing, the number of hooks observed was estimated from the product of hooks-between-floats and the number of baskets observed. Oceanography covariates (sea surface temperature, chlorophyll-*a* (Chl-a), and distance from the coast) were extracted at the lowest resolution possible and aggregated to match the resolution of each dataset. Species targeting clusters were applied following k-means clustering of observed catch proportions as described in Tremblay-Boyer et al. (2019).

2.2 Length frequency for assessments

Length-frequency information as extracted from observer records. All measurements were standardised to fork-length using $FL = 0.9110 \cdot TL + 0.8210$. Fork length distributions were plotted in space and time, by flag and target fishery in order to evaluate trends between fisheries that catch shortfin mako shark.

2.3 Catch reconstruction

Overall fishing related mortality was estimated as the product of overall catch, discarding and fish condition (Figure 1). For each of these components of fishery interactions, data were variable in the geographical coverage and information content, and we employed a series of models for these different components in order to estimate total fishing related mortality.

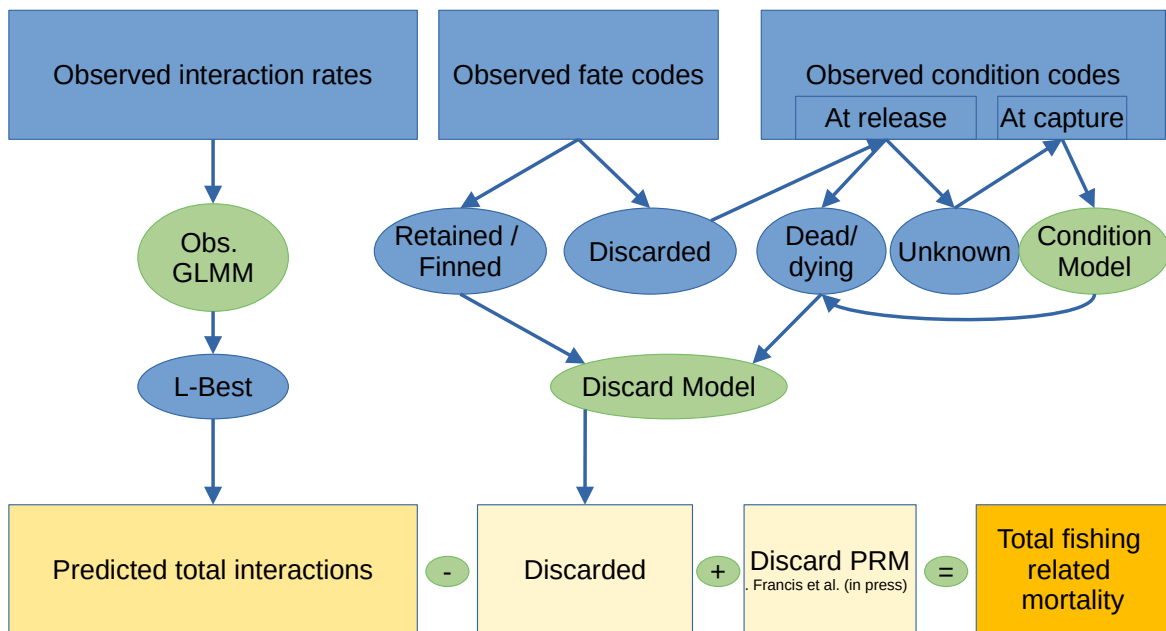


Figure 1: Illustration of the over-all approach used to reconstruct fishing related mortality. Data sources are shown in blue, models and assumptions in green, resulting estimated catch components are shown in orange. Observer catches (interactions) were estimated from observer data, then scaled to overall predicted interactions using the L-BEST dataset. These estimates were then scaled by estimates of live discards based on observer discard and condition information, as well by post-release mortality estimates for blue shark.

2.3.1 Prediction of catch rates from observed sets

Overall catches (interactions) were estimated from observer catch rates using generalised linear mixed model. Previous approaches to reconstruct catches for this species have also been based on observer catch data (see Tremblay-Boyer and Takeuchi 2016, Peatman et al. 2018 Neubauer et al. 2021b). The basis for these methods is similar: a model of catch-per-unit-effort (CPUE)

is built based on observed sets and relevant covariates, and the model is then used to predict catch based on total effort (e.g., L-BEST for longline data) by fleet across the assessment region.

The previous approaches differ in the modelling framework used to build the catch rate model, and the covariates considered. Tremblay-Boyer and Takeuchi (2016) used generalised linear models (GLMs) with splines for oceanographic covariates to predict catches in unobserved strata. Peatman et al. (2018) used Generalised Estimating Equations (GEEs) to model catch rates using a delta-lognormal model structure. The GEE framework allows for the correlation between observed sets in the same observer trips to be accounted for. Catch predictions and uncertainty were estimated with a Monte Carlo simulation approach drawing samples from modelled catch distributions.

We used the approach used by Neubauer et al. (2021b) (similar to Tremblay-Boyer and Takeuchi 2016) to model catch rates of shortfin mako shark in observer data. We employed generalised linear mixed models with splines for oceanographic predictors, estimated within the general Bayesian linear model framework “*brms*” (Burkner 2017). In contrast Neubauer et al. (2021b), used negative binomial models, which have been used for other bycatch species (Tremblay-Boyer et al. 2019), and are often preferred for highly skewed distributions with large amounts of zeros.

A key difference of the present modelling to previous approaches is the use of blocked cross validation to obtain an ensemble-weighted prediction of absolute catch over the assessment area. Previous catch reconstructions typically attempted to find a single best model from a set of candidate models to fit observer catch rates and predict catches across the total longline effort. This approach, while using cross validation in recent studies (Tremblay-Boyer et al. 2019, Neubauer et al. 2021b), ignores the spatio-temporal correlation structure in the datasets used for inference, as well as the non-representative sampling that is provided by observer data: observers are not placed at random across the fleet, but are rather disproportionately present on vessels of certain CCMs. These patterns can lead to strong bias in model selection based on traditional information-criterion or cross-validation-based model selection (Roberts et al. 2017).

Blocked cross-validation can provide a way to reduce bias in model selection (Roberts et al. 2017). Due to computational complexity, we here only tried a single blocking strategy – blocking by CCM. To this end, we fitted a range of candidate models (Table 2) with each CCM removed from the analysis, and then assessed predictive accuracy for the hold-out data for all models. Weights for each model and holdout set were estimated using Bayesian stacking of posteriors Yao et al. 2018. We then applied a second layer of weights, determined by the relative importance of each flag in the total effort dataset. The rationale here is that we want to up-weight model ensembles for CCMs that account for most of the total effort, since predicted catches will be disproportionately affected by strata with high effort. The combined weights (products) were then averaged across holdout sets to give a final ensemble weight.

All models were run using observer records aggregated to the resolution of the L-BEST dataset (i.e., $5^\circ \times 5^\circ$, flag, month) as the response, while allowing for non-linearity in CPUE with effort

by including a non-linear term for the number of hooks set per stratum in a subset of models.

All models included spline formulations (estimated as random effects in brms) for oceanographic habitat predictors for SST and Chl-a. In addition to oceanographic predictors, some models included a random effect for the vessel flag, area and their interaction with year effects (Table 1). The latter effects be used to predict catches for strata (flags/areas) without any observer coverage. Month was fitted as a random effect in the model, and targeting cluster was fitted as a fixed effect. A spline by month and longitude and latitude was used to adjust for within-season spatio-temporal trend in habitat preference (Kai et al. 2017) that are not well described by the predictors in the model.

The most complex model was written as:

```
f(y) ~ s(log(hooks), by=Lat5) + (1|month) + s(SST) + s(Lon5, Lat5, by=month) +
s(Chl-a) + target_cluster + (1 | flag_id) + (1 | year(area):flag_id)
```

for $f(y)$ the log-transformed rate of the negative binomial response. Alternative models omitted the flag (or area) year interactions, the non-linear scaling with effort (hooks) or its variation by latitude.

Models were fitted with eight separate Markov Chain Monte Carlo chains with 2000 iterations each, including 1000 iterations burn-in period that was discarded from posterior samples. Convergence, as judged by marginal and multivariate scale reduction factors (SRF) across 8 chains (at convergence of MCMC runs, the MSRF (or Rhat) is one).

2.3.2 Extrapolation of observed catch rates to WCPo-wide effort

Predictions to the L-BEST dataset were performed on the basis of available variables in the L-BEST dataset. Targeting practice was assumed to be described by the inferred targeting clusters. We avoided predicting on the basis of additional gear characteristics, such as HBF, as these are not consistently available, and uncertainty from imputing such values on the basis of other characteristics cannot be straightforwardly propagated to catch estimates.

2.3.3 Adjusting for discarding and condition at release

Predicted catches are in the form of total interactions - i.e., some of the catch is not retained and released alive, such that fishing related mortality may be substantially different than interactions alone might suggest. This is especially relevant since recent CMMs for non-retention of sharks have lead to noticeable increases in sharks being cut free and/or discarded (Brouwer et al. 2021).

We assumed 100% mortality for retained and/or finned sharks (Figure 1). In addition, for discarded sharks, any sharks that had a condition at release of 'Dead' or 'Alive - dying' were classified as retained. Although information about condition at release is more frequently

recorded in recent years, but records prior to 2015 often had fate codes indicating discard (e.g., Discarded - other reason; or Discarded, shark damage), but had missing condition-at-release information. Nevertheless, these data often had information on the condition at capture. In order to obtain a better picture of discard mortality prior to 2015, we used a binomial GLMM to infer the condition at release (i.e., dead or likely dying vs. alive and healthy) from the condition at capture (cond code), sex, vessel and flag. In contrast to previous analyses, which attempted to estimate this relationship from data for the species in question only, we included data across all mako species, porbeagle and blue sharks, with a fixed effect for species accounting for differences in species survival as a function of condition at capture. The final model for the expected number of mortalities for a given number of records in each stratum was then:

```
condD.num | trials(records) ~ (1 | flag_id) + (1 | vessel_id) +
species + sex_code + cond_code
```

Note that we do not use a temporal variable in this model as most of the data (>53 000 records) with both condition at release and condition at recapture recorded occurs post 2015 (>47 000 of all records). This temporal split in the dataset largely precludes any strong inferences on changes in handling mortality over time for a given condition at capture. Nevertheless, the model above allows us to predict the expected condition of over 112,000 discarded individuals for which the condition at release was not recorded.

To estimate trends in discarding, we used the recorded and imputed discard status (dead or alive, as recorded or estimated by the condition model) to estimate trends in live-discarded individual by flag and latitudinal stratum. The model for mako shark fate was similar, therefore, to the condition model. However, its main purpose was to estimate a rate by year, fleet and latitudinal stratum (LL) that could be applied to estimated catches. The model was written as:

```
FateD.num | trials(records) ~ (1 | flag_id) + (1 | vessel_id) +
species + LL + s(year, LL, species)
```

Models were fitted using MCMC sampling in ‘brms’ as outlined above. We applied the 25%, 50% (median) and 75% percentiles of the posterior distribution of predicted live-discards, discounted by a 17% post-release mortality (Common Oceans (ABNJ) Tuna Project 2019), to predicted catches (posterior median and 90th percentile of predicted catches) to derive the total fishing related mortality used in the stock assessment.

2.4 Logsheet CPUE standardisation

Log-sheet CPUE was standardised using a standard set of grooming rules and models across a number of fleets. Specifically, based on predicted catches, we conducted independent standardisation analyses for New Zealand (> 35°S and < 45°S), Australia (split at 35°S), Japan

(split at 35°S), and a combination of logsheet data from a range of flags operating in the high seas (FJ, CN, VU, TW, KR). We included TW in this set because a stand-alone standardisation of their logsheet CPUE provided highly variable trends that were not easily interpreted.

All analyses used a set of common grooming rules:

- vessels had to have reported positive SMA catches for at least 3 years;
- vessels had to have reported at least 10 events with SMA captures; and,
- only vessel-years with at least one positive catch were retained.

We compared reporting rates (i.e., proportion of positive sets) between observer records and logsheet data where possible, using predictions from the observer catch-reconstruction to compare with operational reporting. Due to concerns about reporting rates for sharks in operational data, we initially fit a hurdle log-normal GLM model for catch rates, including a separate binomial model that could capture reporting aspect of the data (Neubauer et al. 2021a). We tested that this assumption does not unduly bias our inference by attempting negative-binomial and zero-inflated negative-binomial models on the same datasets. Relatively simple GLM models were chosen for these standardisation in order to facilitate rapid iterations on the models across all analyses and collaborators.

A standard set of predictors was prepared for all analyses, including oceanographic predictors (SST, Chl-a, distance from nearest land). The latter entered the model as splines, while vessel effects, target cluster and month effects were fixed effects in the model. We excluded Chl-a and distance from coast as these variables were highly correlated with SST in some analyses, and we aimed to keep analyses as consistent as possible.

All analyses were diagnosed using tools outlined in Bentley et al. (2012) . These include detailed analyses on the fleet composition and its effect on CPUE trends, as well as standard model fit diagnostics for GLMs.

2.4.1 Adjusting CPUE for estimates of rates of cutting-free of shortfin mako

Due to recent non-retention measures (WCPFC 2019), rates of discards and cutting-free of sharks before they are brought on board, suggests that recent CPUE for many CCMs may under-estimate mako abundance. CPUE being a measure of local density, it ideally measures encounter rates. If reporting rates of these encounters are decreasing as animals are cut free, CPUE may be negatively biased in recent years. To account for potential biases from cutting free in log-sheet CPUE, we fit a binomial model to the proportion of sharks that were recorded as cut free by flag and year. The model emulates the discard fate model, and models the number of cut free animals relative to total captures as

```
FateD.num | trials(records) ~ (1 | flag_id) + (1 | vessel_id) +
(1 | species) + LL + s(year, LL)
```

3. RESULTS

3.1 Length frequency data

Length frequency data were sparse across the fishery, and length frequencies highly variable among years, fisheries and fleets. Length frequency sampling showed little consistent variation by sex, with males dominating the samples (Figure 2) in some years. While large individuals (>250 cm) were mainly caught in swordfish target sets, their occurrence was variable among years, and sampling in that fishery was infrequent (Figure 3). Small shortfin mako were predominantly caught in southern bluefin target sets, and sporadically appear in other target fisheries (i.e., bigeye, yellowfin) in the mid-1990s and early 2000s, including albacore and swordfish target sets.

Spatial sampling did not show consistent trends, and the largest individuals appeared to occur in samples at the eastern boundary of the WCPO, between 15 and 30°South (Figure 4). Small individuals occurred around the northern North Island of New Zealand, and also near the equator.

Spatial inferences about length frequency samples are complicated by strong temporal patterns in sampling. Most samples initially came from observers on Australian and Japanese vessels mainly operating in the southern Tasman Sea (1990-2000; Figure 5). Between 2000 and the late 2010s, samples came mostly from New Zealand observers on New Zealand and Japanese charter vessels operating in New Zealand fishery waters. Since the mid-2010s, Chinese-Taipei, Fiji, Japan and New Zealand have supplied the bulk of the length frequency samples.

Spatial length frequency patterns are reflected by flag (Figures 6, 7), with Australian, Japanese and New Zealand samples from southern latitudes showing strong peaks in small (age zero) individuals. Samples from these areas also contained larger individuals in roughly equal proportions, indicating co-occurrence of new recruits and larger individuals up to about 250 cm. In lower latitudes, length frequencies had more large individuals, especially from flags fishing in distant and tropical waters (i.e., Fiji, Chinese Taipei).

Comparing growth according to the Bishop et al. (2006) growth curve, (coloured histograms in Figure 6, 7, 8), suggested that samples in the main low latitude peak were age 5+.

3.2 Models of catch rates based on observer data

3.2.1 Observer data

Observer records were highly heterogeneous in space and time, with early observer effort concentrated in high-latitude fisheries around south-eastern Australian waters (Figures 9, 11), and a subsequent shift to New Zealand waters for much of the 2000s. Since the late 2010s, a large number of hooks have been observed in higher latitudes on Fijian, Chinese Taipei and Japanese-flagged vessels.

Observed shortfin mako captures largely mirror trends in observer coverage, with large

numbers of observed SMA/MAK captures in Australian and New Zealand waters in the 1990s and 2000s, respectively (Figures 12, 14). Recent observer coverage in fleets from Fiji and Chinese Taipei lead to an increase in observer reported SMA catch in those fisheries. Nominal CPUE by flag and observer programme were highly variable, owing to the low number of total observed captures (Figures 15, 17, 18). Trends in low latitudes indicate a decline in nominal CPUE in these areas, however, CPUE was already low relative to other areas and the decline coincides with a strong increase in observer coverage. Nominal CPUE was highest between -45°South and -15°South, with CPUE hotspots in northern New Zealand and South Australia.

3.2.2 Historical catch reconstructions

The blocked cross-validation approach to selecting an ensemble for predicting total captures did not select a single best model across all hold-out sets; rather it retained a model set with no clear best model (Figure 24, Table 3). Predictions were therefore based on a set of 18 models that included predictions from models that predicted high catches, and models predicting low catches. The latter were models with (generally) non-linear effects of effort on CPUE. Diagnostics for the combined ensemble prediction suggested that the model ensemble overpredicted higher quantiles for some strata, especially early years (Figures A-1), and for flags and areas that account for less prediction effort, but high CPUE, such as New Zealand and Australia (Figures A-2, A-3). Nevertheless, our predictions showed relatively good alignment with operationally reported captures in highly observed fisheries such as New Zealand and Australia.

Total predicted interactions peaked at near 100,000 individuals per year across the overall South Pacific (Figure 23). Predictions from catch reconstructions suggested highest habitat suitability and CPUE in Tasmanian/South Australian and New Zealand waters (Figure 21), with an over-all higher abundance at latitudes between 30 and 40°S, owing to the influence of preferred SST at these latitudes (Figure 22). Consequently, predicted catch rates were highest in the southwest WCPO and the Tasman Sea (Figure 21).

Areas around Indonesia had intermediate estimated catch rates from the observer model, however, these areas lacked observer coverage, and corresponding uncertainty was very high (Figure 21). This uncertainty drove very high median catch estimates for this area, owing to the high effort in L-BEST. These numbers inflated the catch estimates considerably, and was considered highly uncertain and implausible. As predicted CPUE was very low north of 15°South, and tracking data shows limited movements of sharks to lower latitudes, we decided to exclude effort north of 15°South from the assessment.

Resulting catch estimates were substantially lower in total after removal of spurious catch predictions north of 15°South (Figures 26, ??). The resulting trends suggested an increase in interactions from about 20,000 individuals in the early 1990s, to around 40,000 individuals around the early 2000s. Interactions subsequently reduced sharply in the first decade of the 2000s, with a slow reduction from 2010 to 2020.

3.2.3 Estimates of discard fate

Discard fate based on reported discarding, and discard conditions, together with inferred condition from the condition code model (Figure A-4), was modelled as a smooth term as a function of time. The model inferred low live-discard rates in low latitudes before 2010, with a steady increase in live discards since then. Average discards in high latitudes were largely driven by New Zealand observer data, indicating a slow increase in live discards over time (Figures 27, 28). Data was sparse for most fleets, and discarding trends by flag have a high degree of uncertainty. Nevertheless, for fleets with high catch and catch rates, inferred trends were relatively well modelled (Figure 28). While discarding in New Zealand and Australia was predicted to follow the more general trend, other fisheries, like Japan and Chinese Taipei, had high retention rates even in recent years, whereas many Pacific Island flagged fleets had high discard rates in recent years (e.g., Fiji, New Caledonia and French Polynesia; Figure 28).

Applying discard estimates and their uncertainty to estimated total interactions, leads to a range of scenarios for total fishing related mortality (Figures 29, 30, 31). Discard scenarios mainly served to scale total mortalities, but did not lead to qualitative differences in trends. Fishing related deaths in low latitudes declined rapidly since ~ 2010, leading to a steady decline since the early 2000s in low latitudes. In high latitudes, catch was high between the mid-1990s and early 2000s, but were steady at much lower levels since 2010, with relatively low uncertainty in recent years regardless of the discard assumptions.

Models for the proportion of individuals cut free suggested a strong increase of this practice in recent years in some fleets, especially in the Pacific Islands and New Zealand. However, data on this practice was sparse and estimates uncertain.

3.3 CPUE standardisation for logsheet CPUE data

Most log-normal standardisation models performed well by standard model-fit diagnostics (see Appendix B). Negative binomial models and their zero-inflated counterparts did not always converge, and did not improve diagnostics or show substantially different trends.

3.3.1 New Zealand CPUE

The operational area for the New Zealand fleet is largely within the New Zealand EEZ, with high CPUE throughout the area. Comparison with observer data suggests that logsheet reporting rates were higher than estimated reporting rates from observer data (??). Nominal CPUE was more closely aligned with CPUE trends derived from the combined observer model (??).

The standardised CPUE was slightly adjusted relative to the unstandardised series (Figure 33; ??). The index shows a strongly increasing trend since the early 2000s after an initial decline in the late 1990s. Two data points in 1999 and 2000 stand out from the time series at being >50% higher than the surrounding years in the times series. These points were not strongly

adjusted in any standardisation model (log-normal, negative binomial). Recent CPUE was low relative to the increase in the index in the early 2000s, possibly owing to fish being cut free and not reported or observed by observers.

The standardising effect of the model was small (Figure ??), and only the addition of a non-linear effect in the effort (number of hooks) contributed to adjust recent CPUE downward. The model suggested catch rates were highest at intermediate water temperatures (15-21°C; Figure ??). Additional diagnostics are given in Appendix B.1.

3.3.2 Japanese low-latitude CPUE

The data from the Japanese fleet was analysed at the Fisheries Resources Institutes (FRI), Japan Fisheries Research and Education Agency. These data are from longline logsheets from vessels fishing between 1994 and 2019, and from the equator South to 60°S within the WCPFC-CA (Figure B-21). The data were split into a tropical component, defined as catch occurring between the equator and 30°S; and a temperate area (30-60°S). The tropical fishery is dominated by catch of albacore, yellowfin and bigeye, while the temperate catch is dominated by albacore and, to a lesser extent, southern bluefin tuna (Figure B-22). The vessels tend to fish across the WCPO north of 10°S. But, south of 10°S they generally fished west of the 180°line of longitude.

Logsheets reporting has changed throughout this time due to changes in regulations (e.g. WCPFC 2019 and its predecessors) governing the retention of sharks. This has reduced the number of sharks retained, which declined after 2011 and has remained relatively low (particularly from 2015 onwards). But, at that time, the number of hooks set and spatial distribution of fishing operations south of the Equator in the WCPFC-CA also dropped appreciably (Figure B-23; Figure B-24). It is considered that these changes are the main contributor to the strong decline in reporting rates of sharks from 2016 onwards, particularly in the tropics (Figure B-25).

The number of hooks between floats for this fleet has remained relatively consistent in the tropical waters at around 15 hooks between floats, but in the temperate waters has increased from <10 prior to 2000, to around 10 hooks between floats in the last two decades (Figure B-26). Branchline length has remained relatively consistent at about 40m both in the tropical and temperate fisheries (Figure B-27). The median floatline length is longer in the tropical fishery (~40m) than the temperate fishery (~20m), suggesting that the vessels set deeper sets targeting bigeye tuna in the tropics compared to the temperate regions.

The positive catch ratios of SMA for the Japanese fleet were highest in temperate waters, and relatively steady near 40% of sets prior to 2011 (Figure B-28). In the tropics, the occurrence of SMA in sets dropped steadily from 20% about 10% between the mid-1990s and 2020. Sets recording the positive catch of SMA were lower by a factor of 2 in the tropics.

Grooming of Japanese logsheet data lead to a large change in the proportion of strata with non-zero catch in recent years (Figure B-29), suggesting that declines in observed occurrence may be related to reporting trends for particular vessels. After retaining only a subset of consistently

reporting vessels, the proportion of sets with positive catch largely remained steady in recent years.

Nominal CPUE in the JP fleet did not markedly change due to grooming (Figure B-30), and was similar between high and low latitudes between 15°S and 45°S. Both series showed an initial decline in CPUE, with a slight increase in CPUE in the early 2000s, and a declining trend since.

Standardised CPUE was very similar to unstandardised CPUE except for the late 1990s, where standardisation adjusted the index downward and lead to a less steep decline (Figure B-31). The adjustment was due to vessel effects in the model, which suggested vessels with high catch rates fishing in the early part of the time series (Figure B-33). Alternative CPUE models had trends more similar to unstandardised CPUE (negative binomial).

Standardisation of high latitude CPUE from JP showed a much stronger adjustment (see appendix B.2) based on active vessels and SST in fishing areas over time, with a shift between colder and warmer areas leading to an adjustment of CPUE from a declining trend to a globally increasing trend.

3.3.3 Australian CPUE

As for the New Zealand flagged fleet, the Australian flagged fleet reported more positive interactions than was estimated by the observer catch-reconstruction predictions (Figure B-55). While nominal CPUE in low latitudes broadly aligned with observer CPUE, showing a broad downward trend over the late 1990s and early 2000s, the nominal CPUE in high latitudes increased and did not mirror trends in observer CPUE. Standardisation of low latitude data showed a considerable standardisation effect that was largely due to reporting changes – a change in vessel keys after 2006 – and gear characteristics that evolved steadily towards using more hooks. As a result, we concluded that these features lead to problems interpreting this index and it was not used for the assessment. In addition, residuals suggested poor fit.

3.3.4 Fijian and Combined Distant Water CPUE

Nominal occurrence and CPUE suggested large changes in reported occurrence and large fluctuations of CPUE within Fiji flagged vessels. Standardised CPUE was strongly increasing in recent years (appendix B.3.4). Residual patterns suggested the model fit was not satisfactory, and alternative models, although providing better fit, produced indices with large fluctuations that were considered implausible. Similarly, poor diagnostics and implausible results from alternative (negative binomial) models meant that we did not retain the combined distant water/low-latitude index (see appendix B.3.5).

3.3.5 Comparing CPUE series

We found that there was little consistency in CPUE trends for Southwest Pacific mako, especially in later years (Figure 33, Figure 33). Trends in the 1990s are relatively uncertain, due to poor observer coverage, and poor reporting of sharks in logsheet data. While early CPUE in the 1990s often showed a decline, recent CPUE in some fleets has been increasing, i.e., New Zealand, while CPUE in other areas has been relatively flat or even declining in recent years. We suggest that this discrepancy may be due to these indices measuring different components of the stock, as evidenced by latitudinal length frequencies.

We found that recent rates of cutting sharks free from lines may have resulted in lower recent CPUE in many fleets if cut-free sharks are not recorded in log-sheets and the possibility that they may not all be seen by observers. To adjust for this, we produced alternative CPUE time series that included the rate of cutting free to provide a more realistic measure of encounter rate of mako sharks. Despite these adjustments we found relatively little consistency in fleet specific CPUE trends, which may hint at either regional abundance patterns, or problems with using logsheet CPUE to index shortfin mako abundance.

4. DISCUSSION

Despite the paucity of length frequency data and the variable coverage of these data both in space and time, there is some indication of nursery habitats in high latitudes. Smaller individuals of recruit and 1 year old size are mainly caught south of 35°S, and at these latitudes the largest individuals are also caught. Samples from these areas also contained larger individuals in roughly equal proportions, indicating co-occurrence of new recruits and larger individuals up to about 250 cm. In lower latitudes, there were more large individuals, especially from flags fishing in distant and tropical waters, and our analysis suggests that samples in these lower latitudes were mainly of fish aged 5+.

Catch-rates in the higher latitudes are also substantially higher, with catch-rates in New Zealand, and to a lesser degree the south Tasman Sea around Tasmania and South Australia, supporting catch rates being higher than elsewhere in the South Pacific. Together with tracking results, our results support the hypothesis that the New Zealand and South Australian fisheries, interacting with newborn and juvenile fish, represent fisheries on nursery areas, whereas older, potentially migrating fish are present at lower densities in oceanic and tropical areas north of New Zealand and southeastern Australia. Nevertheless, these fisheries were predicted to have captured nearly twice the total number of SMA during peak catches in the 1990s and early 2000s.

Although our combined weighted catch-reconstruction model (Figure 25) produced a catch series that generally agrees with the series from other recent catch reconstruction models from the mid-2000s to the late 2010s (Peatman et al. 2018). The present analysis continues the downward trend to 2020, whereas the previous analysis ended in an upward trend for the final two years. However, both analyses show a declining trend in overall catch from the early

2000s, but with much greater uncertainty for the present analysis, owing to the large spread in ensemble models that are used for catch predictions. The earlier part of the catch timeseries, from 1990 to the early 2000s is also highly uncertain, showing an over-all inclining trend with increases in longline effort during that time. Significant peaks in catch were predicted in the late 1990s and again in the early 2000s.

It is unclear to what degree latitudinal representation in observer data affects catch reconstruction models used for shark assessments. A significant proportion of early catch was predicted to have come from high latitude fisheries, especially during the mid-late 1990s. As these fisheries dominate observer effort during this period, high latitude catches may be relatively accurate compared to low-latitude catches at the time. The latter may be unduly inferred from CPUE trends in higher latitudes. Our model shows high uncertainties in predicted captures in this early period, but it is unclear to what degree the model can capture fundamental uncertainties associated with observer coverage.

We trialled a new way to predict over-all captures of sharks from observer data using blocked cross validation, aiming to overcome representation issues over time, where flags with significant effort may be under-represented over periods in the observer dataset. Models were therefore weighted by their predictive power for each flag, as well as the total effort for each fleet. This “grouped blocking” strategy is only one of a range of possible strategies, such as temporal, spatial or spatio-temporal blocking. We hypothesize that the grouped blocking approximates other types of blocking strategies to some degree, and was thought to be the most parsimonious approach in the present case - given the computational burden of this type of analyses in the Bayesian setting used for catch reconstruction predictions. Adding alternative strategies was not an option within the project time-frame. However, we suggest this as an important future research avenue – in recent shark stock assessments, a lot hinges on reconstructed catch histories, and finding methods to improve their accuracy is an important research task.

In addition to the representation issues with observer data, it is unknown how well shark species were recorded by different observer programmes over time. It is possible the CPUE from observer records in early periods is biased by non-identification of shark species. It may be possible to extend the current approach by imputing shark species for records with unknown species identification. This would essentially combine approaches taken in previous shark assessments (e.g., Tremblay-Boyer and Takeuchi 2016). In addition, logsheet reported catch could be used to provide lower bounds on estimates for poorly observed areas (i.e., via a left-censored data approach). Such an integrated catch-reconstruction model may overcome deficiencies in the present and past attempts at reconstructing catch time-series for under-reported sharks or rays. In summary, we recommend further targeted work on reconstructing shark and other catch histories based on observer data (and, potentially, other data sources), in order to better understand and quantify key uncertainties in catch histories.

Catch estimates were substantially lower after the removal of spurious catch predictions north of 15°South (Figure 26). Alternative assumptions, for example longitudinal restrictions

to areas east of 140°East, did not substantially change the picture due to low catch rates near the equator. The resulting trends suggested an increase in interactions from about 20,000 individuals in the early 1990s, to around 40,000 individuals around the early 2000s. Interactions subsequently reduced sharply in the first decade of the 2000s, with a slow reduction from 2010 to 2020.

We found that there was little consistency in CPUE trends for Southwest Pacific mako, especially in later years (Figure 33, Figure 34). Trends in the 1990s are relatively uncertain, due to poor observer coverage, and poor reporting of sharks in logsheet data. While early CPUE in the 1990s often showed a decline, recent CPUE in some fleets has been increasing, i.e., New Zealand, and CPUE in other areas has been relatively flat or even declining in recent years. We suggest that this discrepancy may be due to these indices measuring different components of the stock, as evidenced by latitudinal length frequencies.

Recent rates of cutting sharks free from lines may have resulted in lower recent CPUE in many fleets if cut-free sharks are not recorded in log-sheets and the possibility that they may not all be seen by observers. To adjust for this, we produced alternative CPUE time series that included the rate of cutting free to provide a more realistic measure of encounter rate of mako sharks. Despite these adjustments, we found relatively little consistency in fleet specific CPUE trends, which may hint at either regional abundance patterns, or problems with using logsheet CPUE to index shortfin mako abundance. We suggest that future research should investigate logsheet reported shark captures in conjunction with observer CPUE with the aim to better understand representation issues for both datasets, leveraging temporal and spatial overlap to calibrate CPUE time series.

The following recommendations are made:

- Future assessments should spend increased effort to reconstruct spatio-temporal abundance patterns for shortfin mako, and develop a better understanding of how these patterns drive regional abundance indices.
- Providing more time, either as inter-sessional projects, or by extending time-frames for shark analyses will allow more thorough investigation of input data quality and trends, which shape assessment choices. In addition, this approach would allow input analyses to be completed in time to be presented to the March pre-assessment workshop prior to the stock assessment commencing. Moreover, this will provide more time for the assessments themselves allowing a more thorough investigation of alternative model structures or assessment approaches.
- Increased effort should be made to re-construct catch histories for sharks (and other bycatch species) from a range of sources. Our catch reconstruction models showed that model assumptions and formulation can have important implications for reconstructed catch. Additional data sources, such as log-sheet reported captures from reliably reporting vessels, may be incorporated into integrated catch-reconstruction models to fill gaps in observer coverage.

ACKNOWLEDGEMENTS

The authors would like to thank SPC, particularly Peter Williams, Emmanuel Schneiter and Aurélien Panizza for providing the WCPFC Members data for these analyses. We would also like to thank Paul Hamer and Jemery Day for constructive discussions throughout this work and for comments on earlier drafts of this report, and the SPC Pre-Assessment Workshop Members for their helpful feedback on the catch reconstruction and CPUE proposals. The authors would also like to thank the SPC for providing the funding for this work through the WCPFC project 111.

5. REFERENCES

- Bentley, N.; Kendrick, T. H.; Starr, P. J., & Breen, P. A. (2012). Influence plots and metrics: Tools for better understanding fisheries catch-per-unit-effort standardizations. *ICES Journal of Marine Science*, 69(1), 84–88.
- Bishop, S. D.; Francis, M. P., & Duffy, C. (2006). Age, growth, maturity, longevity and natural mortality of the shortfin mako shark (*Isurus oxyrinchus*) in New Zealand waters. *Marine and Freshwater Research*, 57(2), 143–154. doi:10.1071/MF05077
- Brouwer, S. & Hamer, P. (2020). 2021-2025 Shark Research Plan. (EB-IP-01 Rev1).
- Brouwer, S. & Harley, S. (2015). Draft Shark Research Plan: 2016-2020. (SC11-EB-WP-01).
- Brouwer, S.; Large, K., & Neubauer, P. (2021). Characterisation of the fisheries catching South Pacific blue sharks (*Prionace glauca*) in the Western and Central Pacific Ocean. (SC17-2021/SA-IP-06).
- Brouwer, S.; Large, K., & Neubauer, P. (2022). Characterisation of the fisheries catching South Pacific shortfin mako sharks (*Isurus oxyrinchus*) in the Western and Central Pacific ocean. (WCPFC-SC18-2022/SA-IP-XX).
- Burkner, P.-C. (2017). brms : An R Package for Bayesian Multilevel Models Using Stan. *Journal of Statistical Software*, 80(1), 1–28. doi:10.18637/jss.v080.i01
- Campana, S. E.; Marks, L., & Joyce, W. (2005). The biology and fishery of shortfin mako sharks (*Isurus oxyrinchus*) in Atlantic Canadian waters. *Fisheries Research*, 73, 341–352.
- Clarke, S. (2009). An alternative estimate of catches of five species of sharks in the Western and Central Pacific Ocean based on shark fin trade data. (SC5-EB-WP-08).
- Clarke, S.; Coelho, R.; Francis, M.; Kai, M.; Kohin, S.; Liu, K. M.; Simpfendorfer, C.; Tovar-Avila, J.; Rigby, C., & Smart, J. (2015). Report of the Pacific shark life history expert panel workshop, 28-30 April 2015. (SC11-EB-IP-13).
- Common Oceans (ABNJ) Tuna Project (2019). Report of the Workshop on Joint Analysis of Shark Post-Release Mortality Tagging Results. (WCPFC-SC15-2019/EB-WP-01).
- Francis, M. P. & Duffy, C. (2005). Length at maturity in three pelagic sharks (*Lamna nasus*, *Isurus oxyrinchus*, and *Prionace glauca*) from New Zealand. *Fish. Bull.*, (103), 489–500.
- Francis, M. P.; Lyon, W. S.; Clarke, S. C.; Finucci, B.; Hutchinson, M. R.; Campana, S. E.; Musyl, M. K.; Schaefer, K. M.; Hoyle, S. D.; Peatman, T.; Bernal, D.; Bigelow, K.; Carlson, J.; Coelho, R.; Heberer, C.; Itano, D.; Jones, E.; Leroy, B.; Liu, K. M.; Murua, H.; Poisson,

- F.; Rogers, P.; Sanchez, C.; Semba, Y.; Sippel, T., & Smith, N. (2022). Post-release survival of shortfin mako (*Isurus oxyrinchus*) and silky (*Carcharhinus falciformis*) sharks released from pelagic tuna longlines in the Pacific Ocean. *In press*.
- Kai, J. T., M. Thorson; Piner, K. R., & Maunder, M. N. (2017). Spatiotemporal variation in size-structured populations using fishery data: an application to shortfin mako (*Isurus oxyrinchus*) in the Pacific Ocean. *Canadian Journal of Fisheries and Aquatic Science*, 74, 175–178. doi:10.1139/cjfas-2016-0327
- Large, K.; Neubauer, P.; Brouwer, S., & Kai, M. (2022). Input data for the 2022 South Pacific Shortfin Mako Shark stock assessment. (WCPFC-SC18-2022/SA-IP-XX).
- Lawson, T. (2011). Estimation of catch rates and catches of Key Shark Species in tuna fisheries of the Western and Central Pacific Ocean using observer data. (SC7-EB-IP-02).
- Neubauer, P.; Large, K., & Brouwer, S. (2021a). Stock assessment for south Pacific blue shark in the Western and Central Pacific Ocean. (WCPFC-SC17-2021/SA-WP-03).
- Neubauer, P.; Large, K.; Kai, M.; Tasi, W., & Liu, K. (2021b). Input data for the 2021 South Pacific blue shark (*Prionace glauca*) stock assessment. (WCPFC-SC17-2021/SA-IP-18).
- Peatman, T.; Bell, L.; Allain, V.; Caillot, S.; Williams, P.; Tuiloma, I.; Panizza, A.; Tremblay-Boyer, L.; Fukufuka, S., & Smith, N. (2018). Summary of longline fishery bycatch at a regional scale, 2003-2017.
- Rice, J. (2012). Alternate catch estimates for silky and oceanic whitetip sharks in Western and Central Pacific Ocean. (SC8-SA-IP-12).
- Roberts, R.; Bahn, V.; Ciuti, S.; Boyce, M. S.; Elith, J.; Guillera-Arroita, G.; Hauenstein, S.; Lahoz-Monfort, J. J.; Schröder, B.; Thuiller, W., et al. (2017). Cross-validation strategies for data with temporal, spatial, hierarchical, or phylogenetic structure. *Ecography*, 40(8), 913–929.
- Tremblay-Boyer, L.; Carvalho, F.; Neubauer, P., & Pilling, G. (2019). Stock assessment for oceanic whitetip shark in the Western and Central Pacific Ocean. (WCPFC-SC15-2019/SA-WP-06).
- Tremblay-Boyer, L. & Takeuchi, Y. (2016). Catch and CPUE inputs to the South Pacific blue shark stock assessment. (SC12-SA-WP-09).
- WCPFC (2019). Conservation and Management Measure for Sharks. (CMM2019-04).
- Williams, P.; Panizza, A.; Falasi, C.; Loganimoce, E., & Schneiter, E. (2020). Status of Observer Data Management. (SC16-2020/ST-IP-02).
- Williams, P. & Ruaia, T. (2021). Overview of tuna fisheries in the Western and Central Pacific Ocean, including economic conditions - 2020. (WCPFC-SC17-2021/GN-IP-01).
- Yao, Y.; Vehtari, A.; Simpson, D., & Gelman, A. (2018). Using stacking to average Bayesian predictive distributions (with discussion). *Bayesian Analysis*, 13(3), 917–1007.

TABLES

Table 1: Model covariates of operational fishing features likely to influence catch rates of shortfin mako shark and environmental variables that may represent habitat of this species (LBEST are databases of the SPC for longline fisheries).

Covariate	Description
Year	Year when the fishing set occurred, treated as categorical .
Flag	Country-assigntation for the vessel performing the fishing set.
Cluster	Predicted targeting strategy for longline fishing set based on k-means clustering of the proportion in the total catch in number of albacore, bigeye, yellowfin, swordfish and other billfish. Cluster composition was predicted based on LBEST records and assuming 4 centres, resulting in a categorical variable with values from 1 to 4. Longline observed set targeting strategy was predicted according to the LBEST classification.
SST	Sea surface temperature aggregated at 5-degree scale for LBEST, obtained from NOAA (https://www.esrl.noaa.gov/psd/data/gridded/data.noaa.oisst.v2.html).
Chl- α	Sea surface chlorophyll- α concentration aggregated at 5-degree scale for LBEST (https://coastwatch.pfeg.noaa.gov/erddap/griddap/erdMH1chlamday).
Dist2Coast	Distance of the set to the nearest coastline, aggregated at 5-degree scale for LBEST.

Table 2: Model specification for the 18 candidate models used in the catch reconstruction.

Model	Model name	Covariates
1	base	(1 year) + (1 month) + s(SST) + s(chla) + target_cluster + t2(Lon5,Lat5, by = month)
2	base.hooks	base + s(log(hooks))
3	base.area	base + (1 area)
4	base.area.hooks	base + s(log(hooks)) + (1 area)
5	base.flag	base + (1 flag_id)
6	base.flag.hooks	base + s(log(hooks)) + (1 flag_id)
7	base.yy	(1 year) + (1 month) + s(SST) + s(chla) + target_cluster + t2(Lon5,Lat5,by = month, by = year))
8	base.hooks.yy	base.yy + s(log(hooks))
9	base.area.yy	base.yy + (1 area)
10	base.area.hooks.yy	base.yy + s(log(hooks)) + (1 area)
11	base.flag.yy	base.yy + (1 flag_id)
12	base.flag.hooks.yy	base.yy + s(log(hooks)) + (1 flag_id)
13	base.lat_hooks	base + t2(log(hooks))
14	base.area.lat_hooks	base + t2(log(hooks)) + (1 area)
15	base.flag.lat_hooks	base + t2(log(hooks)) + (1 flag_id)
16	base.lat_hooks.yy	base.yy + t2(log(hooks))
17	base.area.lat_hooks.yy	base.yy + t2(log(hooks)) + (1 area)
18	base.flag.lat_hooks.yy	base.yy + t2(log(hooks)) + (1 flag_id)

Table 3: Ensemble cross-validation weight for each of the 18 candidate models used in the catch reconstruction. Ensemble weight calculated as the product of the estimated weight of each holdout (flag_id) set in a model averaged across holdout sets to give a final ensemble weight for each model

Model	Model name	Enseble weight
1	base	0.03051890
2	base.hooks	0.01020800
3	base.area	0.09822988
4	base.area.hooks	0.01515643
5	base.flag	0.04224692
6	base.flag.hooks	0.06172245
7	base.yy	0.07937600
8	base.hooks.yy	0.10100842
9	base.area.yy	0.10146614
10	base.area.hooks.yy	0.09458341
11	base.flag.yy	0.05741019
12	base.flag.hooks.yy	0.05509361
13	base.lat_hooks	0.02077188
14	base.area.lat_hooks	0.01953487
15	base.flag.lat_hooks	0.03527741
16	base.lat_hooks.yy	0.10704528
17	base.area.lat_hooks.yy	0.01098080
18	base.flag.lat_hooks.yy	0.05936940

FIGURES

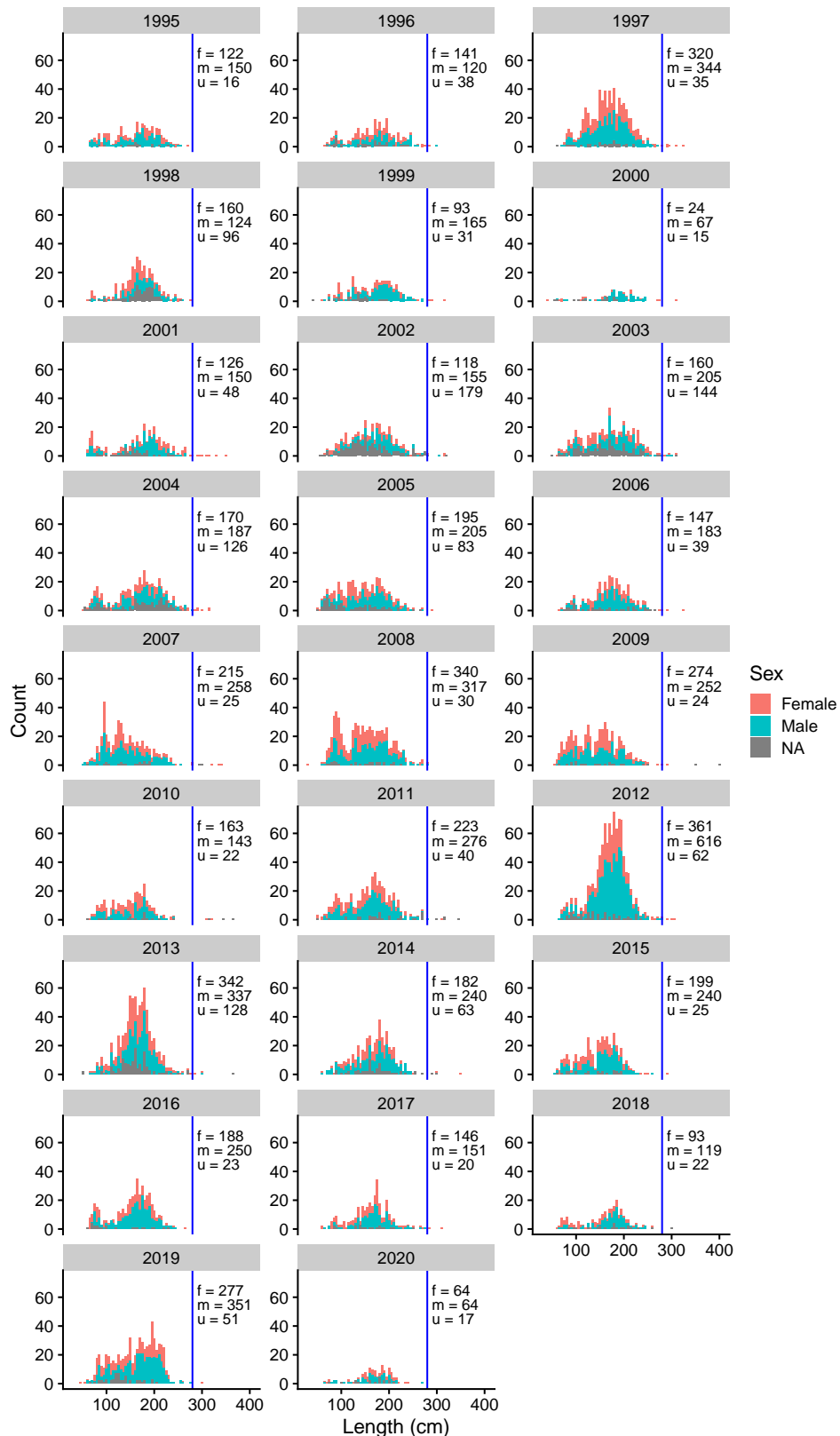


Figure 2: Length frequencies of observer - sampled shortfin mako shark by sex and year. The length at maturity for females is indicated with the vertical line.

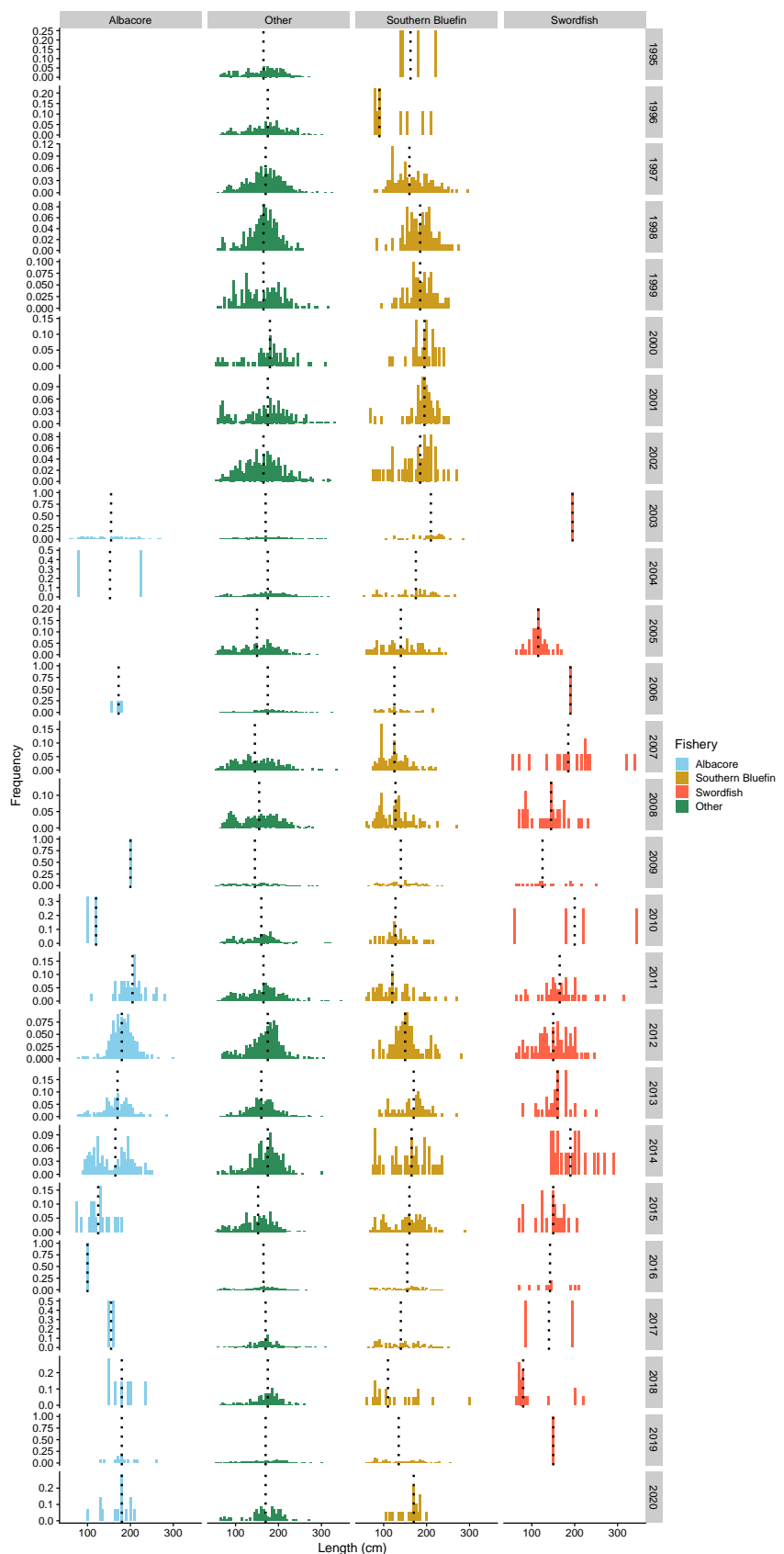


Figure 3: Length frequencies of observer - sampled shortfin mako shark in target fisheries by year. The median length for each year is indicated with the dashed vertical line.

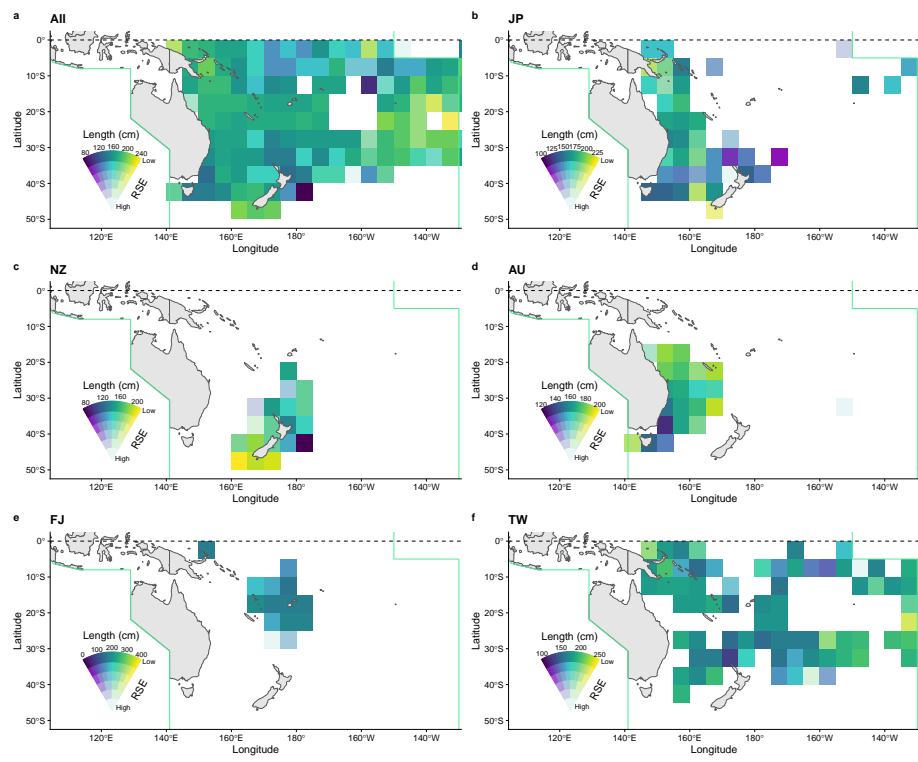


Figure 4: Maps of average length shaded by variability in lengths (SE of mean length). Samples are from a) Combined dataset, b) Japanese, c) New Zealand, d) Australian, e) Fijian, and f) Chinese Taipei.

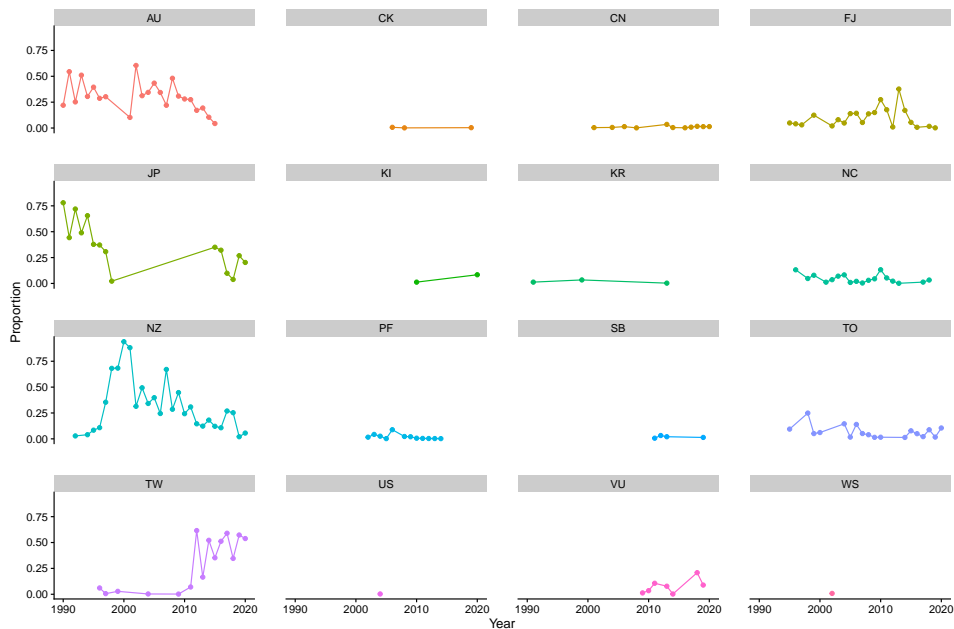


Figure 5: Proportional sampling effort over time by flag in the observer dataset.

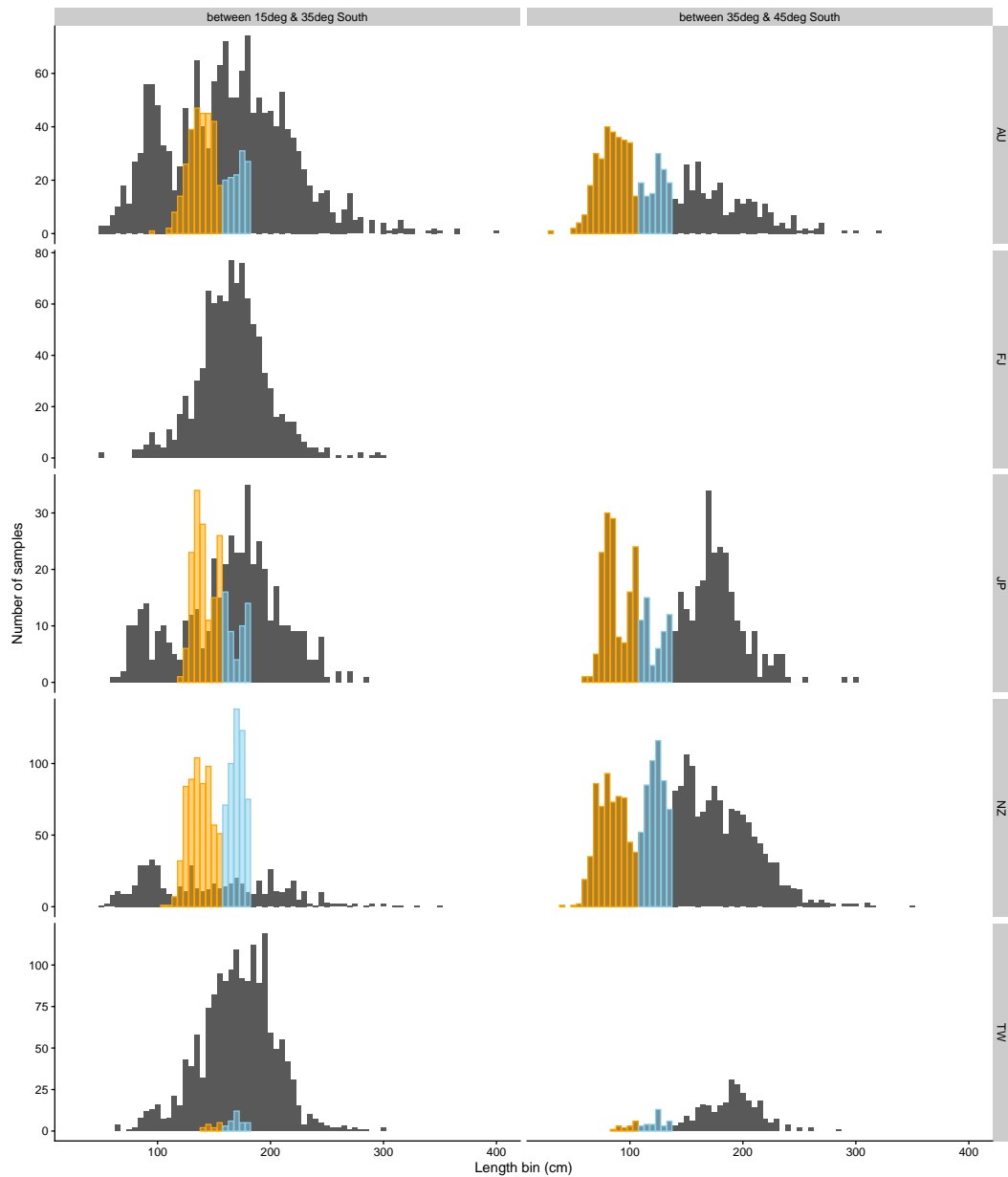


Figure 6: Length frequencies by flag for flags with reasonable amounts of samples. Orange and blue histograms approximately show samples of age - 0 recruits and 1 - year - olds grown according to Bishop et al. (2006) over 5 years respectively.

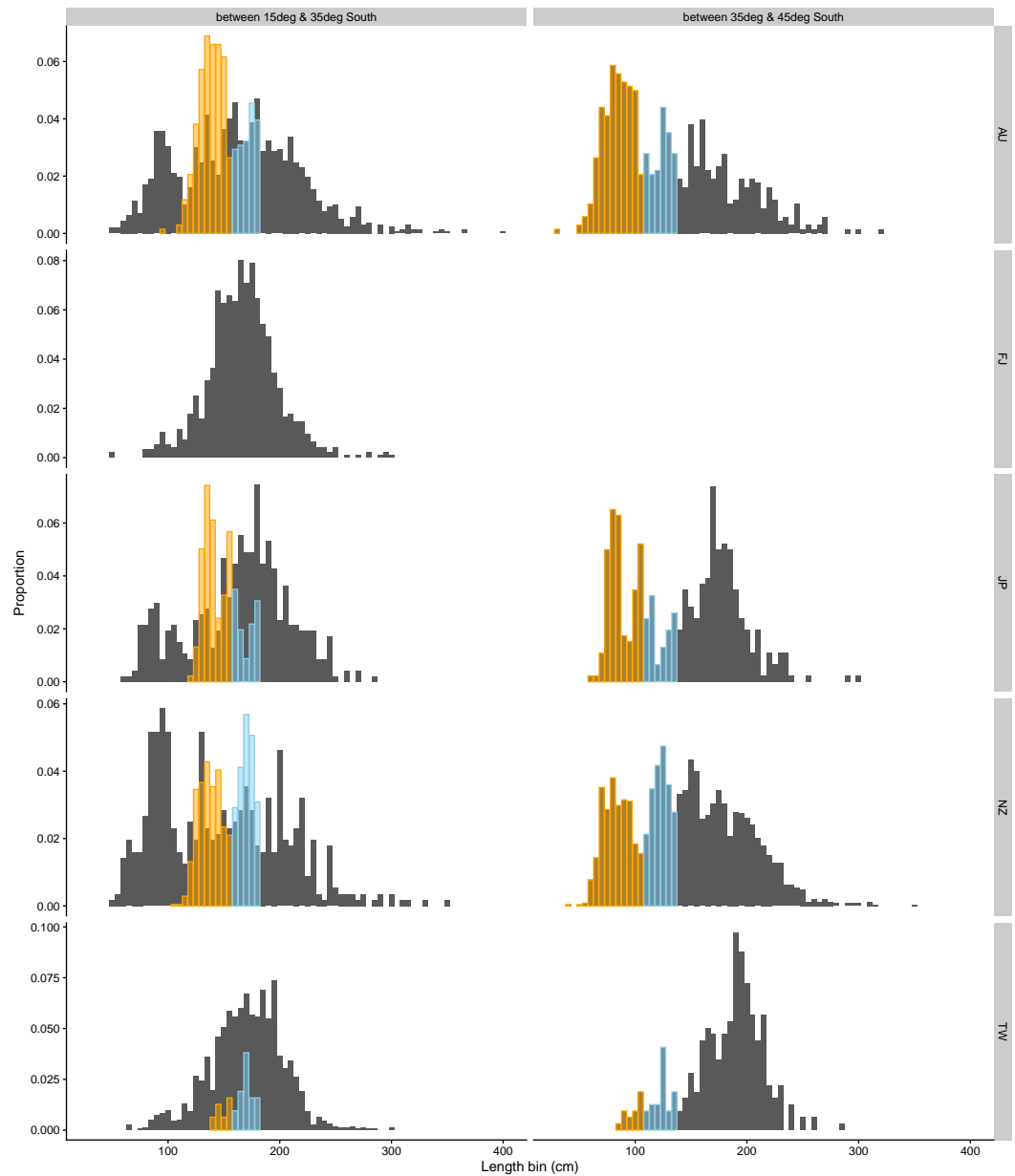


Figure 7: Length proportions by flag for flags with reasonable amounts of samples. Orange and blue histograms approximately show samples of recruits and 1 - year - olds grown according to Bishop et al. (2006) over 5 years, respectively.

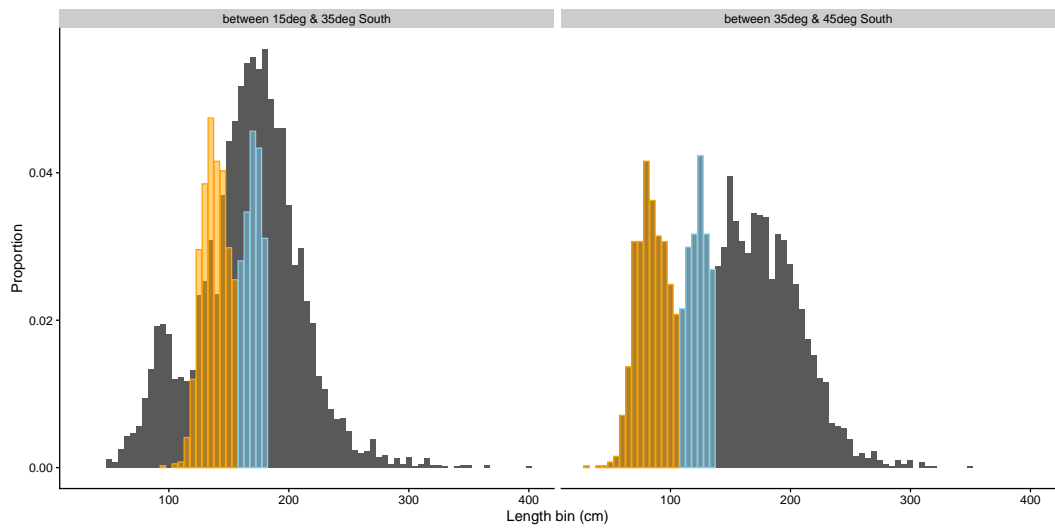


Figure 8: Length proportions by latitudinal strata for flags with reasonable amounts of samples. Orange and blue histograms show samples of recruits and 1-year-olds grown according to Bishop et al. (2006) over 5 years, respectively. Samples of 1-year old fish appear to align with the common fishery peak at 180–200cm in lower latitudes, suggesting a lag of around 6 years from birth to the peak of low latitude LFs.

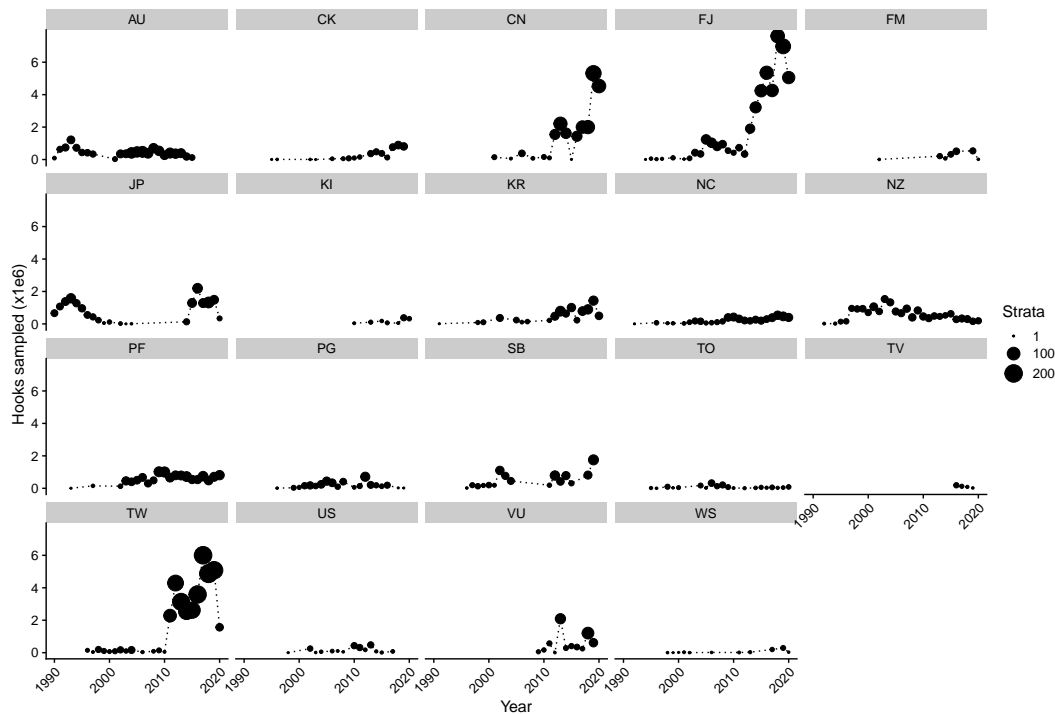


Figure 9: Number of observed hooks by fleet. Strata refer to observed 5x5 degree pixels by month, year, target cluster, and fleet.

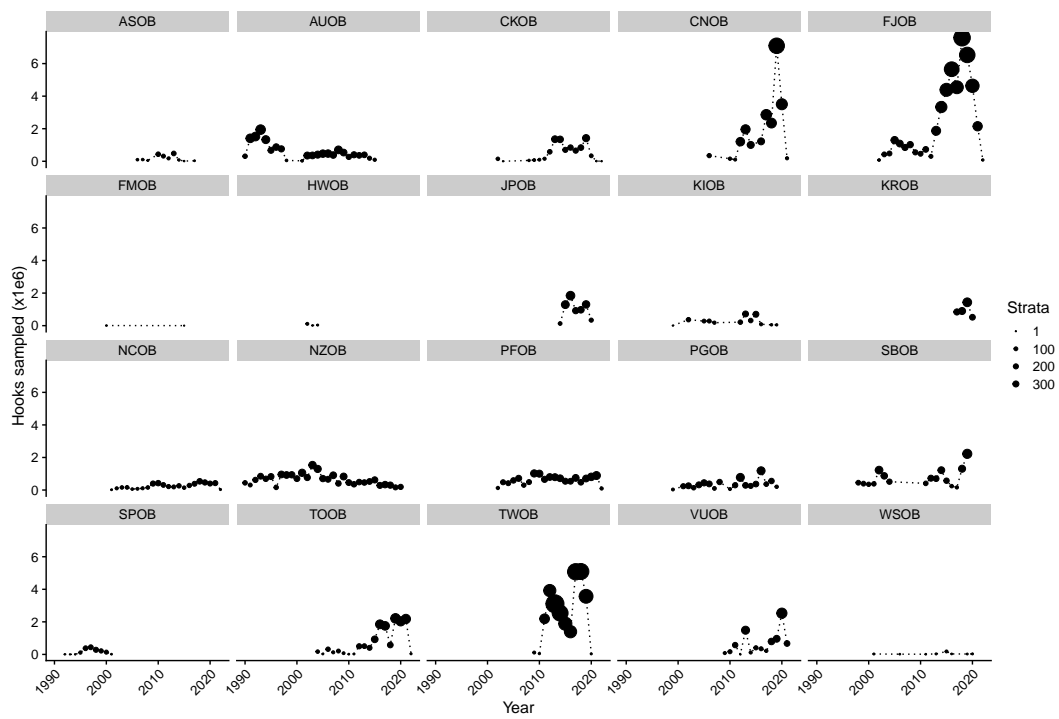


Figure 10: Observed hooks by observer programme. Strata refer to observed 5x5 degree pixels by month, year, target cluster, and fleet.

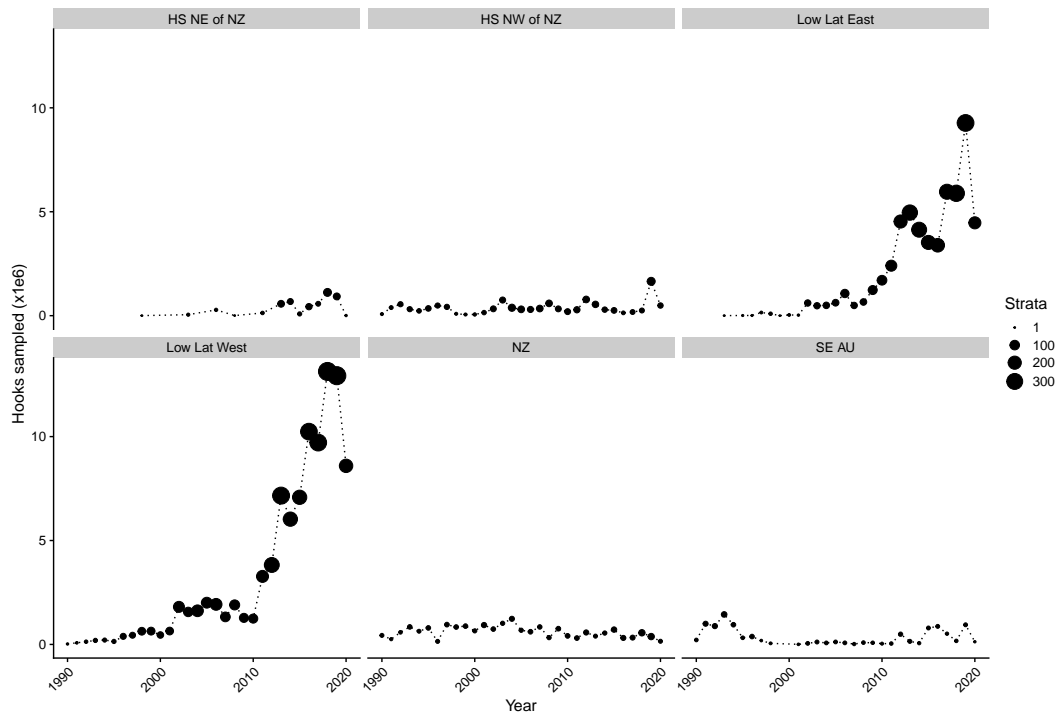


Figure 11: Number of observed hooks by area. Strata refer to observed 5x5 degree pixels by month, year, target cluster, and fleet.

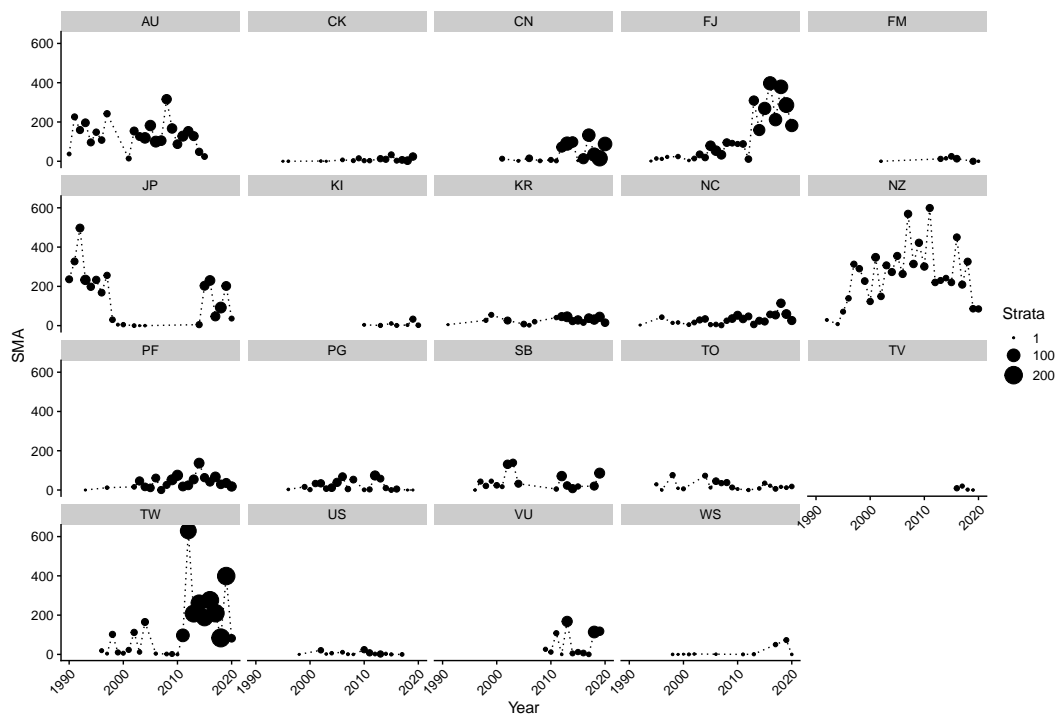


Figure 12: Observed shortfin mako shark interactions by fleet. Strata refer to observed 5x5 degree pixels by month, year, target cluster, and fleet.

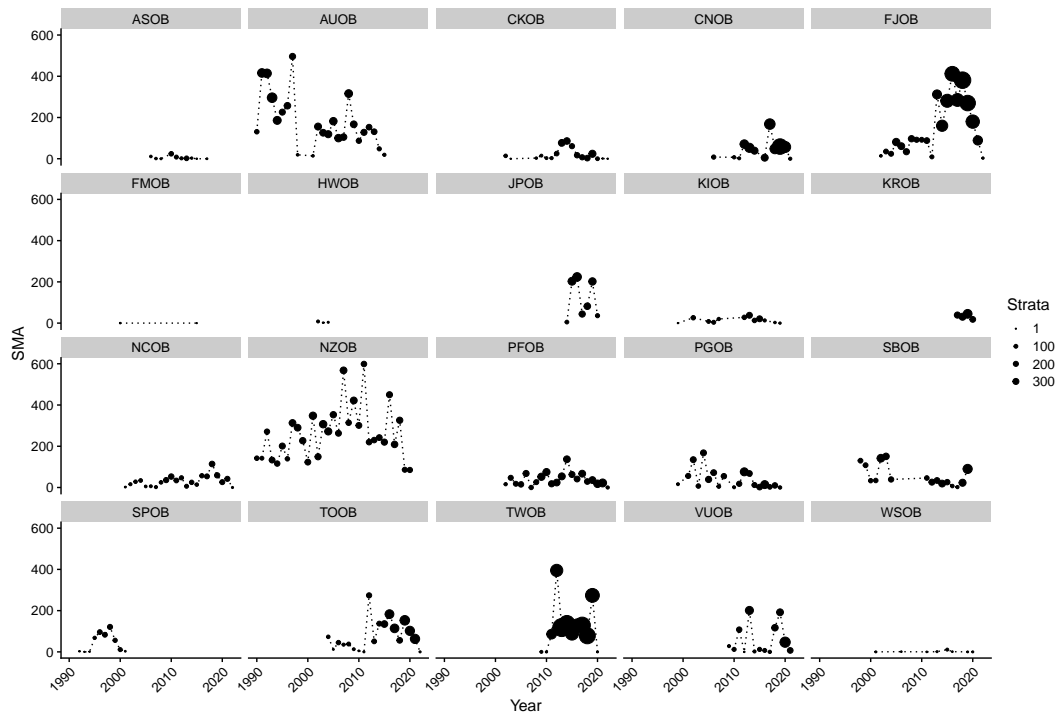


Figure 13: Observed shortfin mako shark interactions by observer programme. Strata refer to observed 5x5 degree pixels by month, year, target cluster, and fleet.

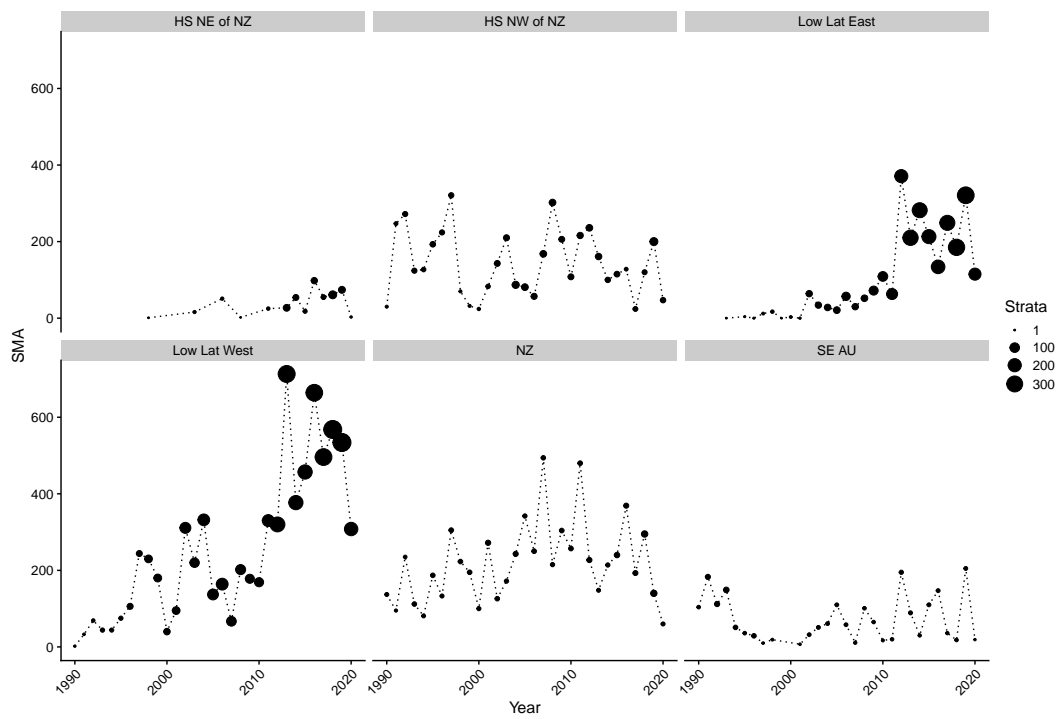


Figure 14: Observed shortfin mako shark interactions by area. Strata refer to observed 5x5 degree pixels by month, year, target cluster, and fleet.

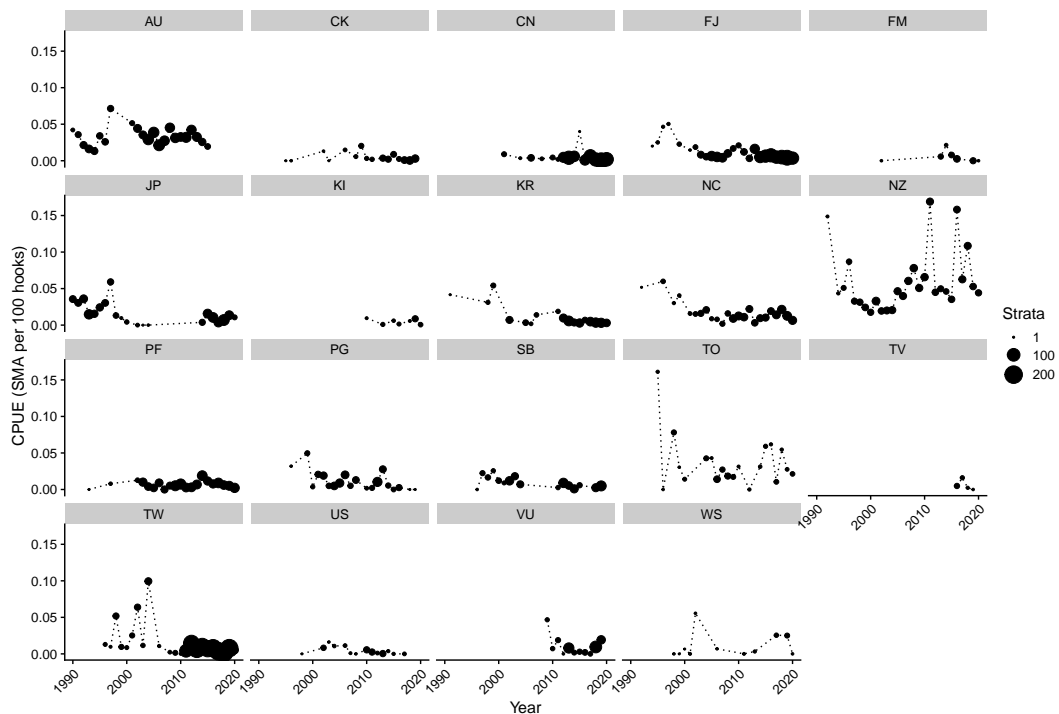


Figure 15: Nominal observed CPUE by fleet. Strata refer to observed 5x5 degree pixels by month, year, target cluster, and fleet.

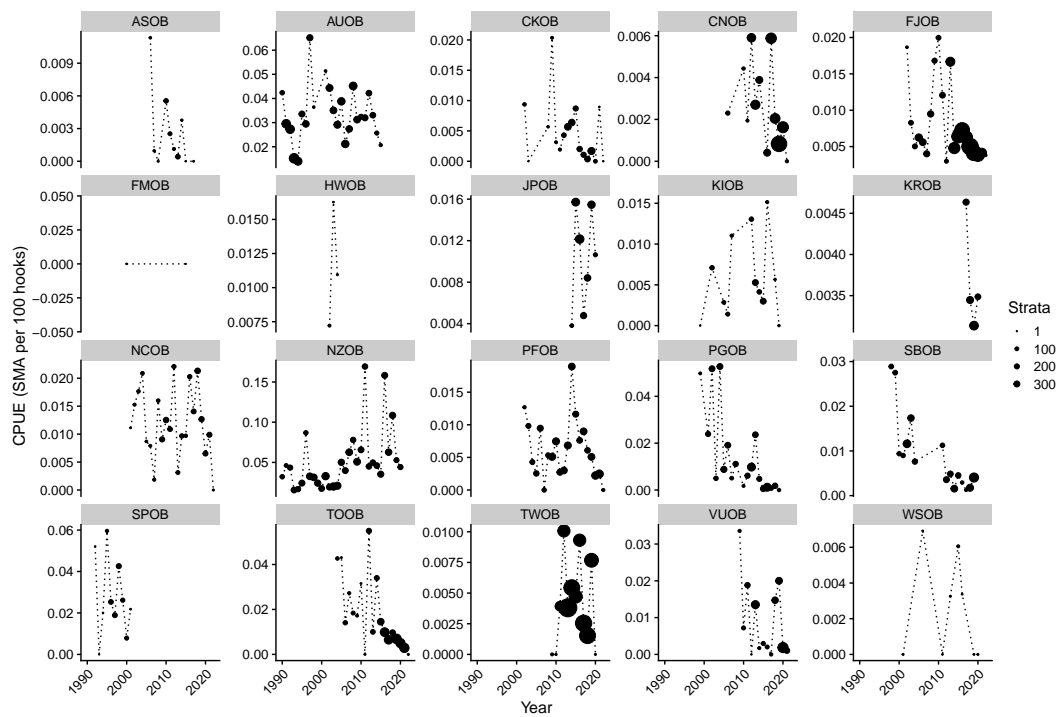


Figure 16: Nominal observed CPUE by observer programme. Strata refer to observed 5x5 degree pixels by month, year, target cluster, and fleet.

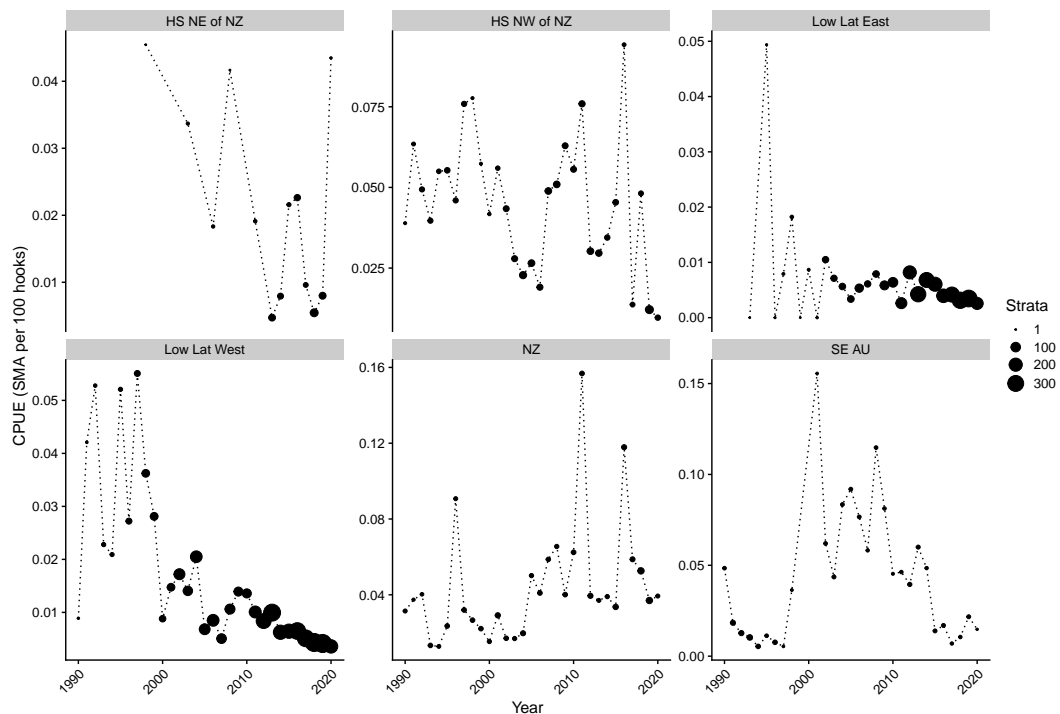


Figure 17: Nominal observed CPUE by area. Strata refer to observed 5x5 degree pixels by month, year, target cluster, and fleet.

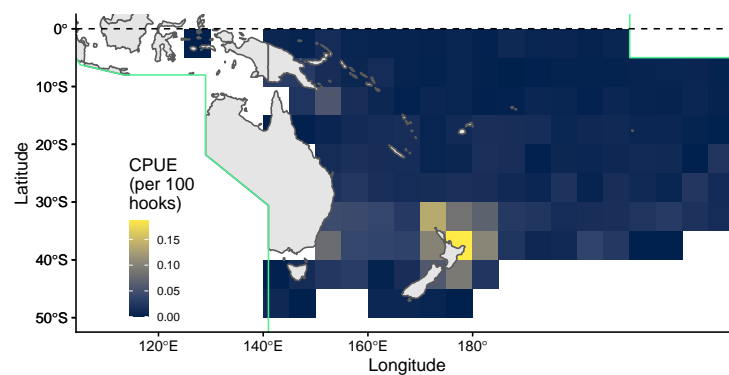
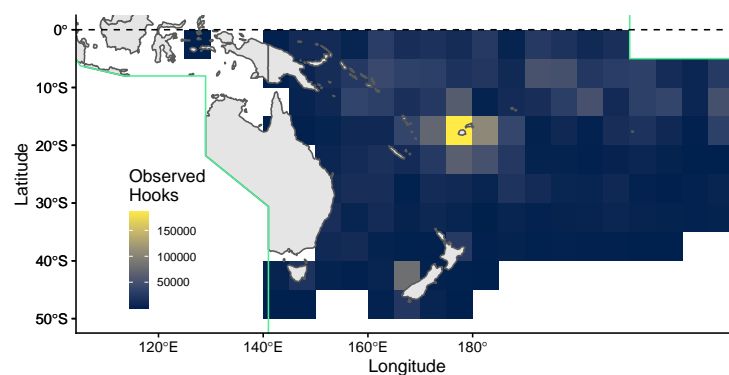


Figure 18: Observed CPUE: (Top) Number of observed hooks by 5x5 degree grid with non-zero shortfin mako shark catch; (bottom) arithmetic mean CPUE across observed strata (5x5, fleet, month).

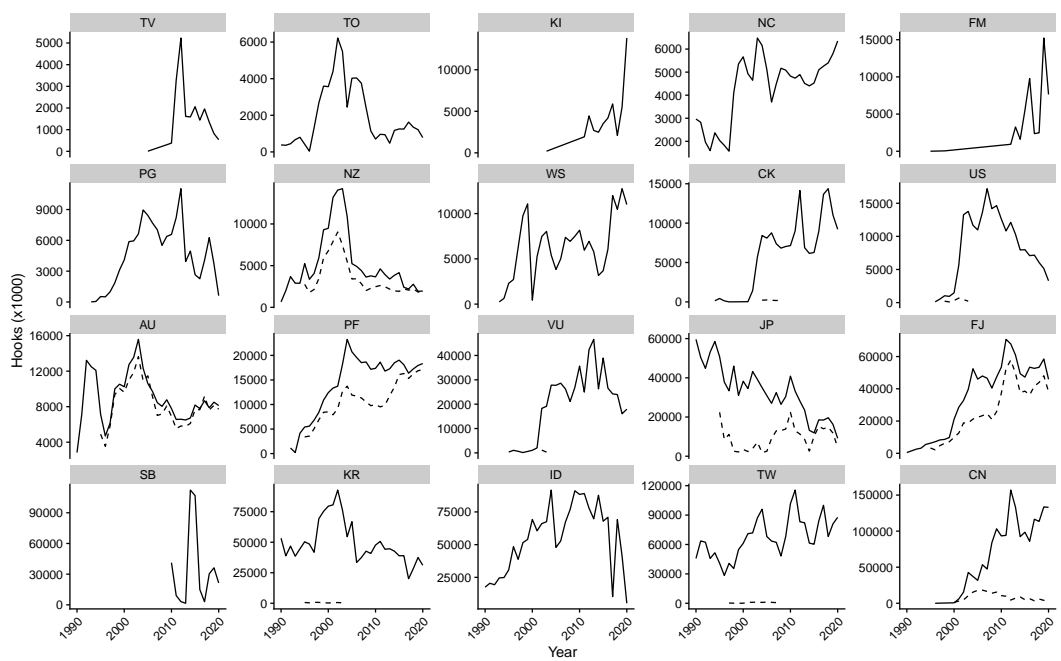


Figure 19: Estimated total hooks by fleet in L-BEST used for predictions of over-all catches of shortfin mako shark, with reported hooks in the operational log-sheet data shown for comparison (dashed lines).

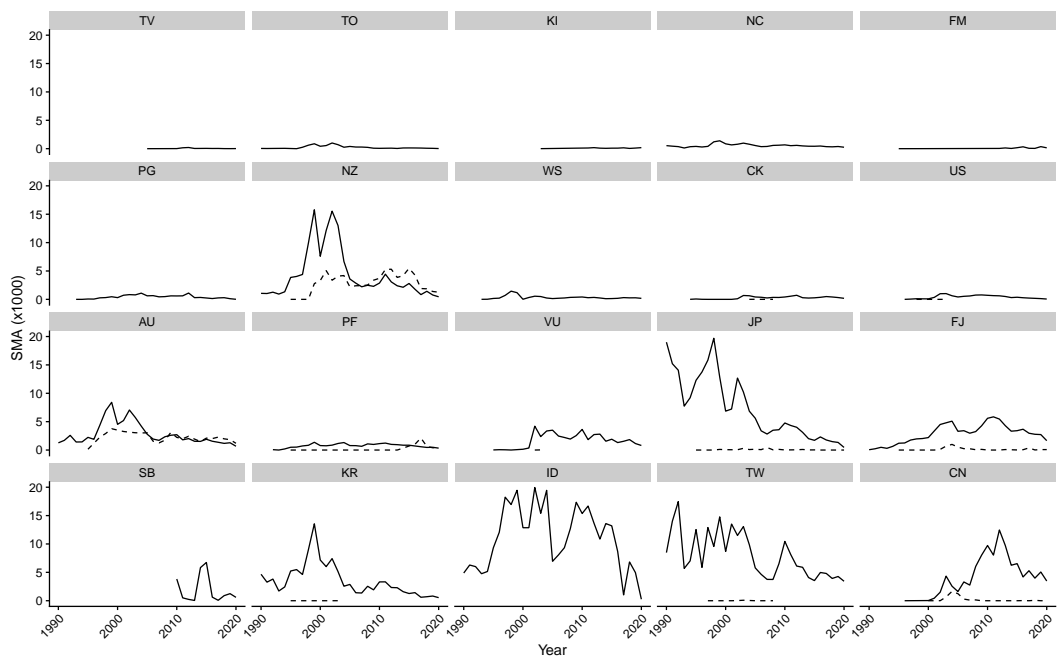


Figure 20: Predicted total shortfin mako shark captures by fleet using the observer catch-rate GLMM in conjunction with L-BEST effort. Reported numbers of shortfin mako shark from the operational log-sheet data shown for comparison (dashed lines).

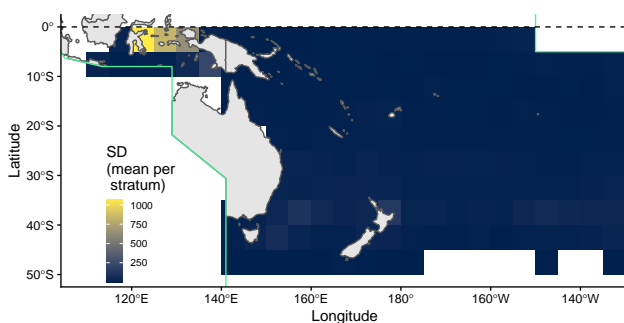
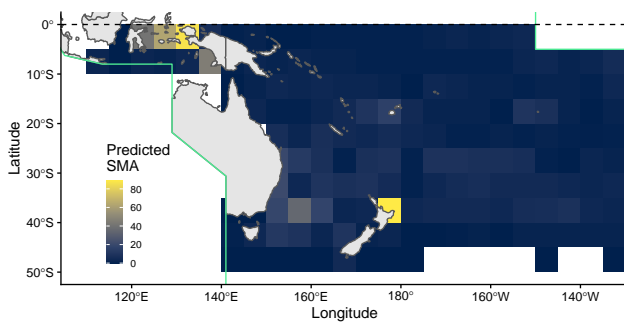
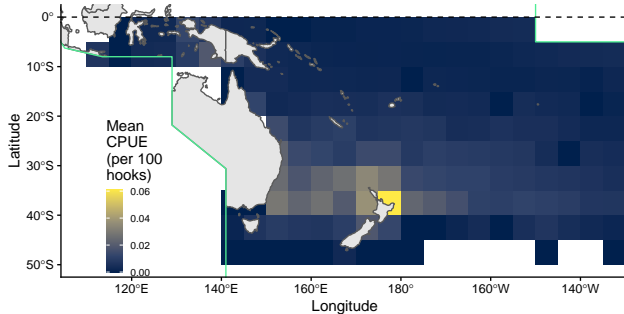


Figure 21: Predicted CPUE surface in terms of (top) predicted mean CPUE per stratum given observed hook numbers and (middle) median predicted numbers of shortfin mako shark per year-month-fleet stratum from the observer catch rate GLMM, (bottom) mean standard deviation of predicted numbers of shortfin mako shark per stratum.

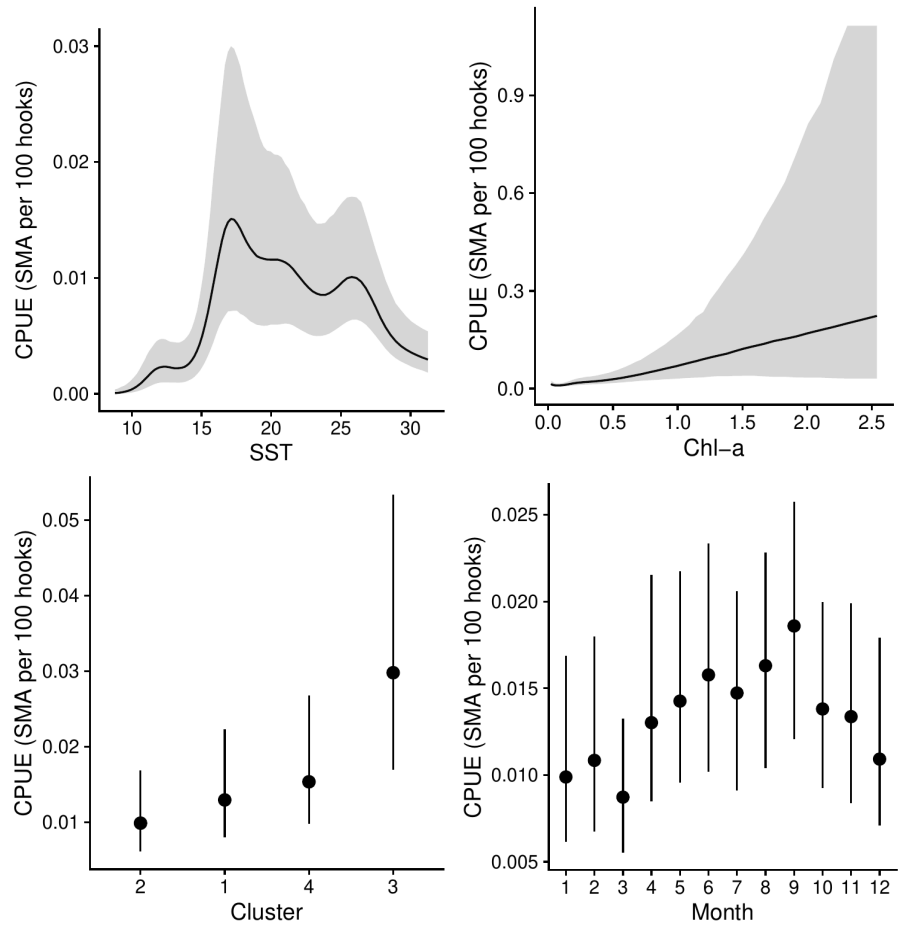


Figure 22: Conditional effects of SST, chlorophyll-a (CHL-a), targeting cluster and month in the observer catch-prediction model.

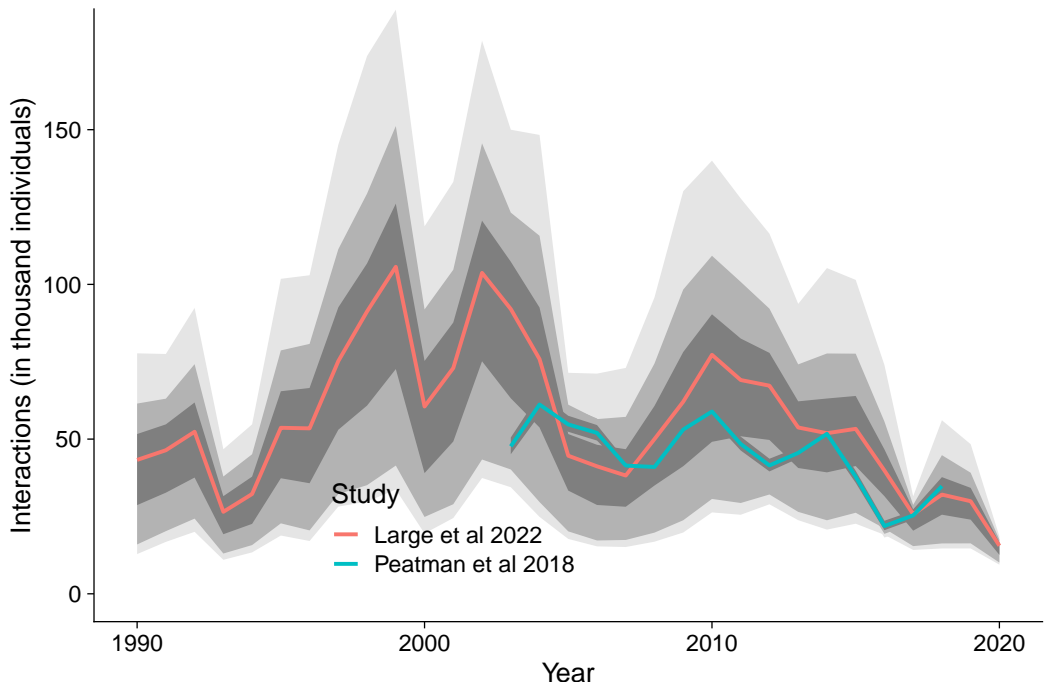


Figure 23: Predicted total shortfin mako shark captures from the combined weighted reconstruction model; posterior median (red); 75% confidence (dark grey) and 80% confidence (light grey). Predictions from Peatman et al. (2018) are shown in blue for comparison.

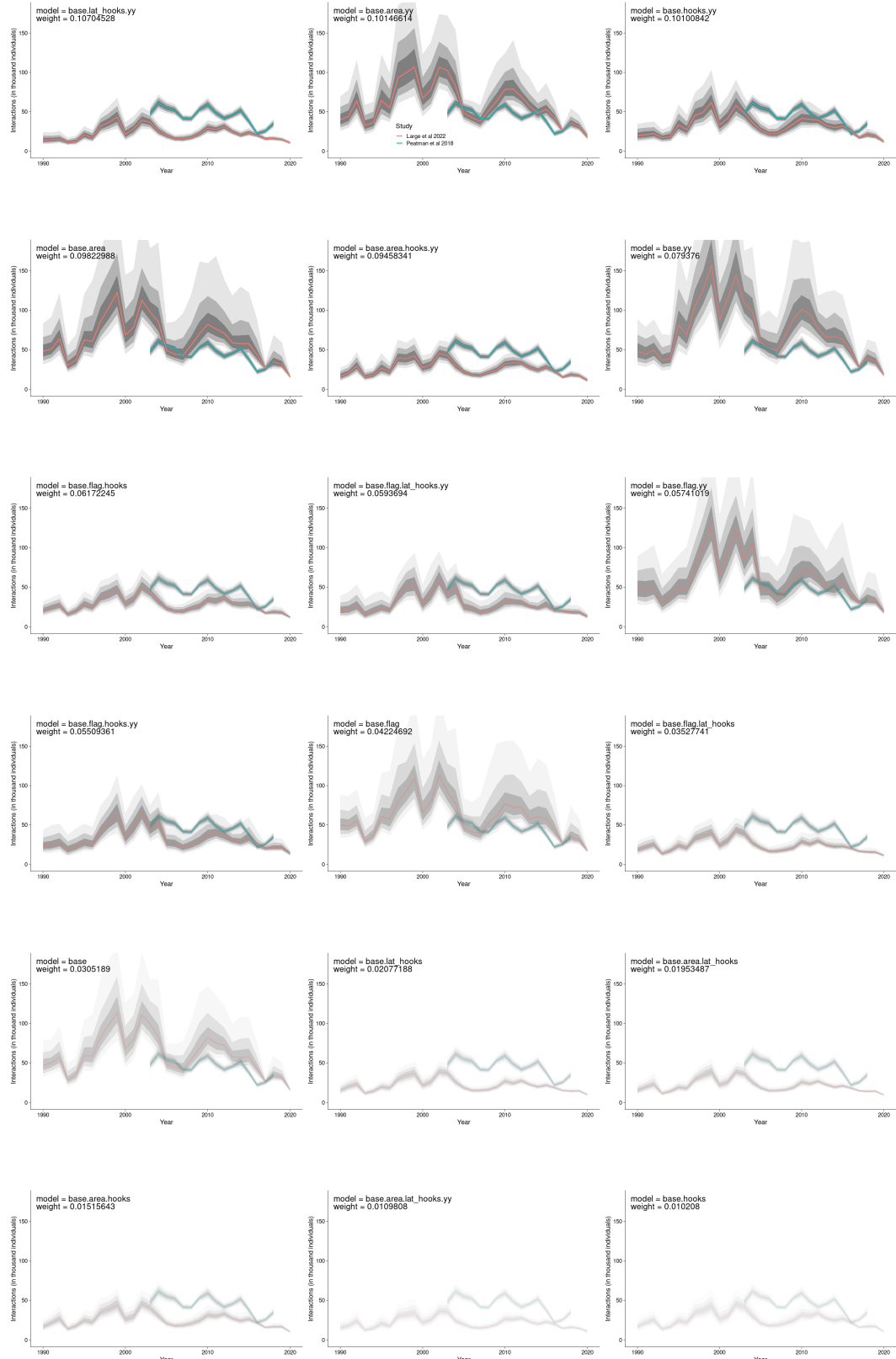


Figure 24: Predicted total shortfin mako shark captures (all latitudes) from the 18 candidate catch reconstruction models (posterior median (red); 75% confidence (dark grey) and 80% confidence (light grey)) using the observer catch-rate GLMM in conjunction with L-BEST effort. Plots are rendered darker (more weight) or lighter (less weight) depending on their contribution in the combined weighted model. Predictions from Peatman et al. (2018) are shown in blue for comparison

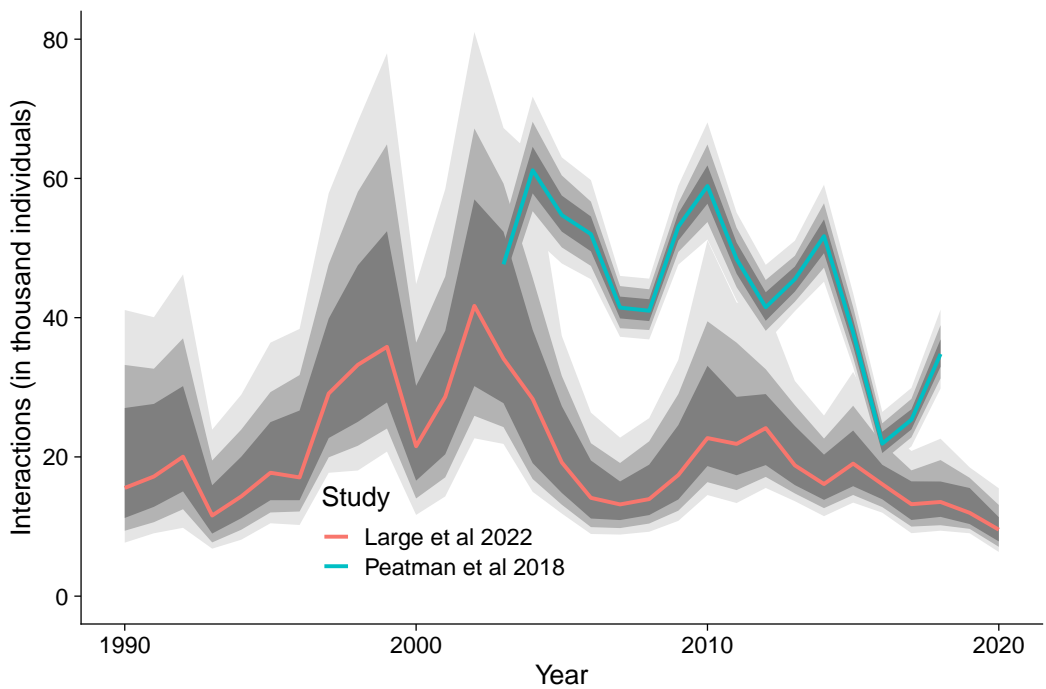


Figure 25: Predicted total shortfin mako shark captures (latitudes between 15°S and 45°S) from the combined weighted reconstruction model; posterior median (red); 75% confidence (dark grey) and 80% confidence (light grey). Predictions from Peatman et al. (2018) are shown in blue for comparison.

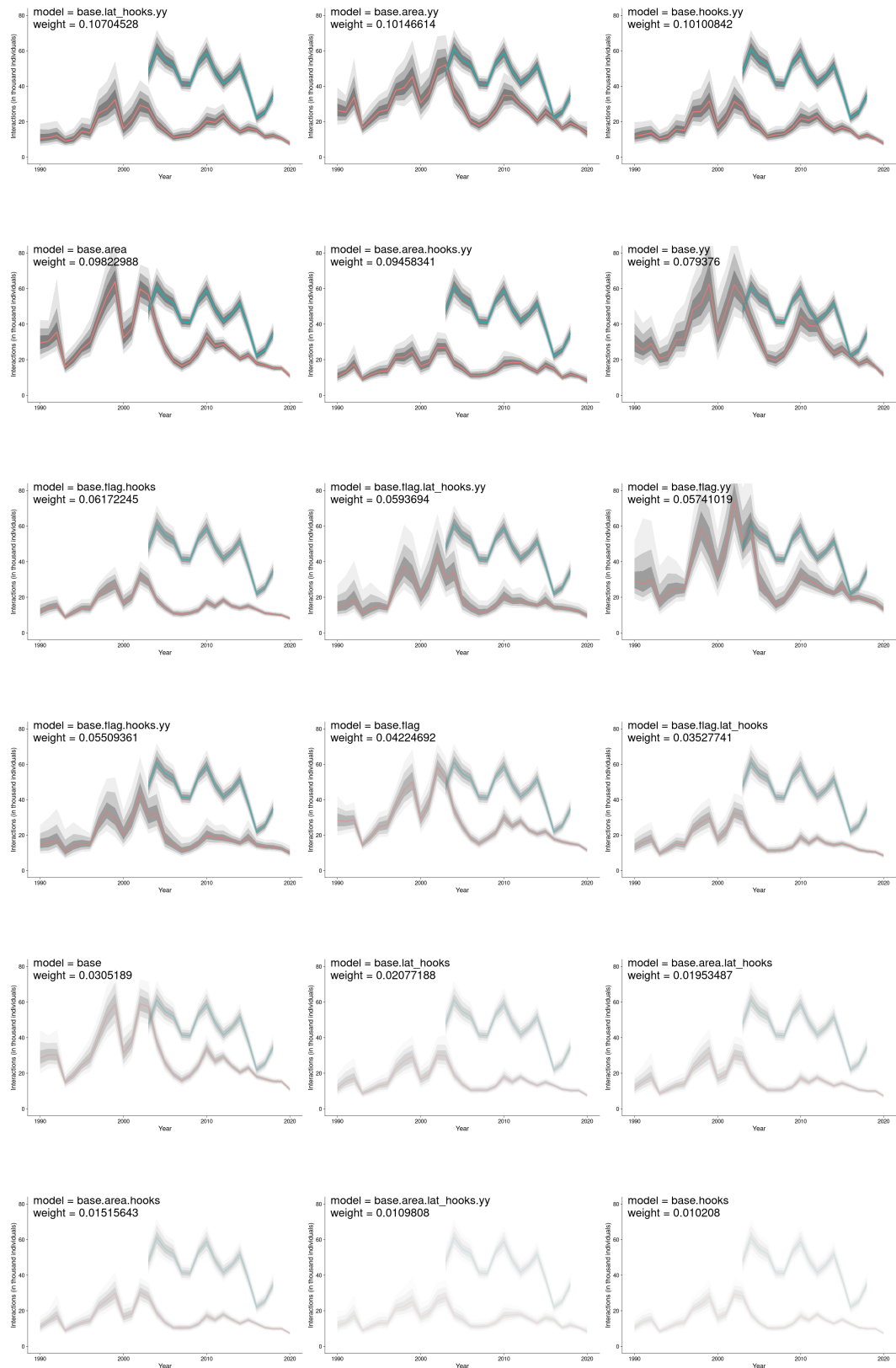


Figure 26: Predicted total shortfin mako shark captures (latitudes between 15°S and 45°S) from the 18 catch candidate reconstruction models (posterior median (red); 75% confidence (dark grey) and 80% confidence (light grey)) using the observer catch - rate GLMM in conjunction with L - BEST effort. Plots are rendered darker (more weight) or lighter (less weight) depending on their contribution in the combined weighted model.

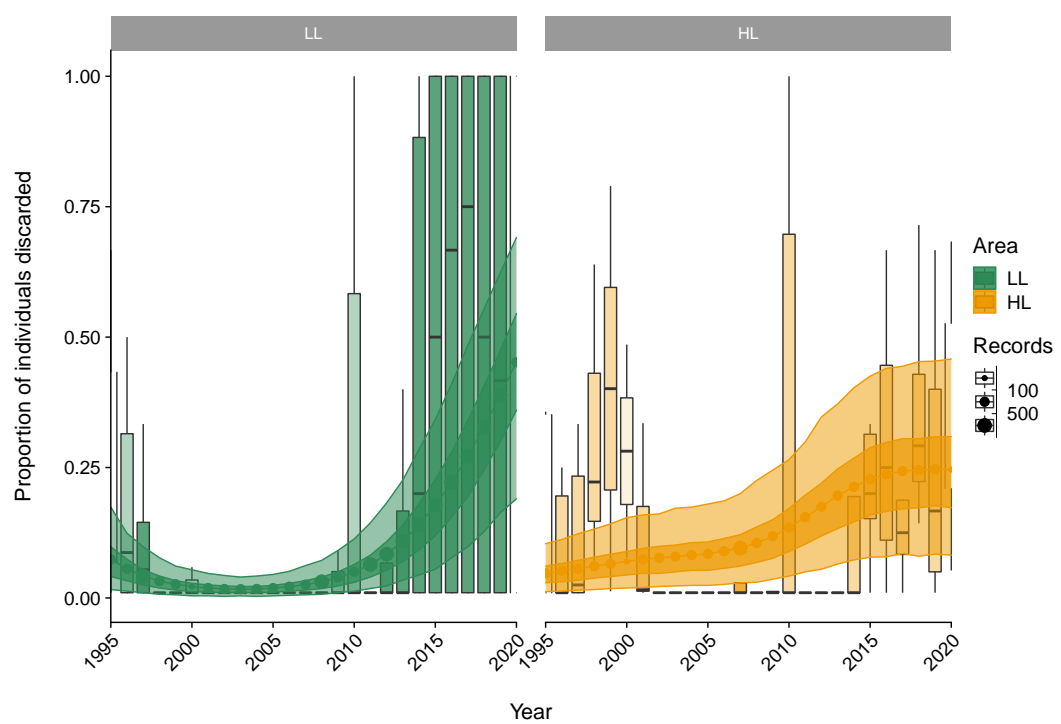


Figure 27: Estimated year effects (expected proportion discarded) for low-latitude and high-latitude (≥ 35 degree South), showing the posterior median, and 75% (dark shade) and 95% (light shade) posterior confidence. The distribution of input data is shown by underlying boxplots.

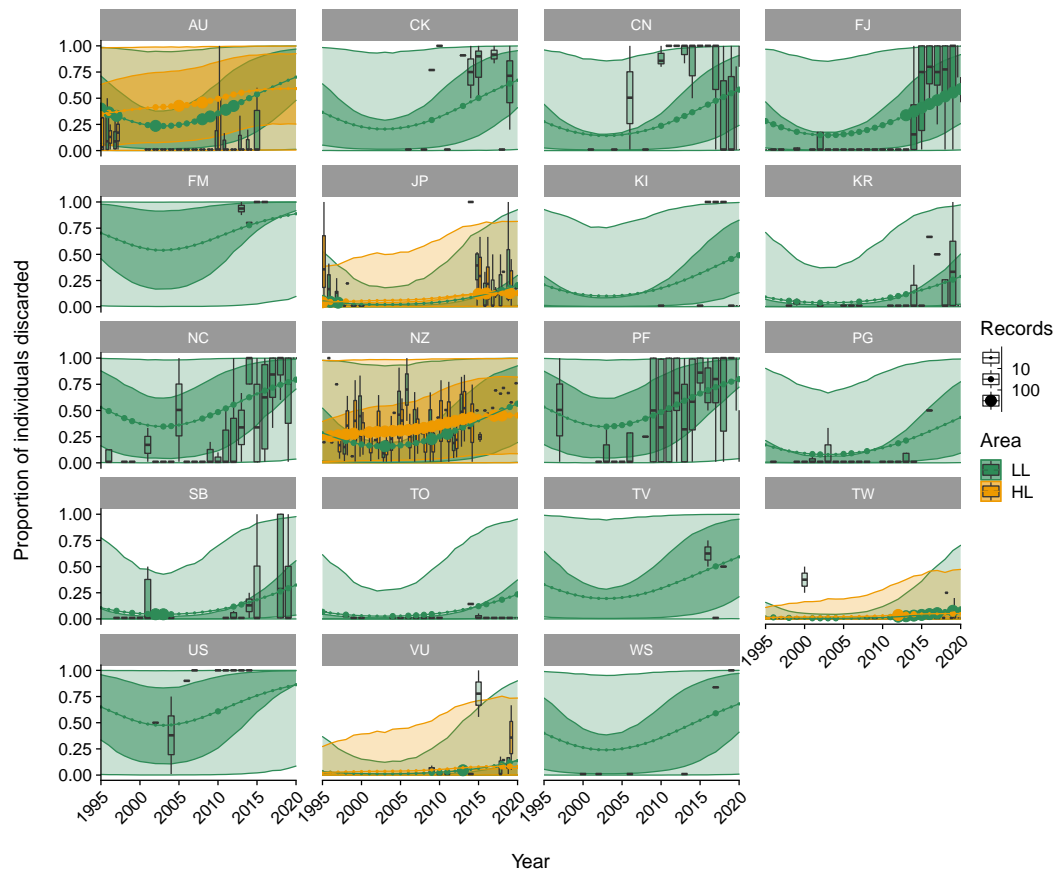


Figure 28: Estimated flag-year effects (expected proportion discarded) for flags in the observer dataset, split along low-latitude and high latitude ($>= 35$ degree South), showing the posterior median, 75% (dark shade) and 95% (light shade) posterior confidence. The distribution of input data is shown by underlying boxplots.

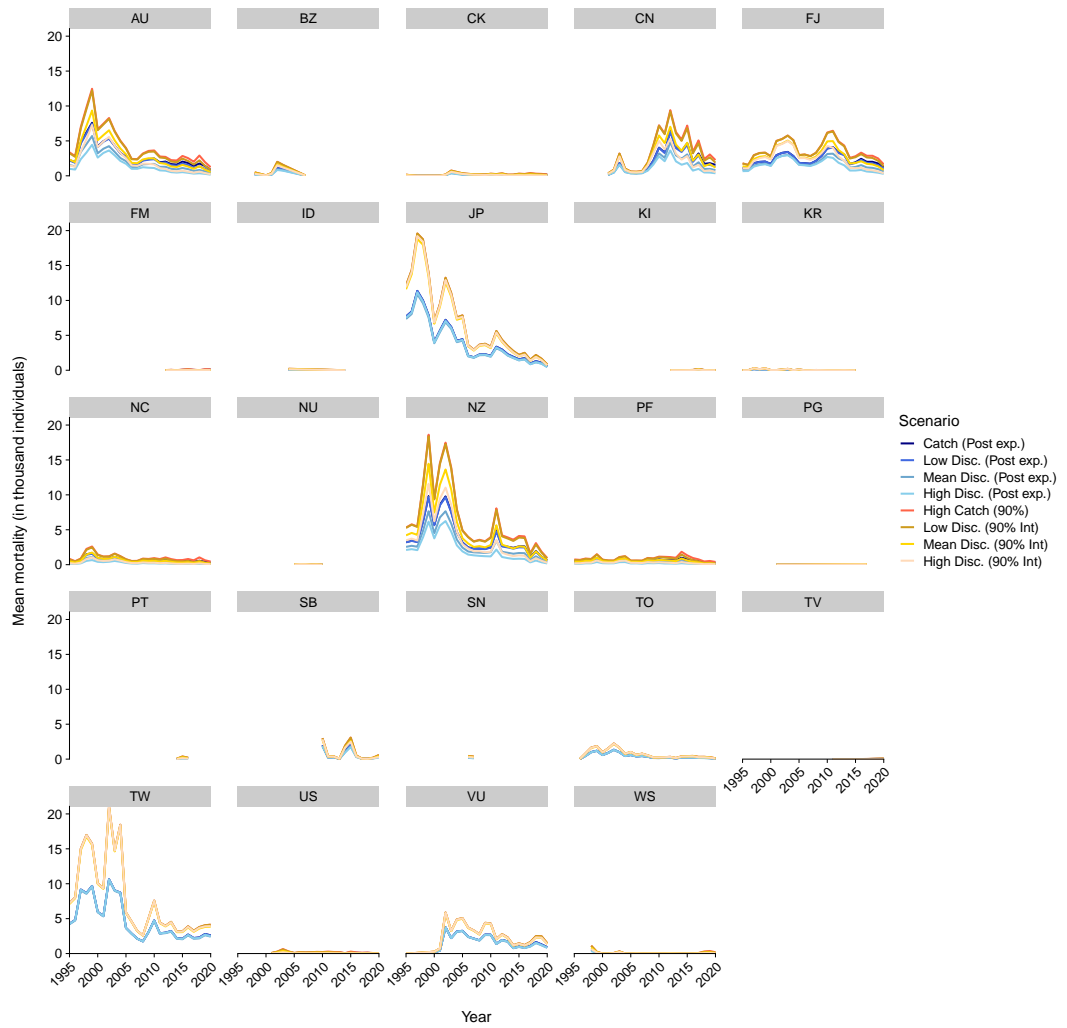


Figure 29: Predicted total fishing related mortality by flag, including 17% post release mortality for live-discarded shortfin mako shark. Catch refers to the posterior median (50%) and 90th percentile (90%) of the predicted catch from the observer catch rate model, low, median and high discard scenarios refer to the 25%, 50% (median) and 75% discard estimates.

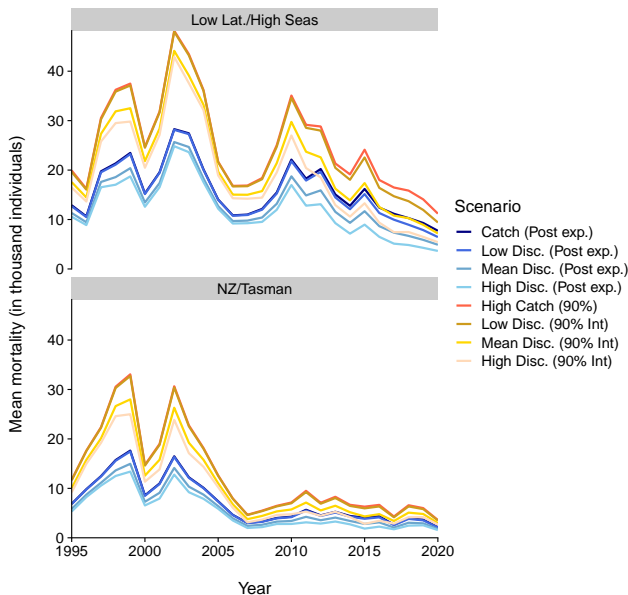


Figure 30: Predicted total fishing related mortality by latitudinal stratum (high [≥ 35 degree South] and low latitude [≥ 35 degree South]), including 17% post release mortality for live-discarded shortfin mako shark. Catch refers to the posterior median (50%) and 90th percentile (90%) of the predicted catch from the observer catch rate model, low, median and high discard scenarios refer to the 25%, 50% (median) and 75% discard estimates. All discard estimates were applied at flag and latitudinal stratum level to over-all interactions.

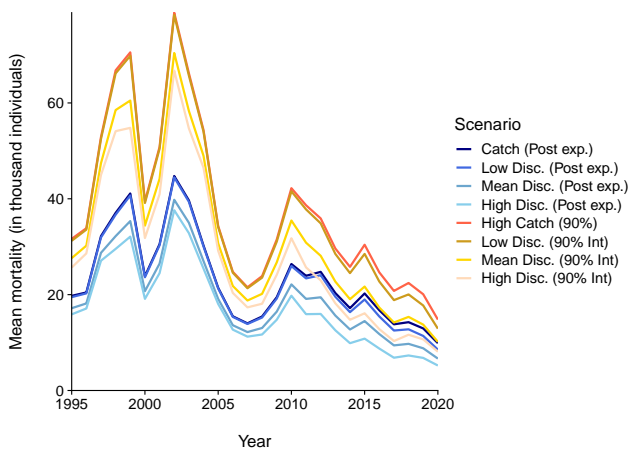


Figure 31: Predicted total fishing related mortality, including 17% post release mortality for live-discarded shortfin mako shark. Catch refers to the posterior median (50%) and 90th percentile (90%) of the predicted catch from the observer catch rate model, low, median and high discard scenarios refer to the 25%, 50% (median) and 75% discard estimates. All discard estimates were applied at flag and latitudinal stratum level to over-all interactions.

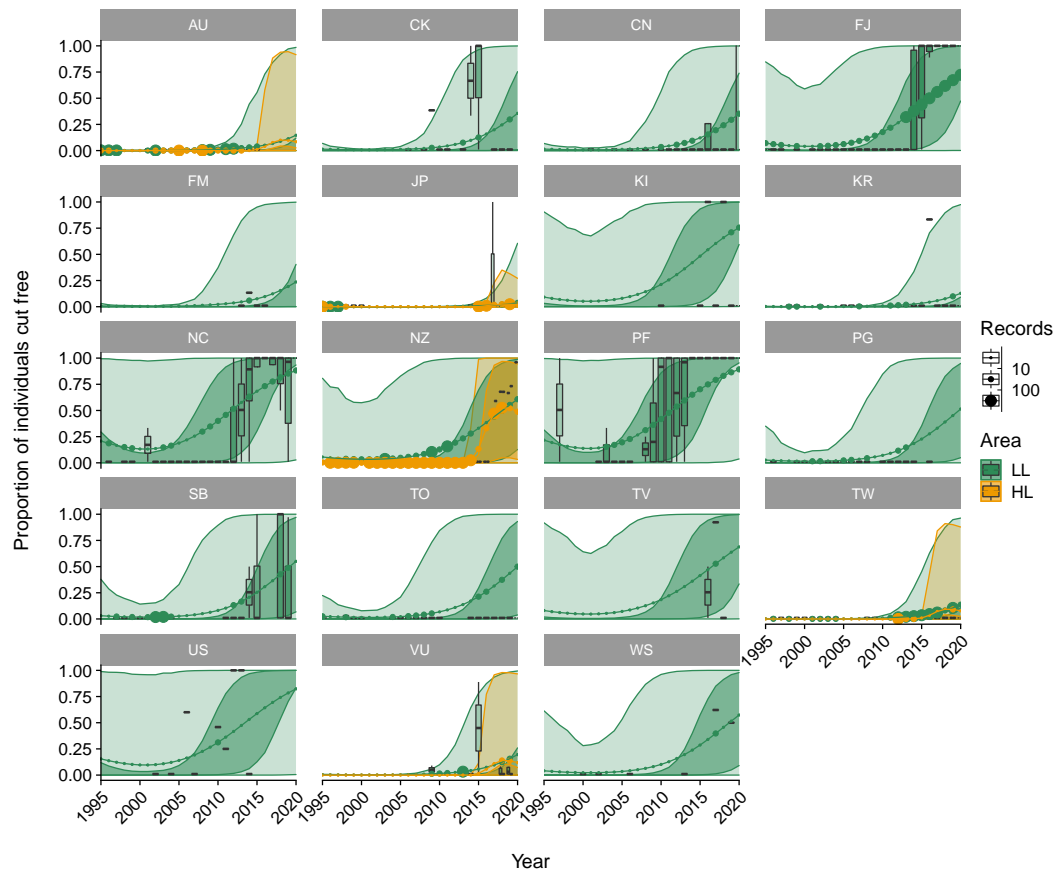


Figure 32: Estimated flag-year effects (expected proportion cut free) for flags in the observer dataset, split along low-latitude and high latitude ($>= 35$ degree South), showing the posterior median, 75% (dark shade) and 95% (light shade) posterior confidence. The distribution of input data is shown by underlying boxplots.

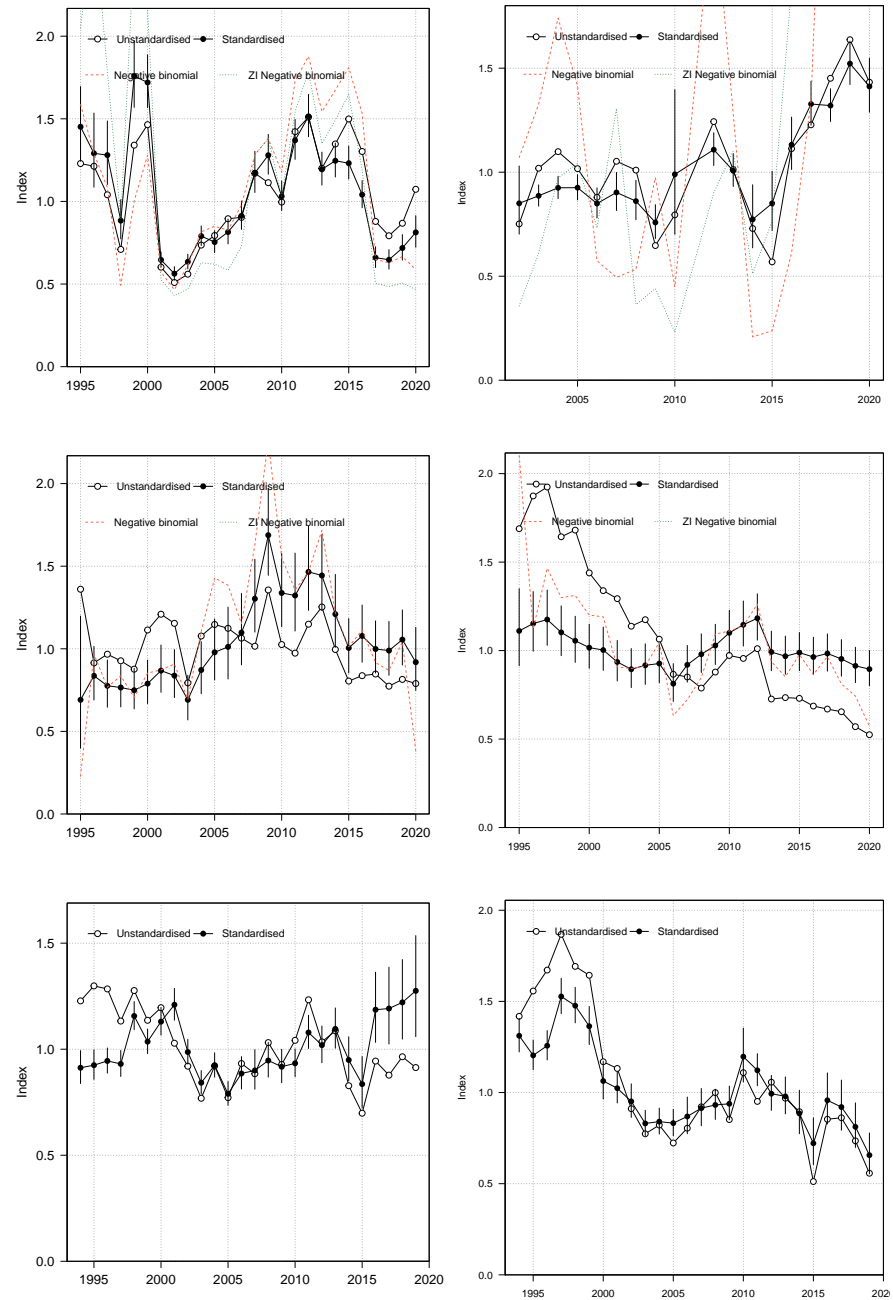


Figure 33: Standardised (closed black circles with standard error) and un-standardised (open circles) CPUE indices for New Zealand (top left), combined high-seas low-latitude fleet (top right), Australian high-latitude (middle-left) and low-latitude (middle-right), Japanese high-latitude (bottom left) and low-latitude (bottom right) fleets, for strata with positive catch. Where successful (i.e., converged), standardised trends from a negative-binomial and zero-inflated negative-binomial model run over the full dataset (including strata with zero values) are also shown for comparison.

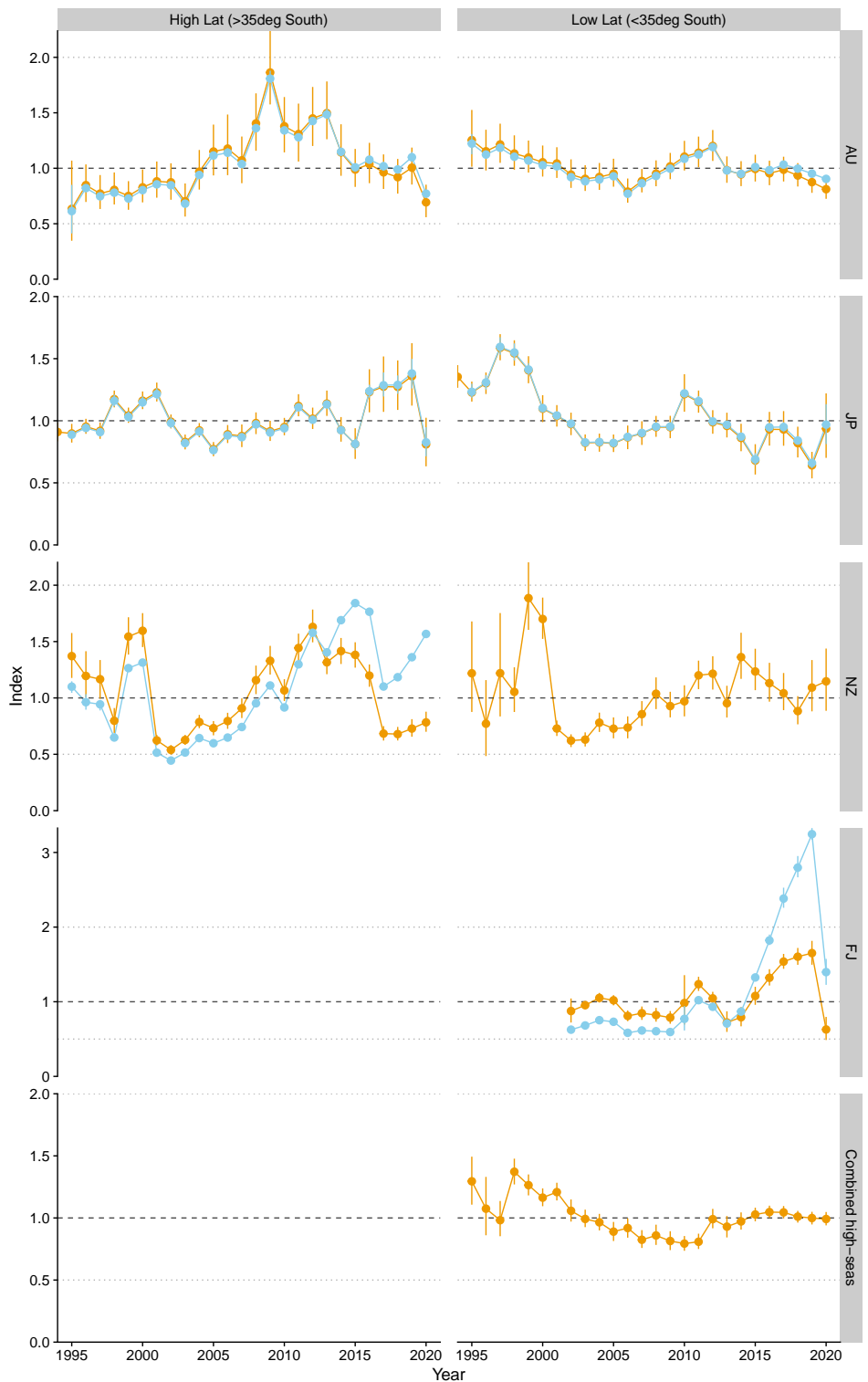


Figure 34: Standardised (circles with standard error) CPUE indices for CCMs included in the log-sheet CPUE analyses (orange), and adjusted by rates of sharks cut-free (blue dots).

APPENDIX A: Observer model diagnostics

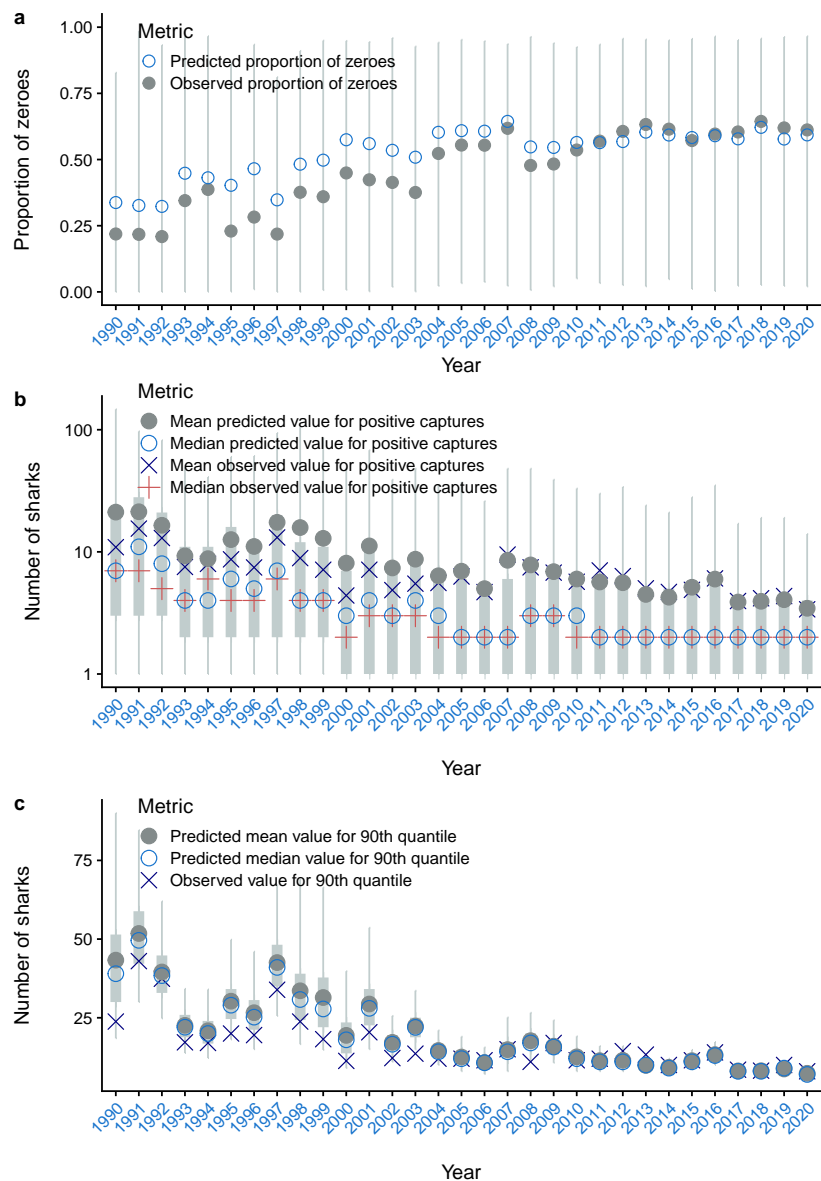


Figure A-1: Diagnostics by model year, with (a) observed and predicted proportion of zero captures, (b) observed and predicted positive captures and (c) dispersion statistics (90% percentile) of observed data and predictions.

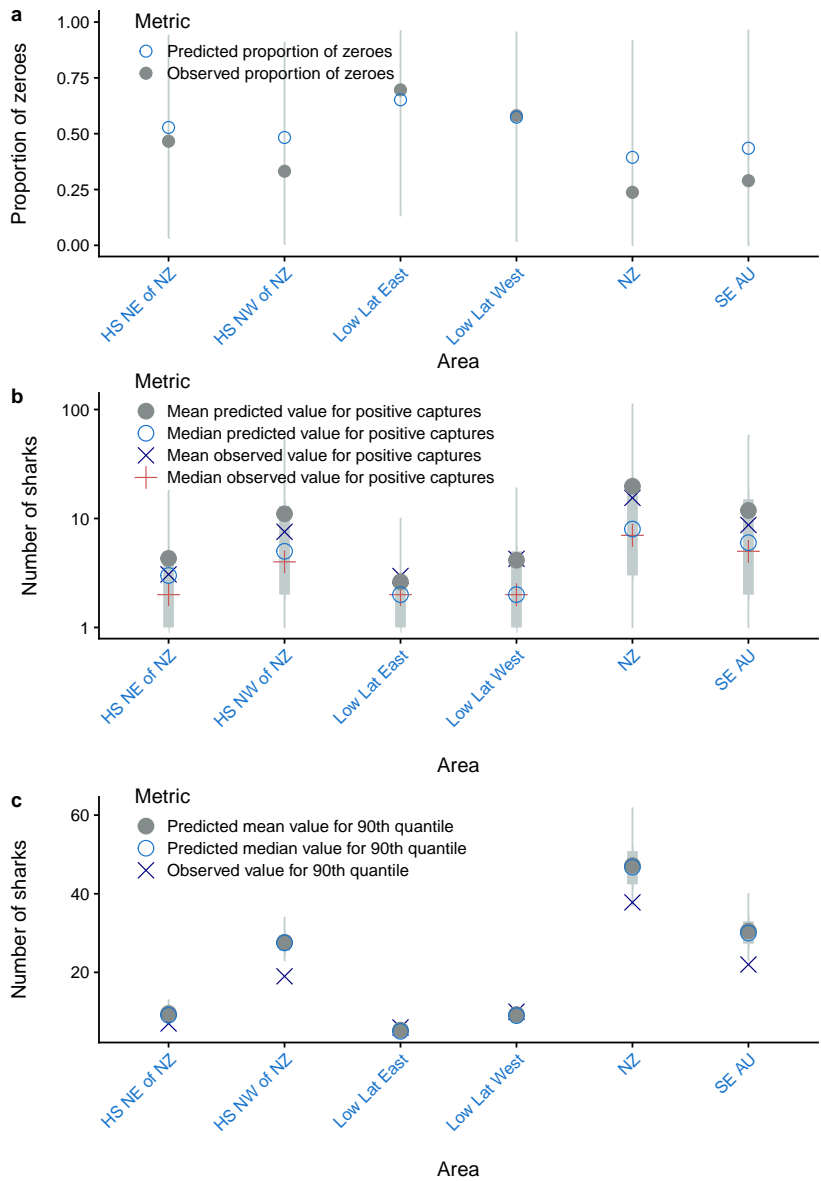


Figure A-2: Diagnostics by model area, with (a) observed and predicted proportion of zero captures, (b) observed and predicted positive captures and (c) dispersion statistics (90% percentile) of observed data and predictions.

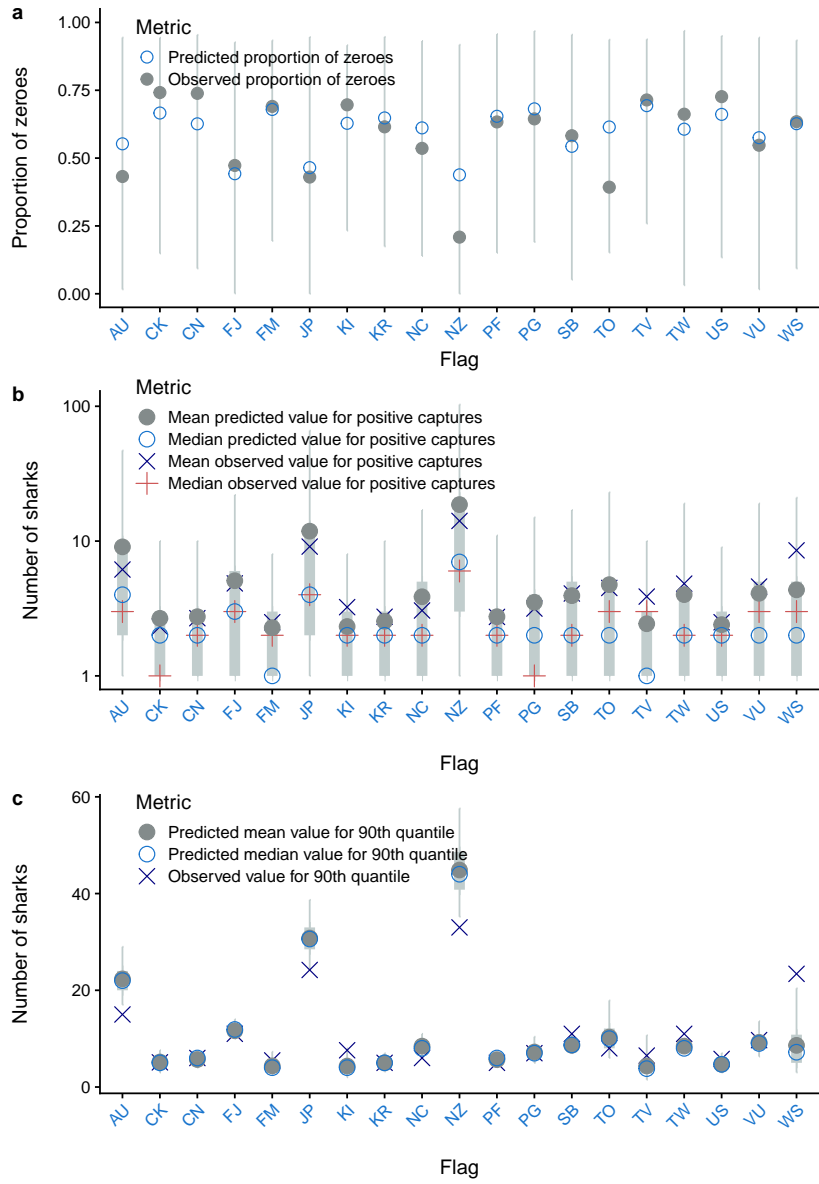


Figure A-3: Diagnostics by flag, with (a) observed and predicted proportion of zero captures, (b) observed and predicted positive captures and (c) dispersion statistics (90% percentile) of observed data and predictions.

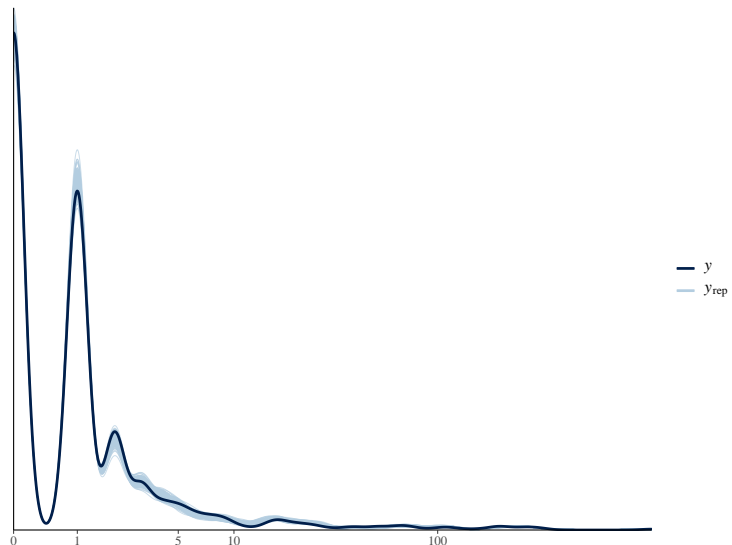


Figure A-4: Posterior predictive check for the release-condition model, showing predicted distribution of number of shortfin mako shark in the category dead or alive - dying (blue draws from the posterior distribution), as well as the observed data distribution (black line).

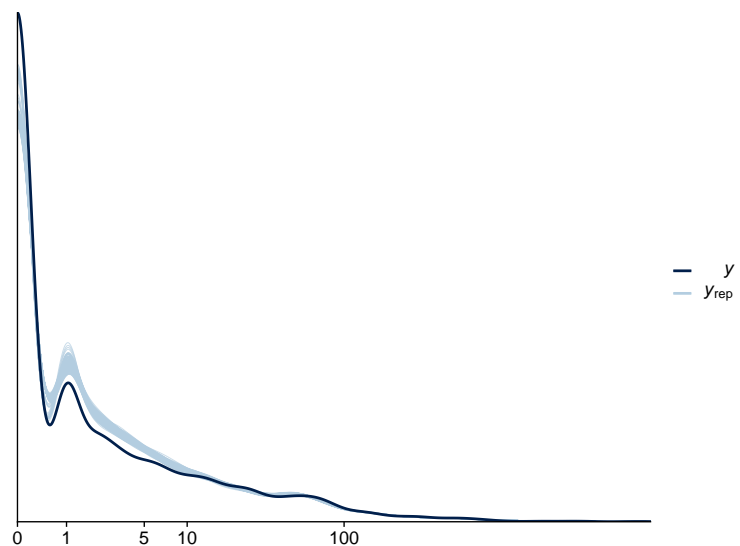


Figure A-5: Posterior predictive check for the fate (discard proportion) model, showing predicted distribution of number of shortfin mako shark in the category "discarded alive" (blue draws from the posterior distribution), as well as the observed data distribution (black line).

APPENDIX B: Logsheets CPUE standardisation diagnostics

B.1 New Zealand fleet high latitude CPUE

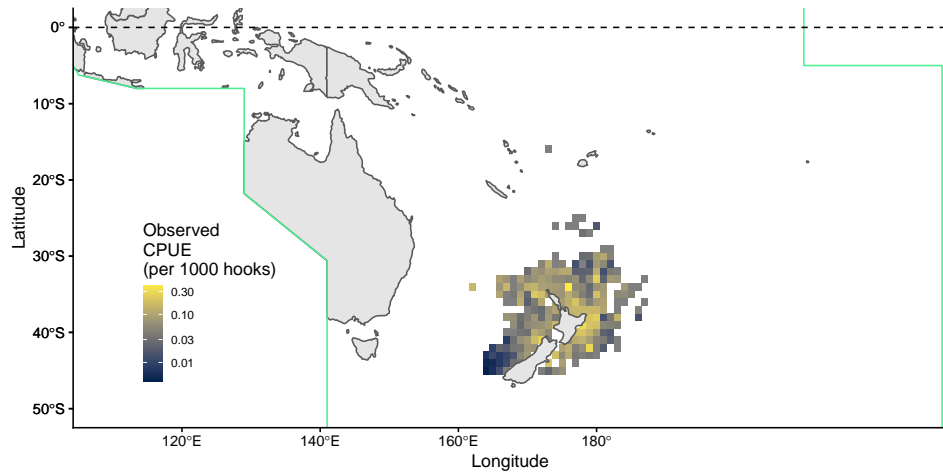


Figure B-6: Maps of average catch rates (CPUE; in number of shortfin mako shark per 100 hooks) for the New Zealand longline fleet.



Figure B-7: Maps of average catch rates (CPUE; in number of shortfin mako shark per 100 hooks) by year for the New Zealand longline fleet.

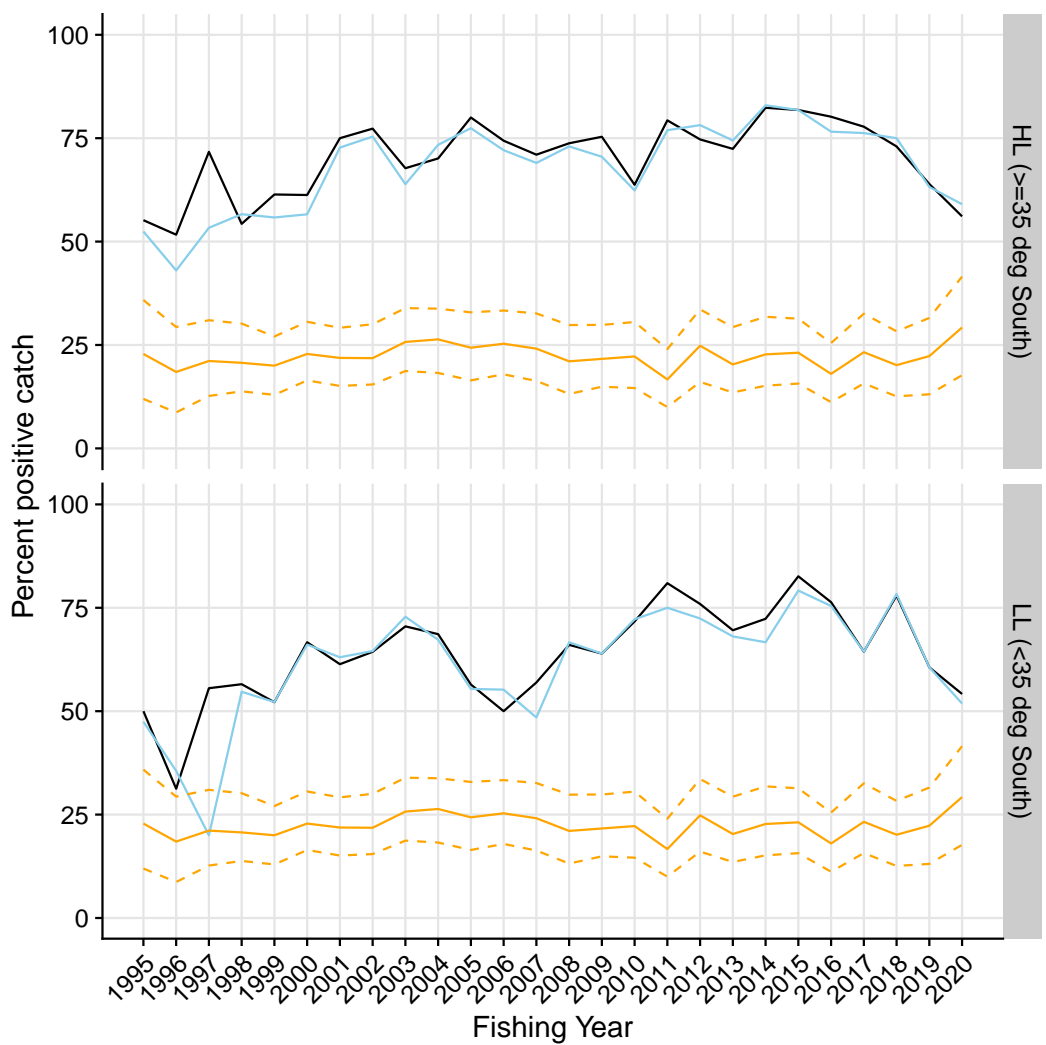


Figure B-8: Proportion of strata for the New Zealand fleet with positive catch by latitudinal stratum. Light blue are initial log-sheet records prior to filtering, the black line is the retained dataset after filtering for consistently reporting vessels. Where available, the corresponding values from observed strata is shown in orange.

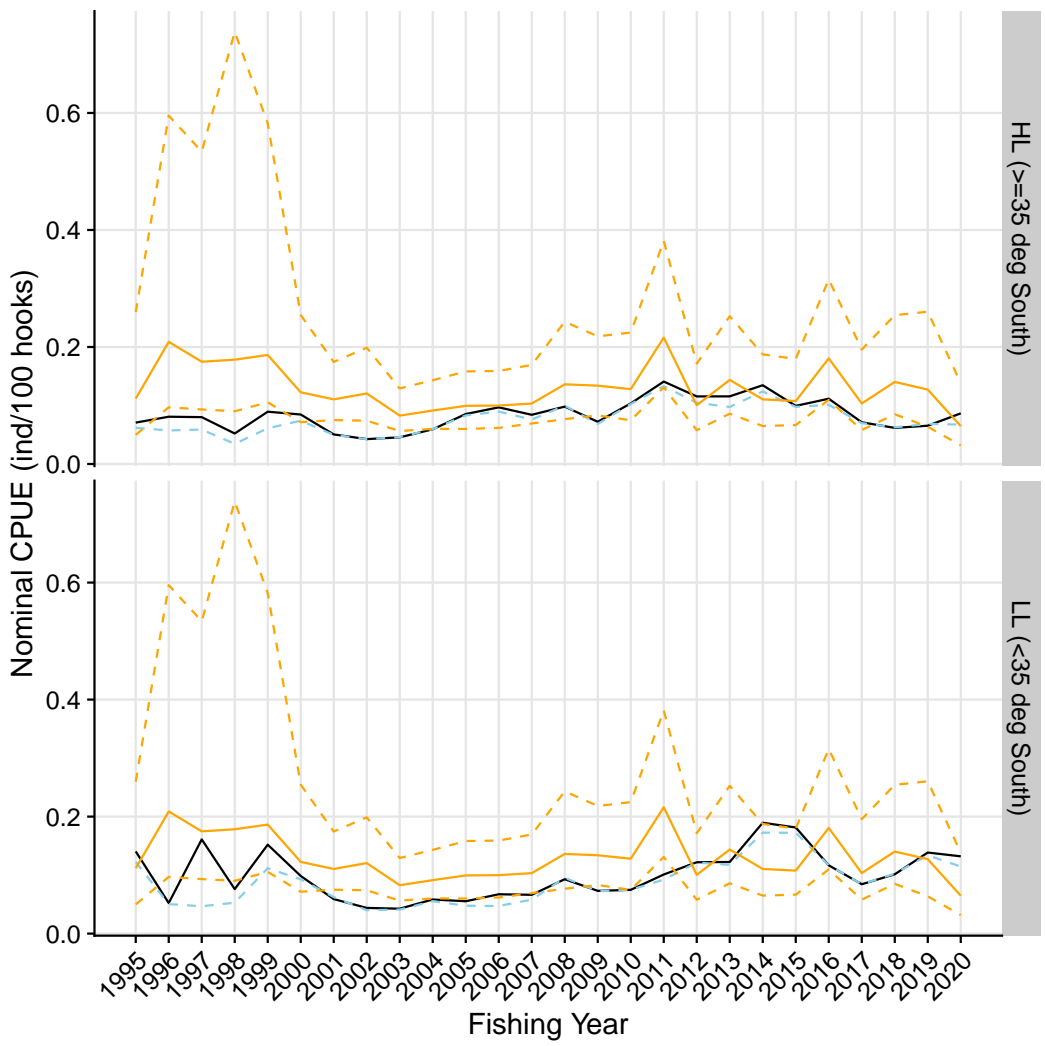


Figure B-9: Nominal CPUE (in number of blue shark per 100 hooks) strata of the New Zealand fleet with positive catch by latitudinal stratum. Light blue are initial log-sheet records prior to filtering, the black line is the retained dataset after filtering for consistently reporting vessels. Where available, the corresponding values from observed strata is shown in orange.

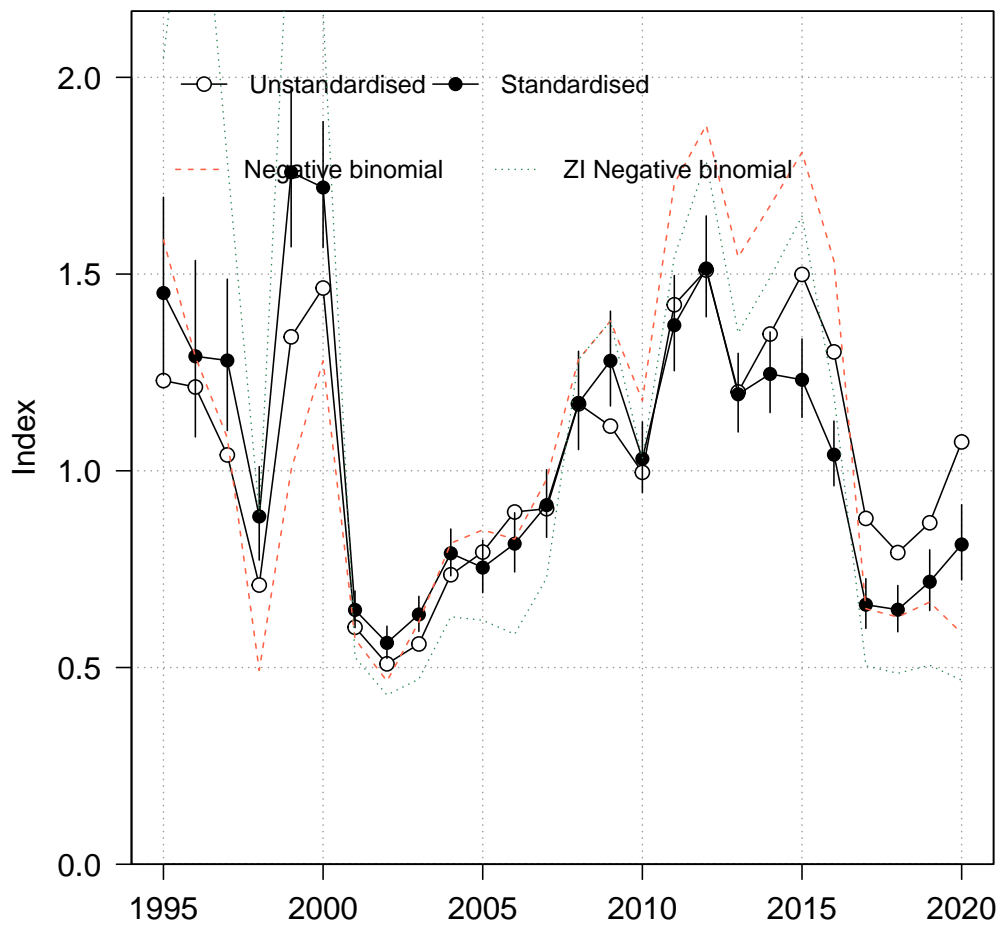


Figure B-10: Standardised (closed black circles with standard error) and unstandardised (open circles) CPUE indices for the New Zealand fleet strata with positive catch. Where successful (i.e., converged), standardised trends from a negative - binomial and zero - inflated negative binomial model run over the full dataset (including strata with zero values) are also shown for comparison.

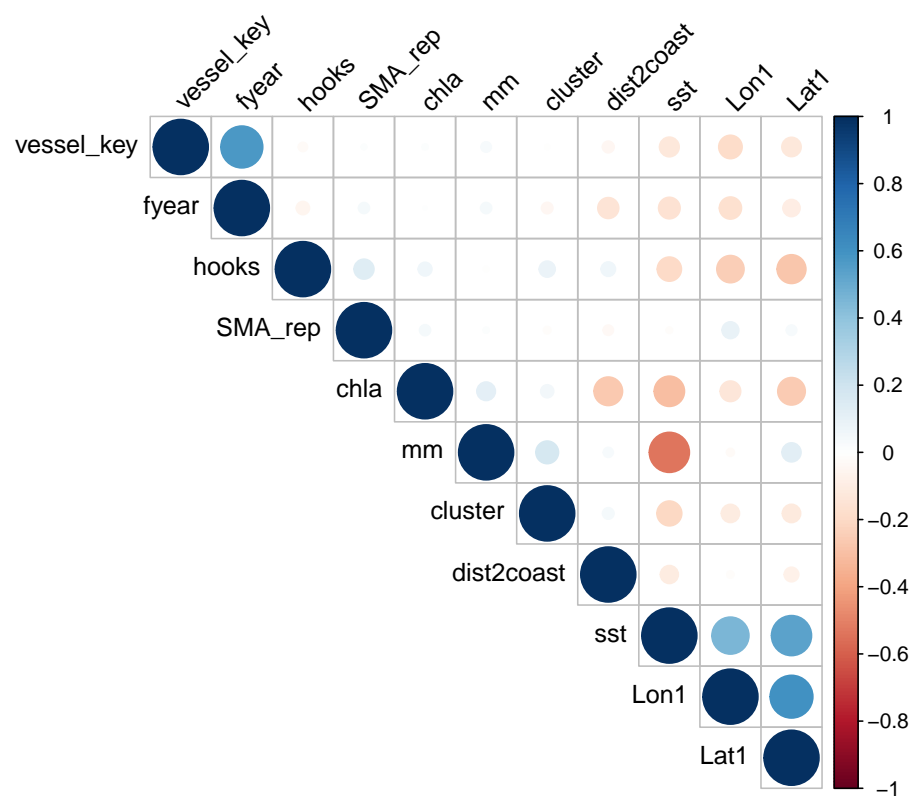


Figure B-11: Correlations amongst potential covariates for CPUE standardisation in the New Zealand fleet. Where necessary, variables were removed to reduce redundancy in the models.

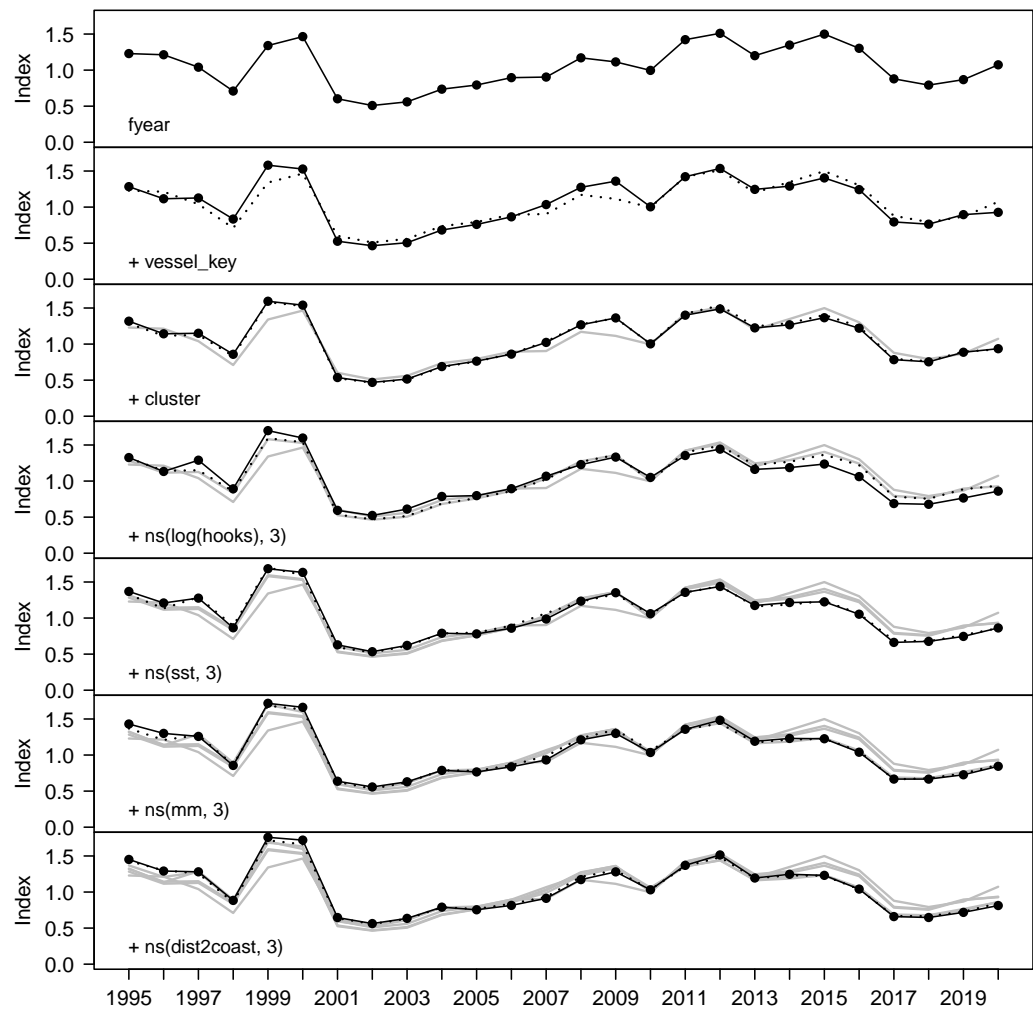


Figure B-12: Step plot for the New Zealand fleet CPUE, showing sequential standardising effects of variables included in the standardisation model.

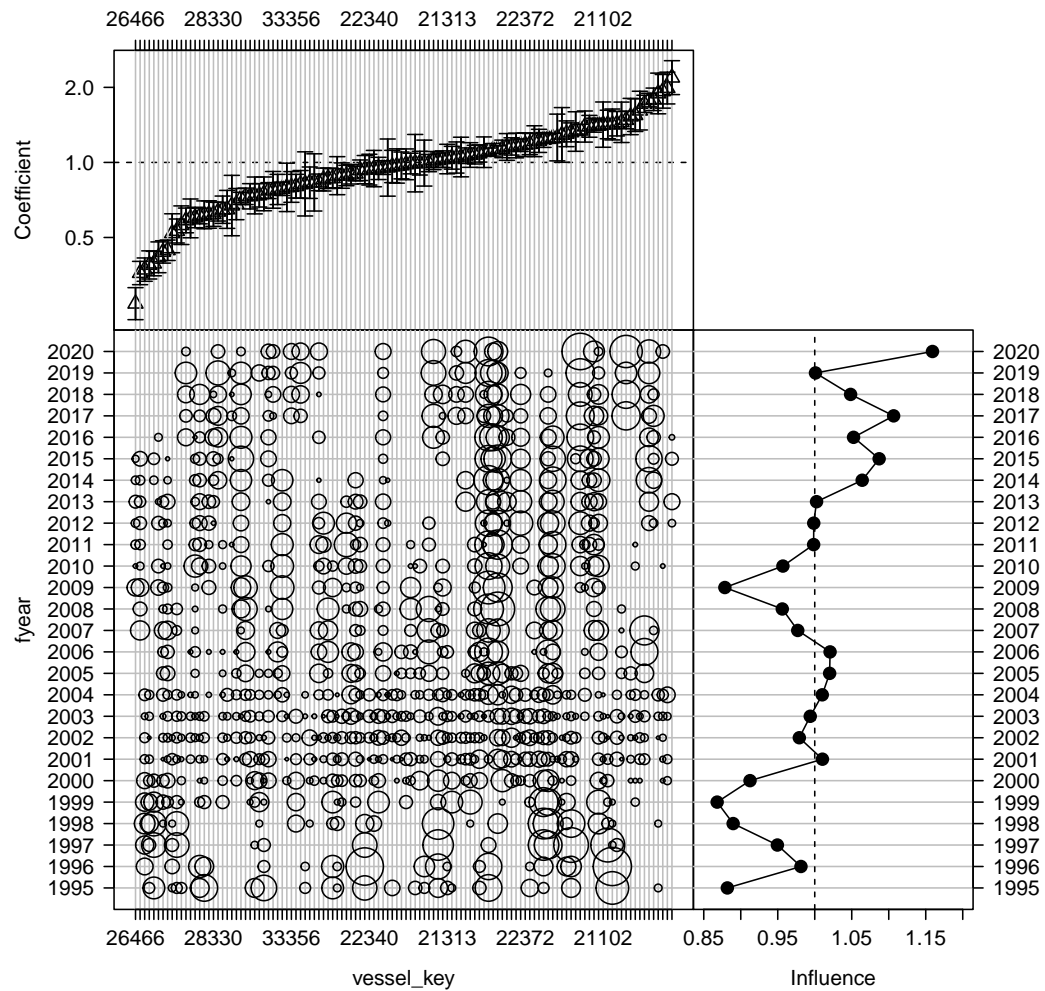


Figure B-13: Influence of fleet composition (vessel keys) for the New Zealand fleet (bubble plot; bubbles scales by effort) on CPUE; influence (right) shows the standardising effect (a positive effect reduces the standardised CPUE by the equivalent amount). Estimated coefficients are given in the top panel.

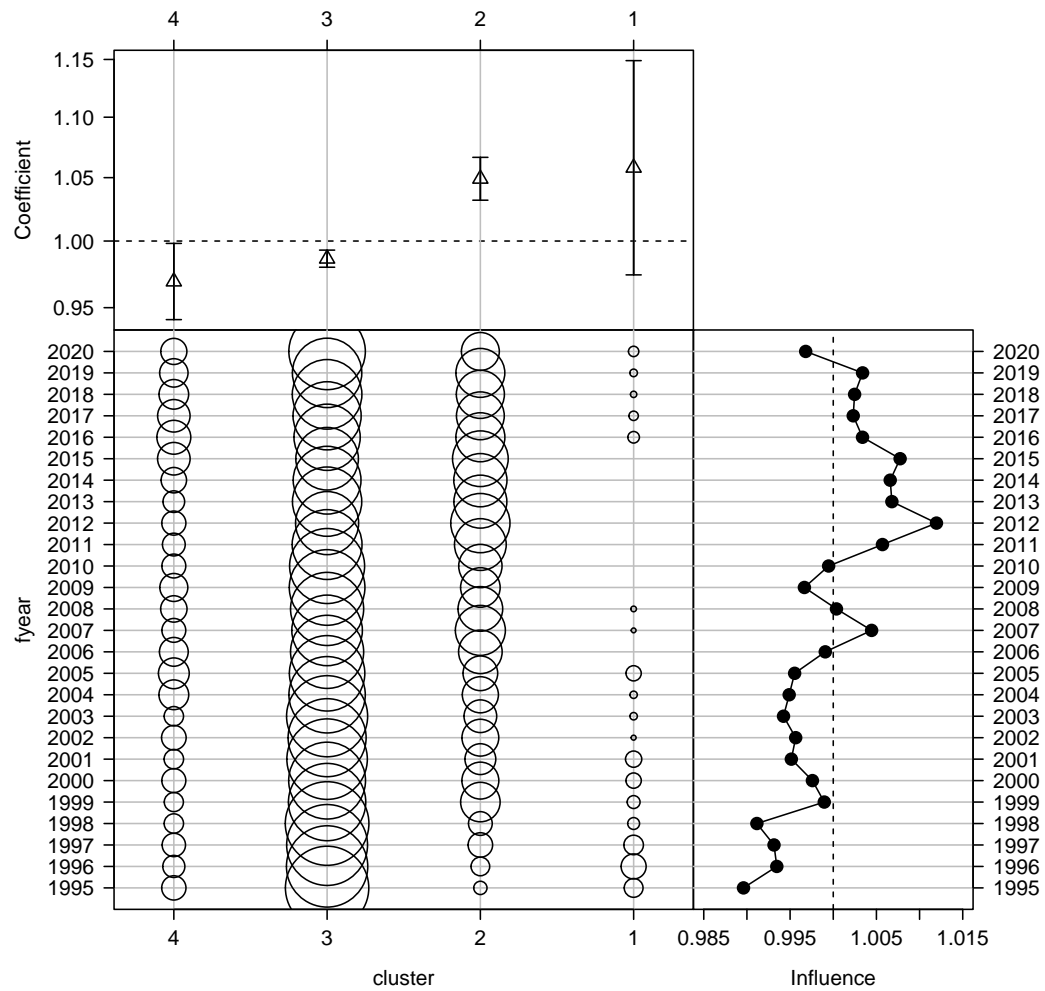


Figure B-14: Influence of targeting cluster for the New Zealand fleet (bubble plot; bubbles scales by effort) on CPUE; influence (right hand plot) shows the standardising effect (a positive effect reduces the standardised CPUE by the equivalent amount). Estimated coefficients are given in the top panel.

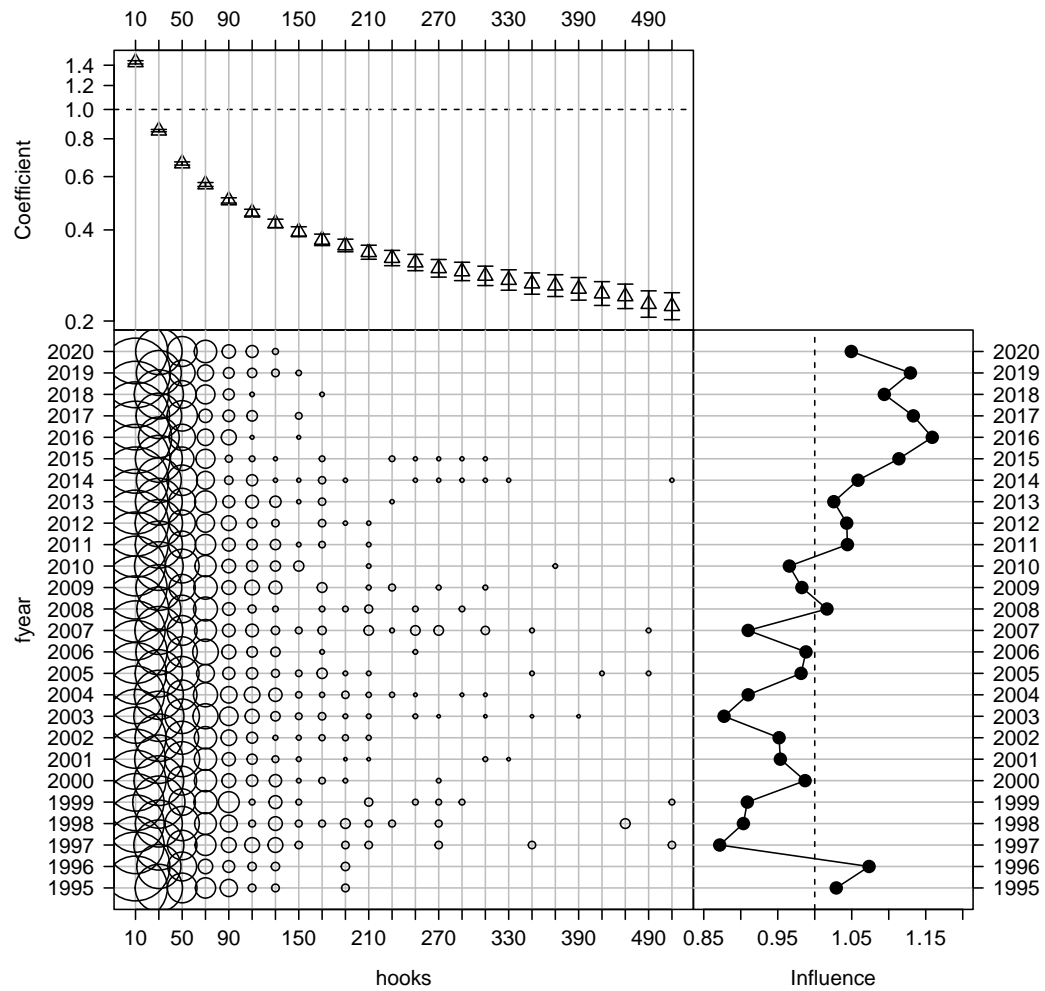


Figure B-15: Influence of number of hooks set per stratum for the New Zealand fleet (bubble plot; bubbles scales by effort) on CPUE; influence (right hand plot) shows the standardising effect (a positive effect reduces the standardised CPUE by the equivalent amount). Estimated coefficients are given in the top panel.

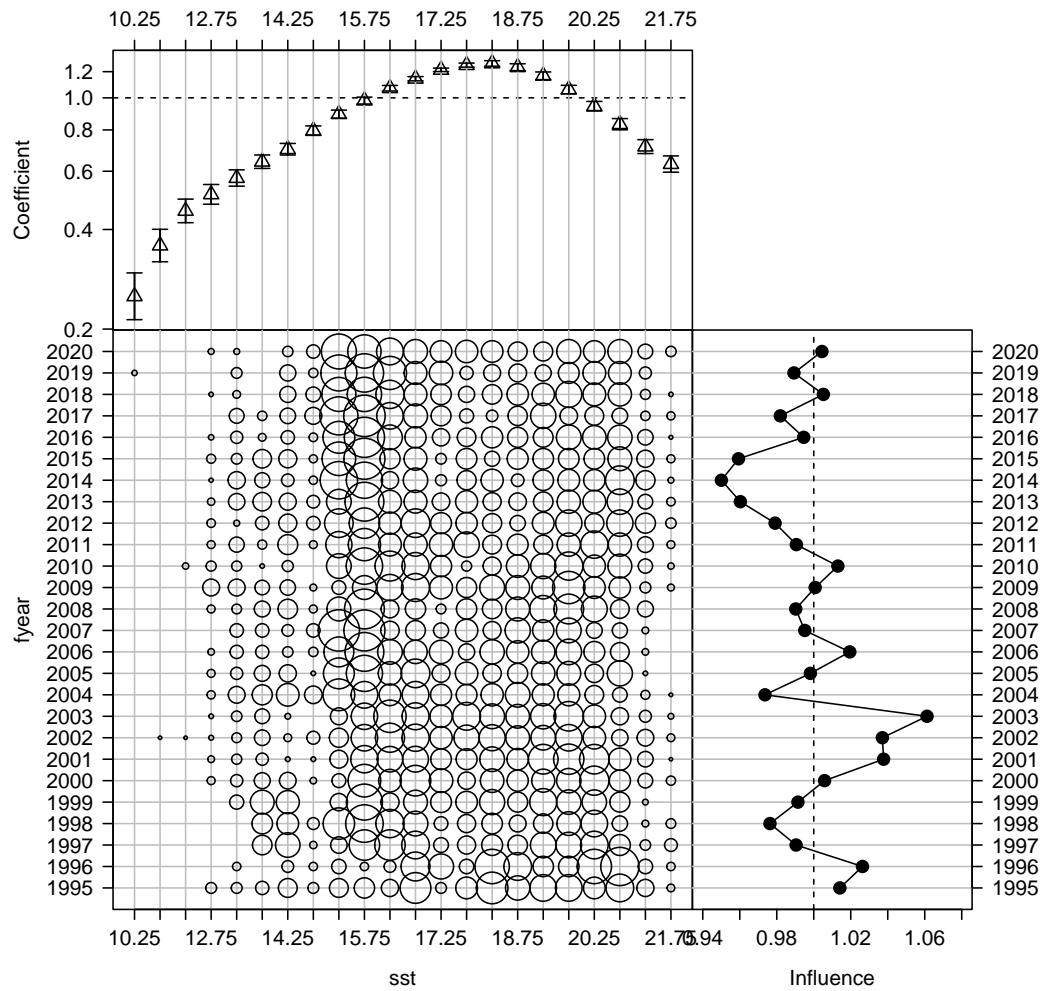


Figure B-16: Influence of sea surface temperature (SST, in degrees Celsius) for the New Zealand fleet (bubble plot; bubbles scales by effort) on CPUE; influence (right hand plot) shows the standardising effect (a positive effect reduces the standardised CPUE by the equivalent amount). Estimated coefficients are given in the top panel.

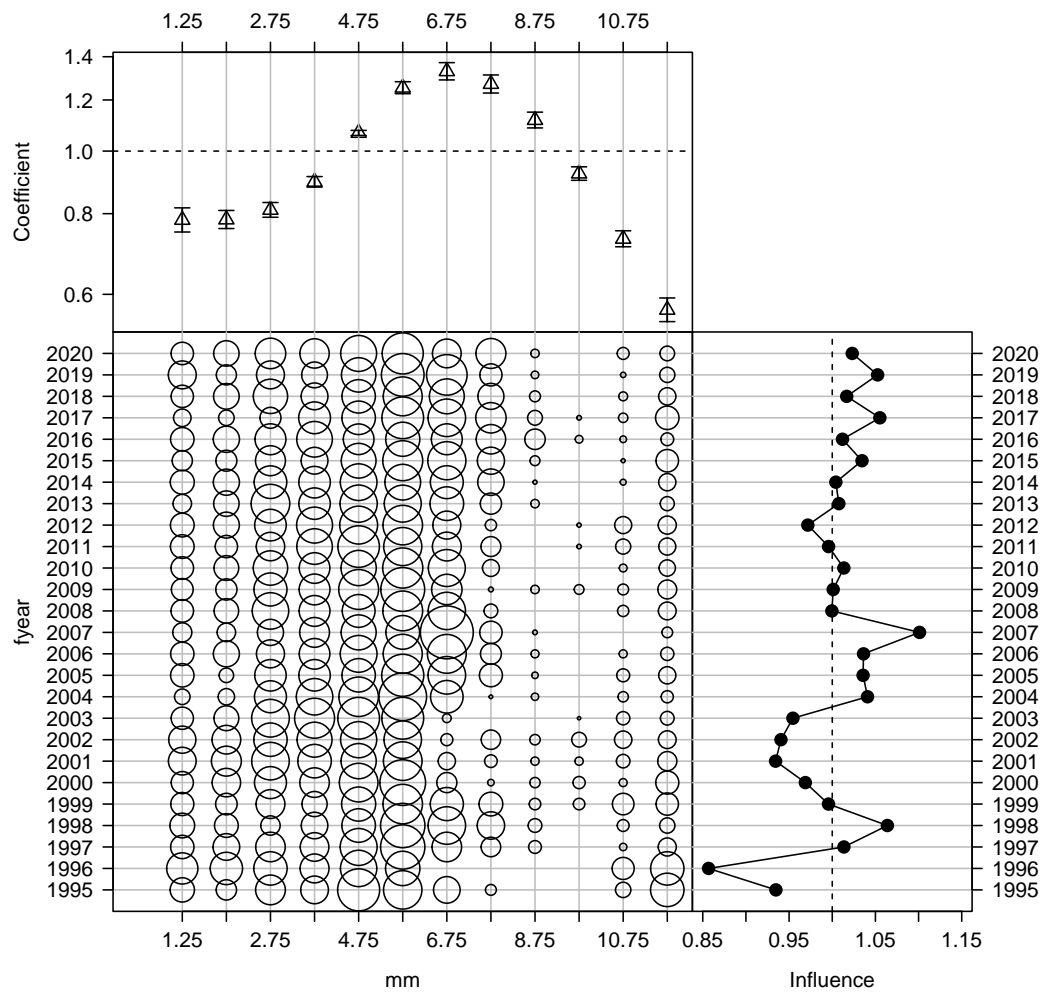


Figure B-17: Influence of month for the New Zealand fleet (bubble plot; bubbles scales by effort) on CPUE; influence (right hand plot) shows the standardising effect (a positive effect reduces the standardised CPUE by the equivalent amount). Estimated coefficients are given in the top panel.

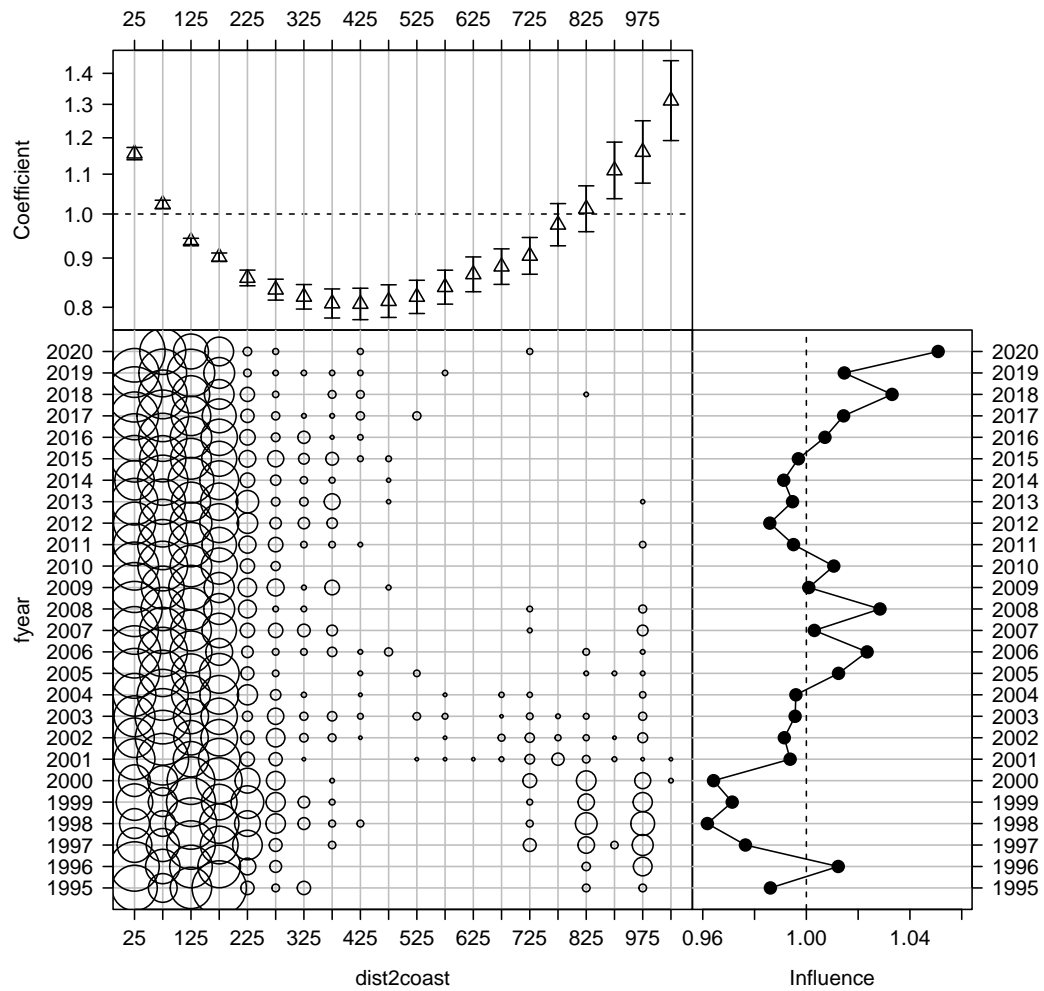


Figure B-18: Influence of distance to coast composition for the New Zealand fleet (bubble plot; bubbles scales by effort) on CPUE; influence (right hand plot) shows the standardising effect (a positive effect reduces the standardised CPUE by the equivalent amount). Estimated coefficients are given in the top panel.

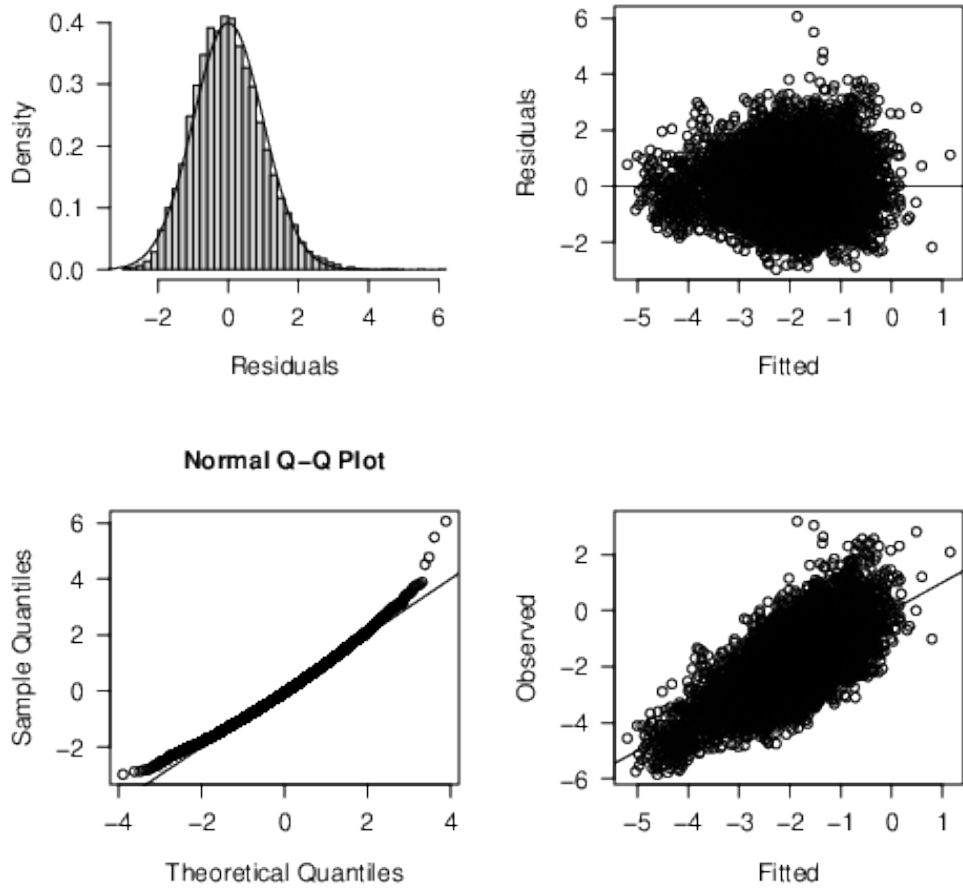


Figure B-19: Diagnostics for the log-normal CPUE standardisation model for the New Zealand fleet strata with positive catch.

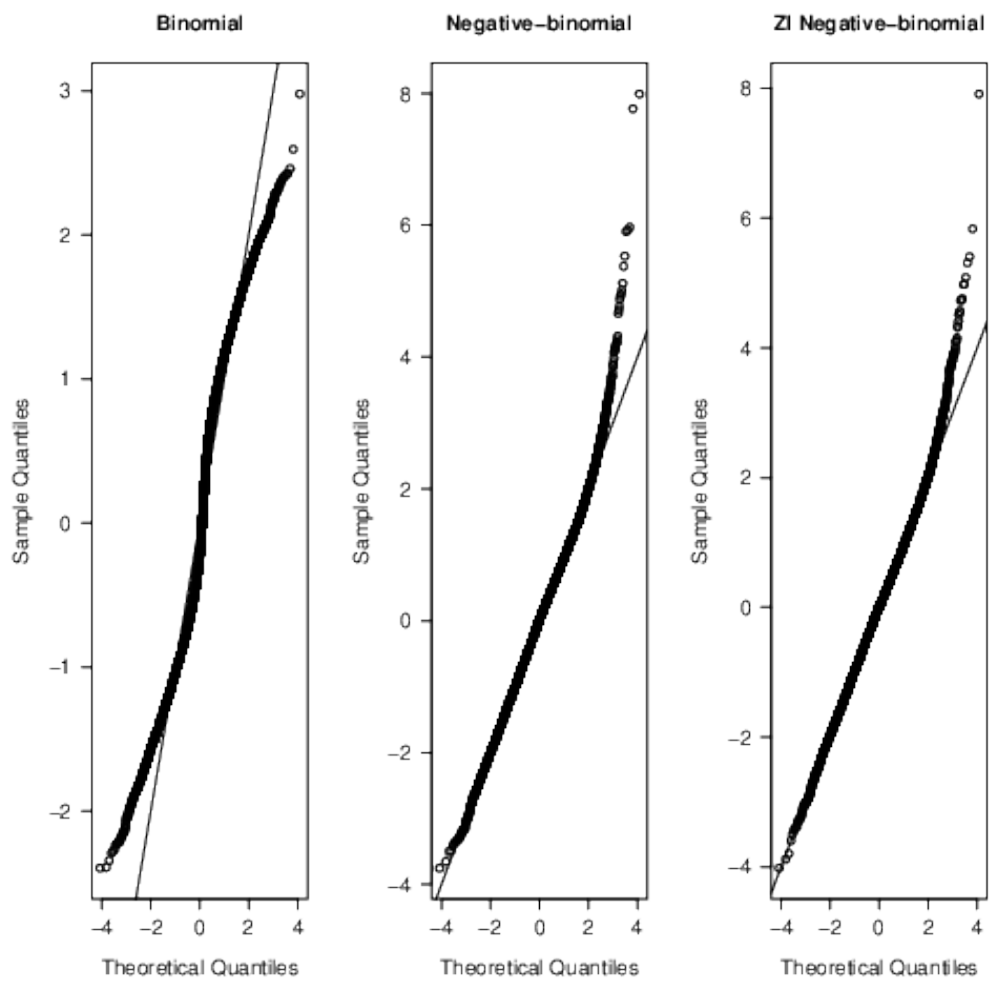


Figure B-20: Quantile residual diagnostics for the binomial component, as well as alternative CPUE standardisation models for the New Zealand fleet strata with positive catch.

B.2 Japan low latitude CPUE

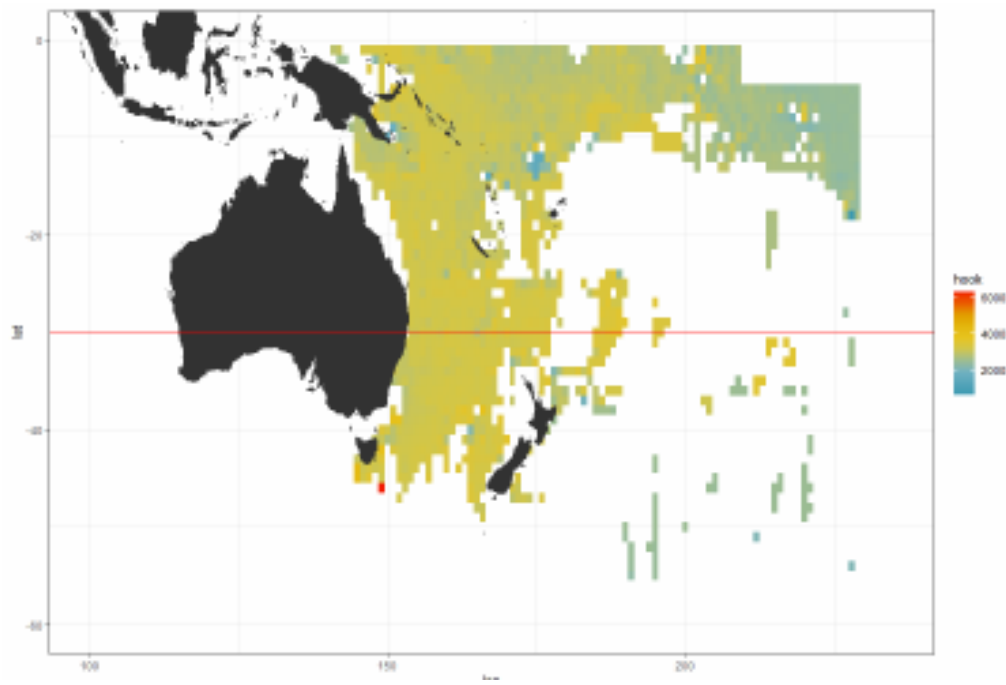


Figure B-21: Operational area of Japanese longline fleets in the southern WCPO from 1994 to 2020 showing the mean number of hooks for 1994-2019.

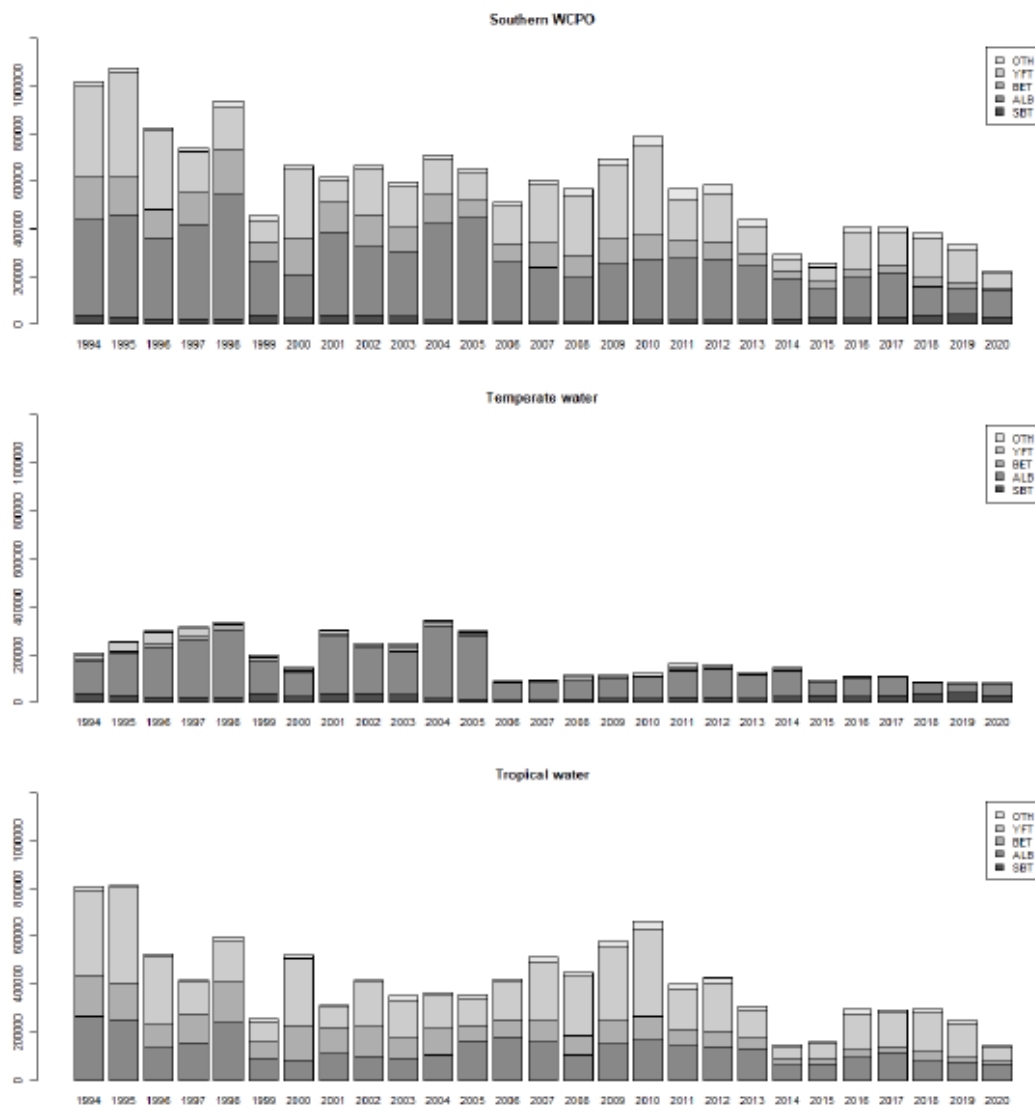


Figure B-22: Annual catch number of target species (OTH: Other species, YFT: Yellowfin tuna, BET: Bigeye tuna, ALB: Albacore, SBT: Southern bluefin tuna) for the Japanese longline fleets in southern WCPO, temperate waters ($30\text{--}60^{\circ}\text{S}$), and tropical waters ($0\text{--}30^{\circ}\text{S}$).

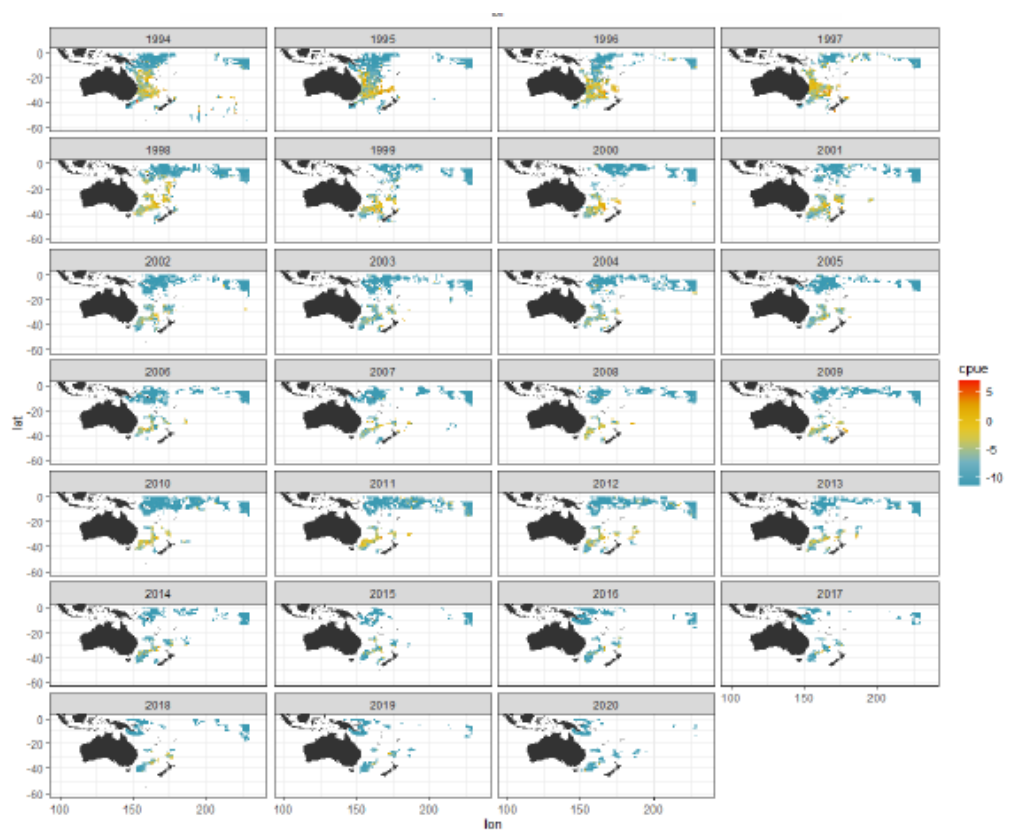


Figure B-23: Operational area of Japanese longline fleets in the southern WCPO from 1994 to 2019 showing the annual changes in the log transformed nominal CPUE of shortfin mako shark from 1994 to 2020.

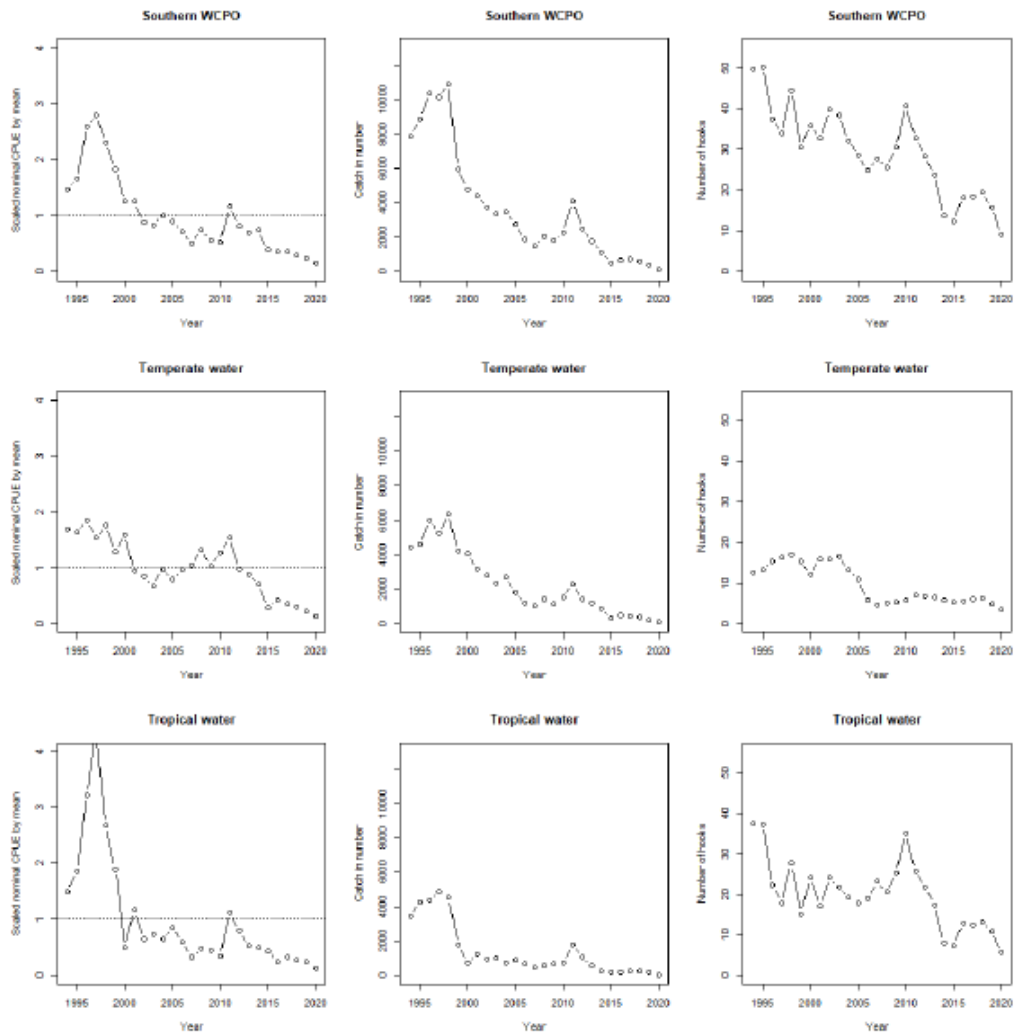


Figure B-24: Annual nominal CPUE of shortfin mako shark, annual catch in number of shortfin mako shark, annual number of hooks in three areas for the Japanese longline fleets: southern WCPO ($0\text{--}60^{\circ}\text{S}$), temperate waters ($30\text{--}60^{\circ}\text{S}$), and tropics ($0\text{--}30^{\circ}\text{S}$).

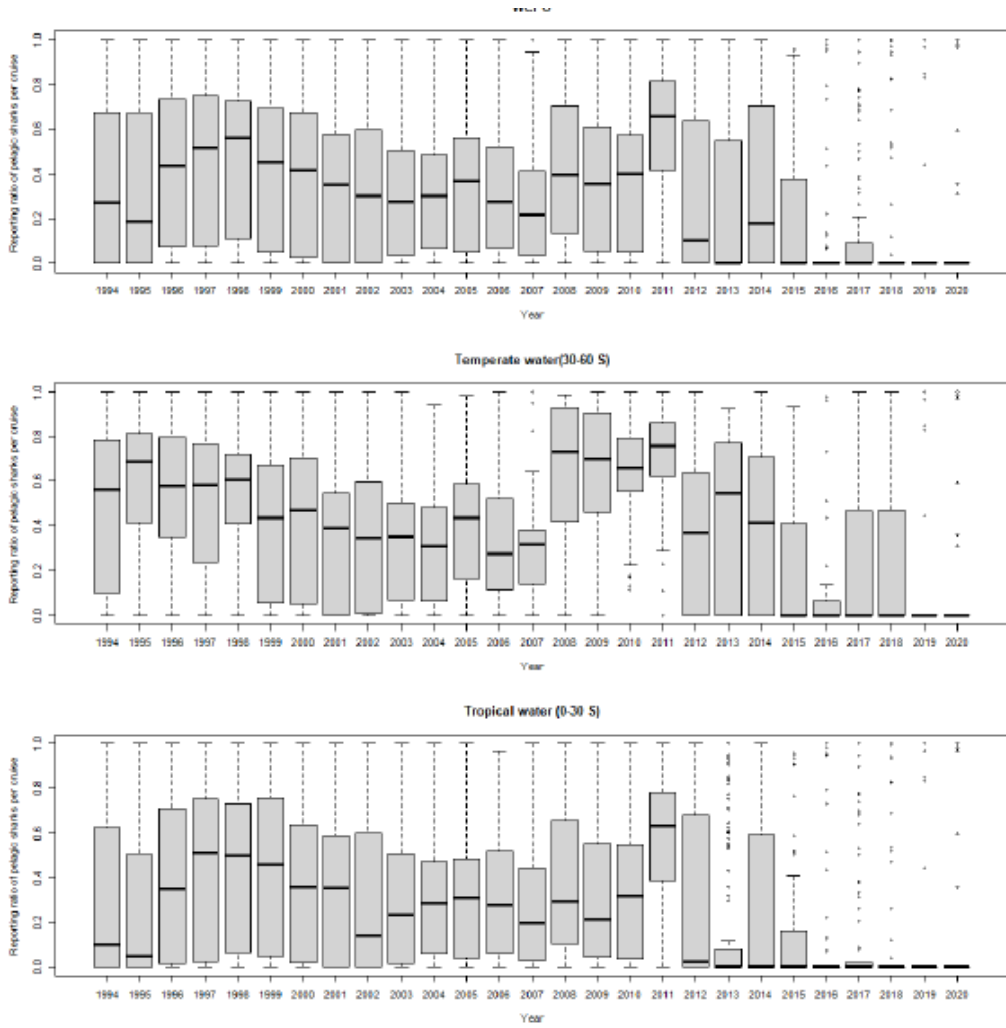


Figure B-25: Annual reporting ratio (RR) of pelagic sharks (shortfin mako shark, mako sharks, porbeagle, silky sharks, oceanic whitetip sharks, thresher sharks, other sharks) in southern WCPO for the Japanese longline fleets. RR was calculated using the number of sets with positive catches of pelagic sharks per total number of sets in a cruise of each vessel. Upper panel is RR in whole area in southern WCPO. Middle panel is RR in the temperate waters. Lower panel is RR in the tropics.

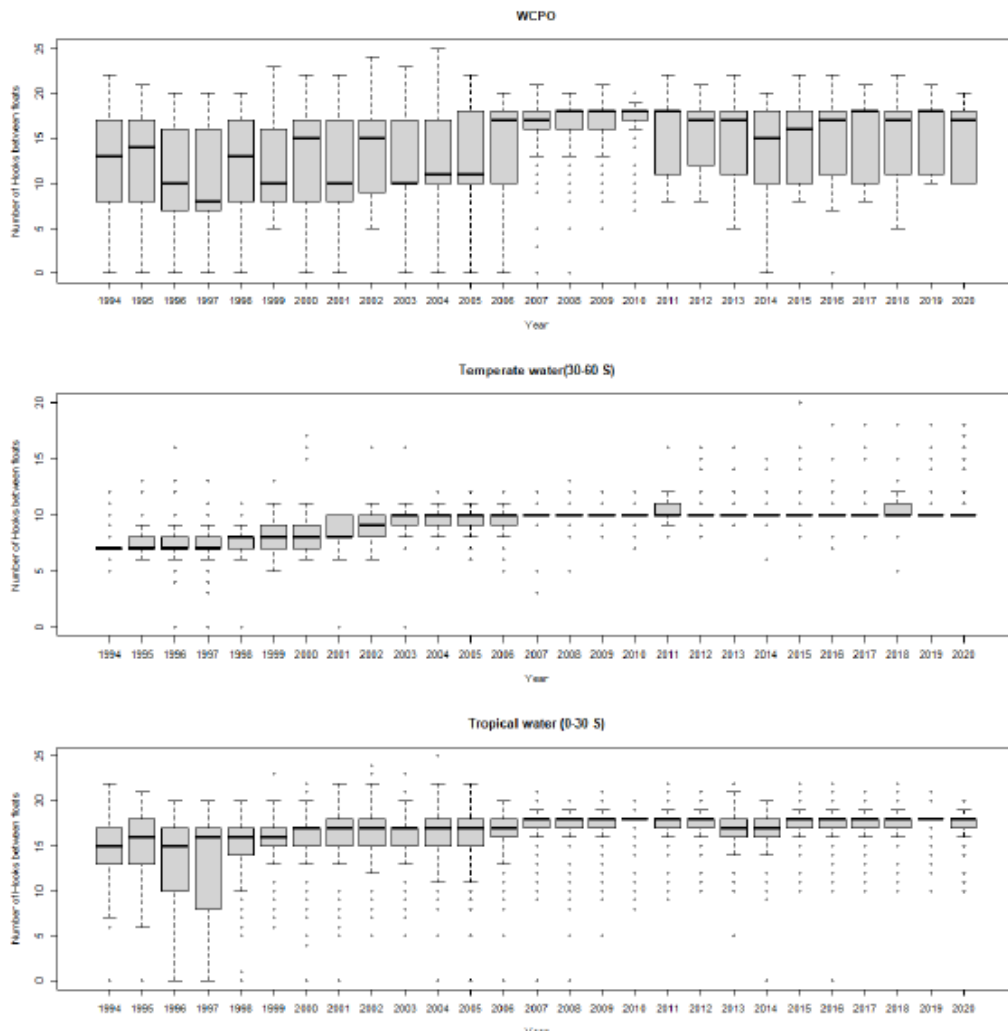


Figure B-26: Annual number of hooks between floats for Japanese fleets in southern WCPO, temperate waters ($30-60^{\circ}\text{S}$), and tropics ($0-30^{\circ}\text{S}$).

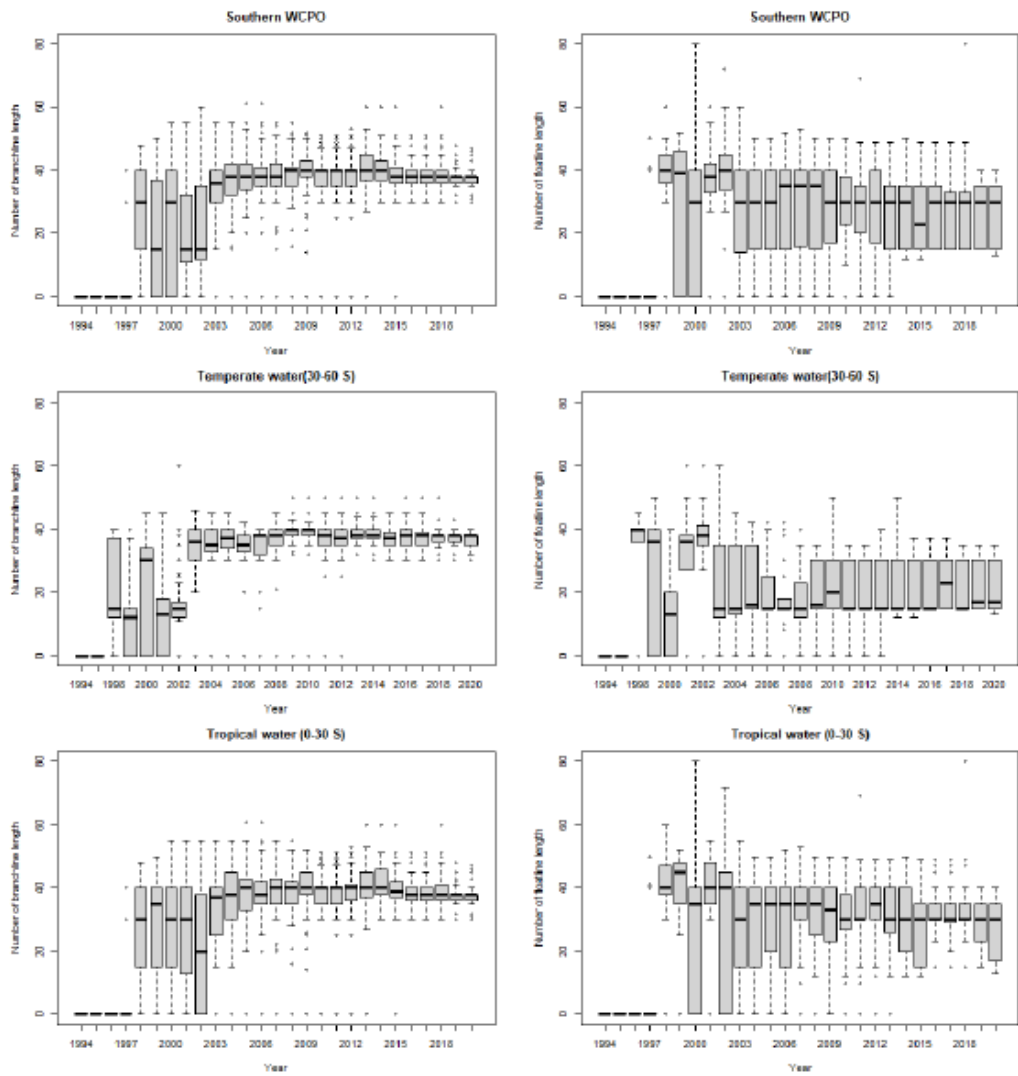


Figure B-27: Annual number of branch-line length (meters) and float-line length (meters) in southern WCPO, temperate waters ($30-60^{\circ}\text{S}$), and tropics ($0-30^{\circ}\text{S}$) for the Japanese longline fleets.

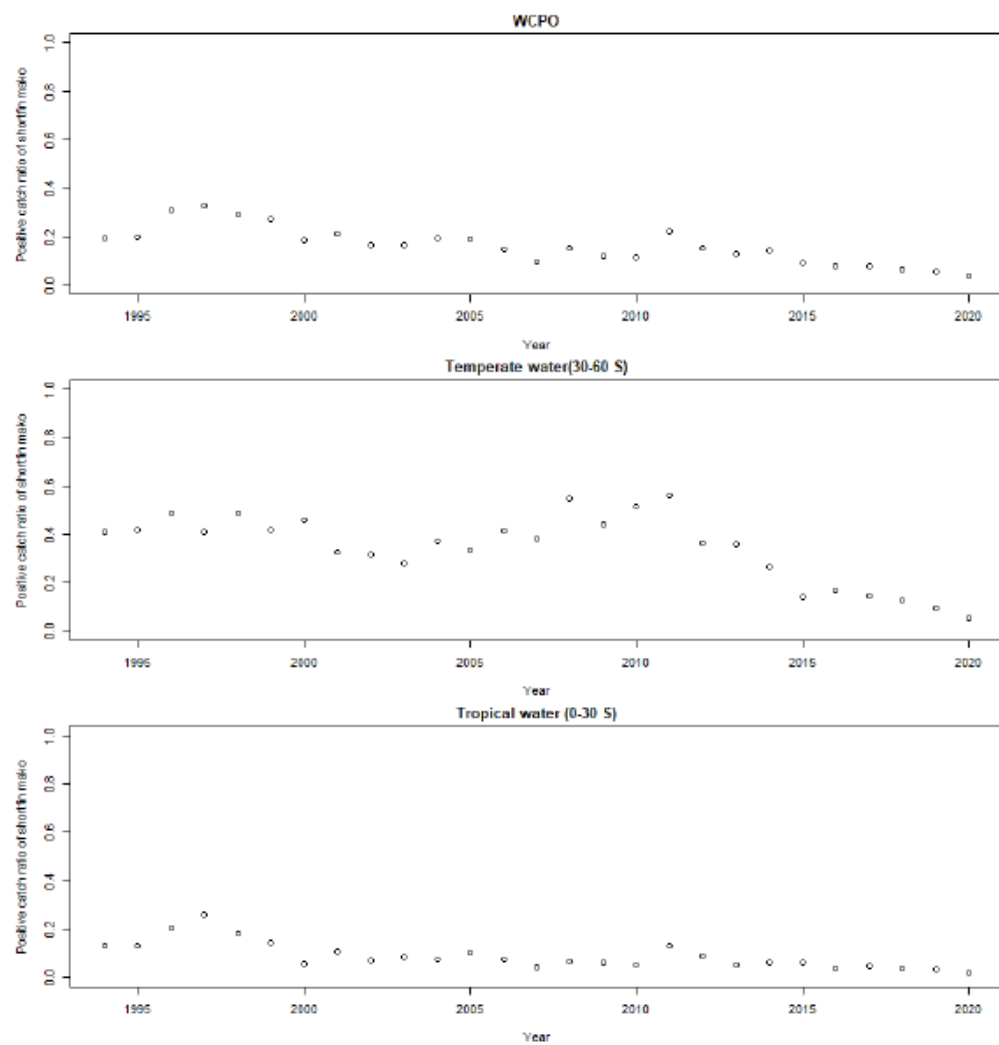


Figure B-28: Annual positive catch ratio of shortfin mako sharks (number of sets with positive catch of shortfin mako shark to total number of sets) for the Japanese longline fleets in southern WCPO, temperate waters ($30-60^{\circ}\text{S}$), and tropics ($0-30^{\circ}\text{S}$).

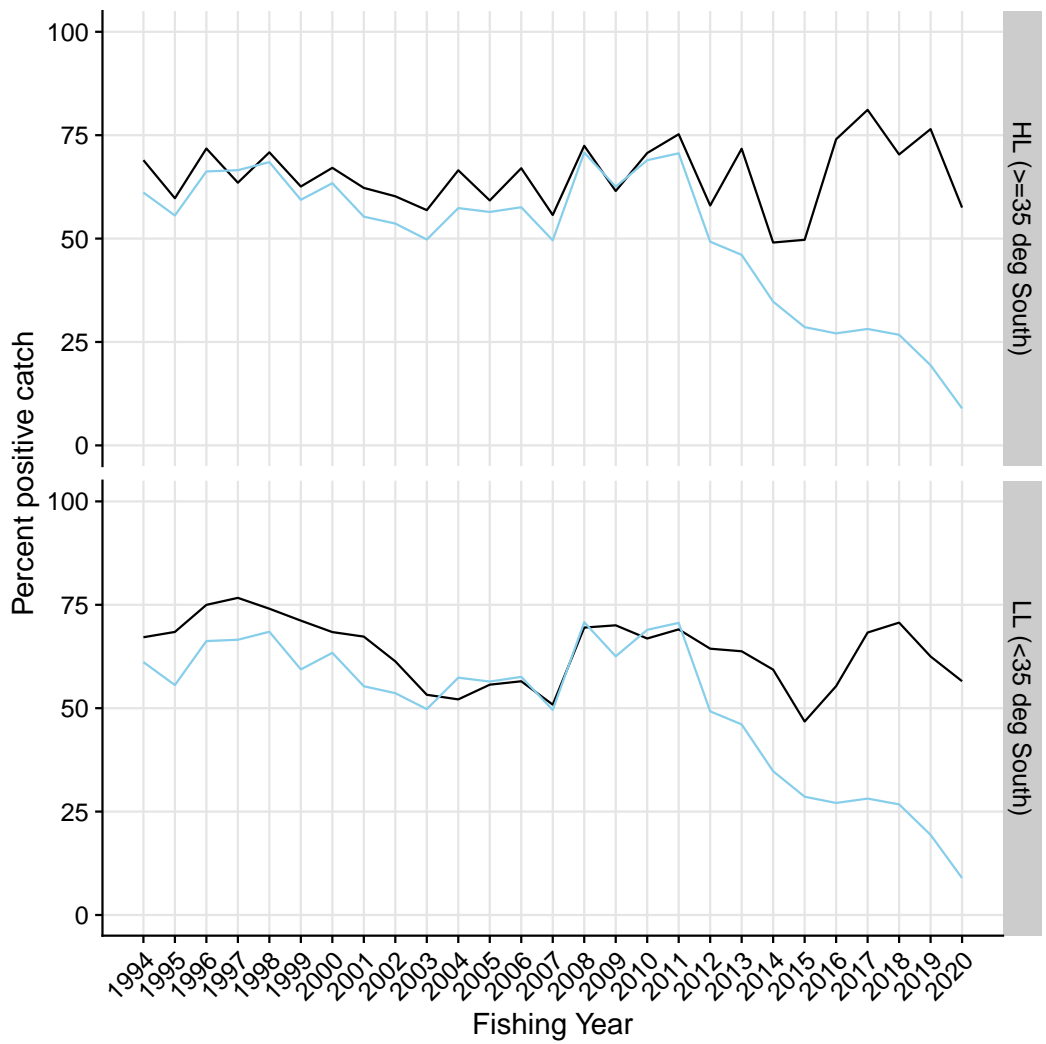


Figure B-29: Proportion of strata for the Japanese fleet with positive catch by latitudinal stratum. Light blue are initial log-sheet records prior to filtering, the black line is the retained dataset after filtering for consistently reporting vessels. Where available, the corresponding values from observed strata is shown in orange.

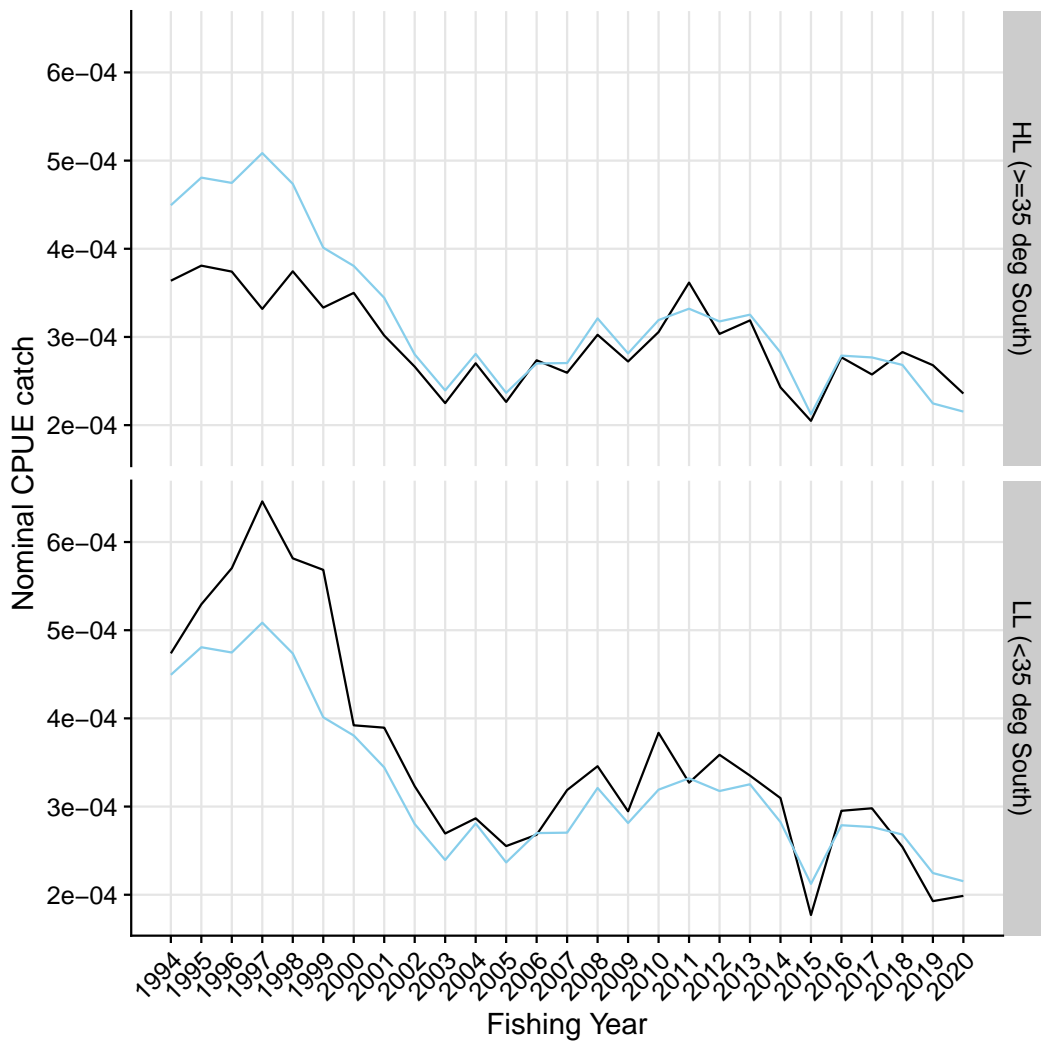


Figure B-30: Nominal CPUE (in number of blue shark per 100 hooks) strata of the Japanese fleet with positive catch by latitudinal stratum. Light blue are initial log-sheet records prior to filtering, the black line is the retained dataset after filtering for consistently reporting vessels. Where available, the corresponding values from observed strata is shown in orange.

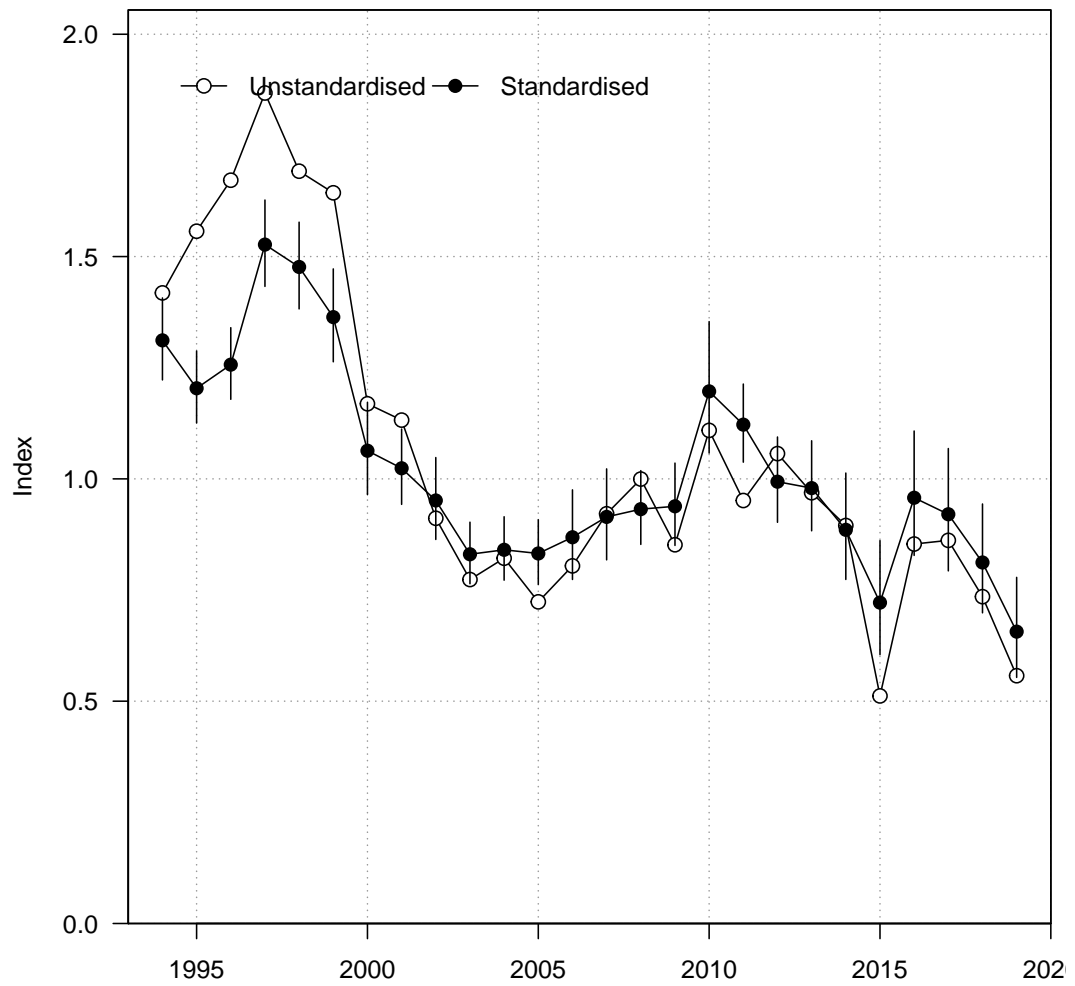


Figure B-31: Standardised (closed black circles with standard error) and unstandardised (open circles) CPUE indices for the Japanese fleet strata with positive catch. Where successful (i.e., converged), standardised trends from a negative - binomial and zero - inflated negative binomial model run over the full dataset (including strata with zero values) are also shown for comparison.

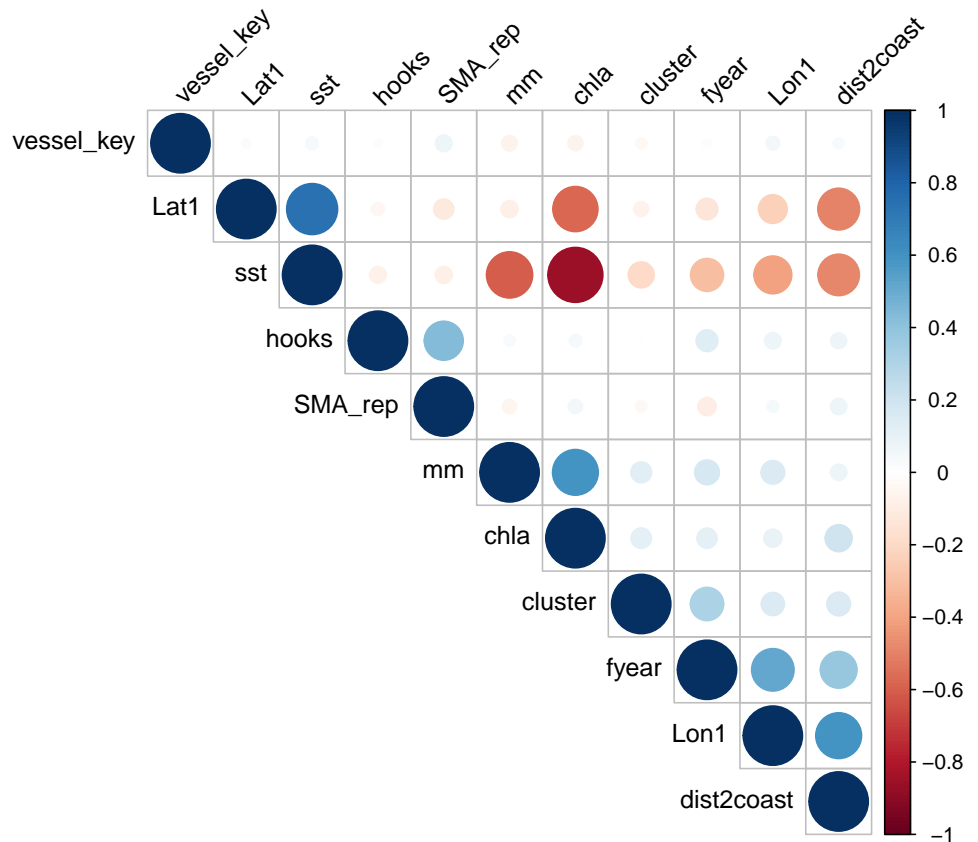


Figure B-32: Correlations amongst potential covariates for CPUE standardisation in the Japanese fleet. Where necessary, variables were removed to reduce redundancy in the models.

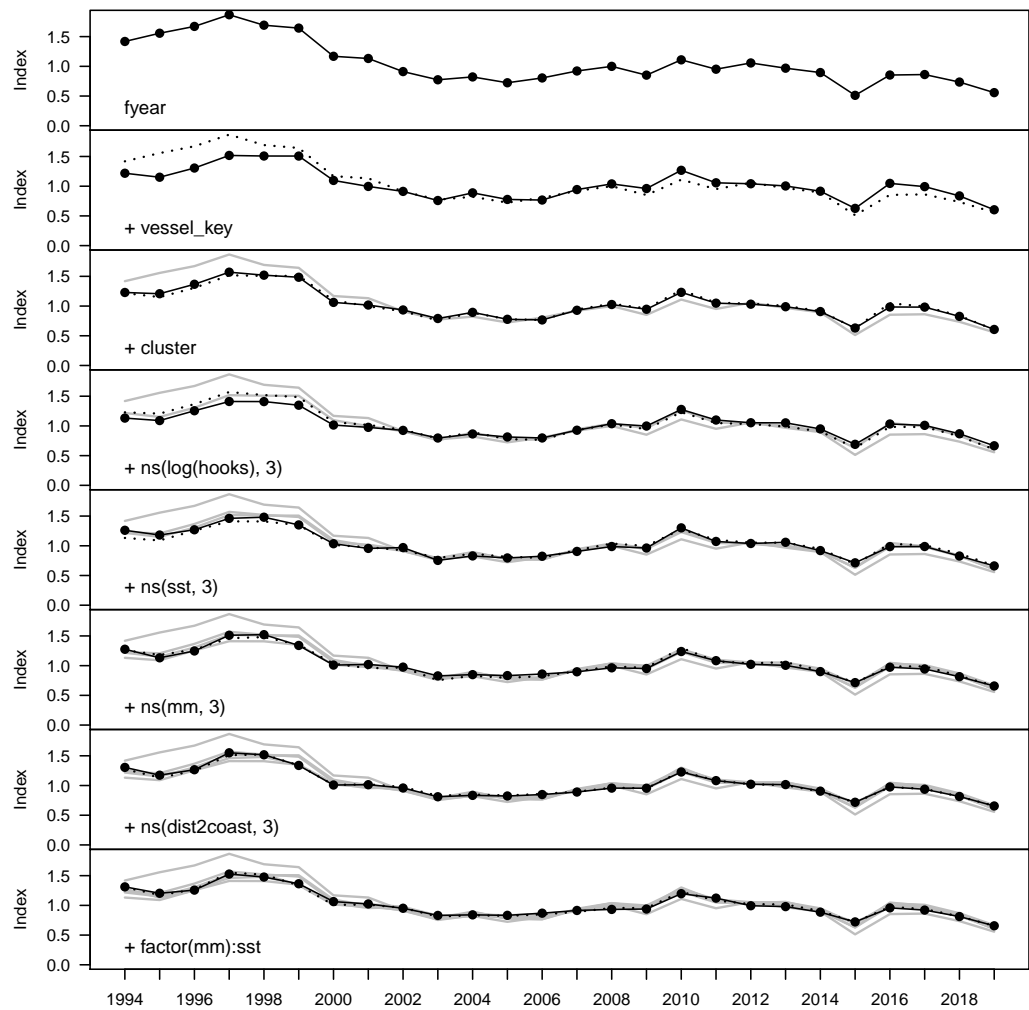


Figure B-33: Step plot for the Japanese fleet CPUE, showing sequential standardising effects of variables included in the standardisation model.

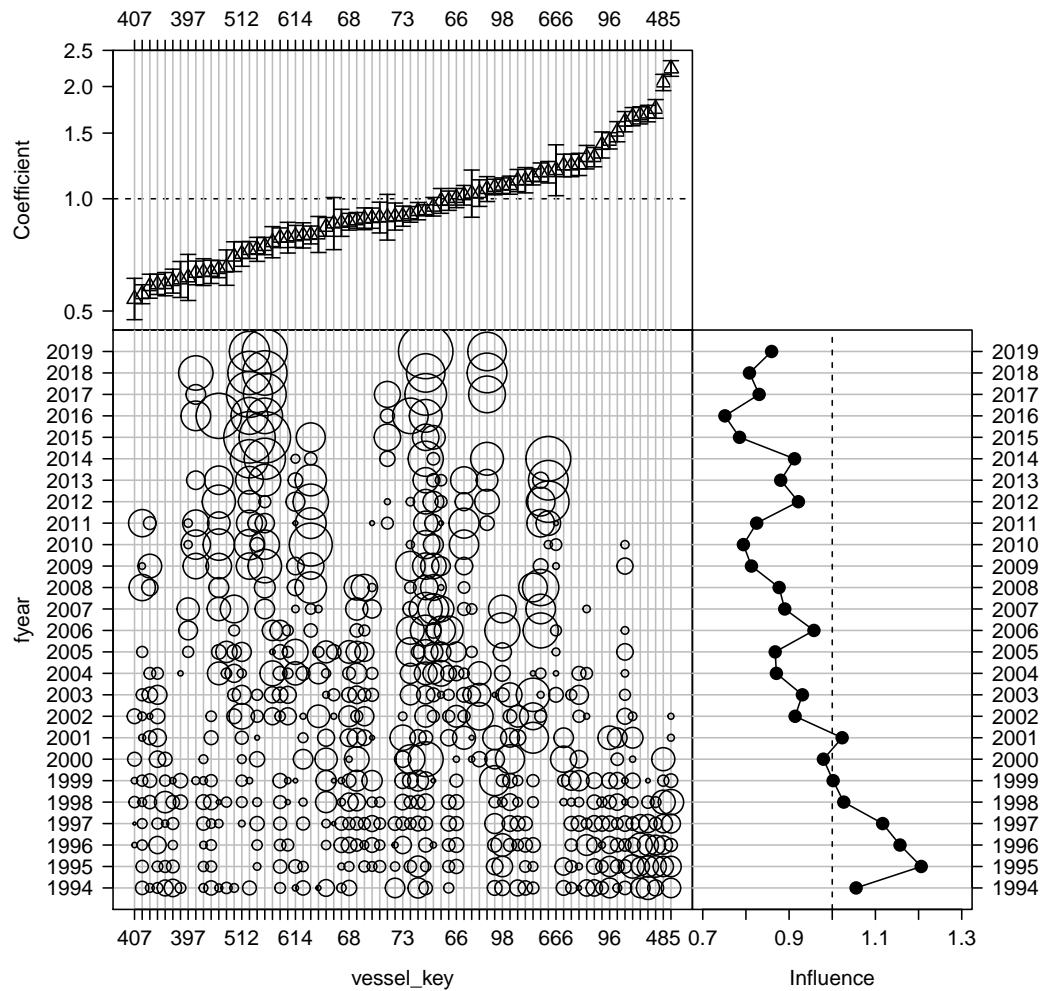


Figure B-34: Influence of fleet composition (vessel keys) for the Japanese fleet (bubble plot; bubbles scales by effort) on CPUE; influence (right) shows the standardising effect (a positive effect reduces the standardised CPUE by the equivalent amount). Estimated coefficients are given in the top panel.

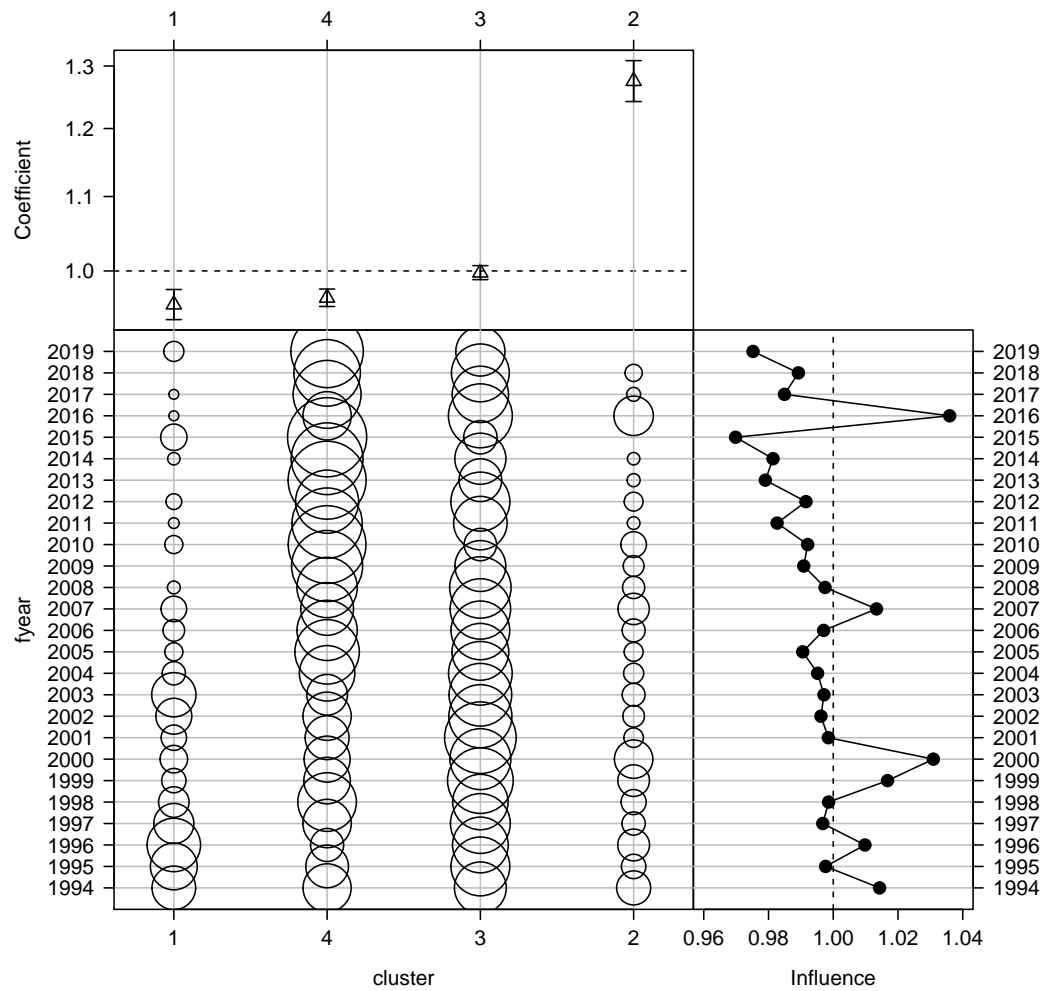


Figure B-35: Influence of targeting cluster for the Japanese fleet (bubble plot; bubbles scales by effort) on CPUE; influence (right hand plot) shows the standardising effect (a positive effect reduces the standardised CPUE by the equivalent amount). Estimated coefficients are given in the top panel.

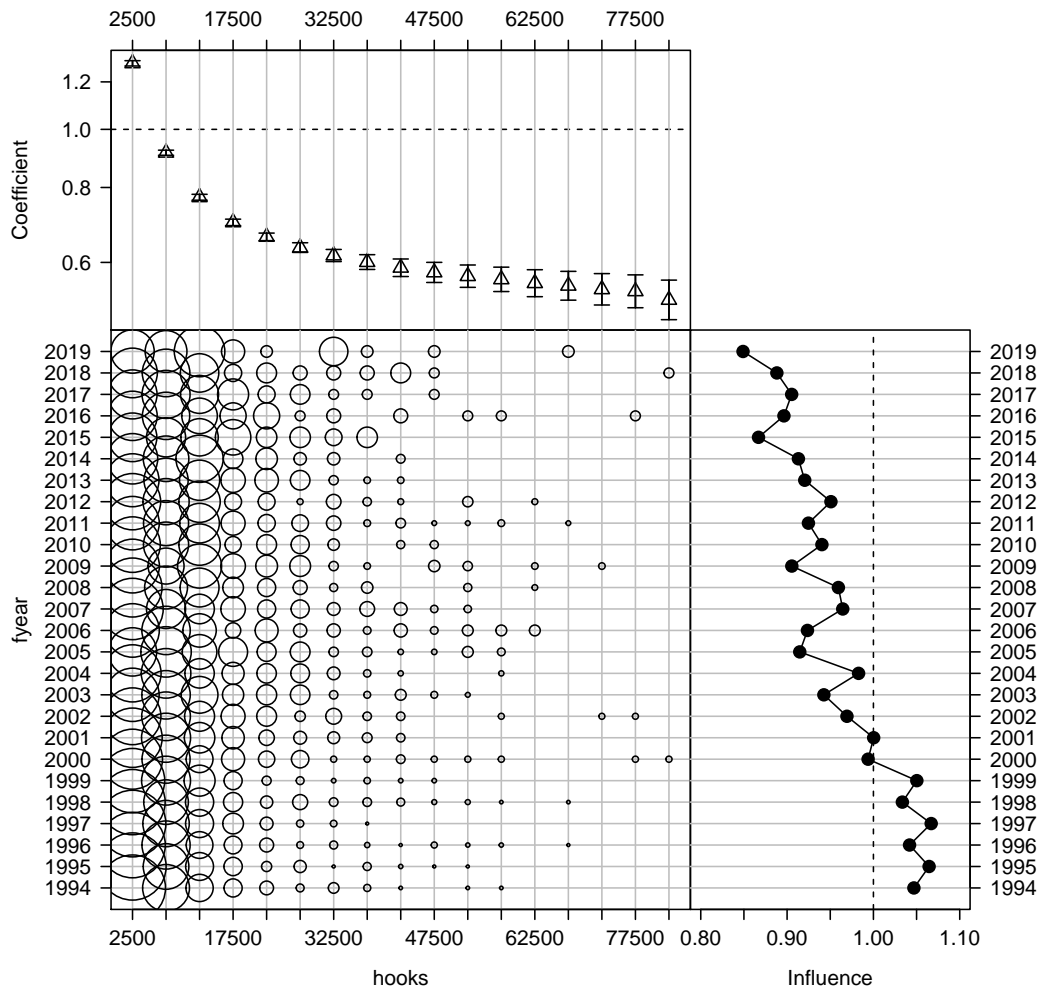


Figure B-36: Influence of number of hooks set per stratum for the Japanese fleet (bubble plot; bubbles scales by effort) on CPUE; influence (right hand plot) shows the standardising effect (a positive effect reduces the standardised CPUE by the equivalent amount). Estimated coefficients are given in the top panel.

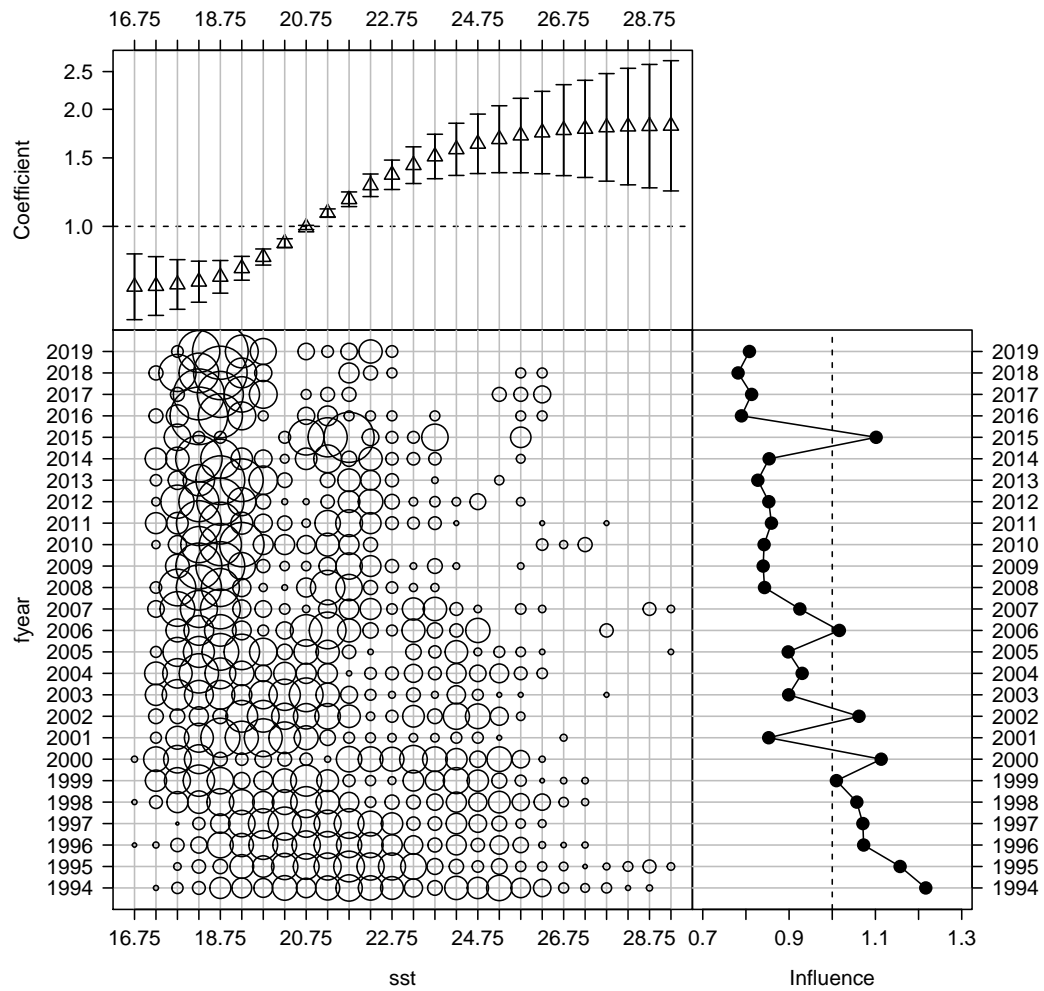


Figure B-37: Influence of sea surface temperature (SST, in degrees Celsius) for the Japanese fleet (bubble plot; bubbles scales by effort) on CPUE; influence (right hand plot) shows the standardising effect (a positive effect reduces the standardised CPUE by the equivalent amount). Estimated coefficients are given in the top panel.

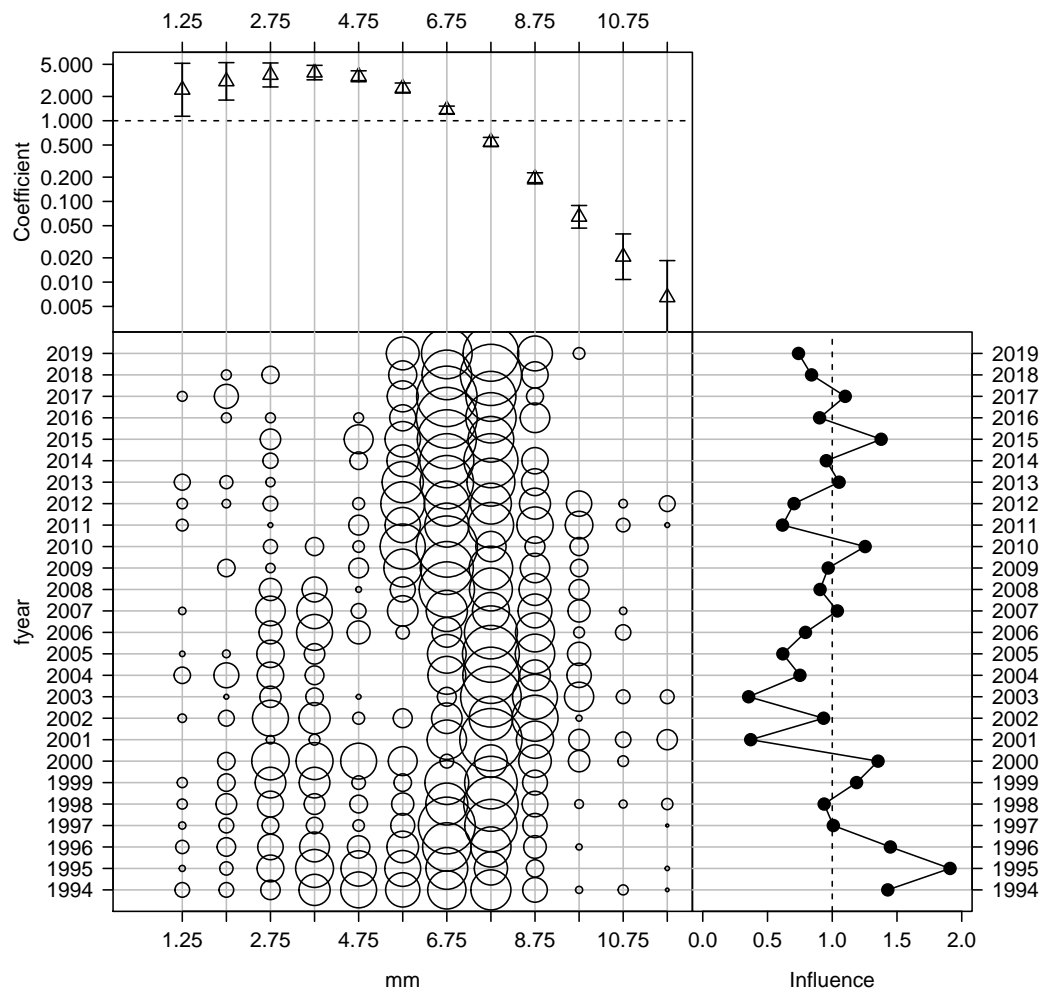


Figure B-38: Influence of month for the Japanese fleet (bubble plot; bubbles scales by effort) on CPUE; influence (right hand plot) shows the standardising effect (a positive effect reduces the standardised CPUE by the equivalent amount). Estimated coefficients are given in the top panel.

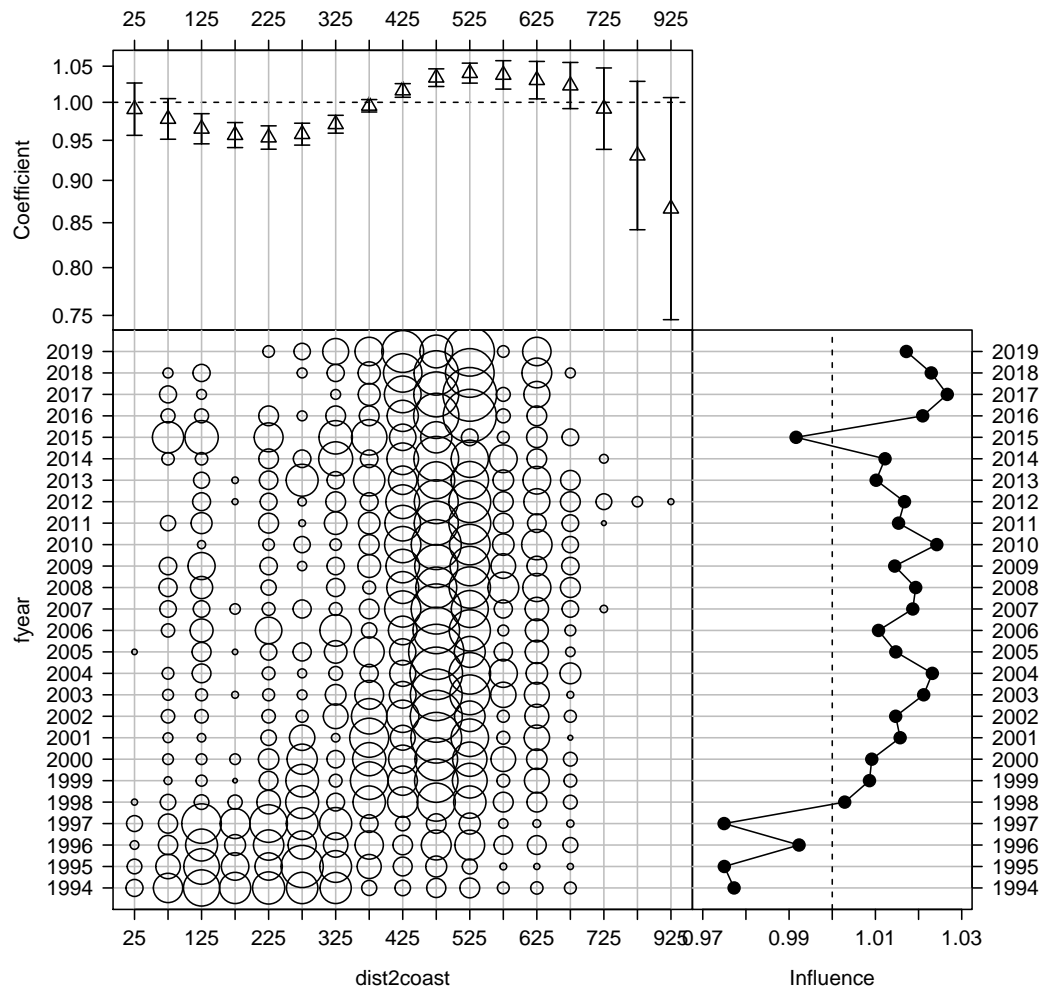


Figure B-39: Influence of distance to coast composition for the Japanese fleet (bubble plot; bubbles scales by effort) on CPUE; influence (right hand plot) shows the standardising effect (a positive effect reduces the standardised CPUE by the equivalent amount). Estimated coefficients are given in the top panel.

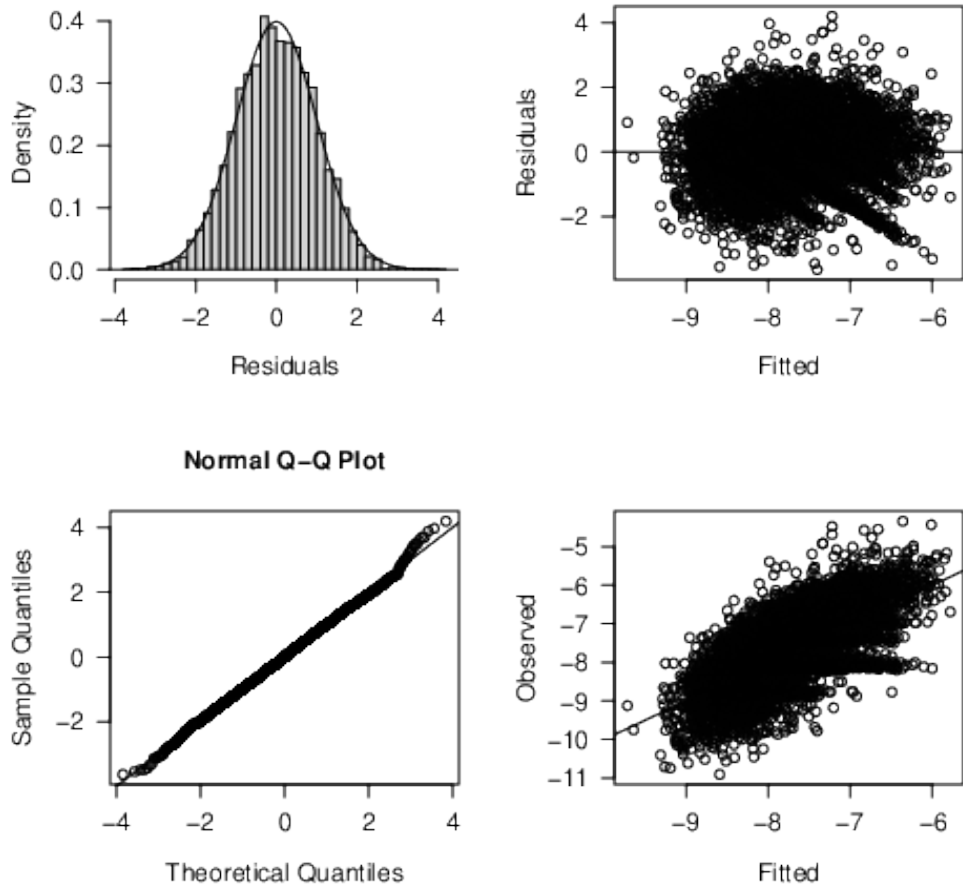


Figure B-40: Diagnostics for the log - normal CPUE standardisation model for the Japanese fleet strata with positive catch.

B.3 Alternative CPUE standardisations

B.3.1 Japan high latitude CPUE

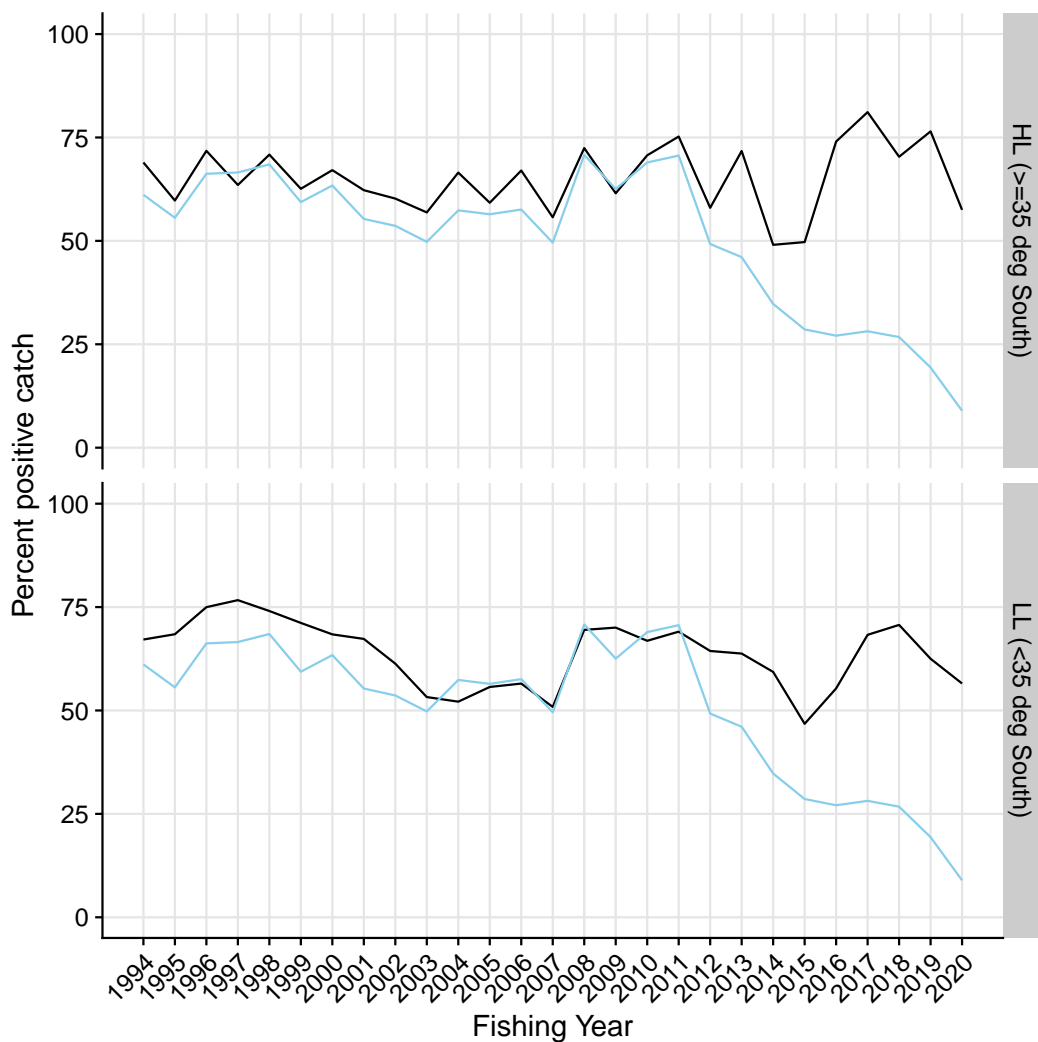


Figure B-41: Proportion of strata for the Japanese fleet with positive catch by latitudinal stratum. Light blue are initial log-sheet records prior to filtering, the black line is the retained dataset after filtering for consistently reporting vessels. Where available, the corresponding values from observed strata is shown in orange.

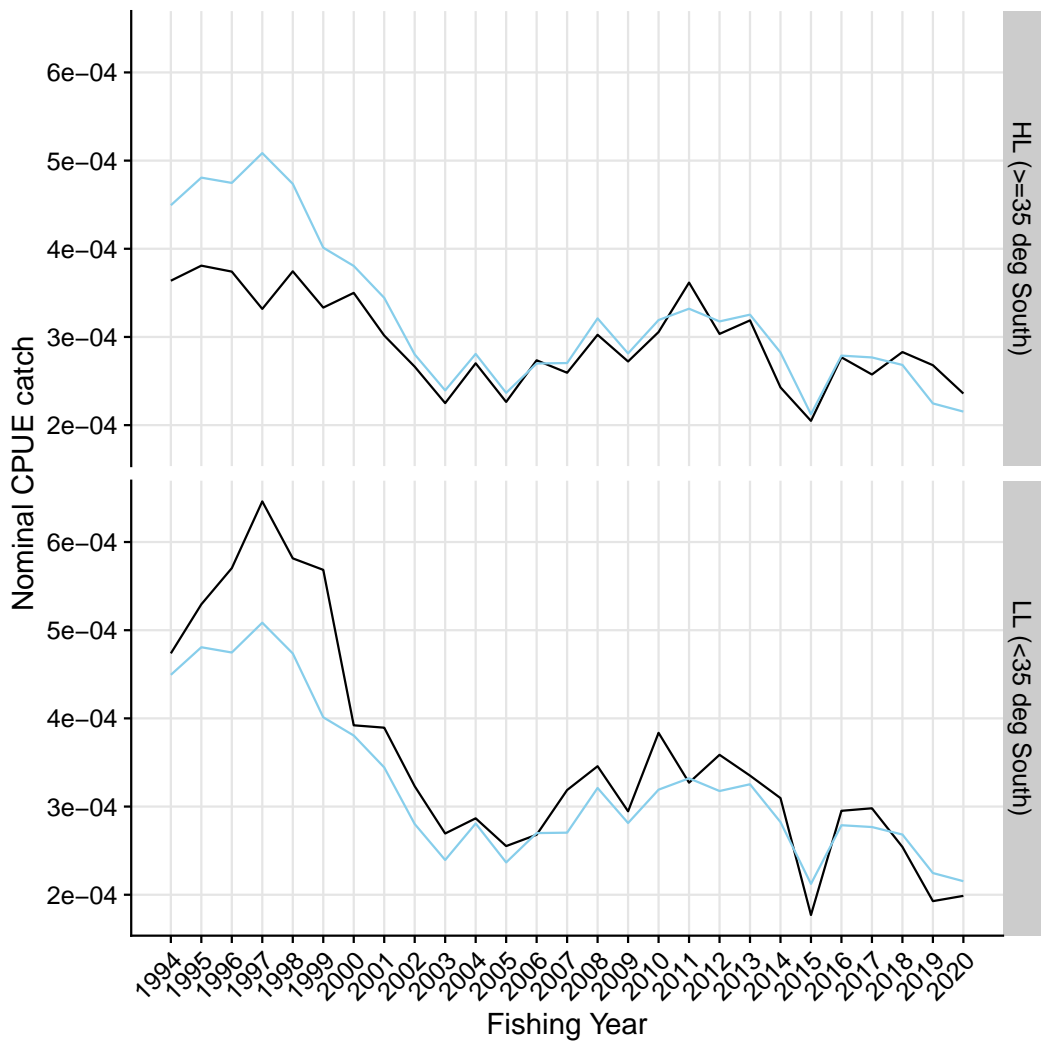


Figure B-42: Nominal CPUE (in number of blue shark per 100 hooks) strata of the Japanese fleet with positive catch by latitudinal stratum. Light blue are initial log-sheet records prior to filtering, the black line is the retained dataset after filtering for consistently reporting vessels. Where available, the corresponding values from observed strata is shown in orange.

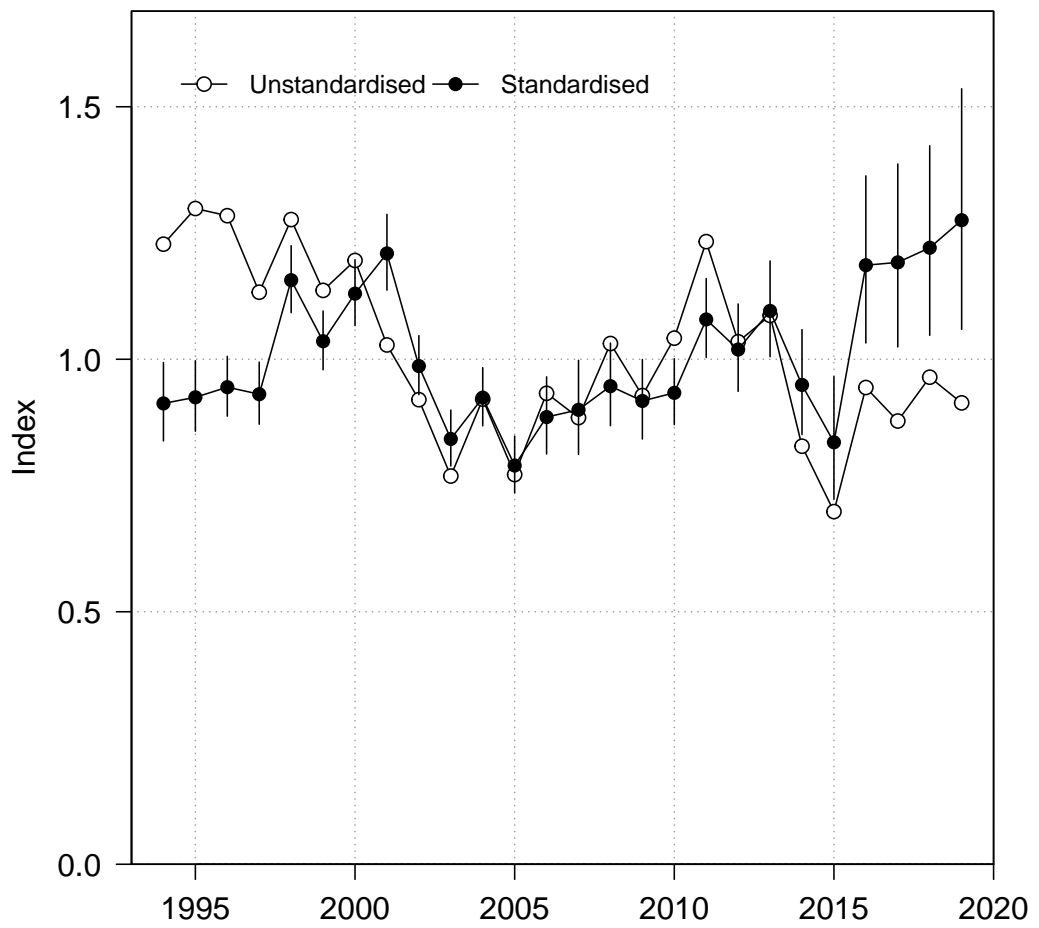


Figure B-43: Standardised (closed black circles with standard error) and unstandardised (open circles) CPUE indices for the Japanese fleet strata with positive catch. Where successful (i.e., converged), standardised trends from a negative - binomial and zero - inflated negative binomial model run over the full dataset (including strata with zero values) are also shown for comparison.

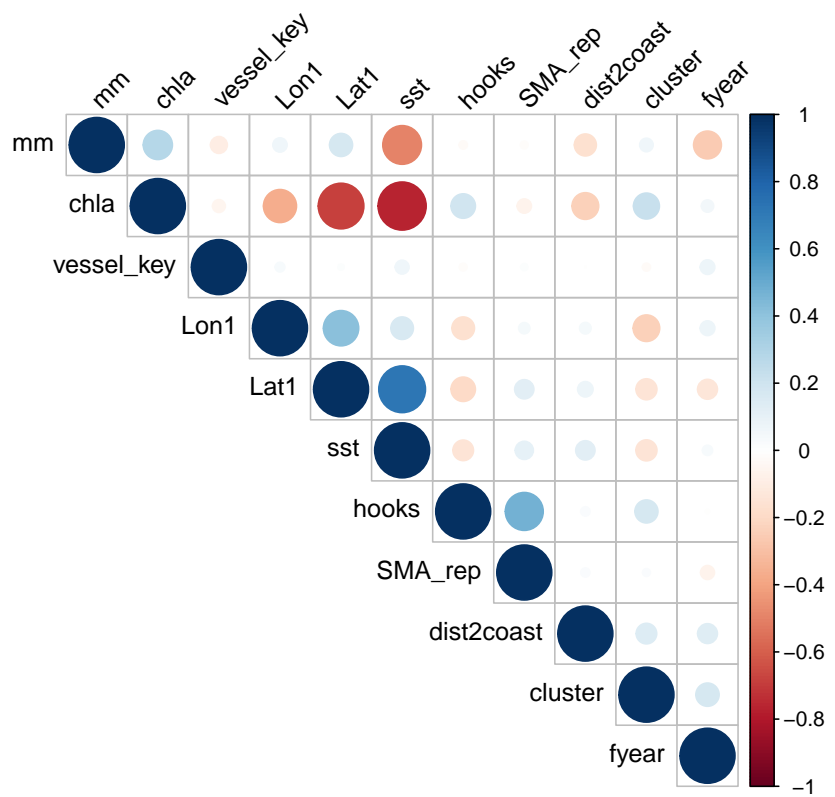


Figure B-44: Correlations amongst potential covariates for CPUE standardisation in the Japanese fleet. Where necessary, variables were removed to reduce redundancy in the models.

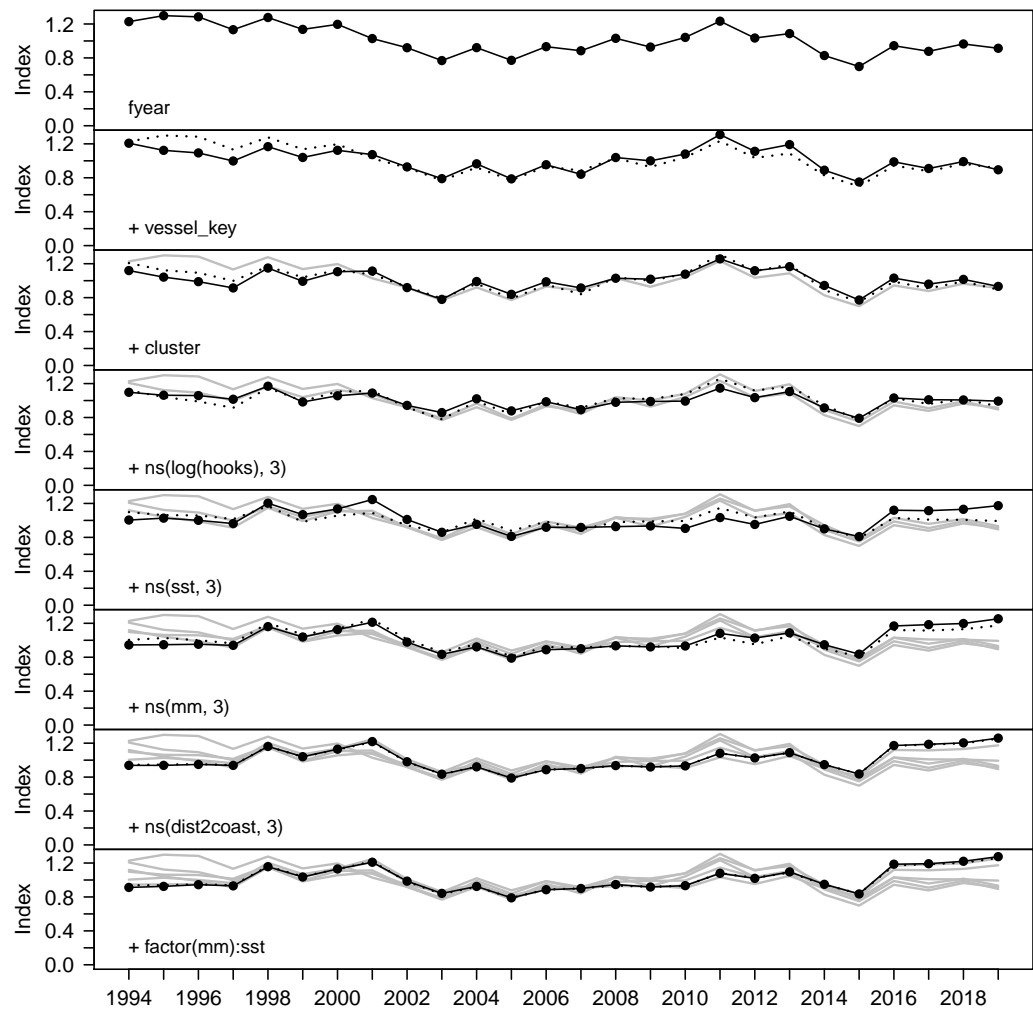


Figure B-45: Step plot for the Japanese fleet CPUE, showing sequential standardising effects of variables included in the standardisation model.

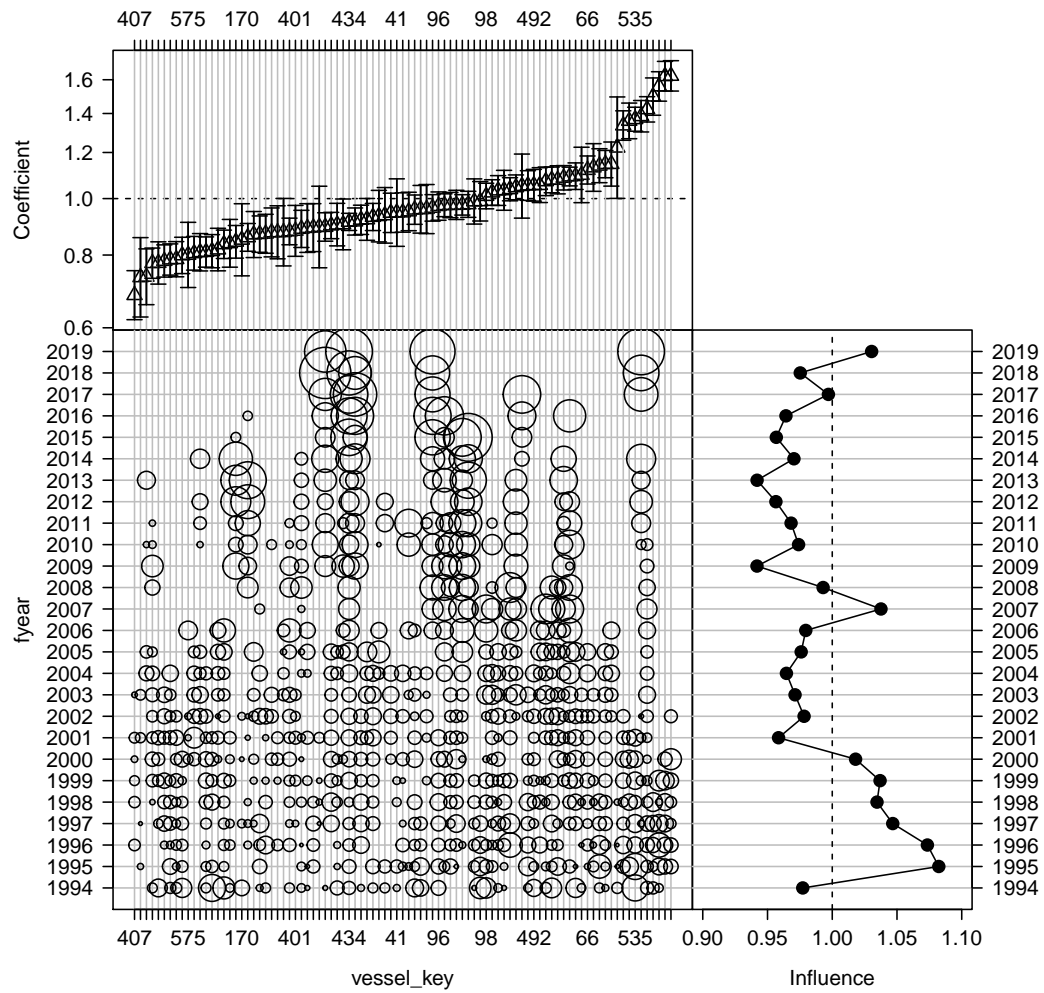


Figure B-46: Influence of fleet composition (vessel keys) for the Japanese fleet (bubble plot; bubbles scales by effort) on CPUE; influence (right) shows the standardising effect (a positive effect reduces the standardised CPUE by the equivalent amount). Estimated coefficients are given in the top panel.

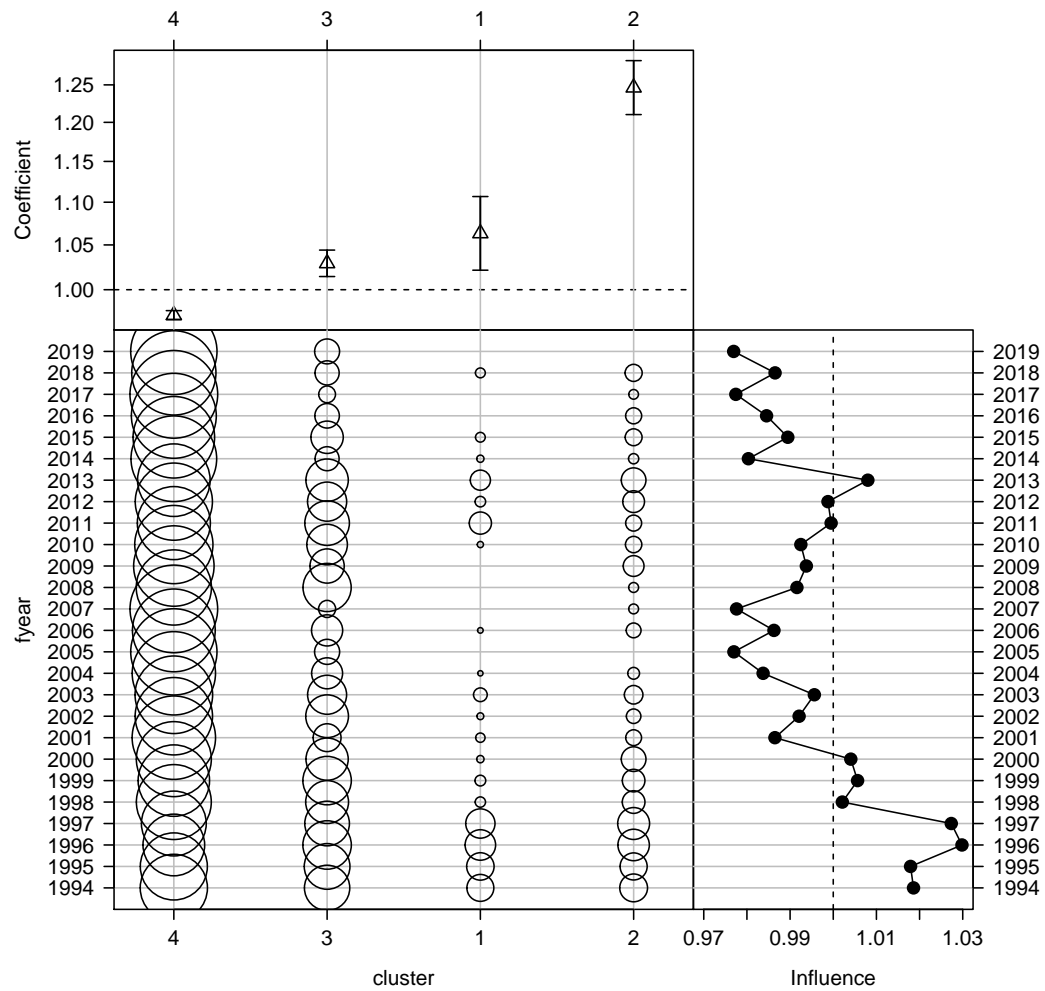


Figure B-47: Influence of targeting cluster for the Japanese fleet (bubble plot; bubbles scales by effort) on CPUE; influence (right hand plot) shows the standardising effect (a positive effect reduces the standardised CPUE by the equivalent amount). Estimated coefficients are given in the top panel.

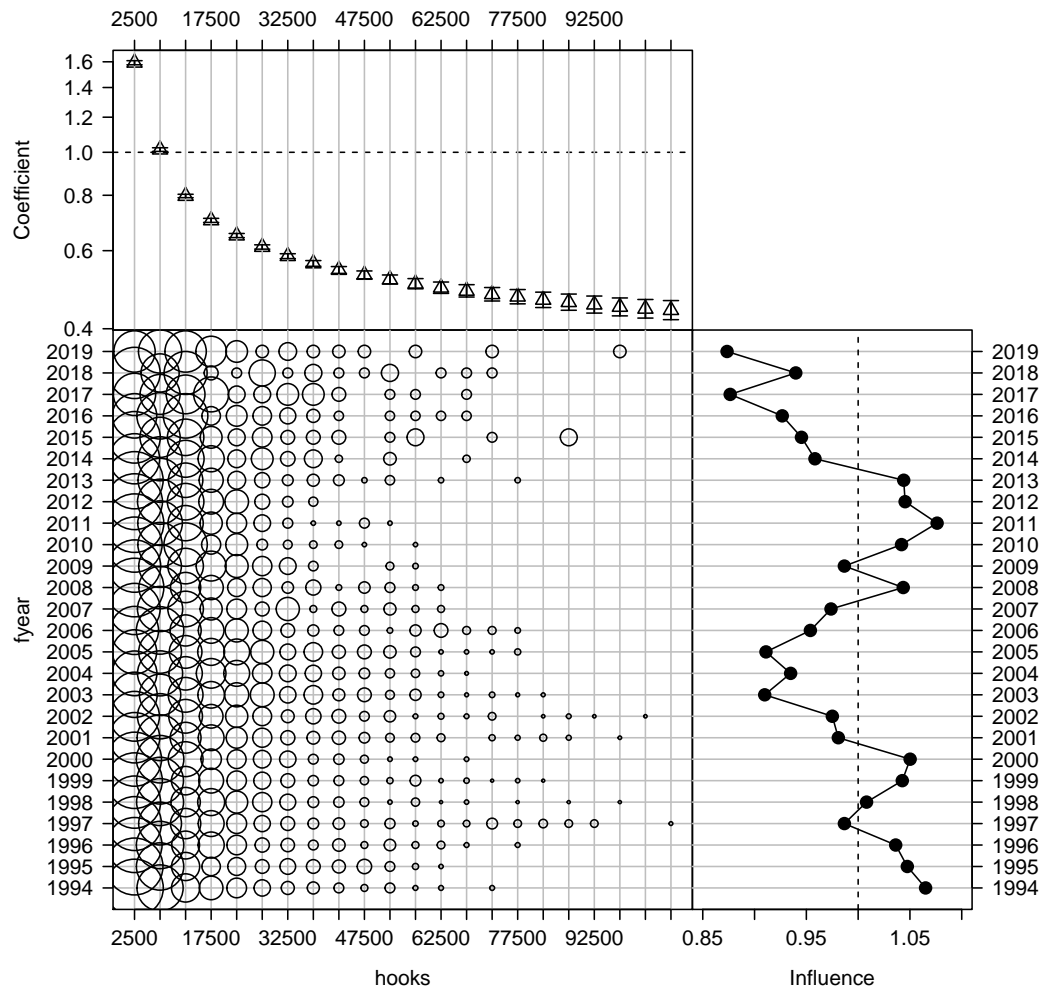


Figure B-48: Influence of number of hooks set per stratum for the Japanese fleet (bubble plot; bubbles scales by effort) on CPUE; influence (right hand plot) shows the standardising effect (a positive effect reduces the standardised CPUE by the equivalent amount). Estimated coefficients are given in the top panel.

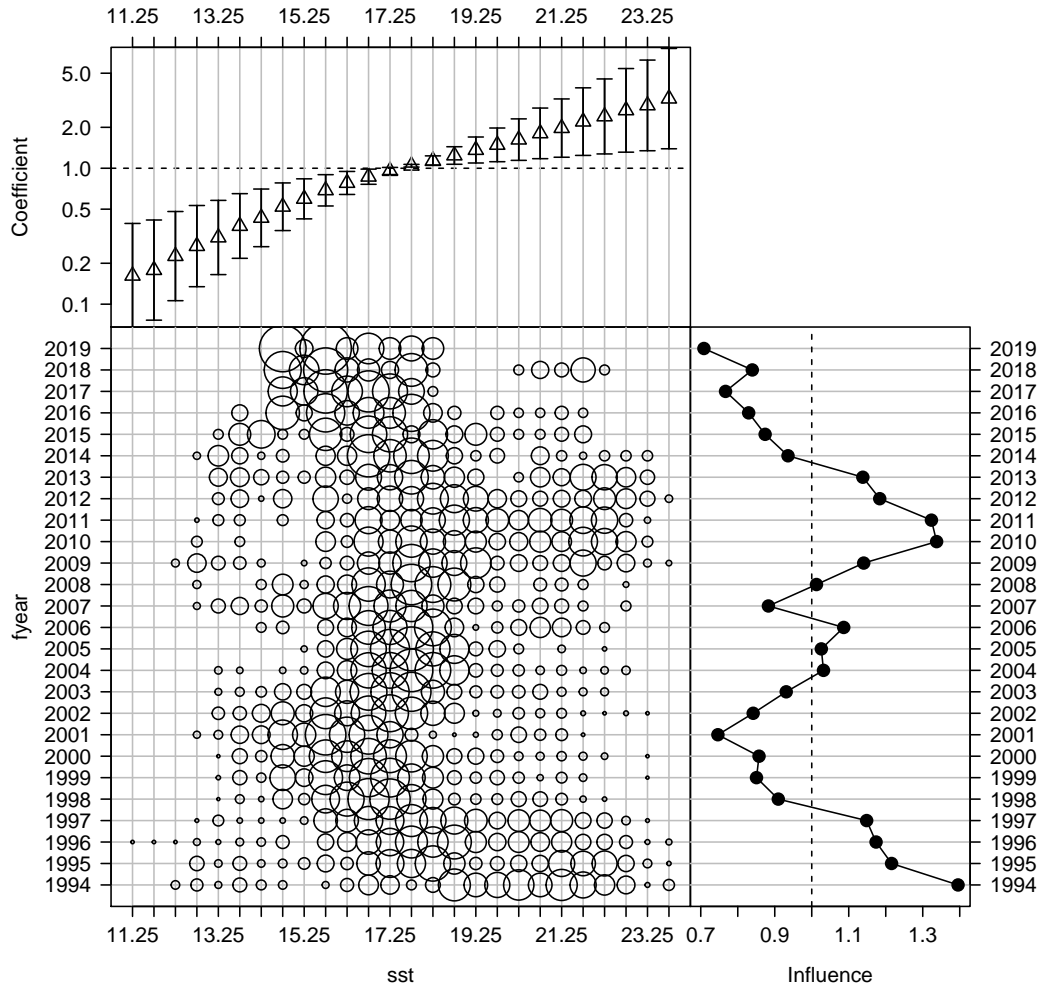


Figure B-49: Influence of sea surface temperature (SST, in degrees Celsius) for the Japanese fleet (bubble plot; bubbles scales by effort) on CPUE; influence (right hand plot) shows the standardising effect (a positive effect reduces the standardised CPUE by the equivalent amount). Estimated coefficients are given in the top panel.

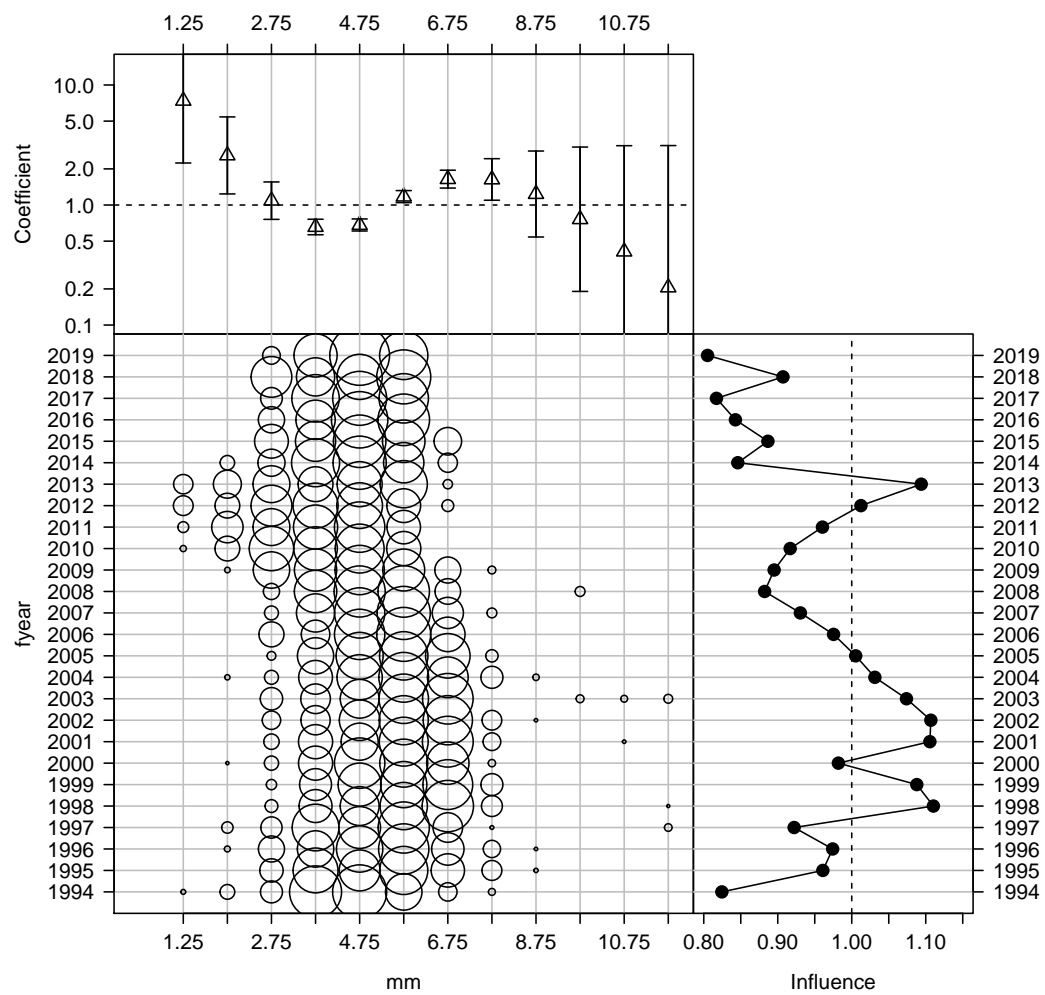


Figure B-50: Influence of month for the Japanese fleet (bubble plot; bubbles scales by effort) on CPUE; influence (right hand plot) shows the standardising effect (a positive effect reduces the standardised CPUE by the equivalent amount). Estimated coefficients are given in the top panel.

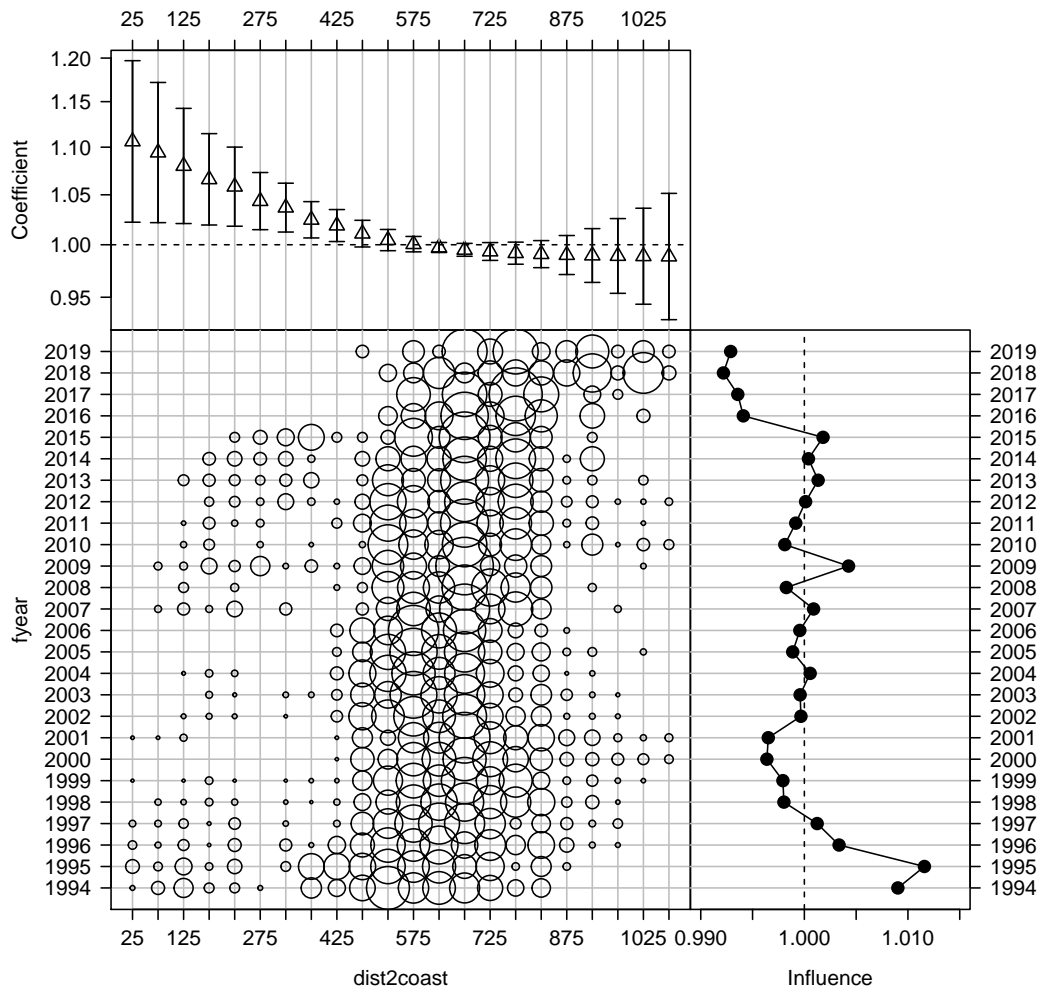


Figure B-51: Influence of distance to coast composition for the Japanese fleet (bubble plot; bubbles scales by effort) on CPUE; influence (right hand plot) shows the standardising effect (a positive effect reduces the standardised CPUE by the equivalent amount). Estimated coefficients are given in the top panel.

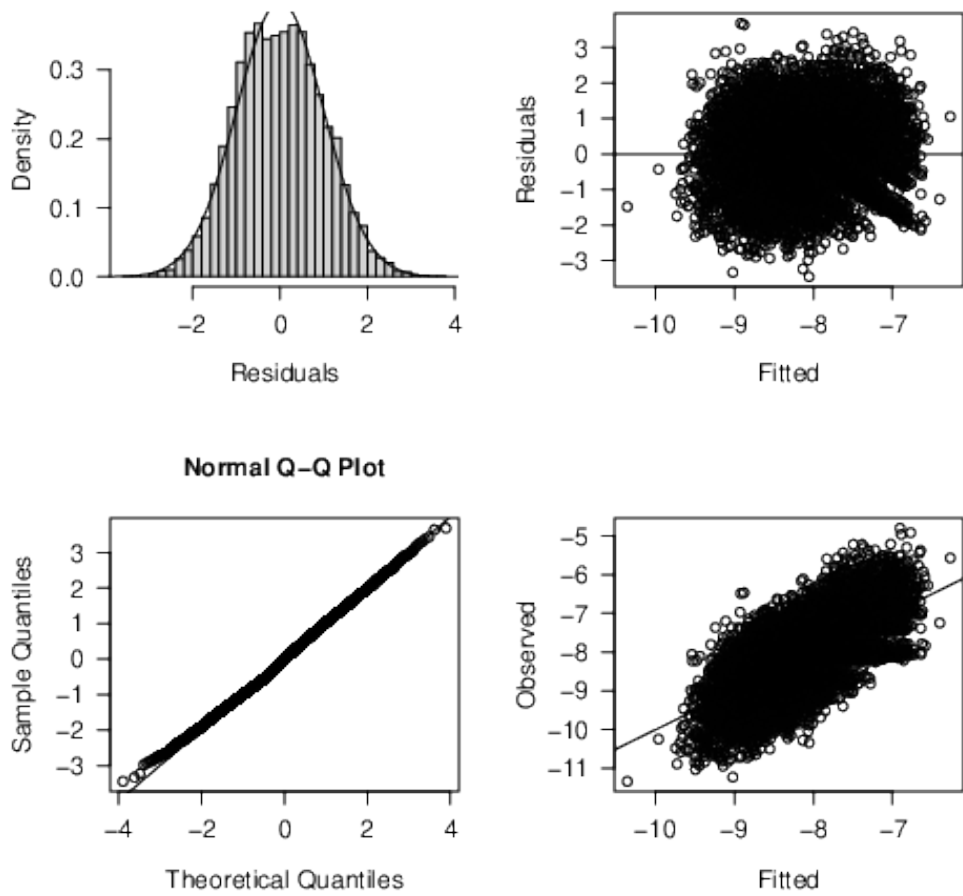


Figure B-52: Diagnostics for the log - normal CPUE standardisation model for the Japanese fleet strata with positive catch.

B.3.2 Australia low latitude CPUE

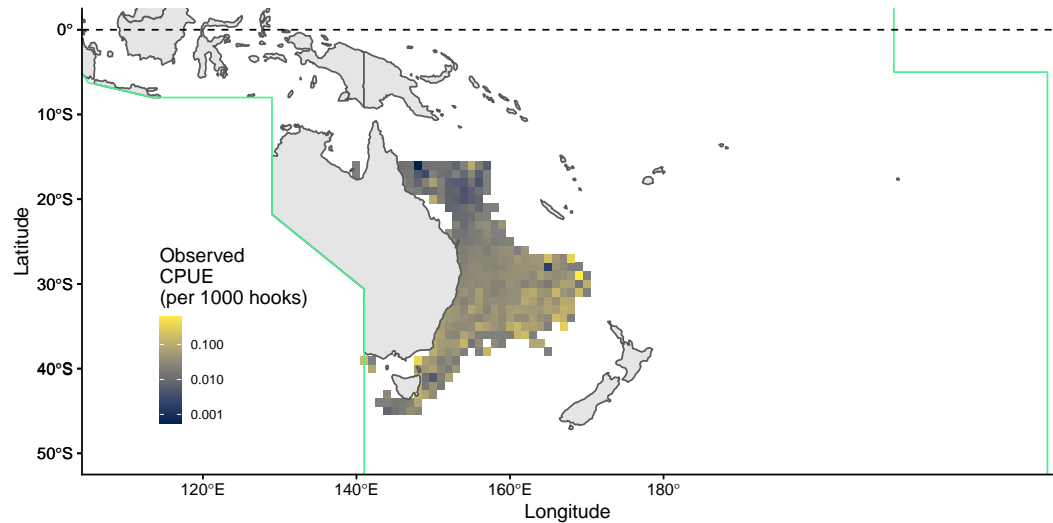


Figure B-53: Maps of average catch rates (CPUE; in number of shortfin mako shark per 1000 hooks) for the Australian longline fleet.

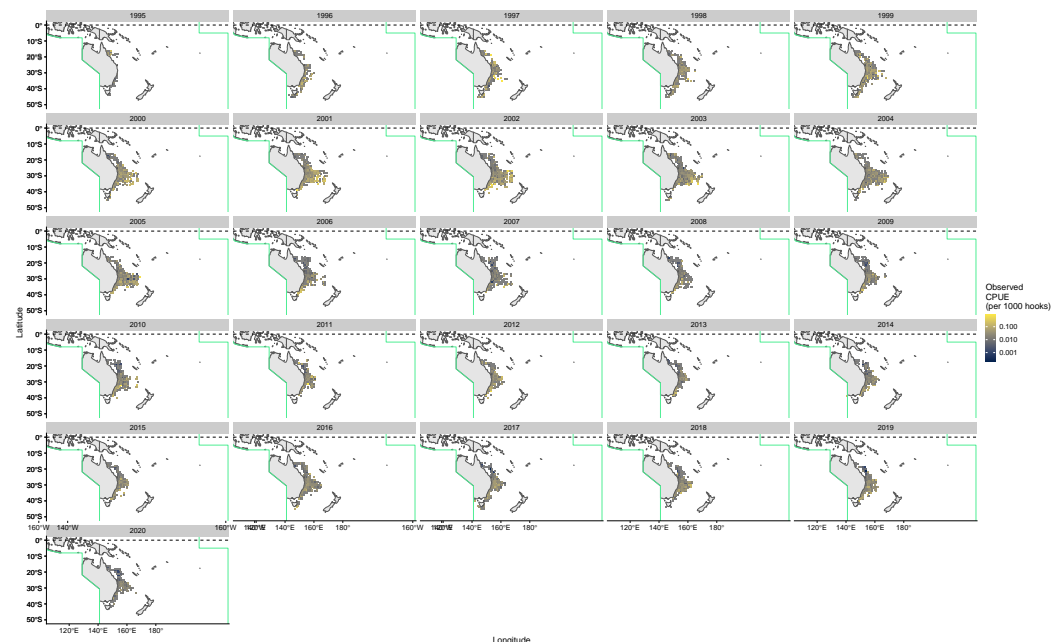


Figure B-54: Maps of average catch rates (CPUE; in number of shortfin mako shark per 1000 hooks) by year for the Australian longline fleet.

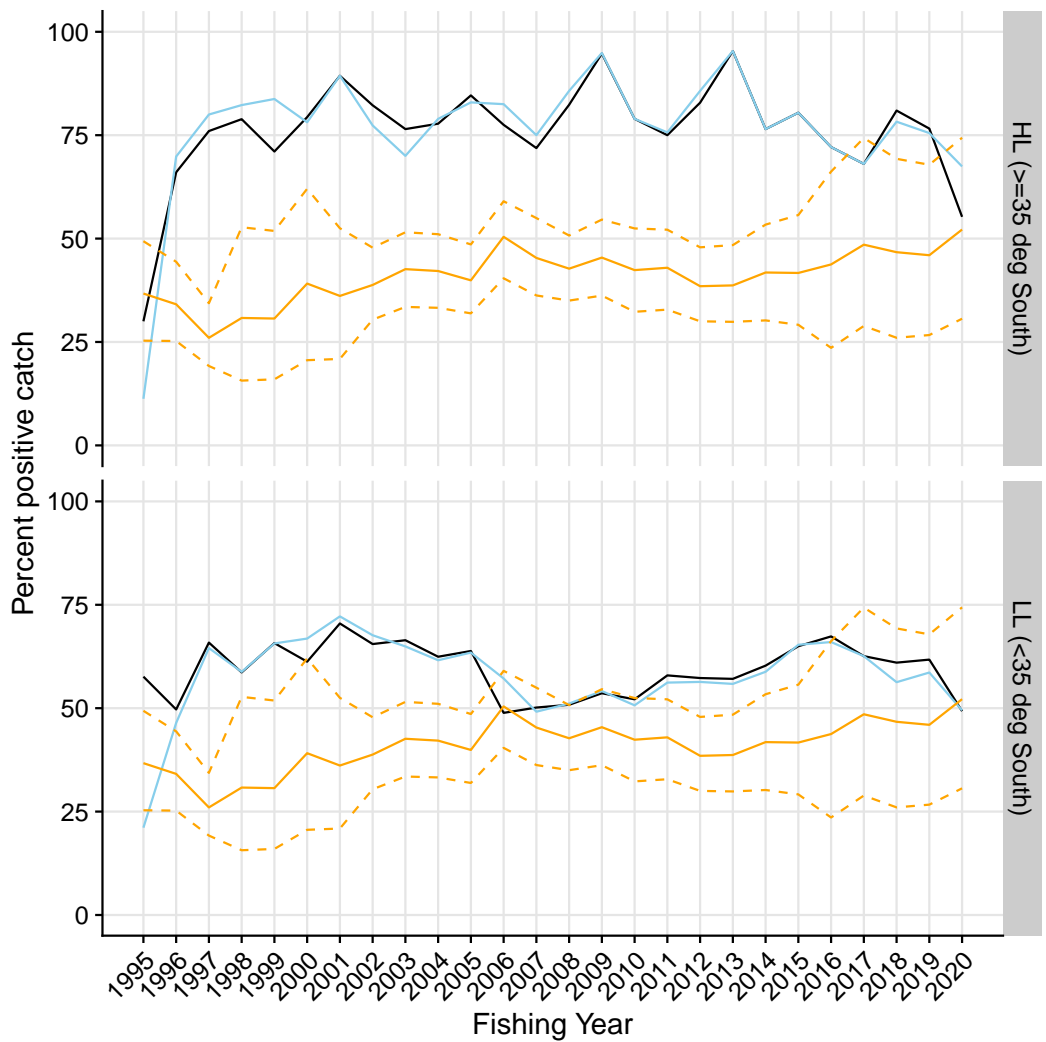


Figure B-55: Proportion of strata for the Australian fleet with positive catch by latitudinal stratum. Light blue are initial log-sheet records prior to filtering, the black line is the retained dataset after filtering for consistently reporting vessels. Where available, the corresponding values from observed strata is shown in orange.

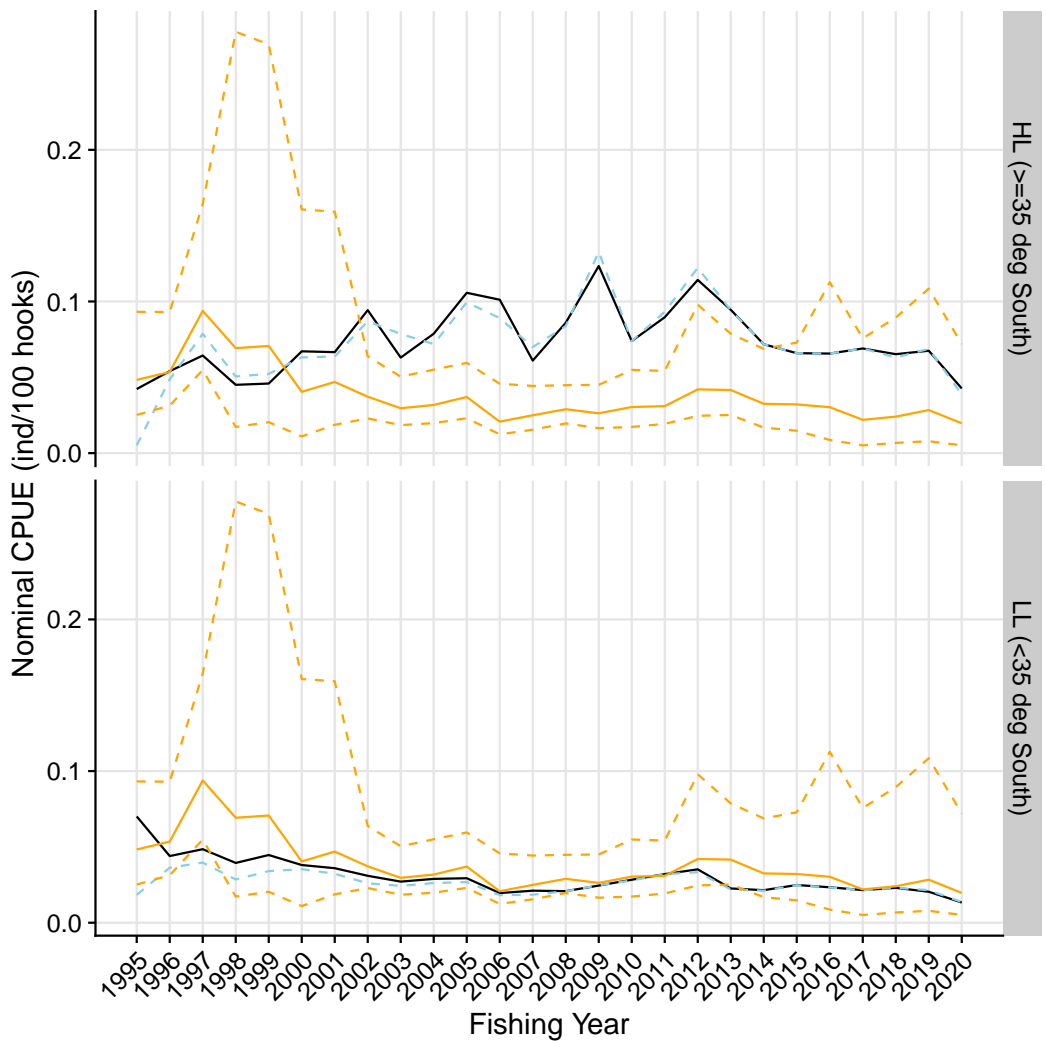


Figure B-56: Nominal CPUE (in number of blue shark per 100 hooks) strata of the Australian fleet with positive catch by latitudinal stratum. Light blue are initial log-sheet records prior to filtering, the black line is the retained dataset after filtering for consistently reporting vessels. Where available, the corresponding values from observed strata is shown in orange.

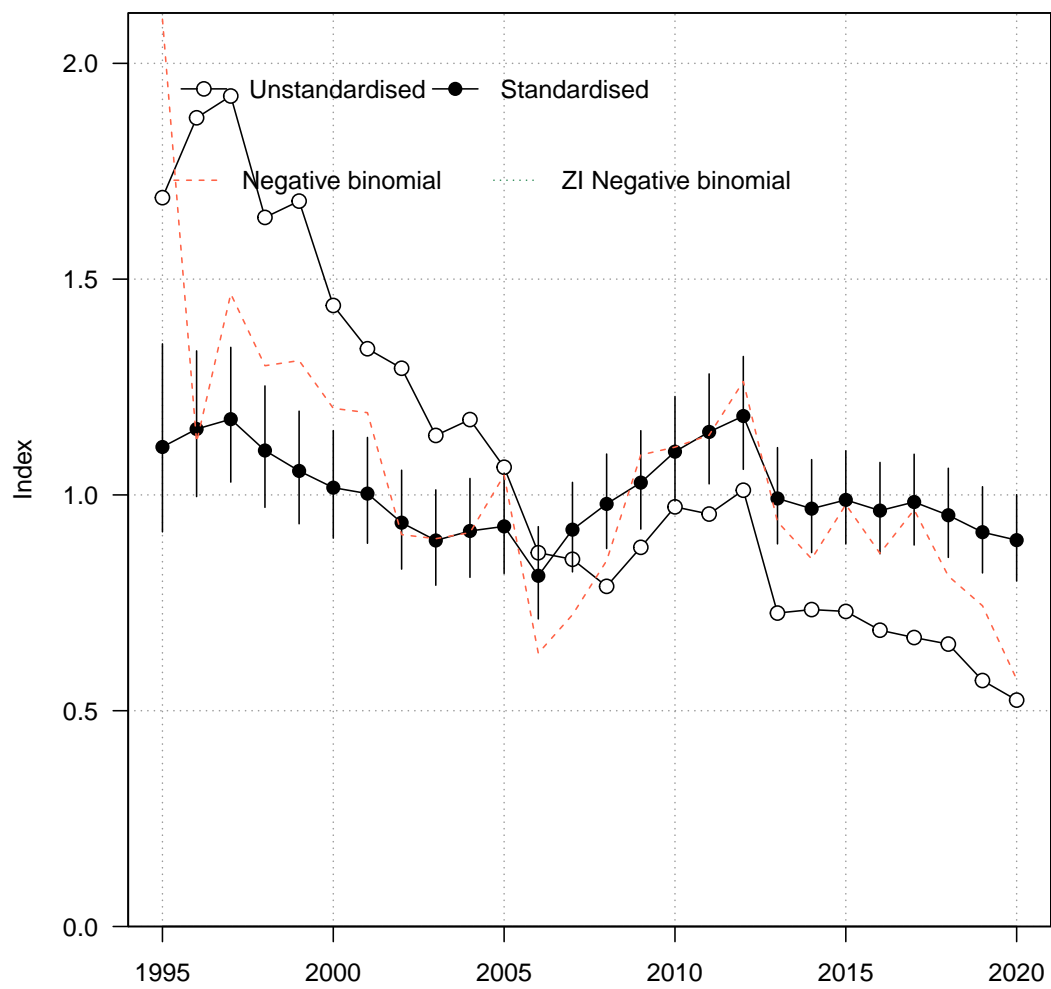


Figure B-57: Standardised (closed black circles with standard error) and unstandardised (open circles) CPUE indices for the Australian fleet strata with positive catch. Where successful (i.e., converged), standardised trends from a negative - binomial and zero - inflated negative binomial model run over the full dataset (including strata with zero values) are also shown for comparison.

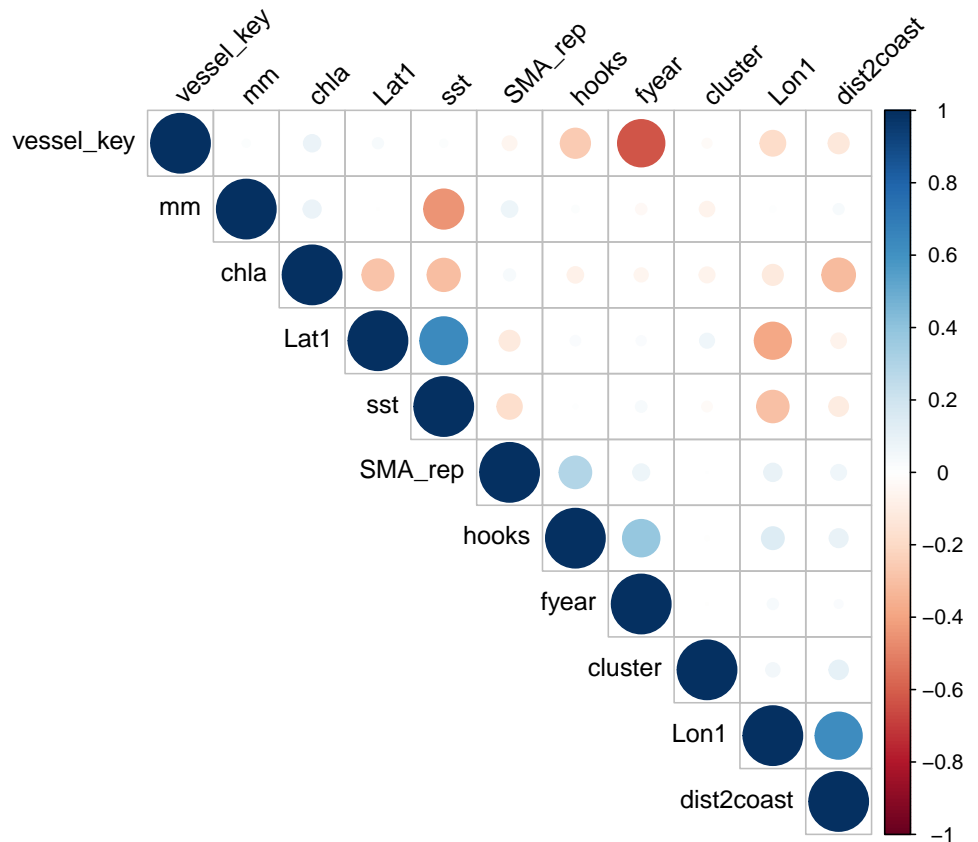


Figure B-58: Correlations amongst potential covariates for CPUE standardisation in the Australian fleet. Where necessary, variables were removed to reduce redundancy in the models.

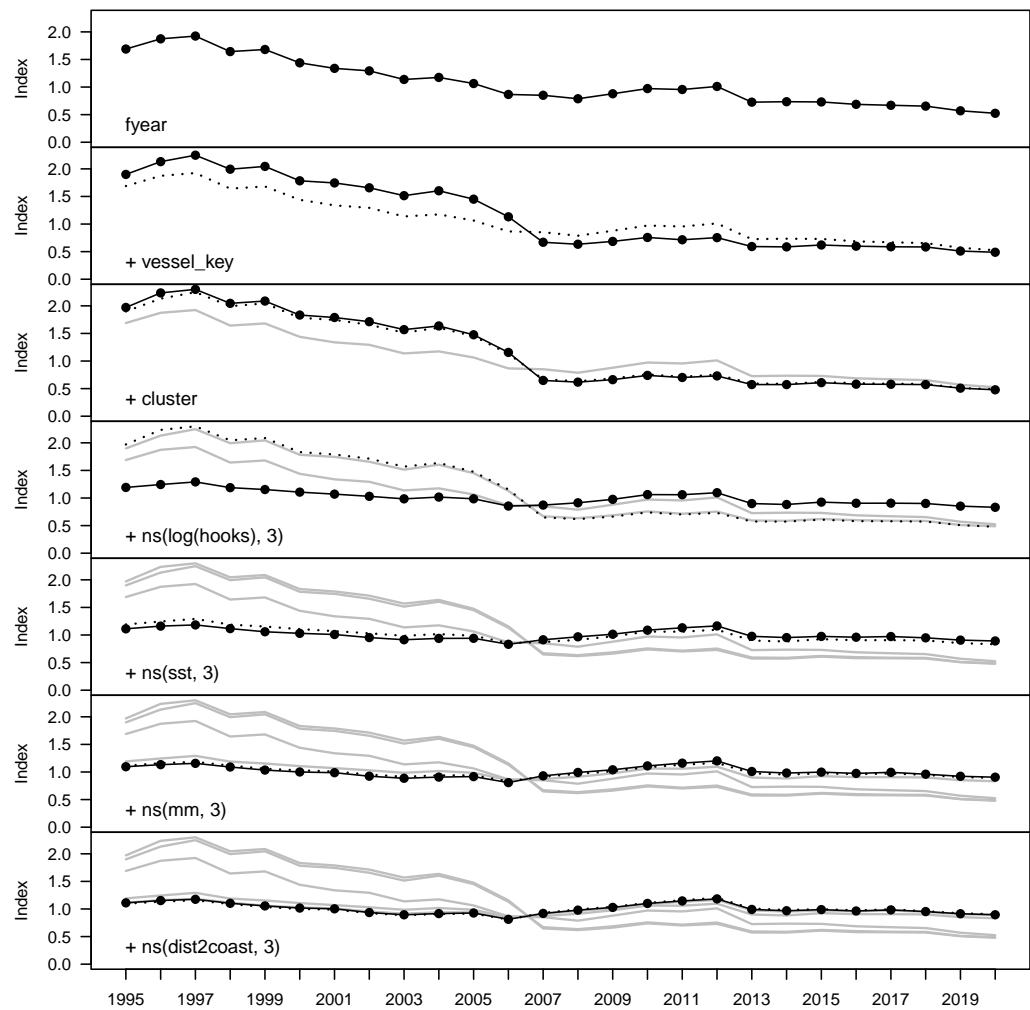


Figure B-59: Step plot for the Australian fleet CPUE, showing sequential standardising effects of variables included in the standardisation model.

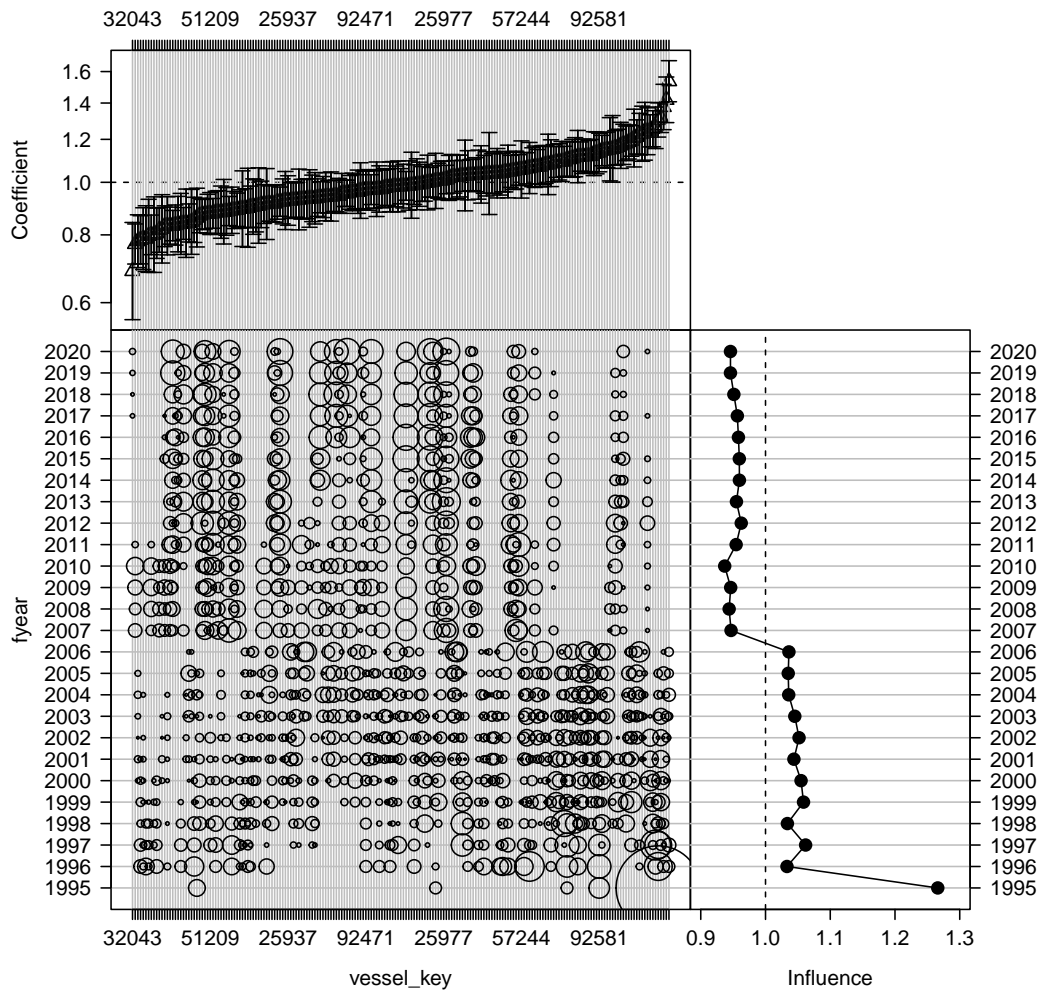


Figure B-60: Influence of fleet composition (vessel keys) for the Australian fleet (bubble plot; bubbles scales by effort) on CPUE; influence (right) shows the standardising effect (a positive effect reduces the standardised CPUE by the equivalent amount). Estimated coefficients are given in the top panel.

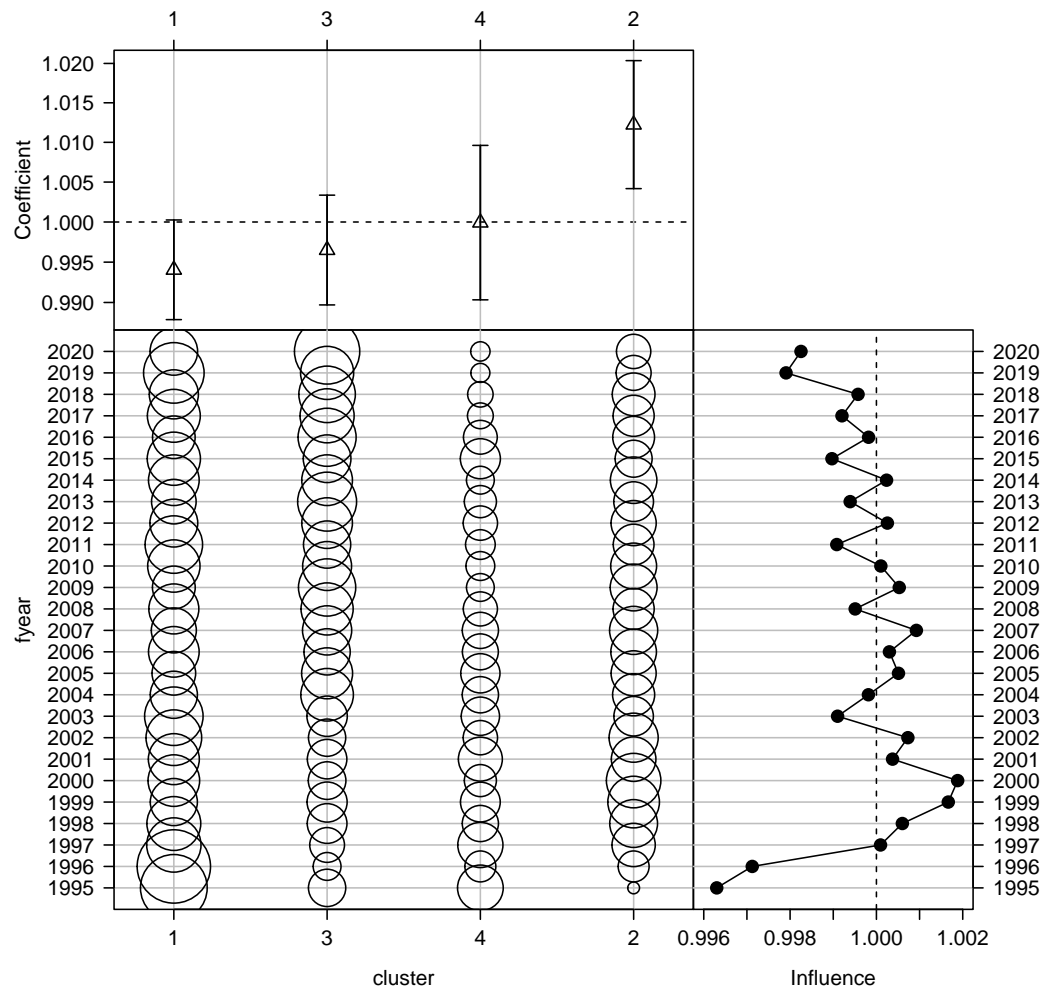


Figure B-61: Influence of targeting cluster for the Australian fleet (bubble plot; bubbles scales by effort) on CPUE; influence (right hand plot) shows the standardising effect (a positive effect reduces the standardised CPUE by the equivalent amount). Estimated coefficients are given in the top panel.

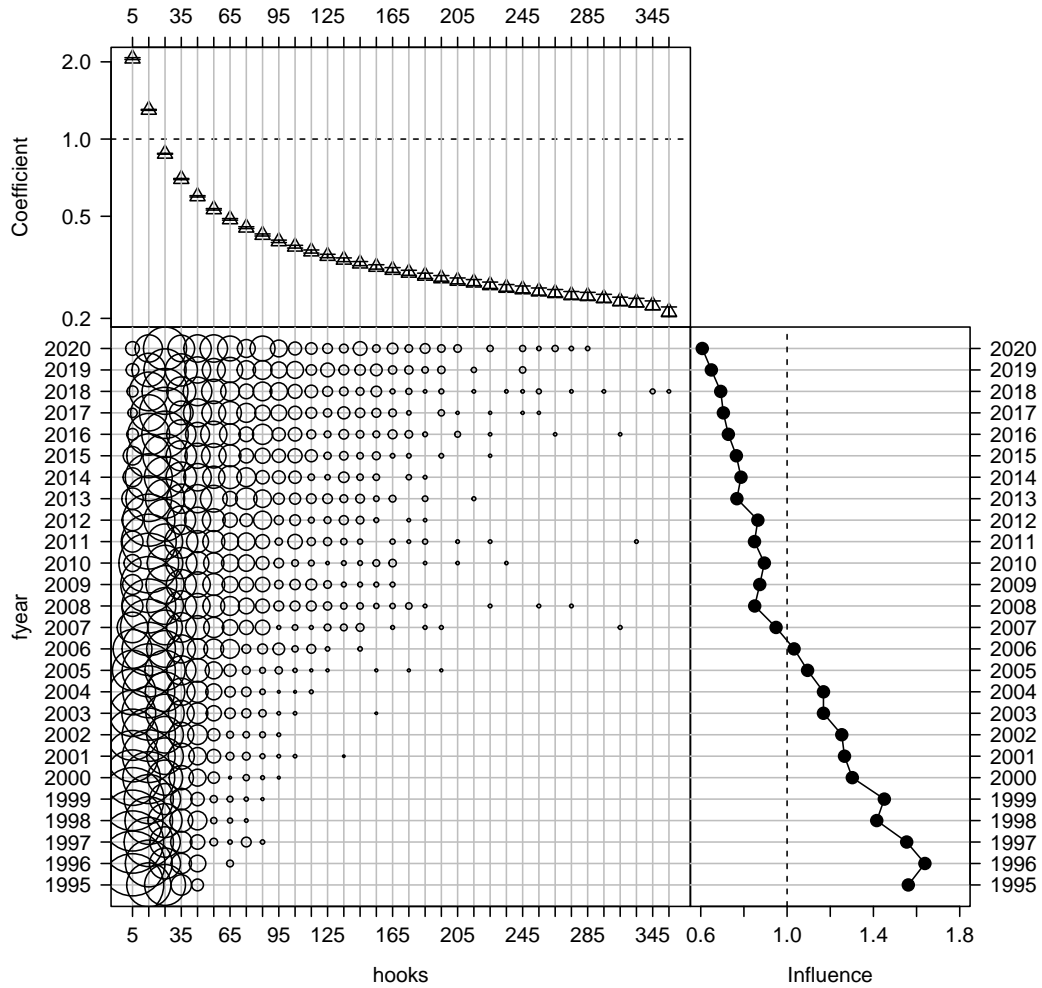


Figure B-62: Influence of number of hooks set per stratum for the Australian fleet (bubble plot; bubbles scales by effort) on CPUE; influence (right hand plot) shows the standardising effect (a positive effect reduces the standardised CPUE by the equivalent amount). Estimated coefficients are given in the top panel.

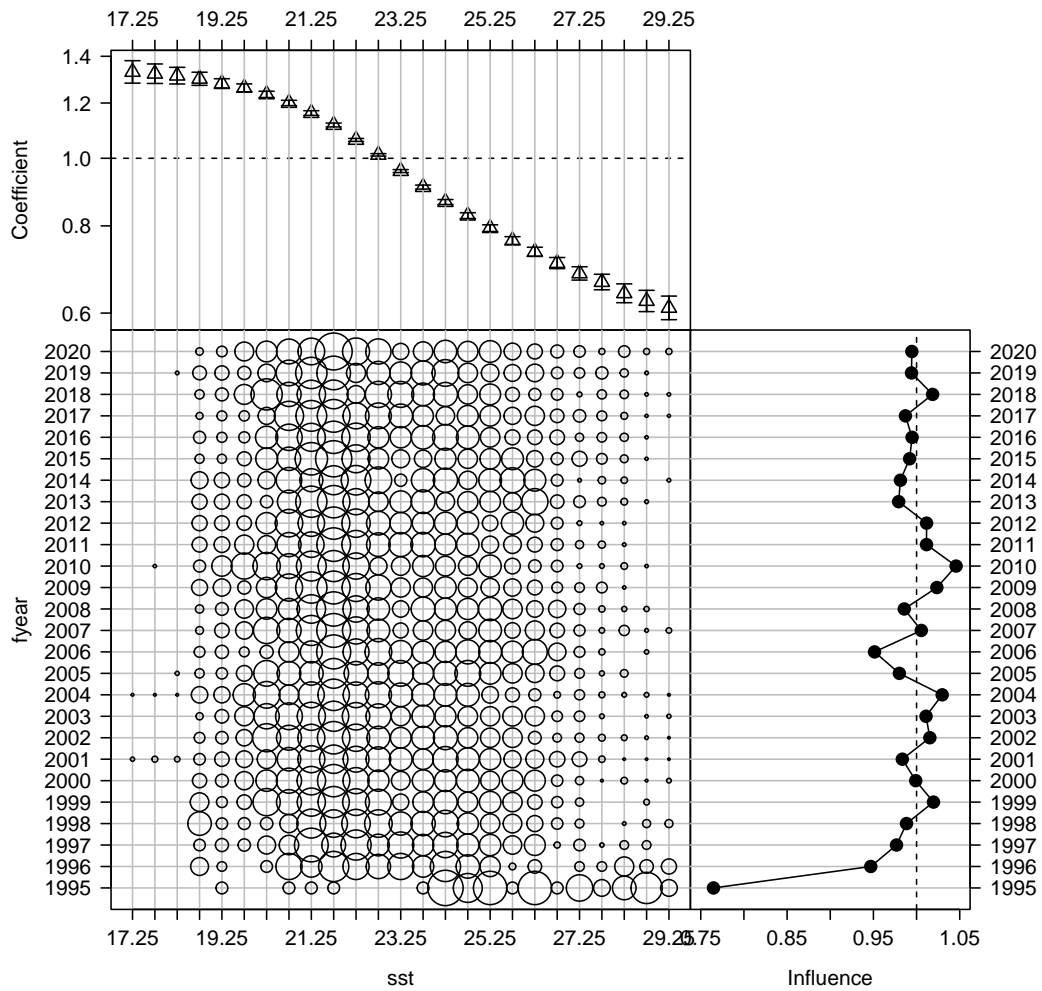


Figure B-63: Influence of sea surface temperature (SST, in degrees Celsius) for the Australian fleet (bubble plot; bubbles scales by effort) on CPUE; influence (right hand plot) shows the standardising effect (a positive effect reduces the standardised CPUE by the equivalent amount). Estimated coefficients are given in the top panel.

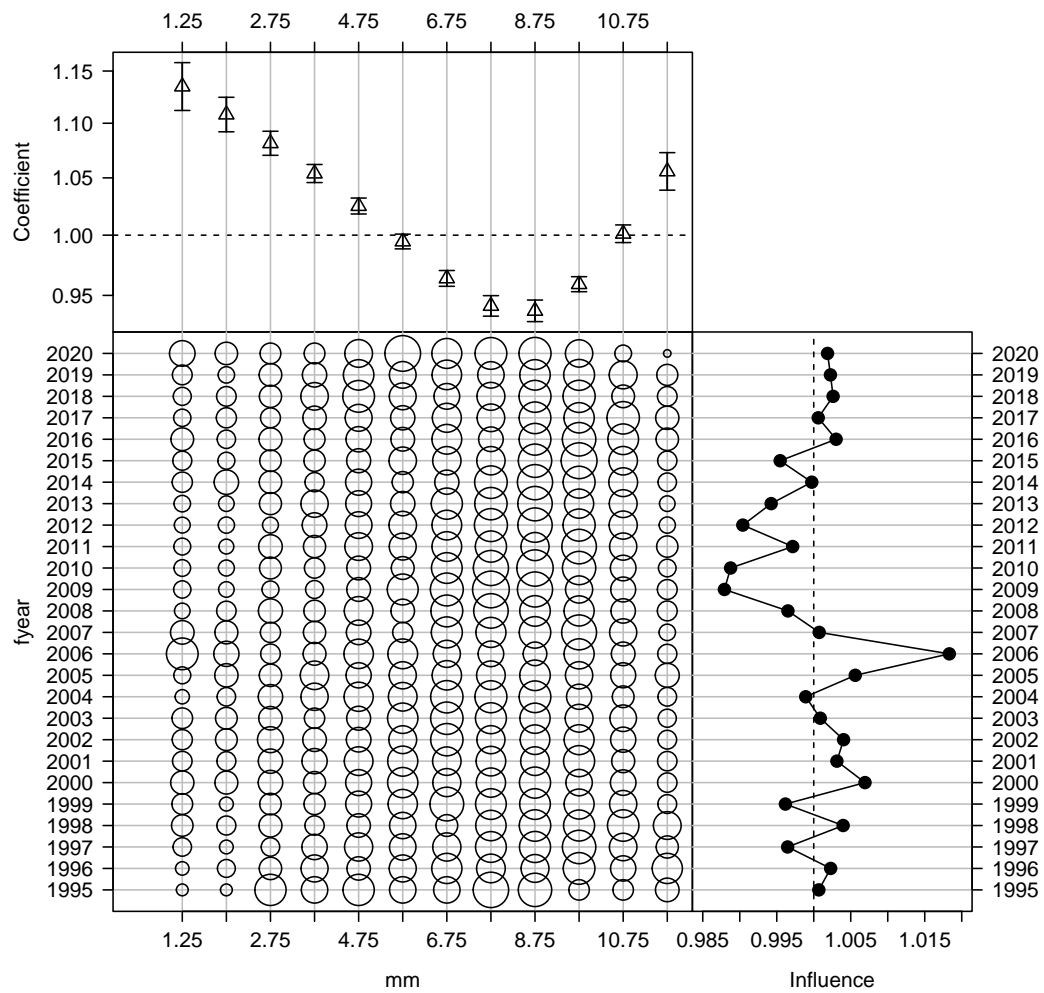


Figure B-64: Influence of month for the Australian fleet (bubble plot; bubbles scales by effort) on CPUE; influence (right hand plot) shows the standardising effect (a positive effect reduces the standardised CPUE by the equivalent amount). Estimated coefficients are given in the top panel.

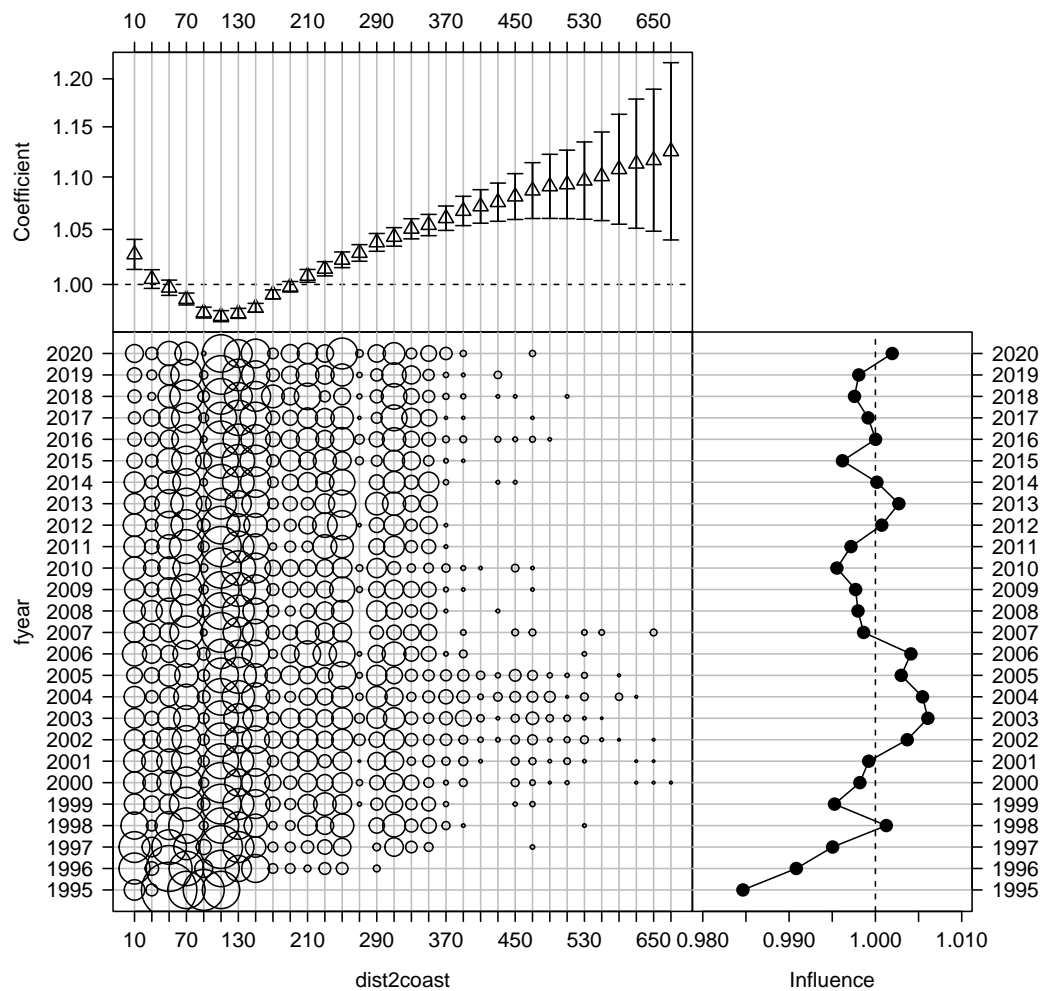


Figure B-65: Influence of distance to coast composition for the Australian fleet (bubble plot; bubbles scales by effort) on CPUE; influence (right hand plot) shows the standardising effect (a positive effect reduces the standardised CPUE by the equivalent amount). Estimated coefficients are given in the top panel.

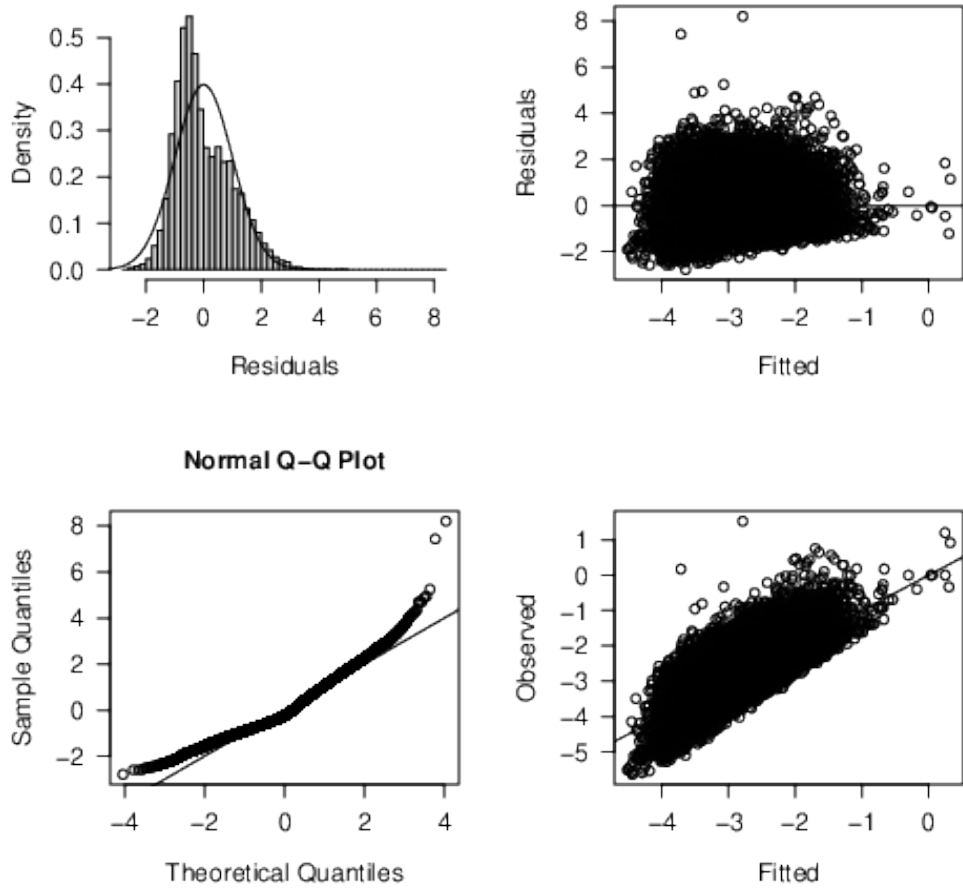


Figure B-66: Diagnostics for the log-normal CPUE standardisation model for the Australian fleet strata with positive catch.

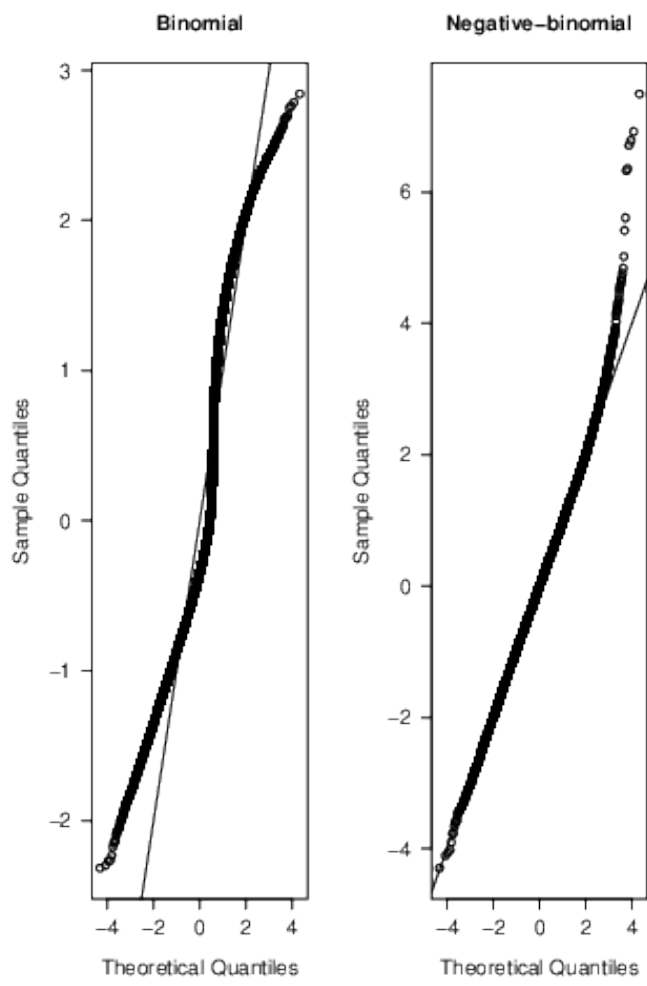


Figure B-67: Quantile residual diagnostics for the binomial component, as well as alternative CPUE standardisation models for the Australian fleet strata with positive catch.

B.3.3 Australia high latitude CPUE

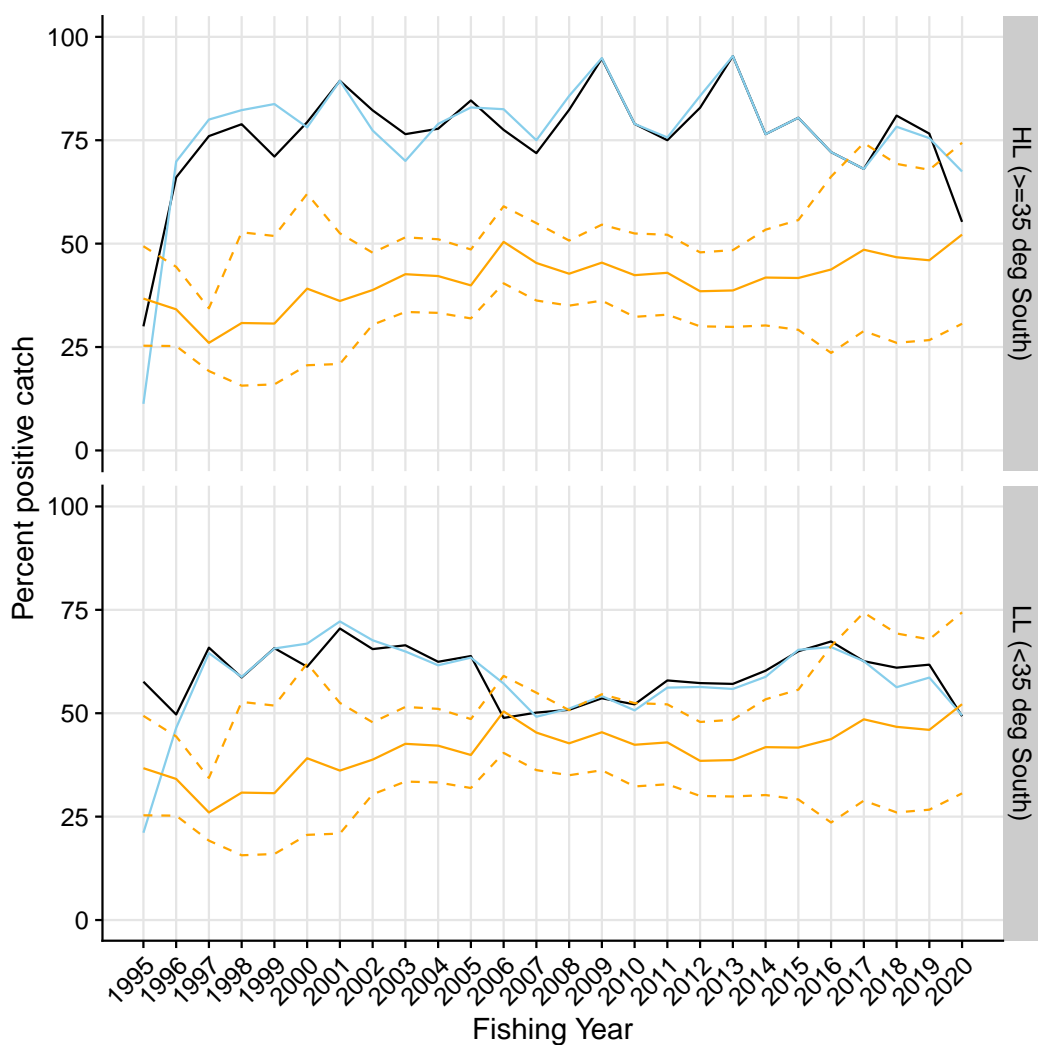


Figure B-68: Proportion of strata for the Australian fleet with positive catch by latitudinal stratum. Light blue are initial log-sheet records prior to filtering, the black line is the retained dataset after filtering for consistently reporting vessels. Where available, the corresponding values from observed strata is shown in orange.

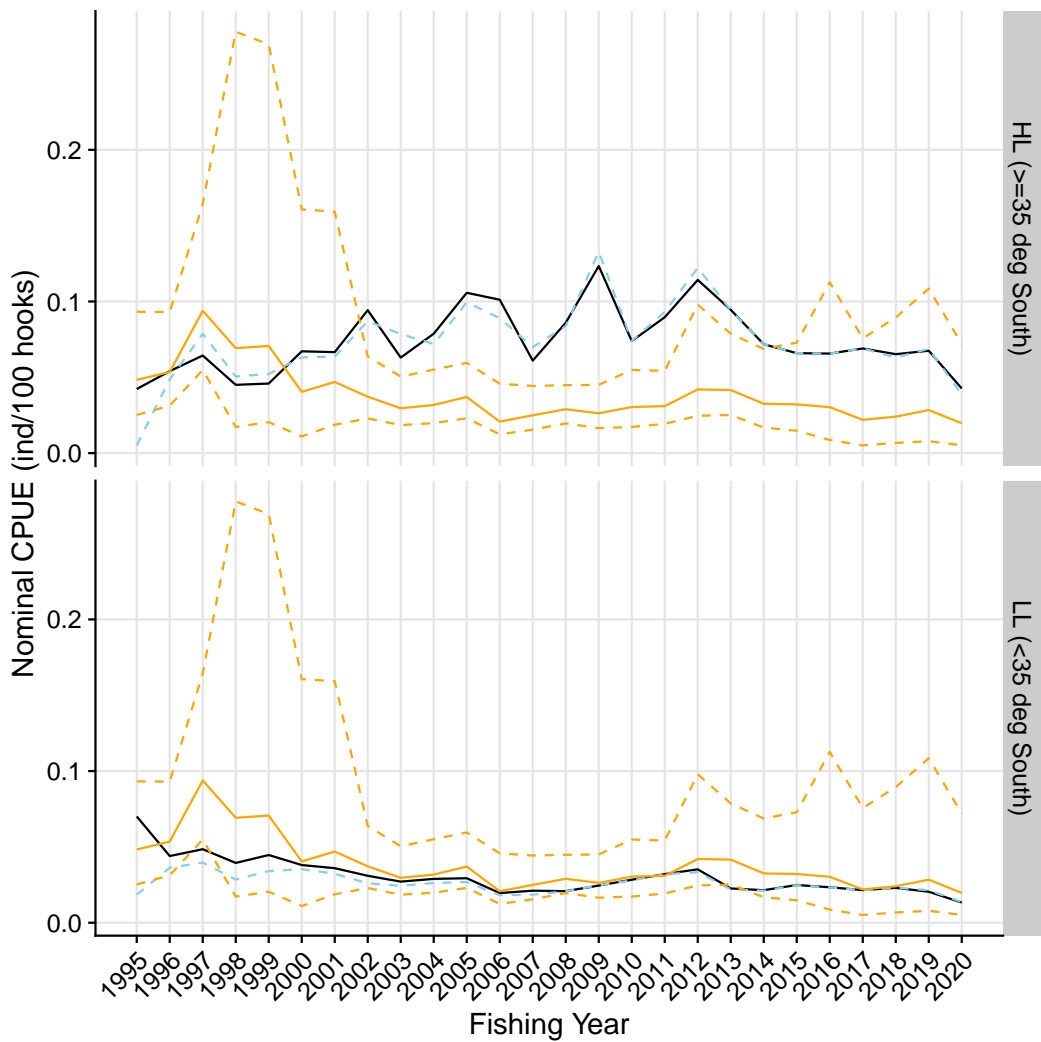


Figure B-69: Nominal CPUE (in number of blue shark per 100 hooks) strata of the Australian fleet with positive catch by latitudinal stratum. Light blue are initial log-sheet records prior to filtering, the black line is the retained dataset after filtering for consistently reporting vessels. Where available, the corresponding values from observed strata is shown in orange.

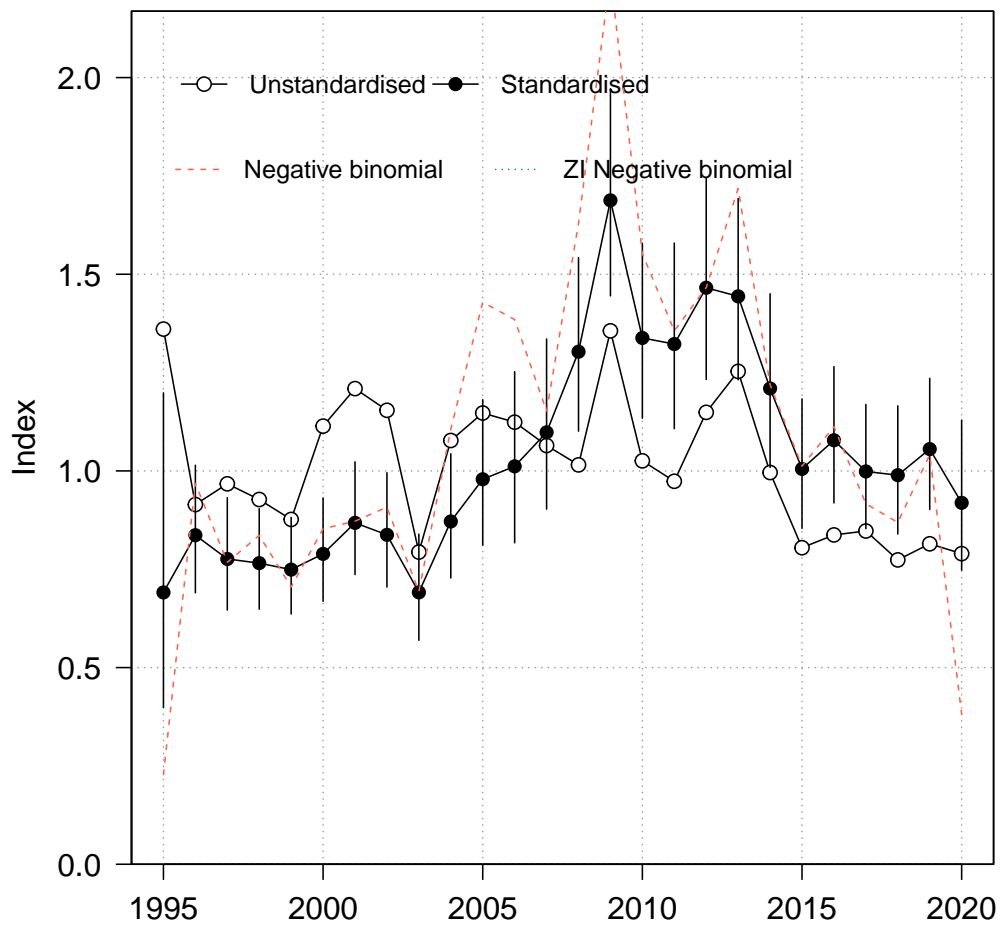


Figure B-70: Standardised (closed black circles with standard error) and unstandardised (open circles) CPUE indices for the Australian fleet strata with positive catch. Where successful (i.e., converged), standardised trends from a negative - binomial and zero - inflated negative binomial model run over the full dataset (including strata with zero values) are also shown for comparison.

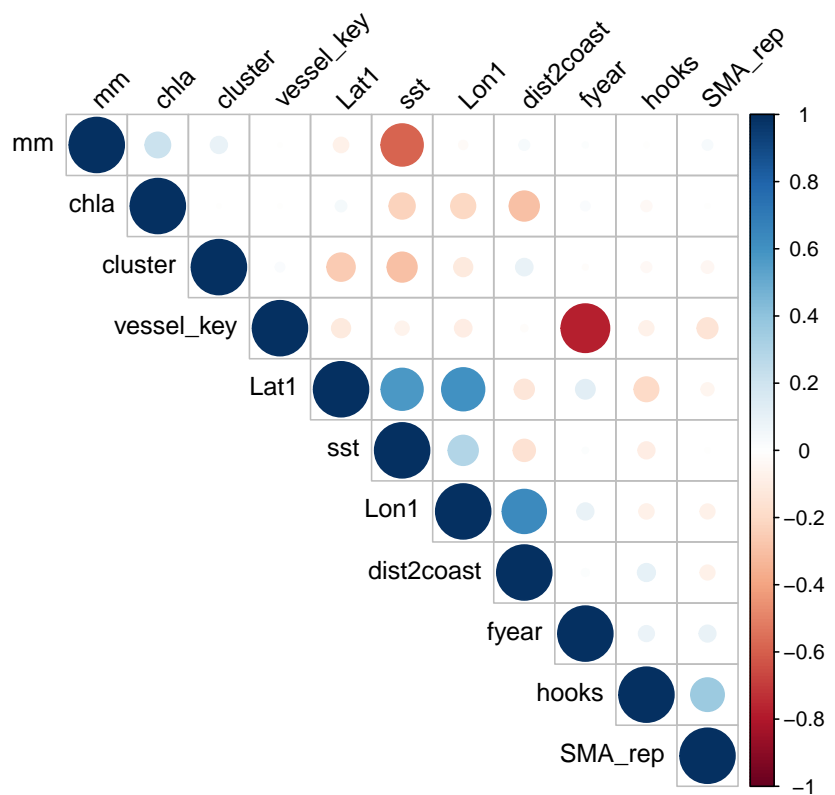


Figure B-71: Correlations amongst potential covariates for CPUE standardisation in the Australian fleet. Where necessary, variables were removed to reduce redundancy in the models.

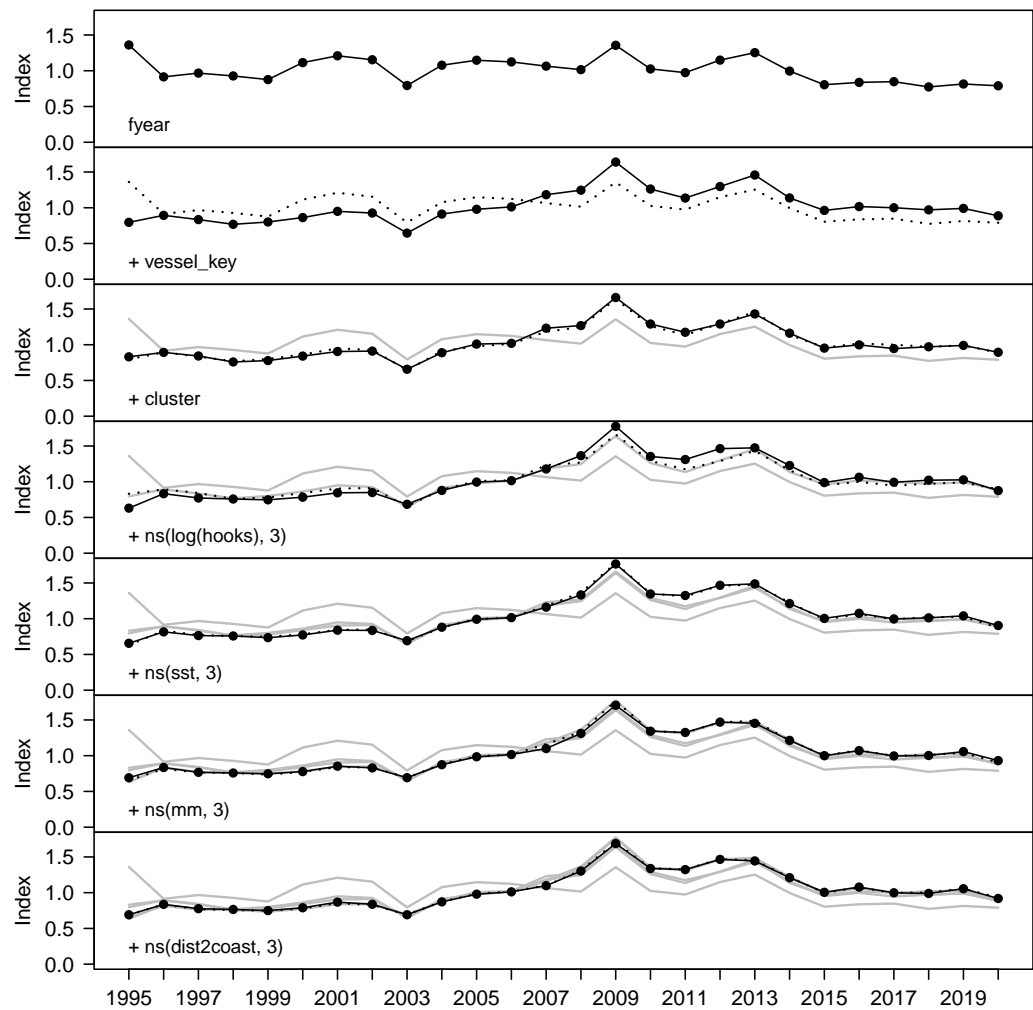


Figure B-72: Step plot for the Australian fleet CPUE, showing sequential standardising effects of variables included in the standardisation model.

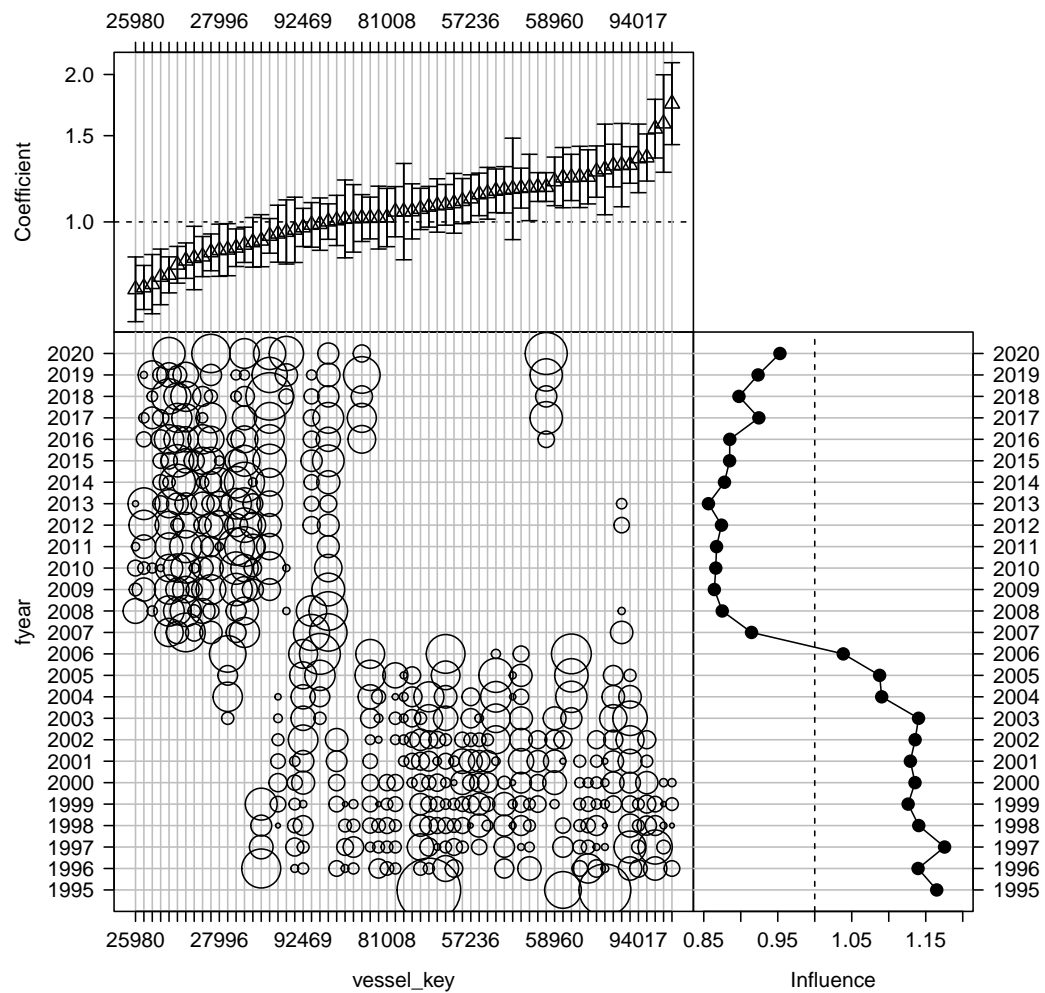


Figure B-73: Influence of fleet composition (vessel keys) for the Australian fleet (bubble plot; bubbles scales by effort) on CPUE; influence (right) shows the standardising effect (a positive effect reduces the standardised CPUE by the equivalent amount). Estimated coefficients are given in the top panel.

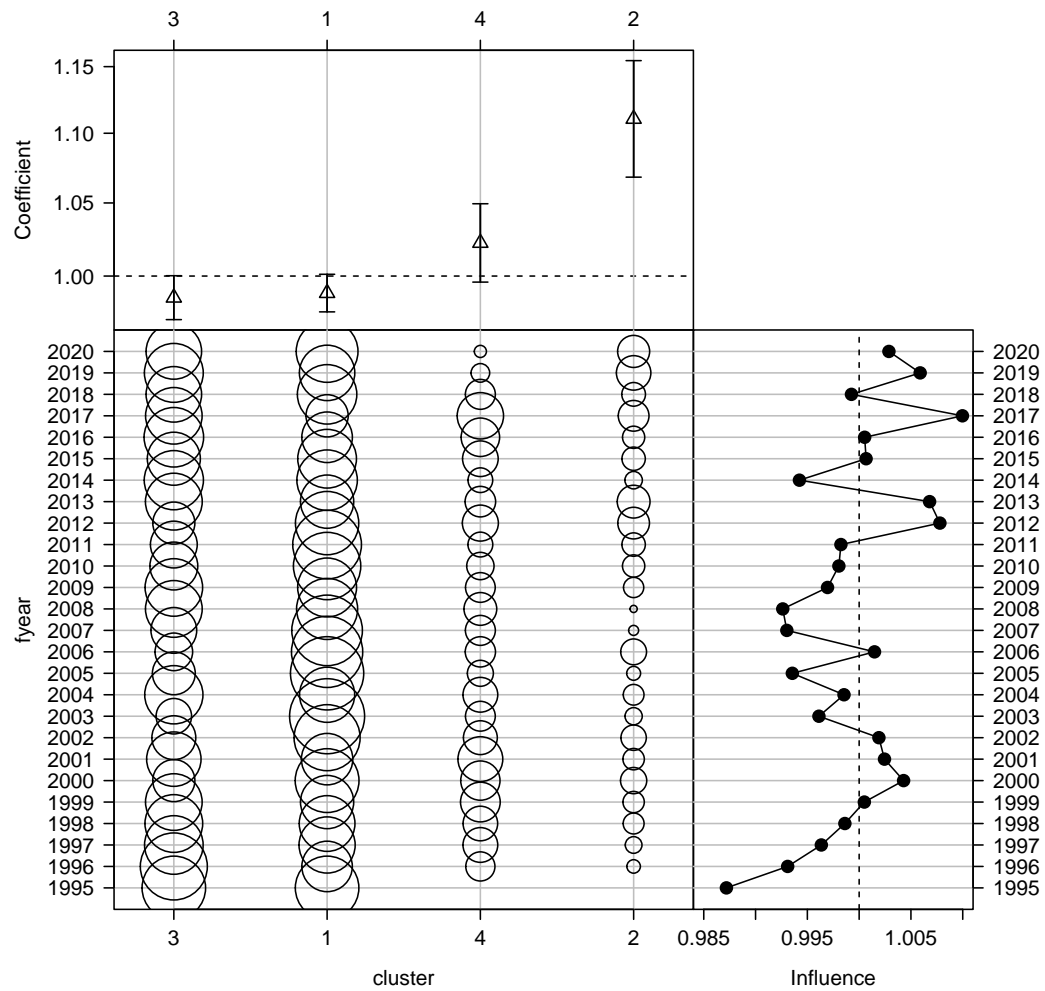


Figure B-74: Influence of targeting cluster for the Australian fleet (bubble plot; bubbles scales by effort) on CPUE; influence (right hand plot) shows the standardising effect (a positive effect reduces the standardised CPUE by the equivalent amount). Estimated coefficients are given in the top panel.

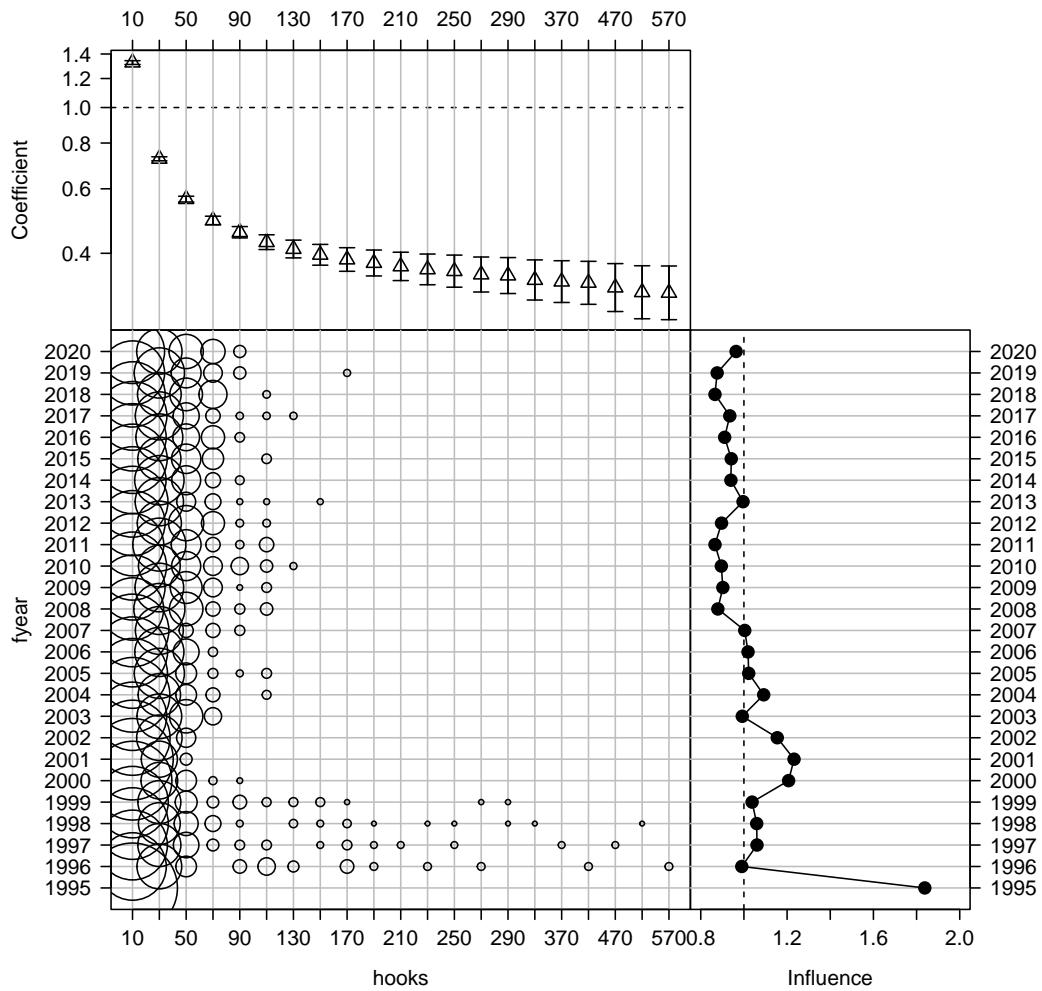


Figure B-75: Influence of number of hooks set per stratum for the Australian fleet (bubble plot; bubbles scales by effort) on CPUE; influence (right hand plot) shows the standardising effect (a positive effect reduces the standardised CPUE by the equivalent amount). Estimated coefficients are given in the top panel.

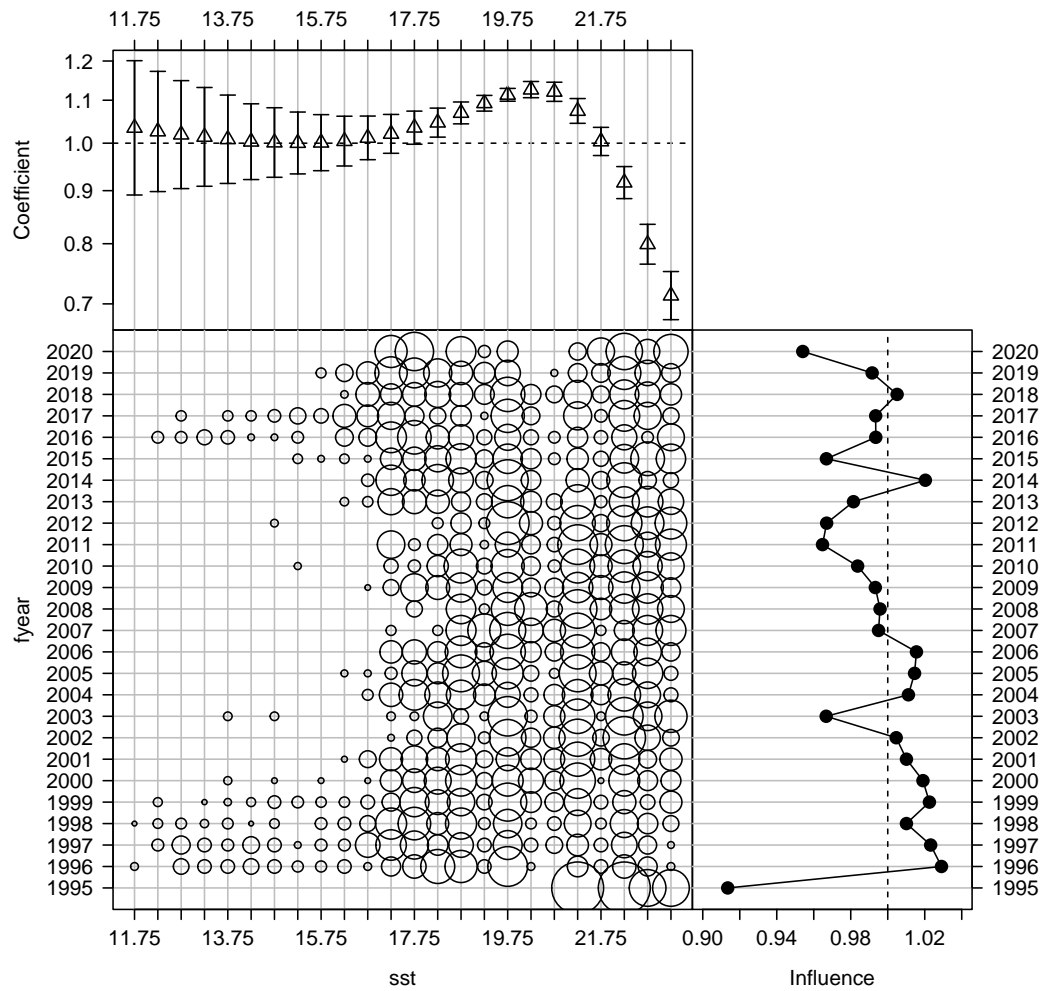


Figure B-76: Influence of sea surface temperature (SST, in degrees Celsius) for the Australian fleet (bubble plot; bubbles scales by effort) on CPUE; influence (right hand plot) shows the standardising effect (a positive effect reduces the standardised CPUE by the equivalent amount). Estimated coefficients are given in the top panel.

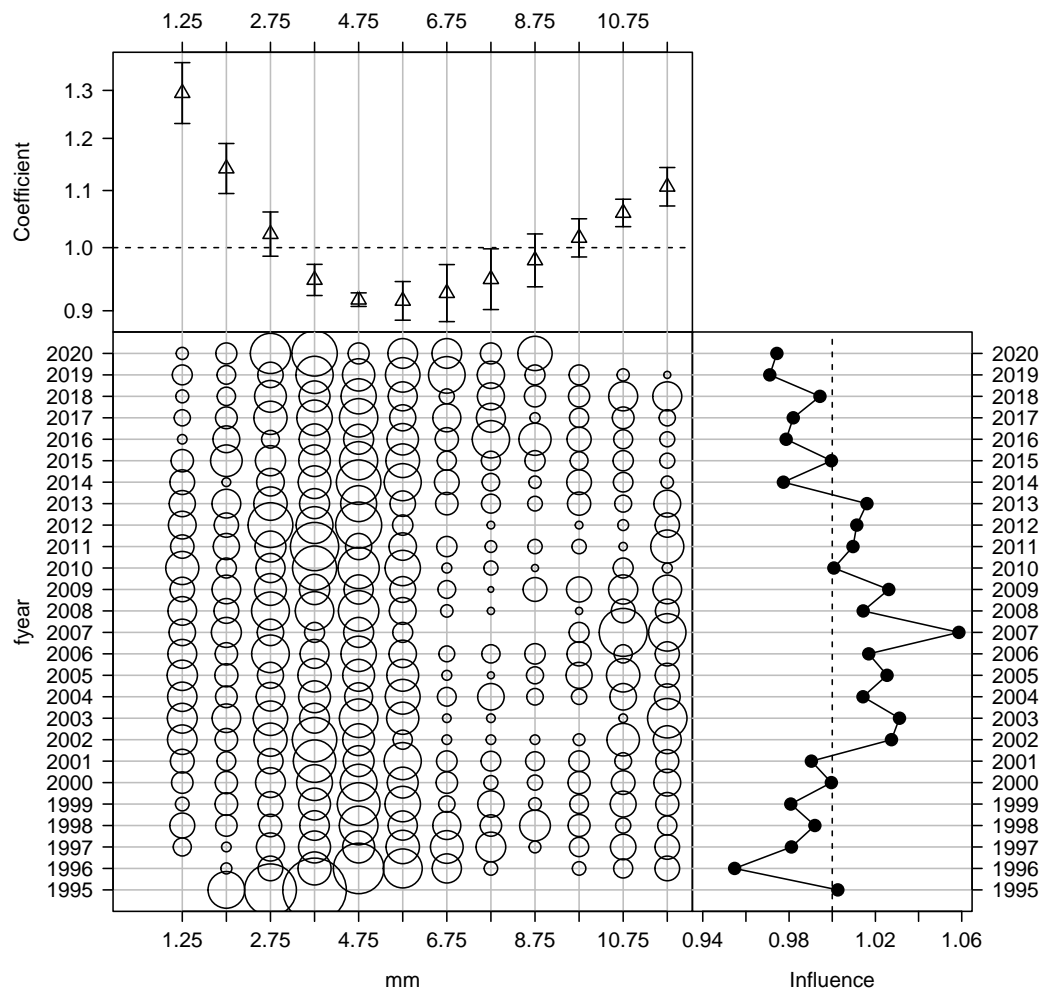


Figure B-77: Influence of month for the Australian fleet (bubble plot; bubbles scales by effort) on CPUE; influence (right hand plot) shows the standardising effect (a positive effect reduces the standardised CPUE by the equivalent amount). Estimated coefficients are given in the top panel.

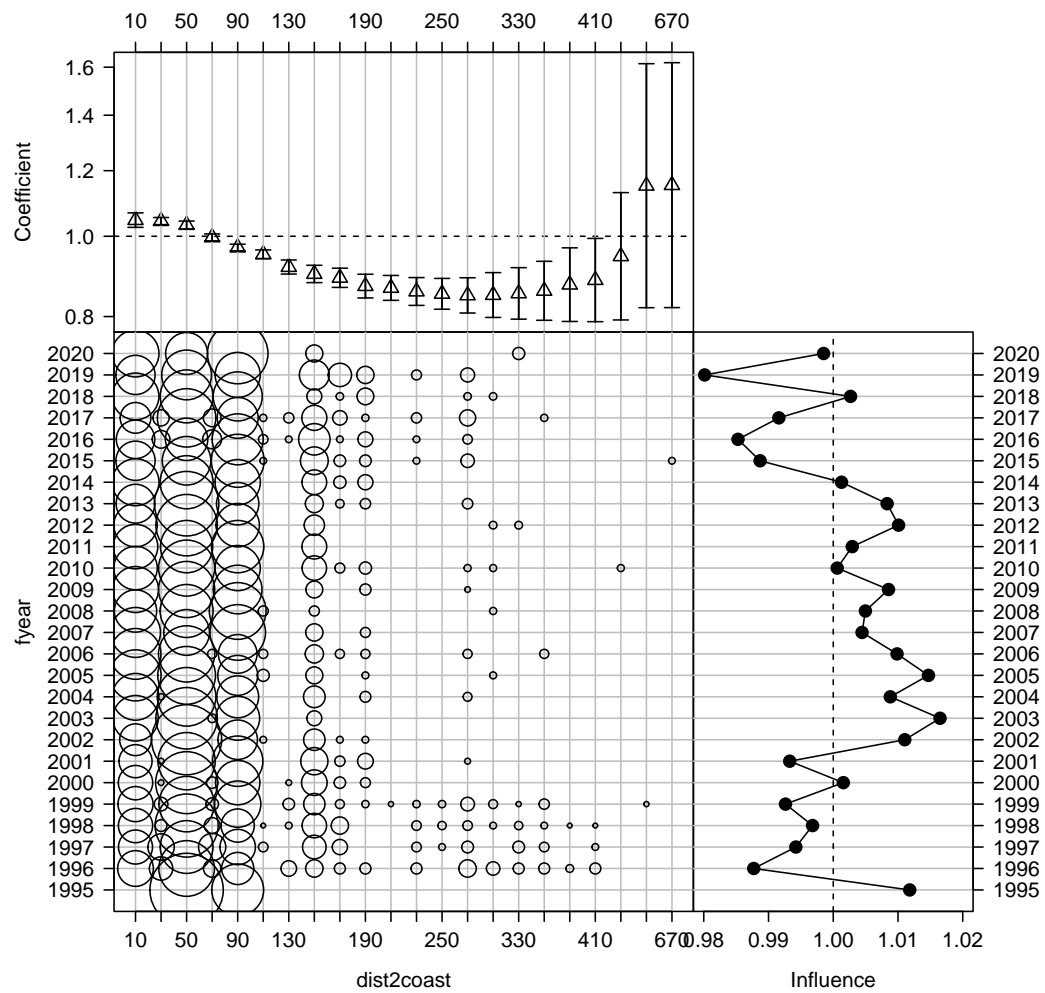


Figure B-78: Influence of distance to coast composition for the Australian fleet (bubble plot; bubbles scales by effort) on CPUE; influence (right hand plot) shows the standardising effect (a positive effect reduces the standardised CPUE by the equivalent amount). Estimated coefficients are given in the top panel.

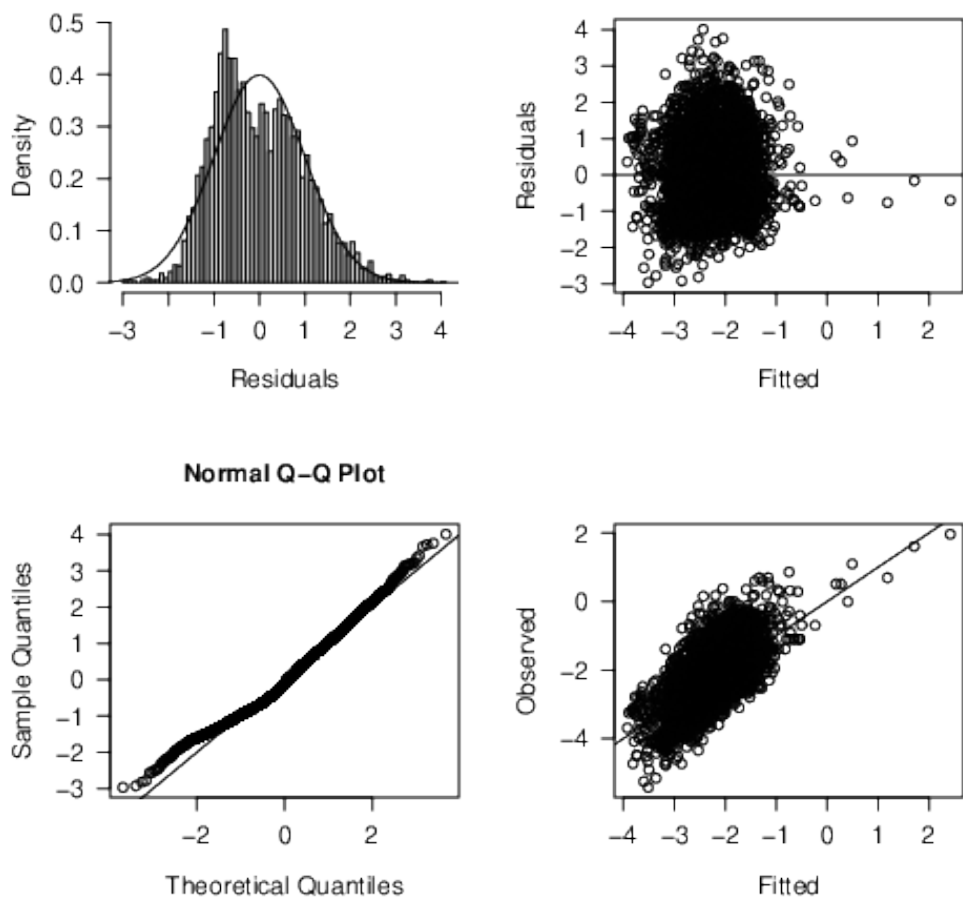


Figure B-79: Diagnostics for the log-normal CPUE standardisation model for the Australian fleet strata with positive catch.

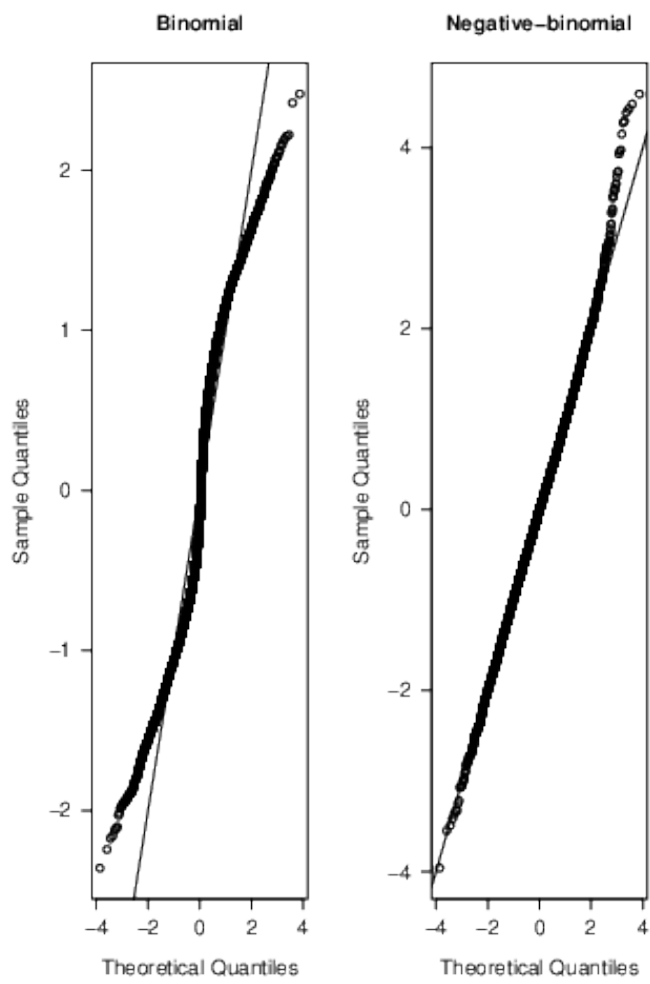


Figure B-80: Quantile residual diagnostics for the binomial component, as well as alternative CPUE standardisation models for the Australian fleet strata with positive catch.

B.3.4 Fiji low latitude CPUE

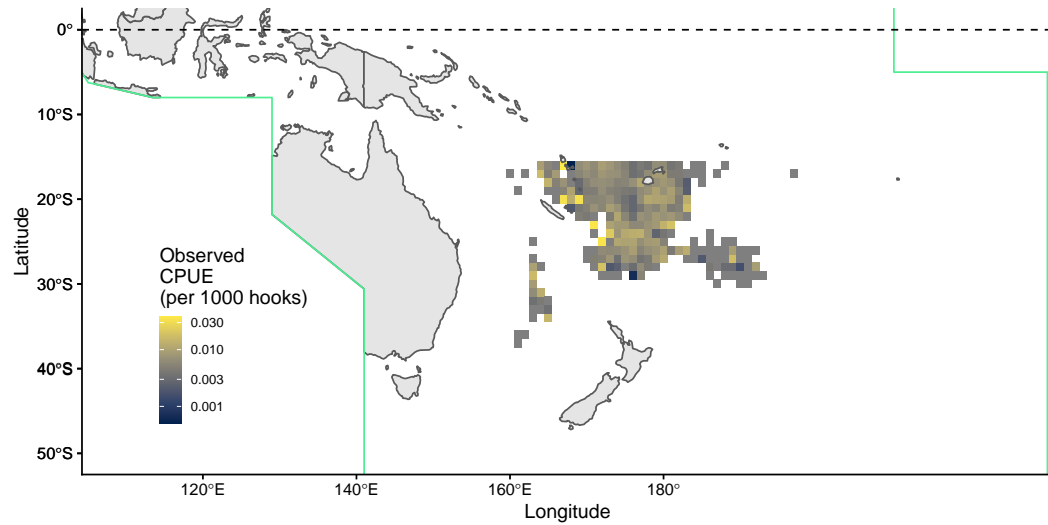


Figure B-81: Maps of average catch rates (CPUE; in number of shortfin mako shark per 100 hooks) for the Fijian longline fleet.

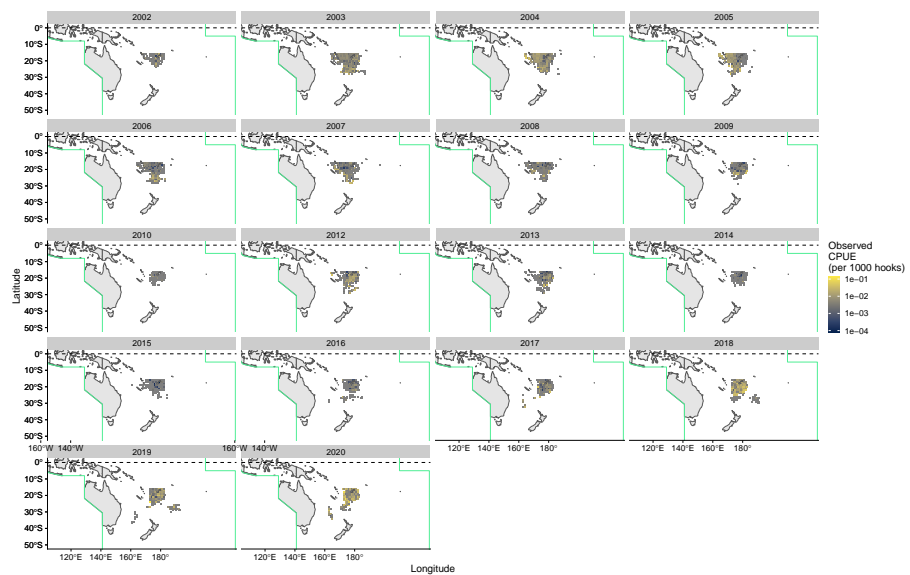


Figure B-82: Maps of average catch rates (CPUE; in number of shortfin mako shark per 100 hooks) by year for the Fijian longline fleet.

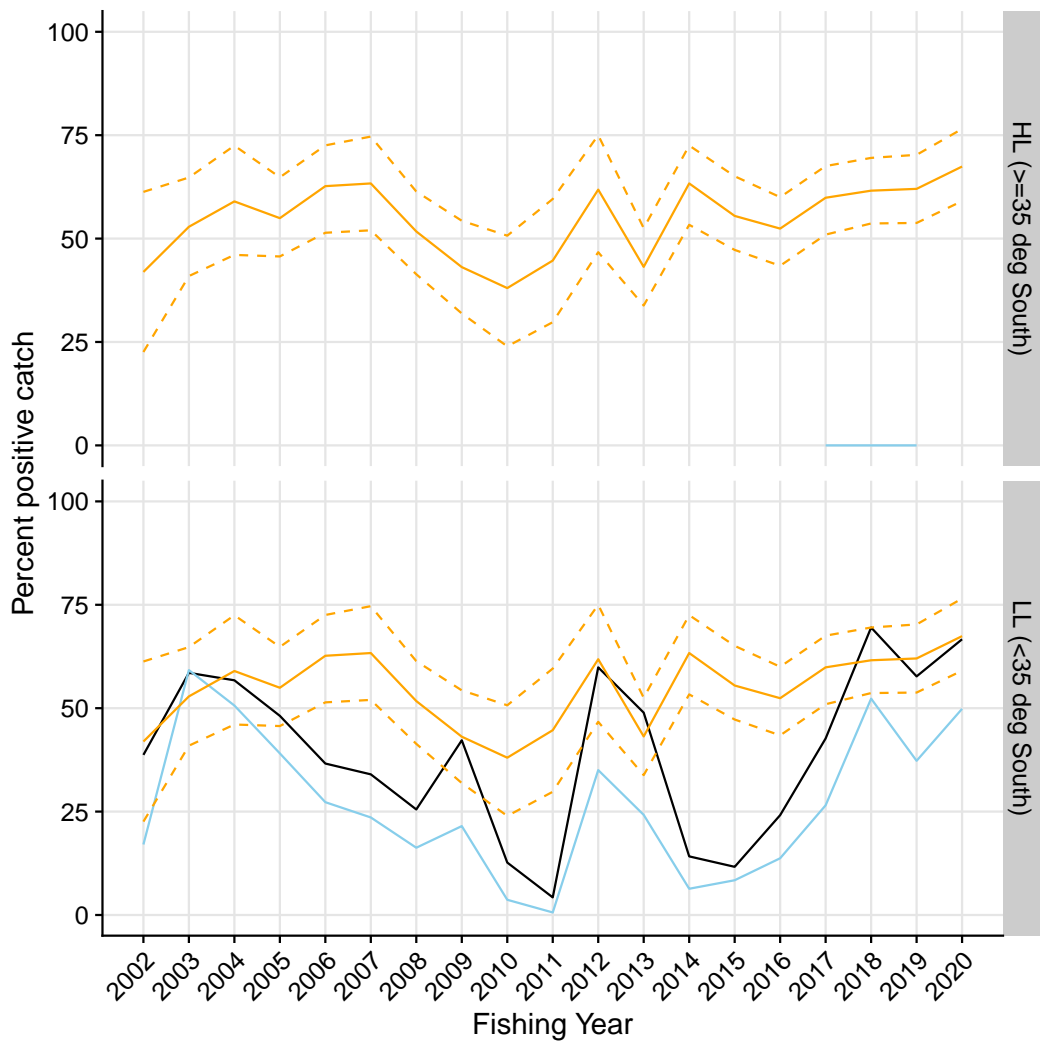


Figure B-83: Proportion of strata for the Fijian fleet with positive catch by latitudinal stratum. Light blue are initial log-sheet records prior to filtering, the black line is the retained dataset after filtering for consistently reporting vessels. Where available, the corresponding values from observed strata is shown in orange.

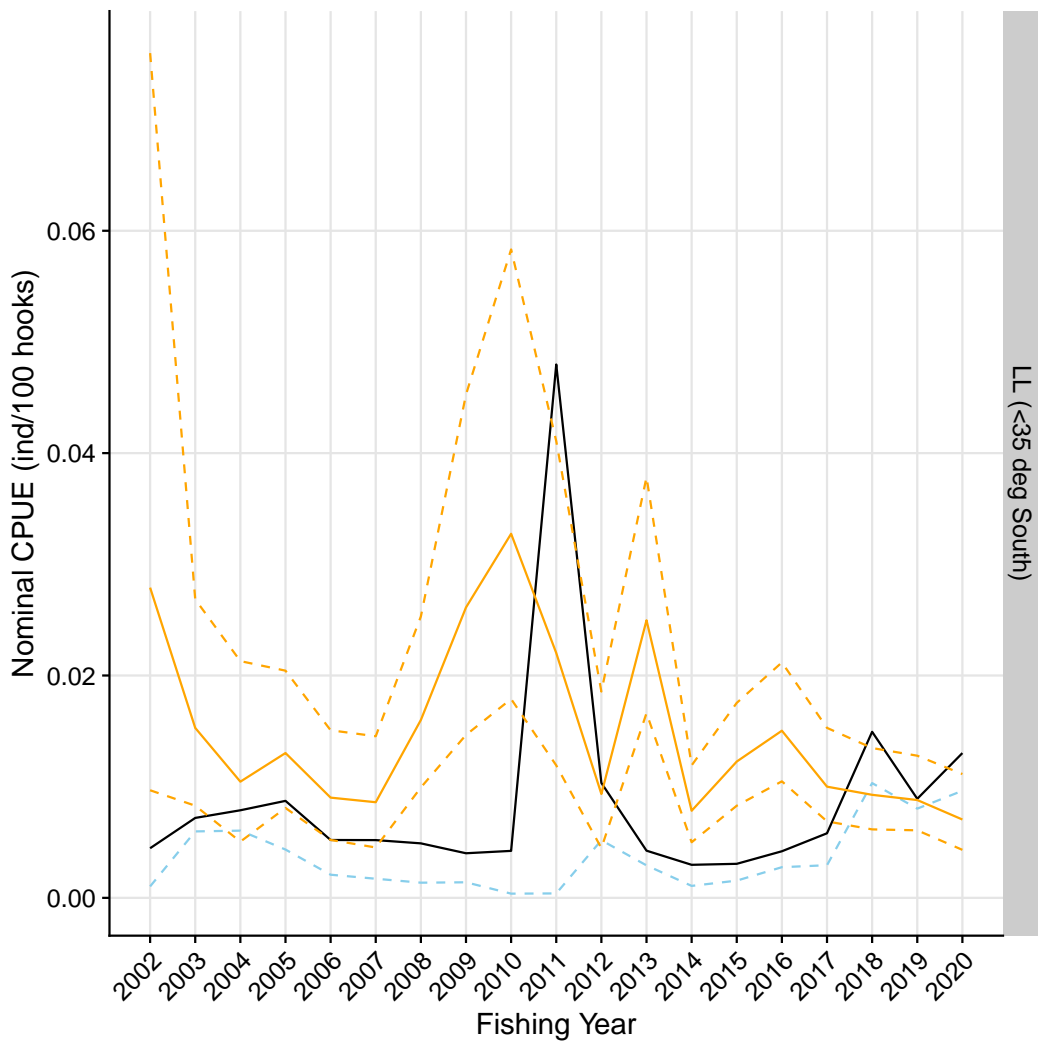


Figure B-84: Nominal CPUE (in number of blue shark per 100 hooks) strata of the Fijian fleet with positive catch by latitudinal stratum. Light blue are initial log-sheet records prior to filtering, the black line is the retained dataset after filtering for consistently reporting vessels. Where available, the corresponding values from observed strata is shown in orange.

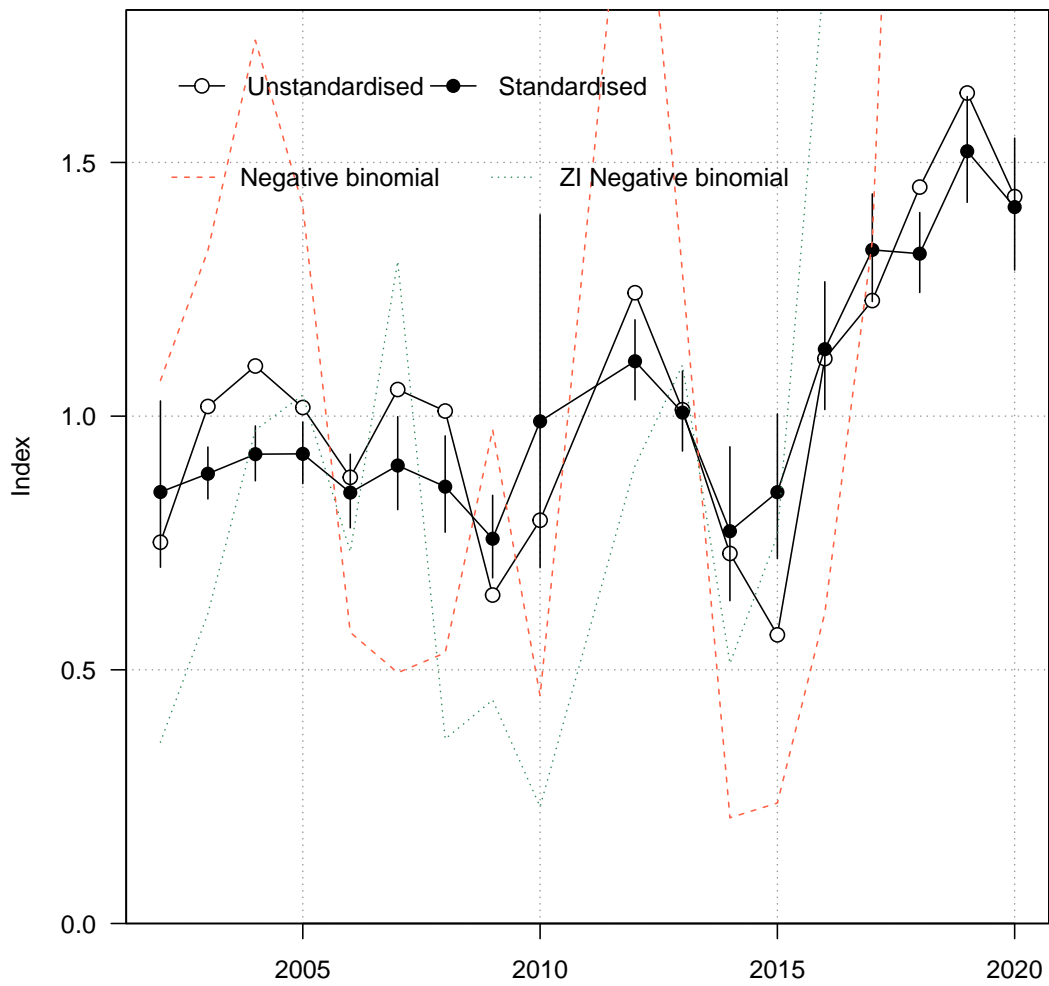


Figure B-85: Standardised (closed black circles with standard error) and unstandardised (open circles) CPUE indices for the Fijian fleet strata with positive catch. Where successful (i.e., converged), standardised trends from a negative - binomial and zero - inflated negative binomial model run over the full dataset (including strata with zero values) are also shown for comparison.

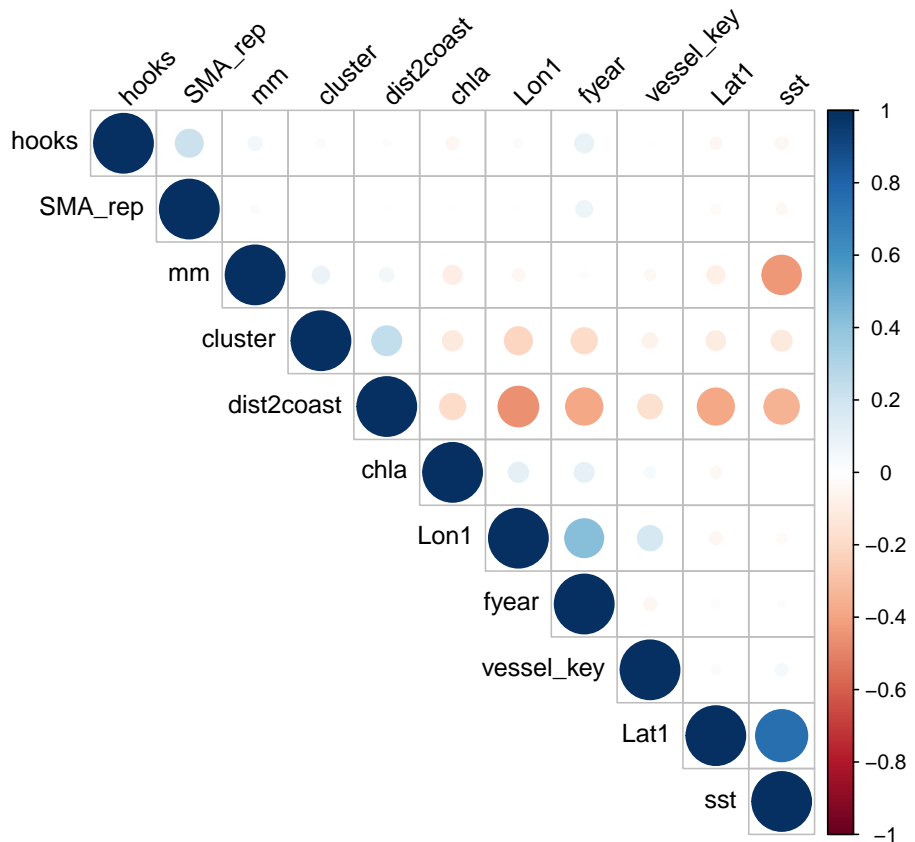


Figure B-86: Correlations amongst potential covariates for CPUE standardisation in the Fijian fleet. Where necessary, variables were removed to reduce redundancy in the models.

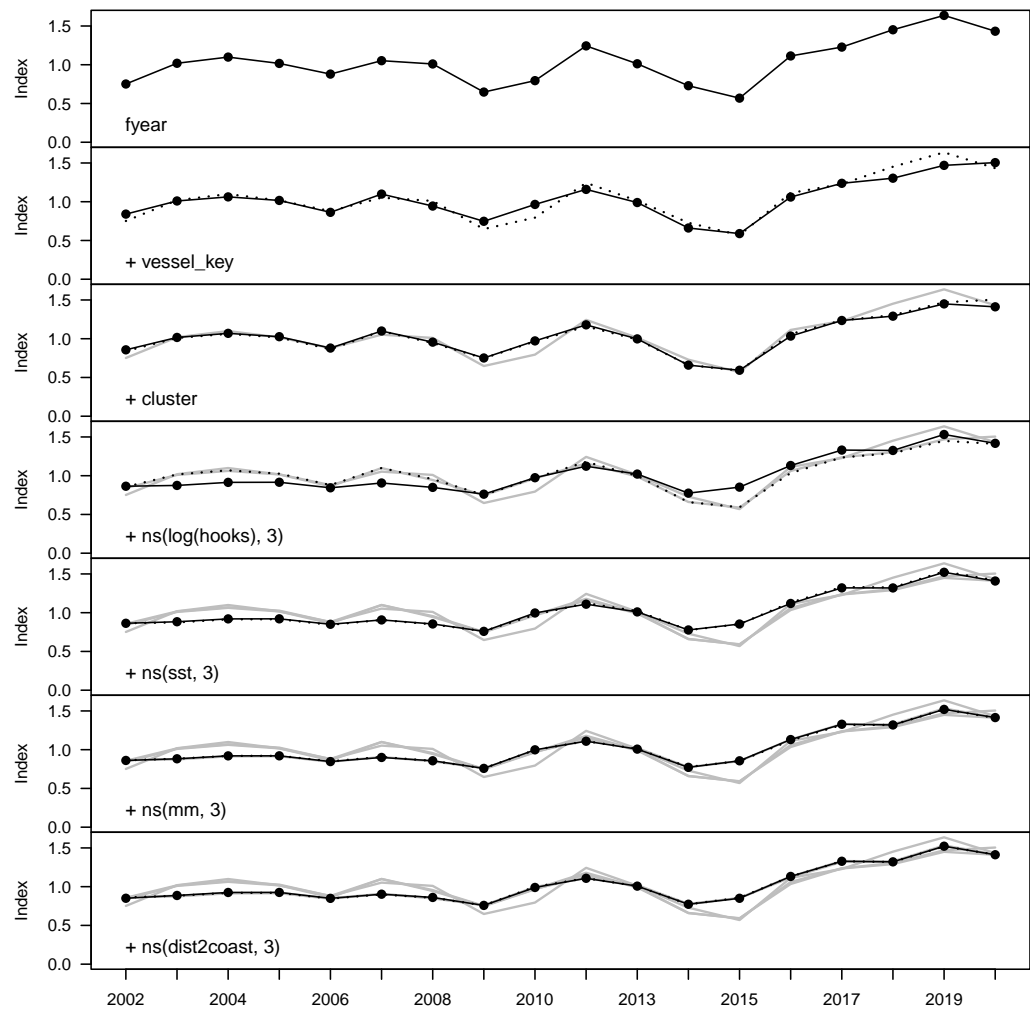


Figure B-87: Step plot for the Fijian fleet CPUE, showing sequential standardising effects of variables included in the standardisation model.

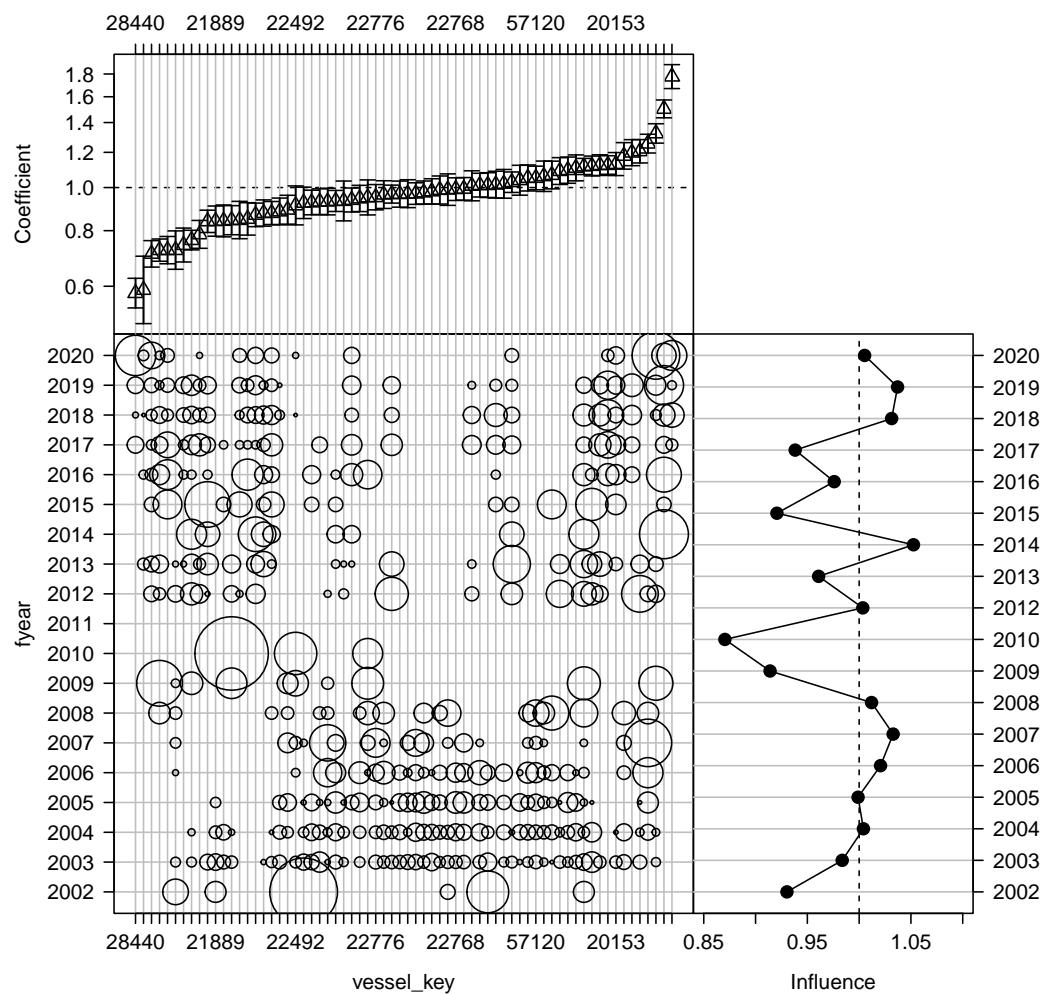


Figure B-88: Influence of fleet composition (vessel keys) for the Fijian fleet (bubble plot; bubbles scales by effort) on CPUE; influence (right) shows the standardising effect (a positive effect reduces the standardised CPUE by the equivalent amount). Estimated coefficients are given in the top panel.

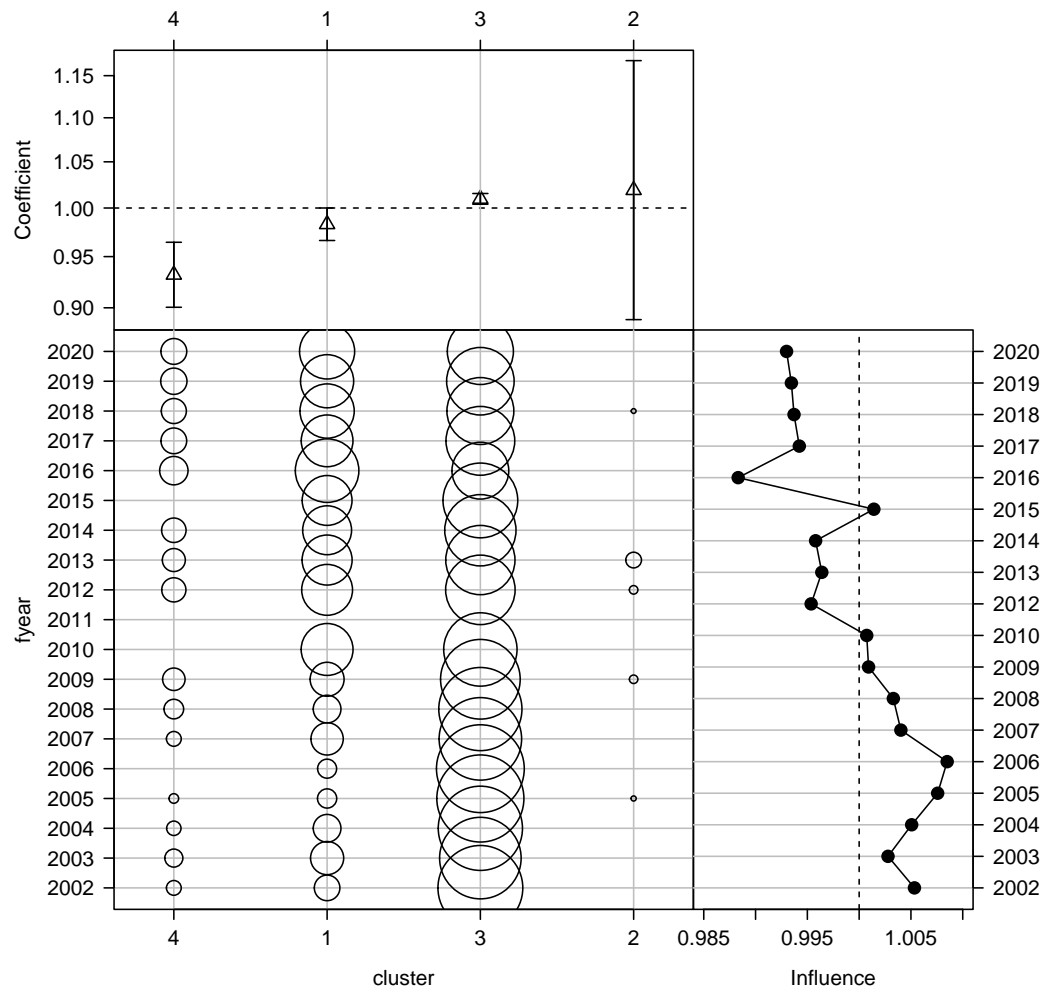


Figure B-89: Influence of targeting cluster for the Fijian fleet (bubble plot; bubbles scales by effort) on CPUE; influence (right hand plot) shows the standardising effect (a positive effect reduces the standardised CPUE by the equivalent amount). Estimated coefficients are given in the top panel.

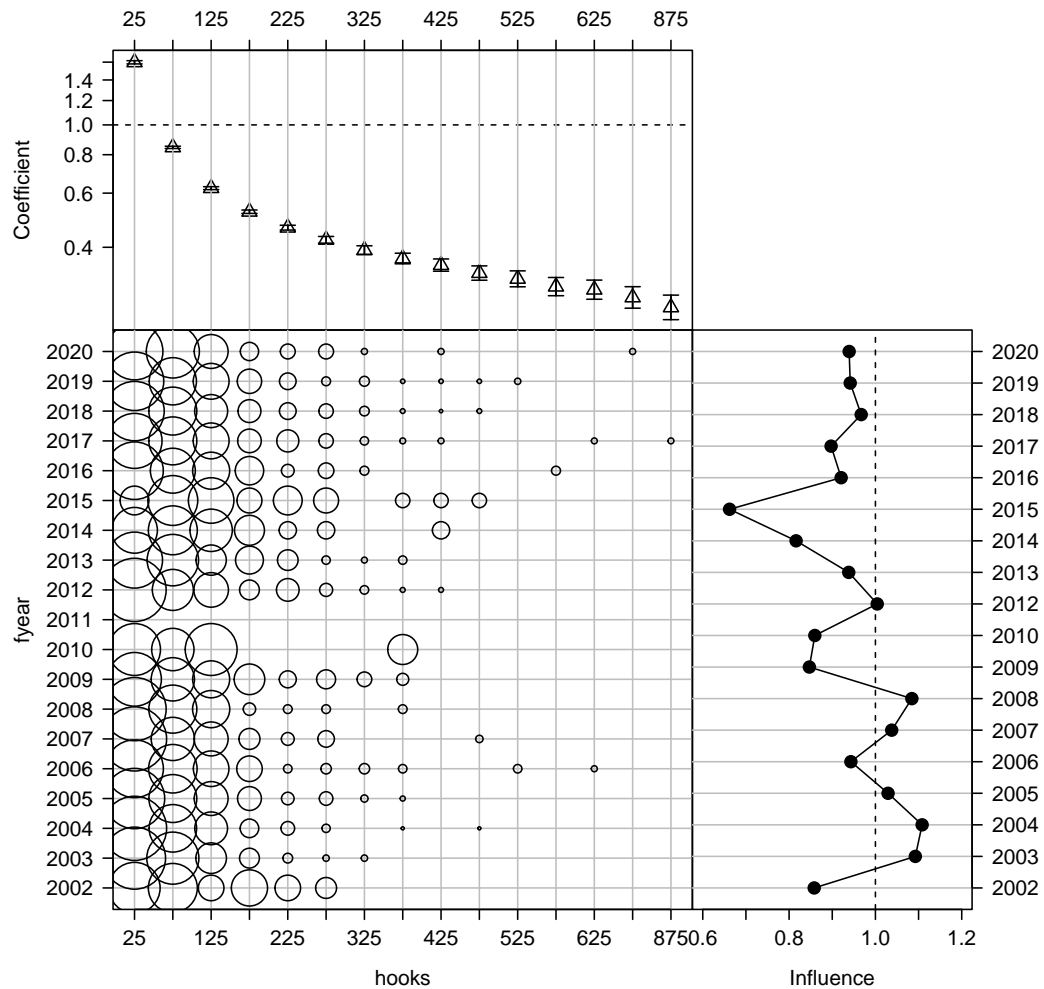


Figure B-90: Influence of number of hooks set per stratum for the Fijian fleet (bubble plot; bubbles scales by effort) on CPUE; influence (right hand plot) shows the standardising effect (a positive effect reduces the standardised CPUE by the equivalent amount). Estimated coefficients are given in the top panel.

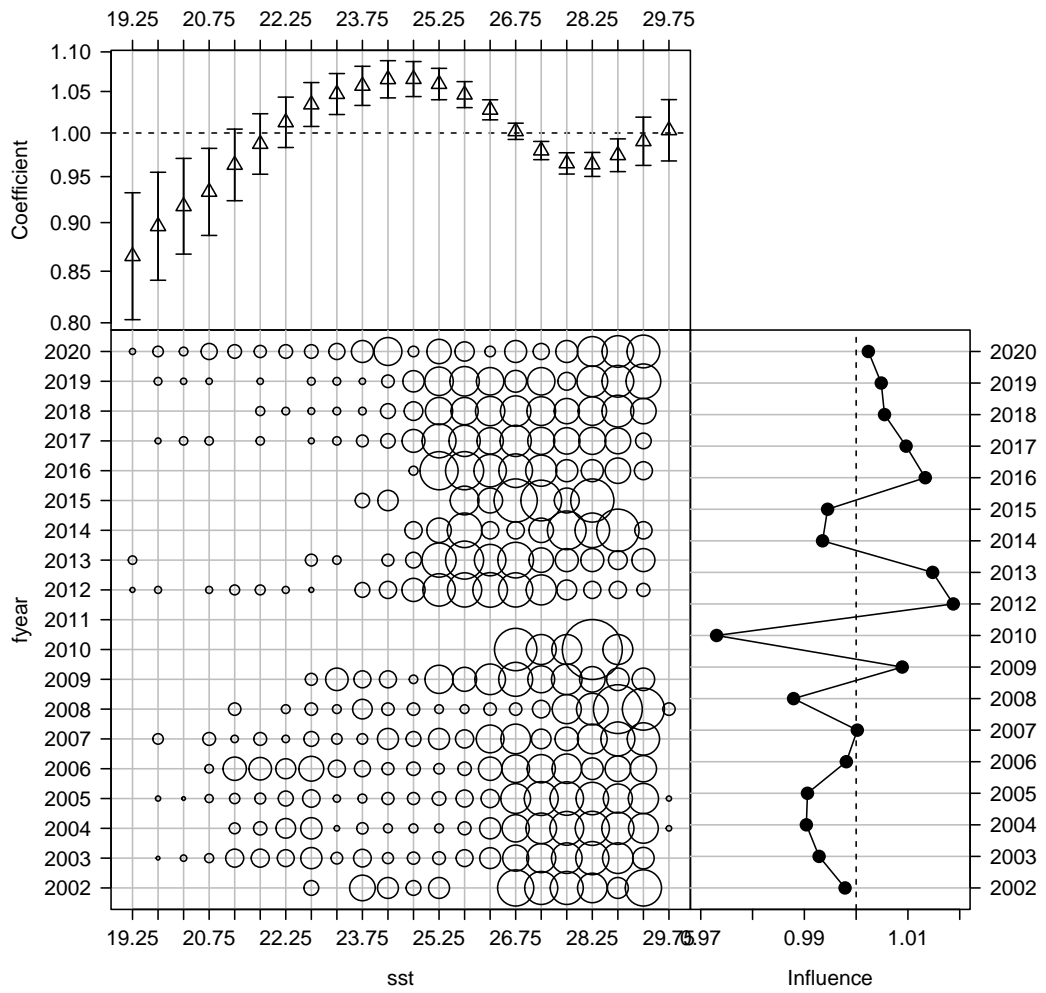


Figure B-91: Influence of sea surface temperature (SST, in degrees Celsius) for the Fijian fleet (bubble plot; bubbles scales by effort) on CPUE; influence (right hand plot) shows the standardising effect (a positive effect reduces the standardised CPUE by the equivalent amount). Estimated coefficients are given in the top panel.

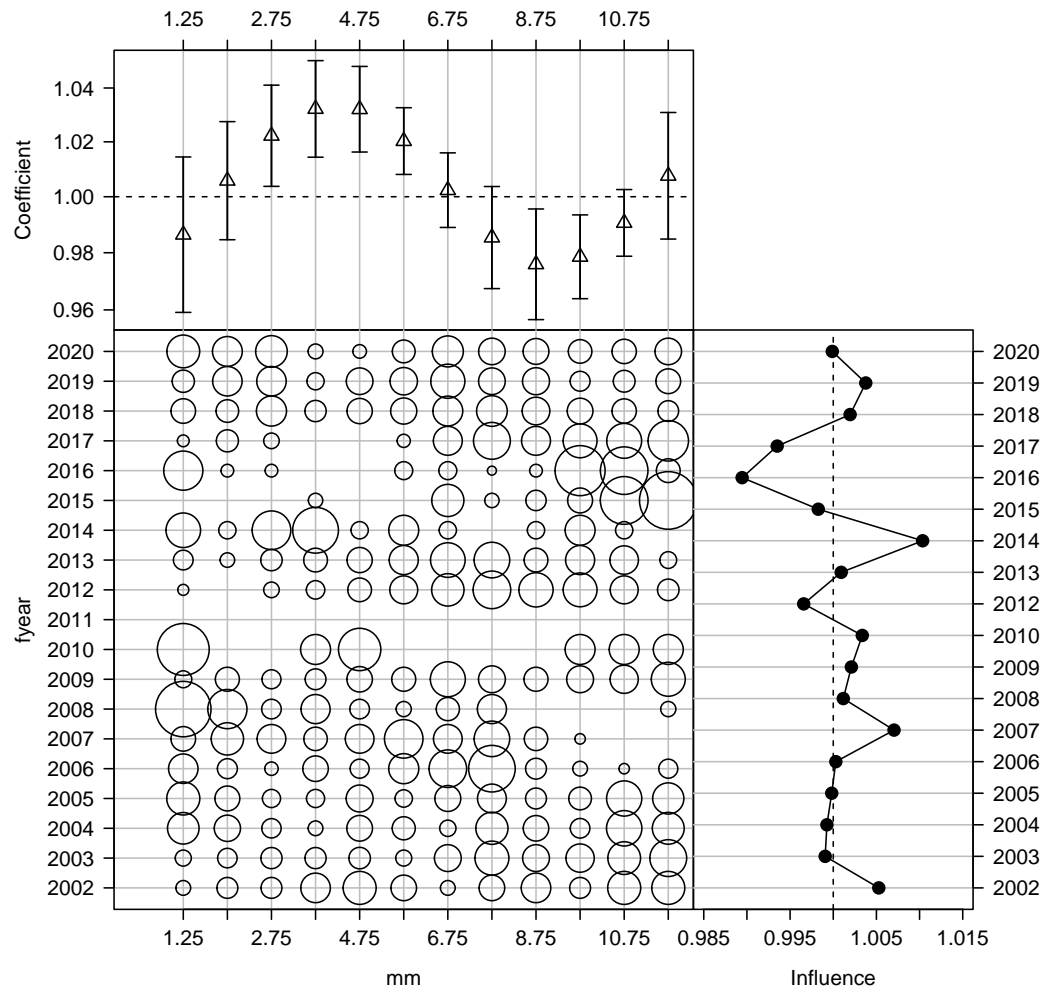


Figure B-92: Influence of month for the Fijian fleet (bubble plot; bubbles scales by effort) on CPUE; influence (right hand plot) shows the standardising effect (a positive effect reduces the standardised CPUE by the equivalent amount). Estimated coefficients are given in the top panel.

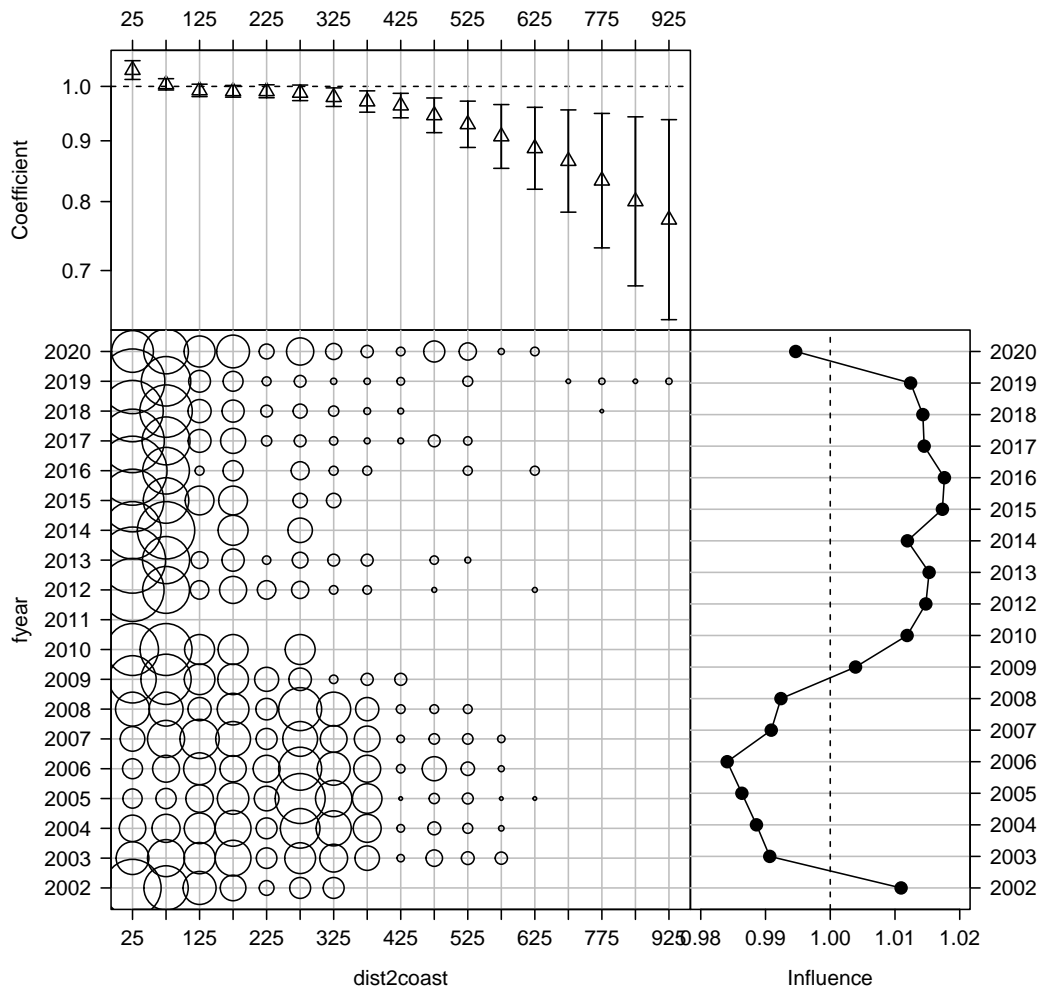


Figure B-93: Influence of distance to coast composition for the Fijian fleet (bubble plot; bubbles scales by effort) on CPUE; influence (right hand plot) shows the standardising effect (a positive effect reduces the standardised CPUE by the equivalent amount). Estimated coefficients are given in the top panel.

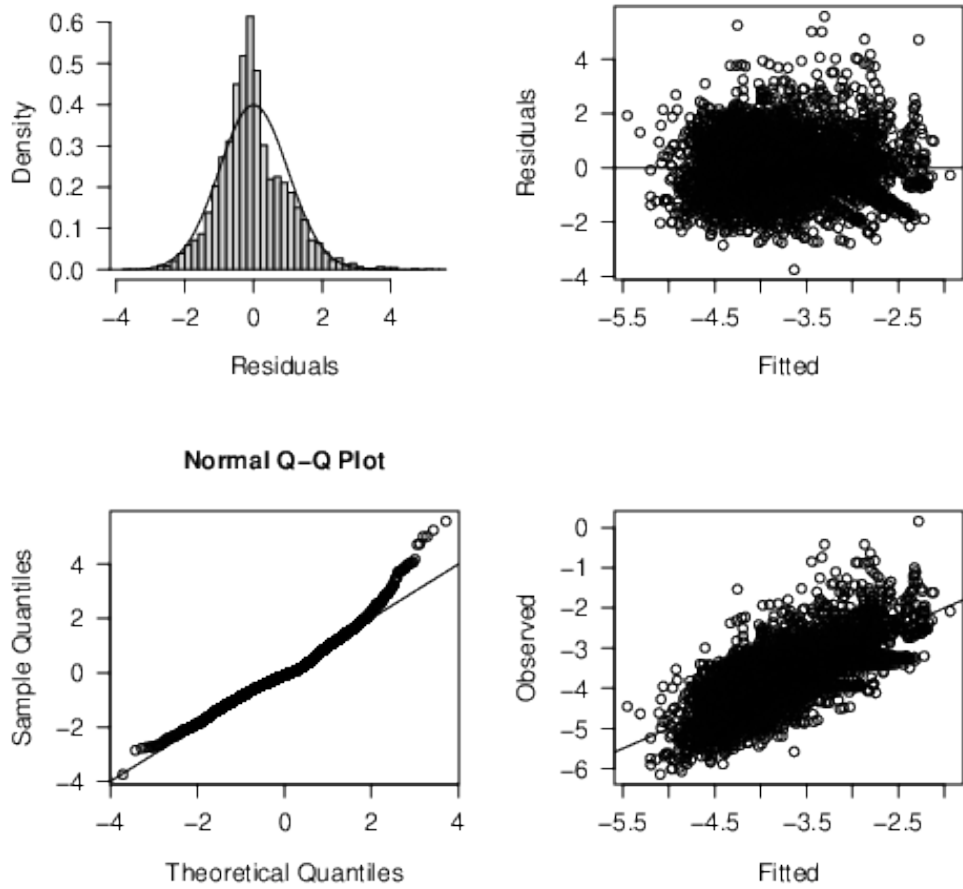


Figure B-94: Diagnostics for the log - normal CPUE standardisation model for the Fijian fleet strata with positive catch.

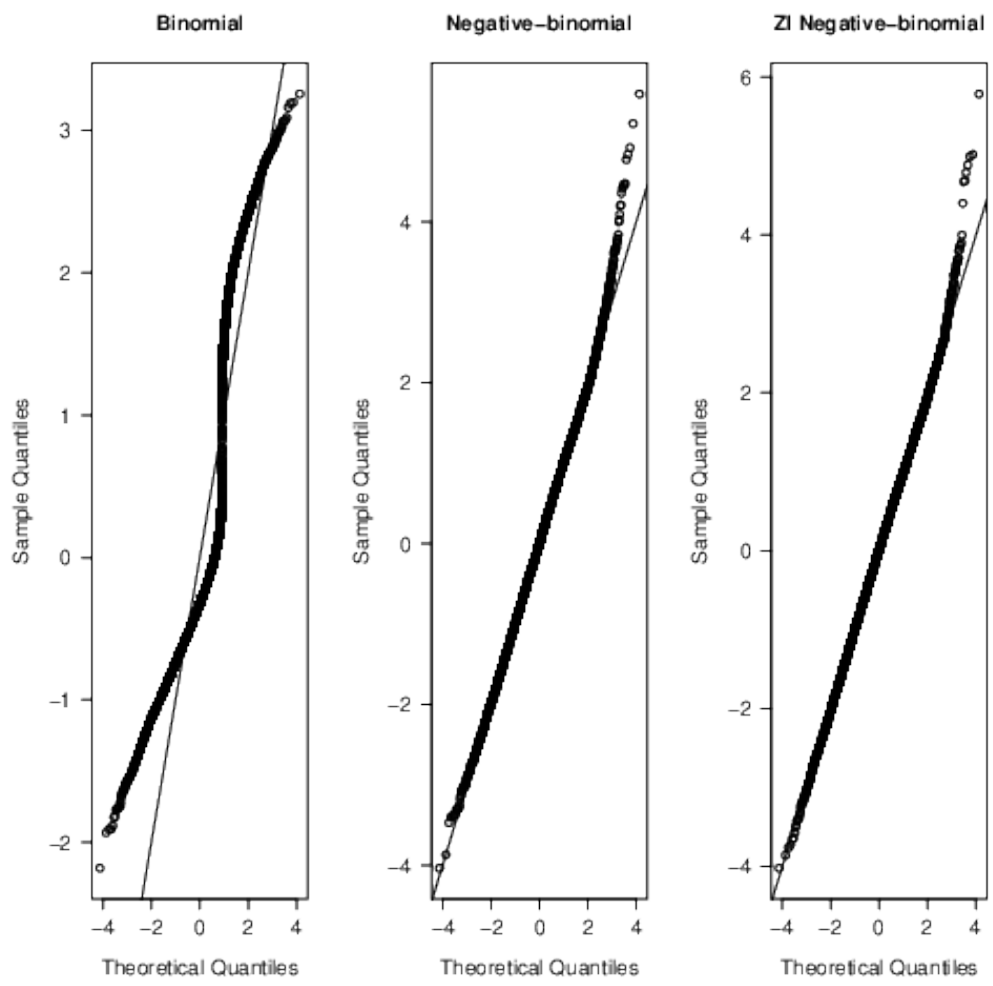


Figure B-95: Quantile residual diagnostics for the binomial component, as well as alternative CPUE standardisation models for the Fijian fleet strata with positive catch.

B.3.5 Combined low latitude CPUE

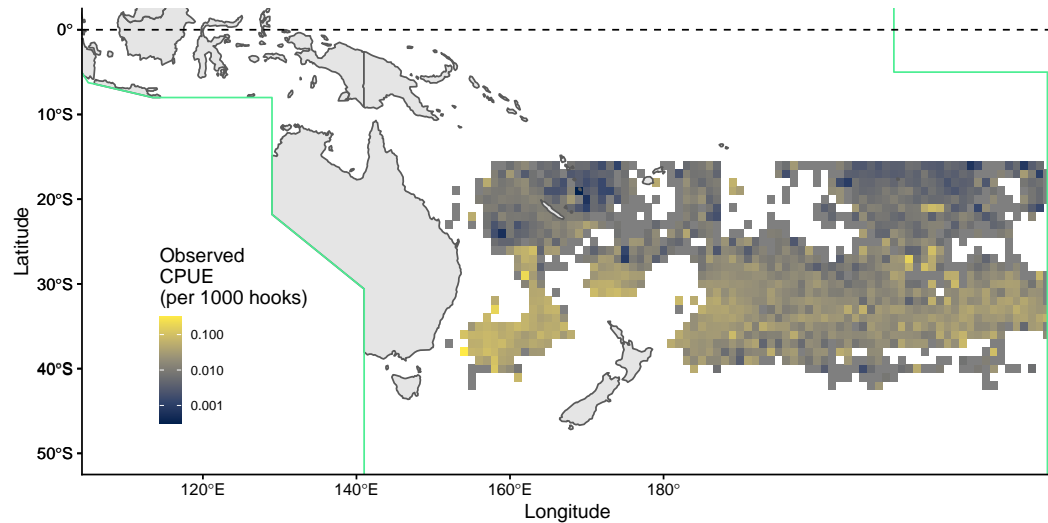


Figure B-96: Maps of average catch rates (CPUE; in number of shortfin mako shark per 1000 hooks) for the distant water longline fleet.

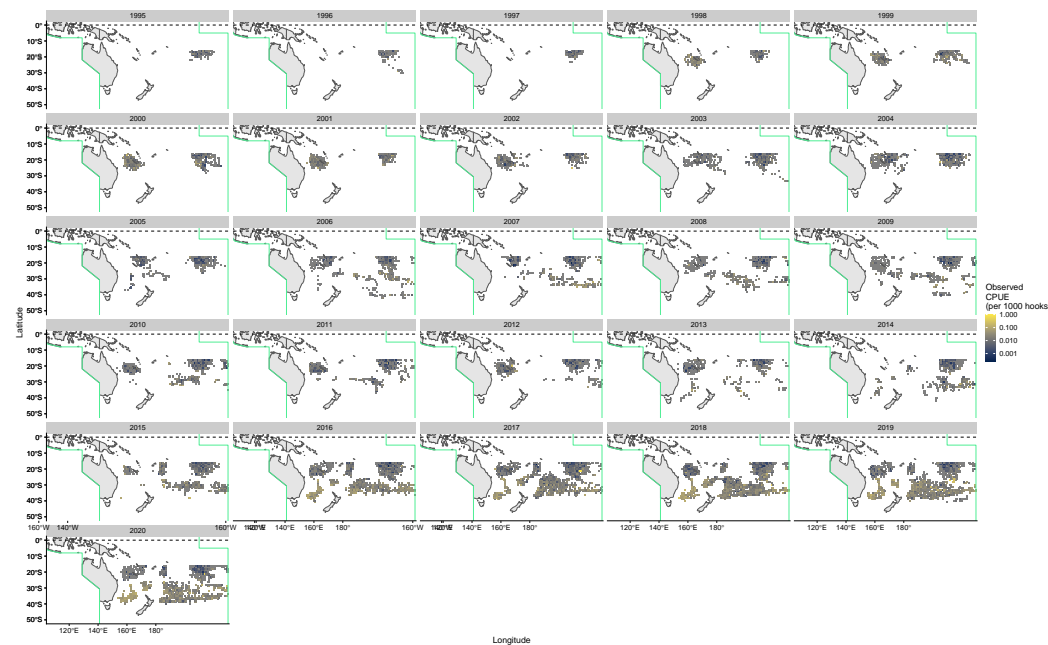


Figure B-97: Maps of average catch rates (CPUE; in number of shortfin mako shark per 100 hooks) by year for the distant water longline fleet.

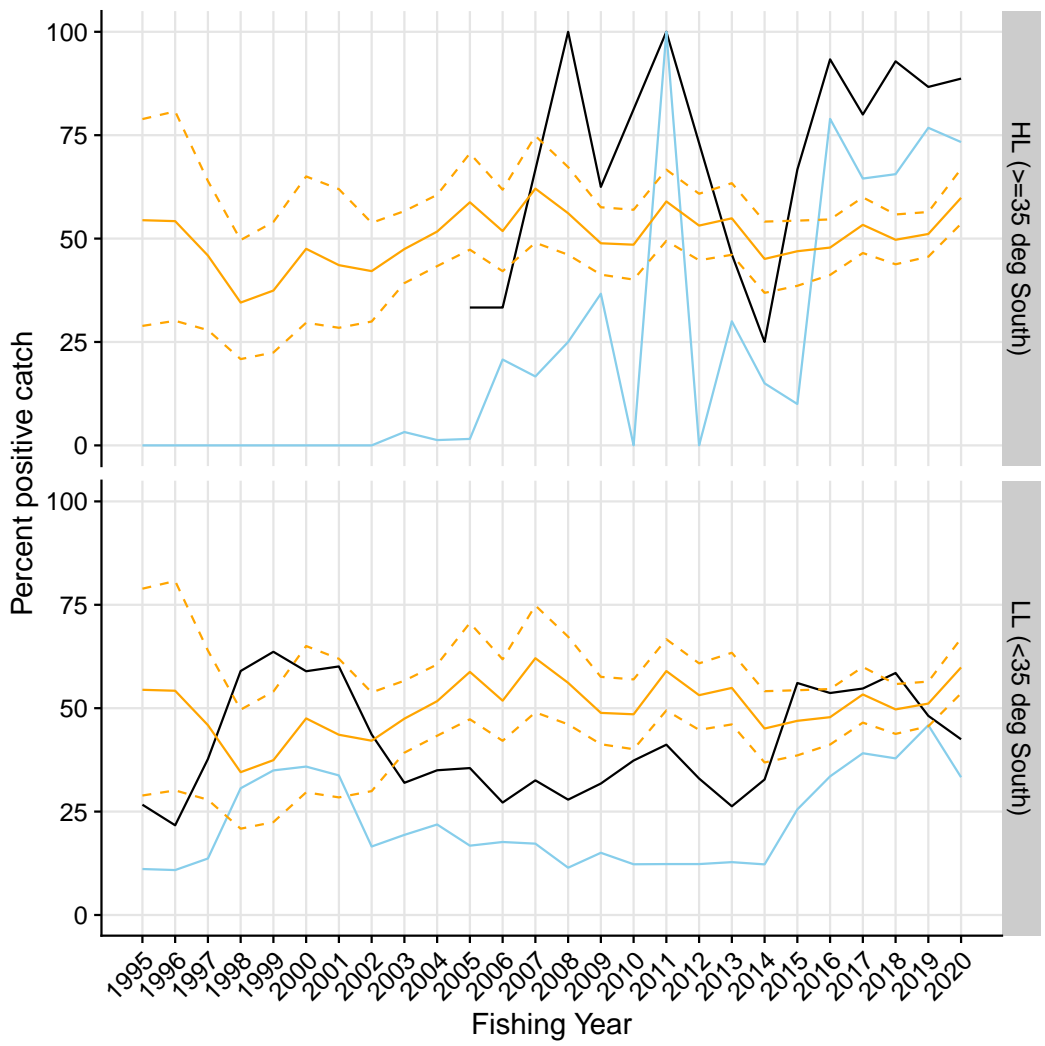


Figure B-98: Proportion of strata for the combined DW low-latitudes (<35 degree South) fleet with positive catch by latitudinal stratum. Light blue are initial log-sheet records prior to filtering, the black line is the retained dataset after filtering for consistently reporting vessels. Where available, the corresponding values from observed strata is shown in orange.

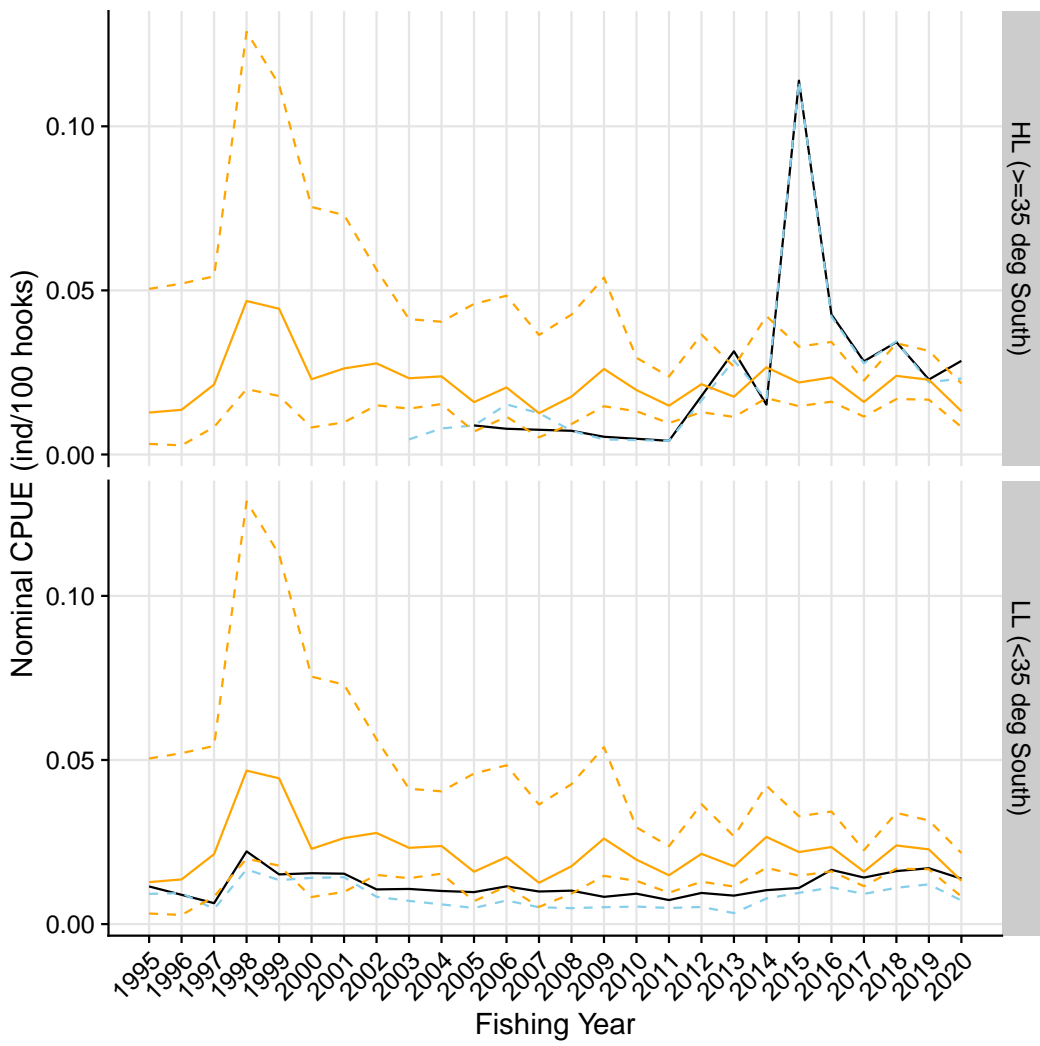


Figure B-99: Nominal CPUE (in number of blue shark per 100 hooks) strata of the combined DW low-latitudes (<35 degree South) fleet with positive catch by latitudinal stratum. Light blue are initial log-sheet records prior to filtering, the black line is the retained dataset after filtering for consistently reporting vessels. Where available, the corresponding values from observed strata is shown in orange.

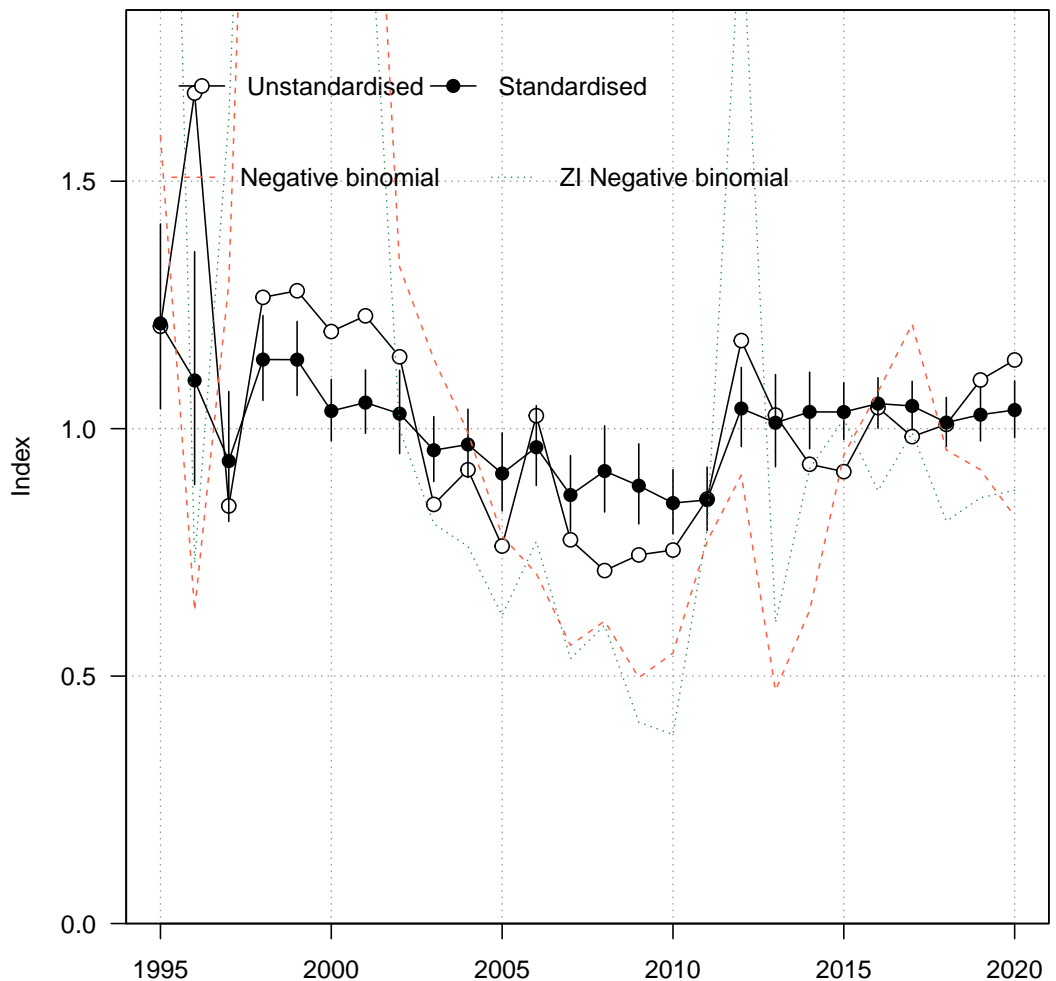


Figure B-100: Standardised (closed black circles with standard error) and unstandardised (open circles) CPUE indices for the combined DW low-latitudes (<35 degree South) fleet strata with positive catch. Where successful (i.e., converged), standardised trends from a negative-binomial and zero-inflated negative binomial model run over the full dataset (including strata with zero values) are also shown for comparison.

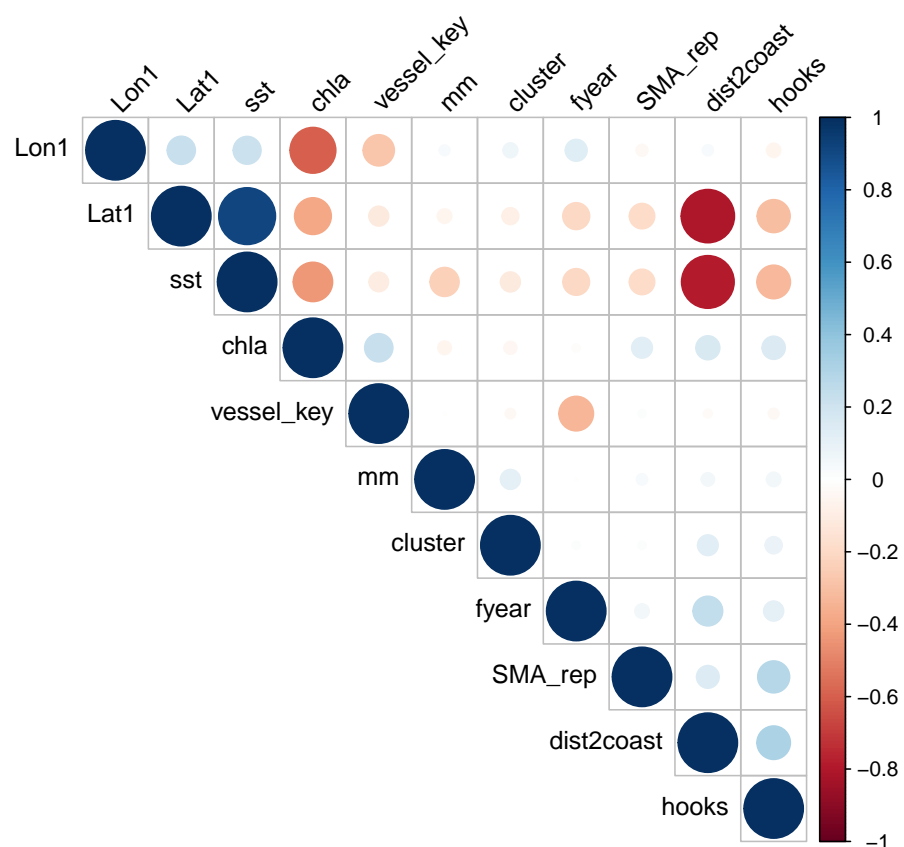


Figure B-101: Correlations amongst potential covariates for CPUE standardisation in the combined DW low-latitudes (<35 degree South) fleet. Where necessary, variables were removed to reduce redundancy in the models.

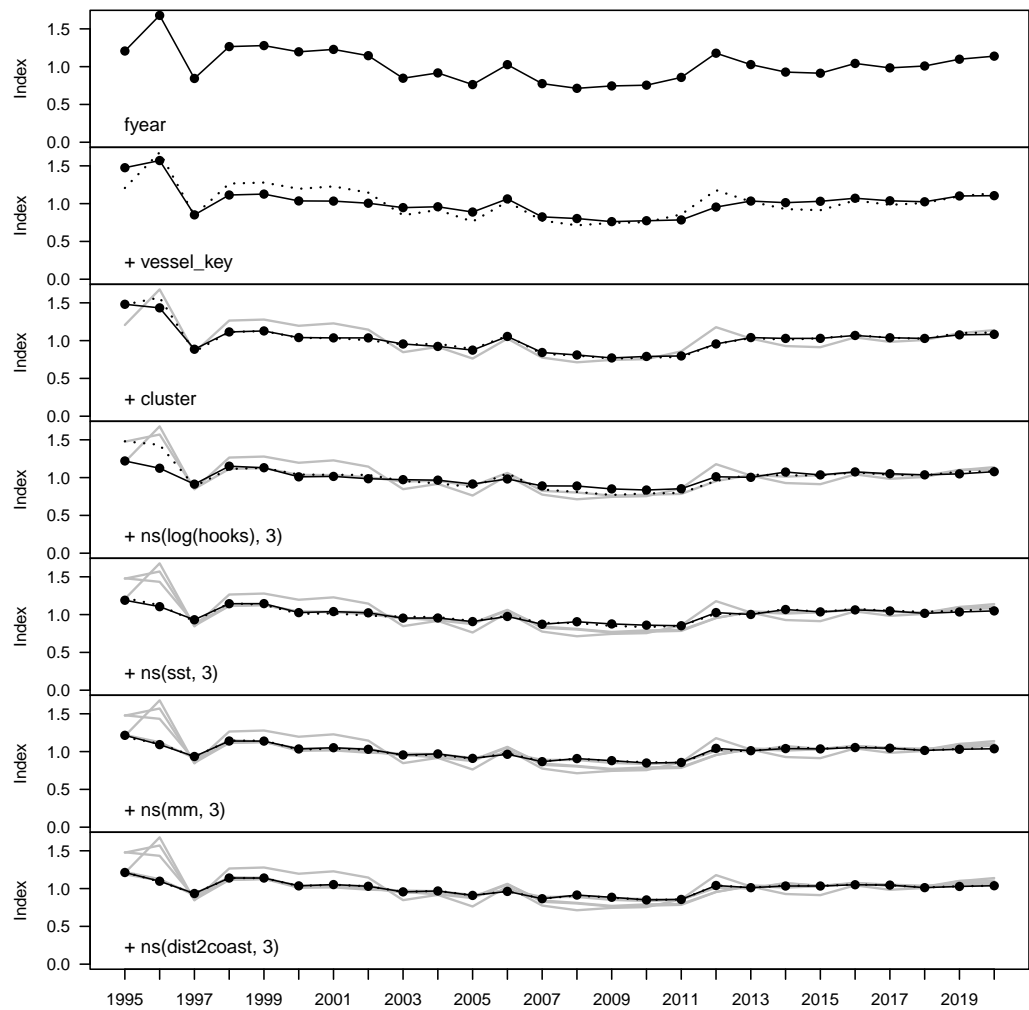


Figure B-102: Step plot for the combined DW low-latitudes (<35 degree South) fleet CPUE, showing sequential standardising effects of variables included in the standardisation model.

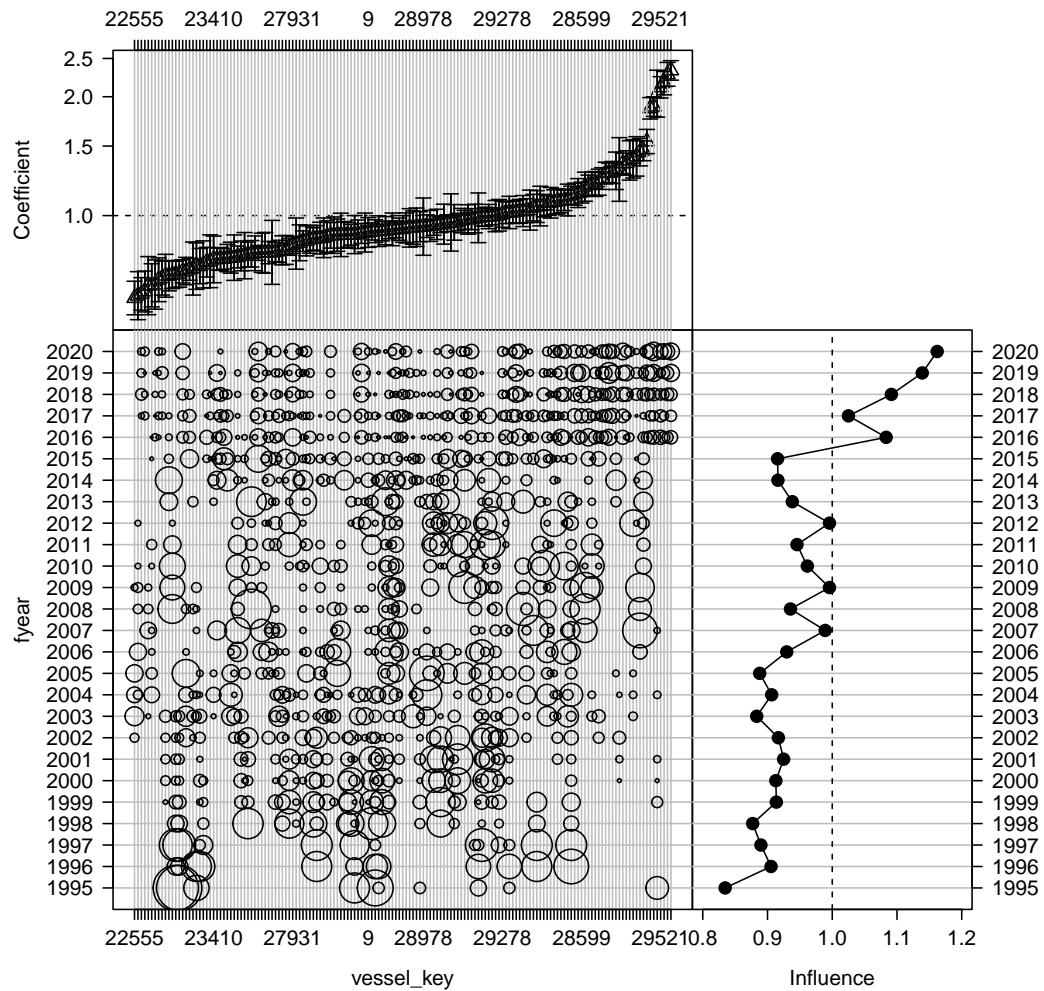


Figure B-103: Influence of fleet composition (vessel keys) for the combined DW low - latitudes (<35 degree South) fleet (bubble plot; bubbles scales by effort) on CPUE; influence (right) shows the standardising effect (a positive effect reduces the standardised CPUE by the equivalent amount). Estimated coefficients are given in the top panel.

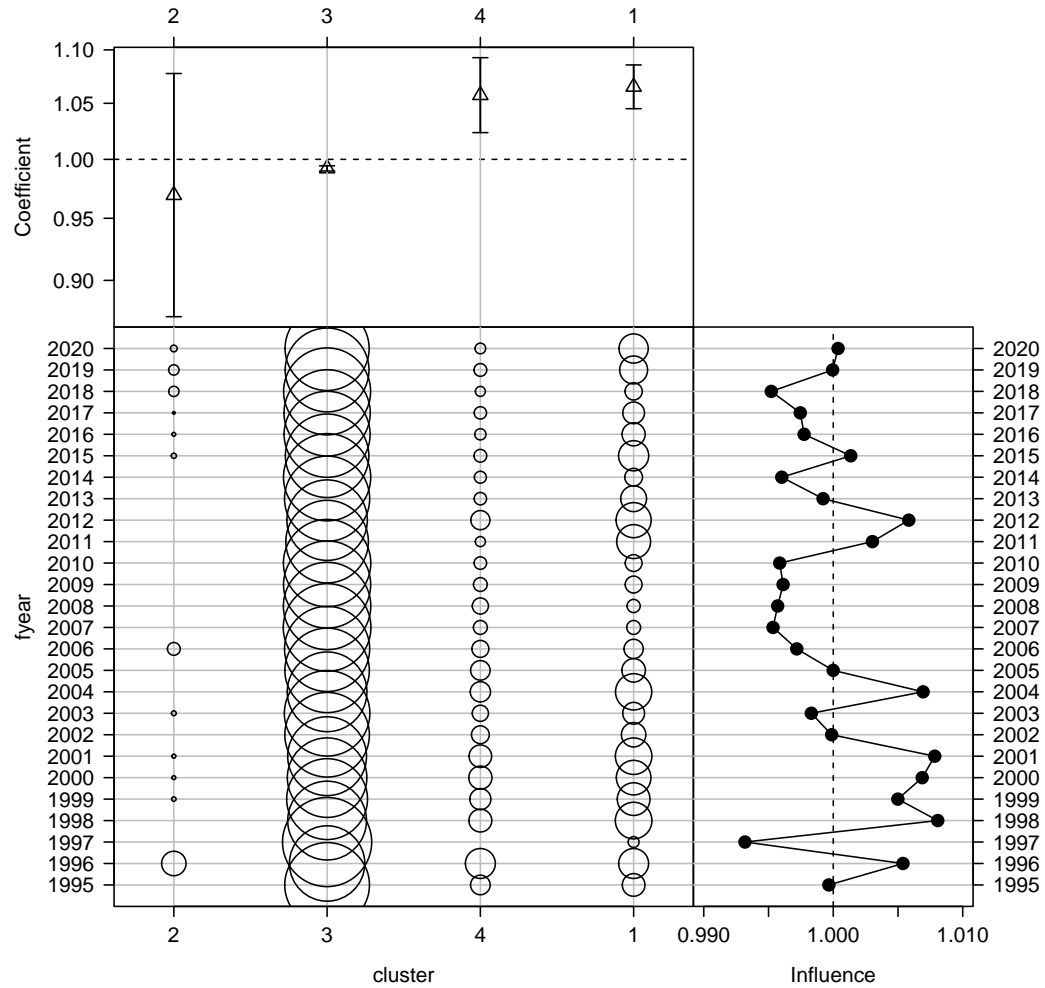


Figure B-104: Influence of targeting cluster for the combined DW low-latitudes (<35 degree South) fleet (bubble plot; bubbles scales by effort) on CPUE; influence (right hand plot) shows the standardising effect (a positive effect reduces the standardised CPUE by the equivalent amount). Estimated coefficients are given in the top panel.

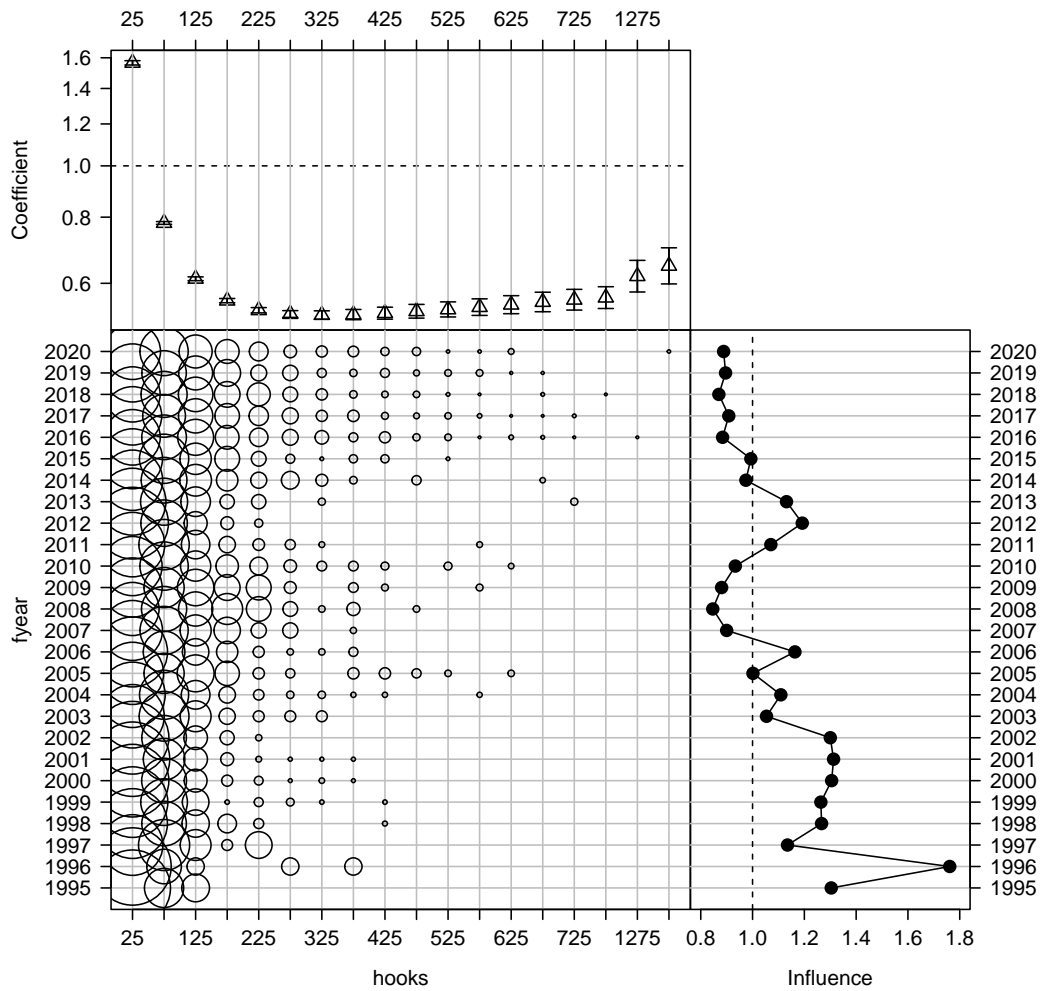


Figure B-105: Influence of number of hooks set per stratum for the combined DW low-latitudes (<35 degree South) fleet (bubble plot; bubbles scales by effort) on CPUE; influence (right hand plot) shows the standardising effect (a positive effect reduces the standardised CPUE by the equivalent amount). Estimated coefficients are given in the top panel.

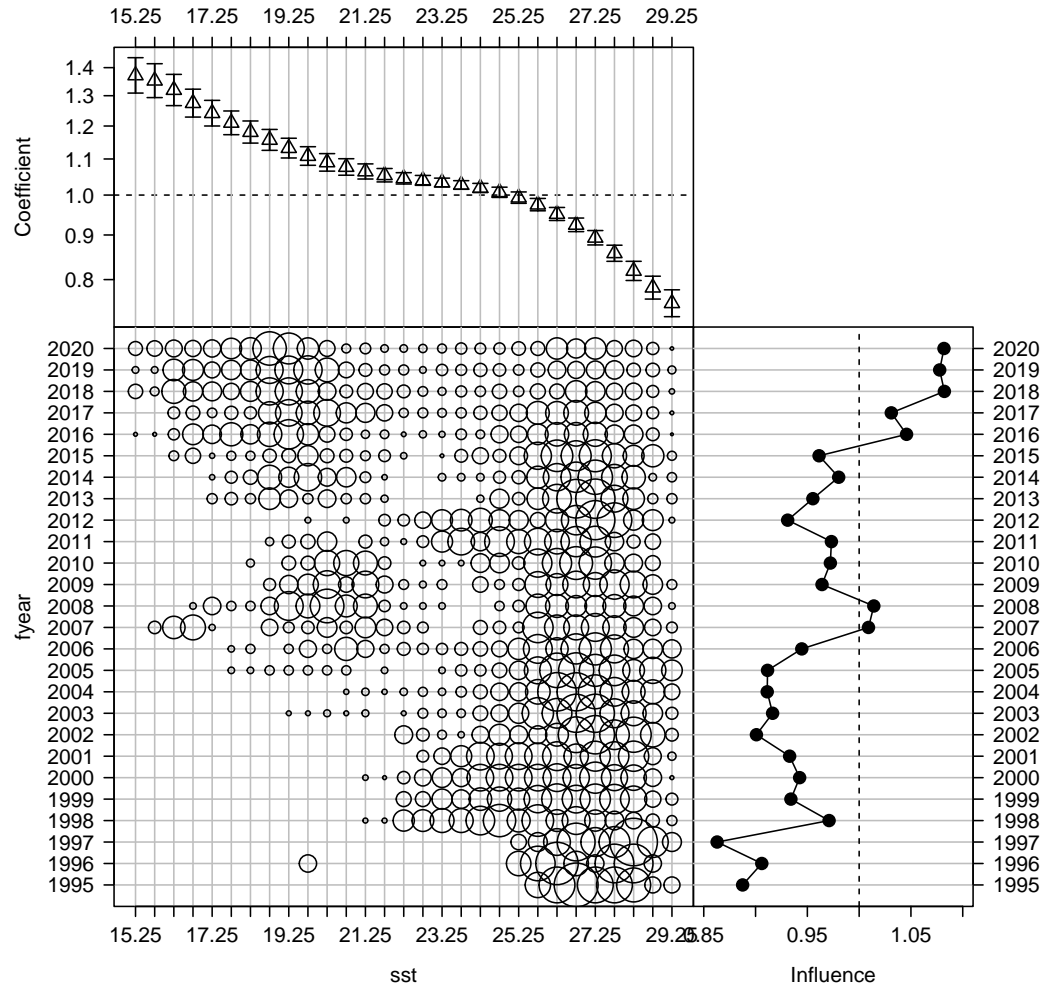


Figure B-106: Influence of sea surface temperature (SST, in degrees Celsius) for the combined DW low-latitudes (<35 degree South) fleet (bubble plot; bubbles scales by effort) on CPUE; influence (right hand plot) shows the standardising effect (a positive effect reduces the standardised CPUE by the equivalent amount). Estimated coefficients are given in the top panel.

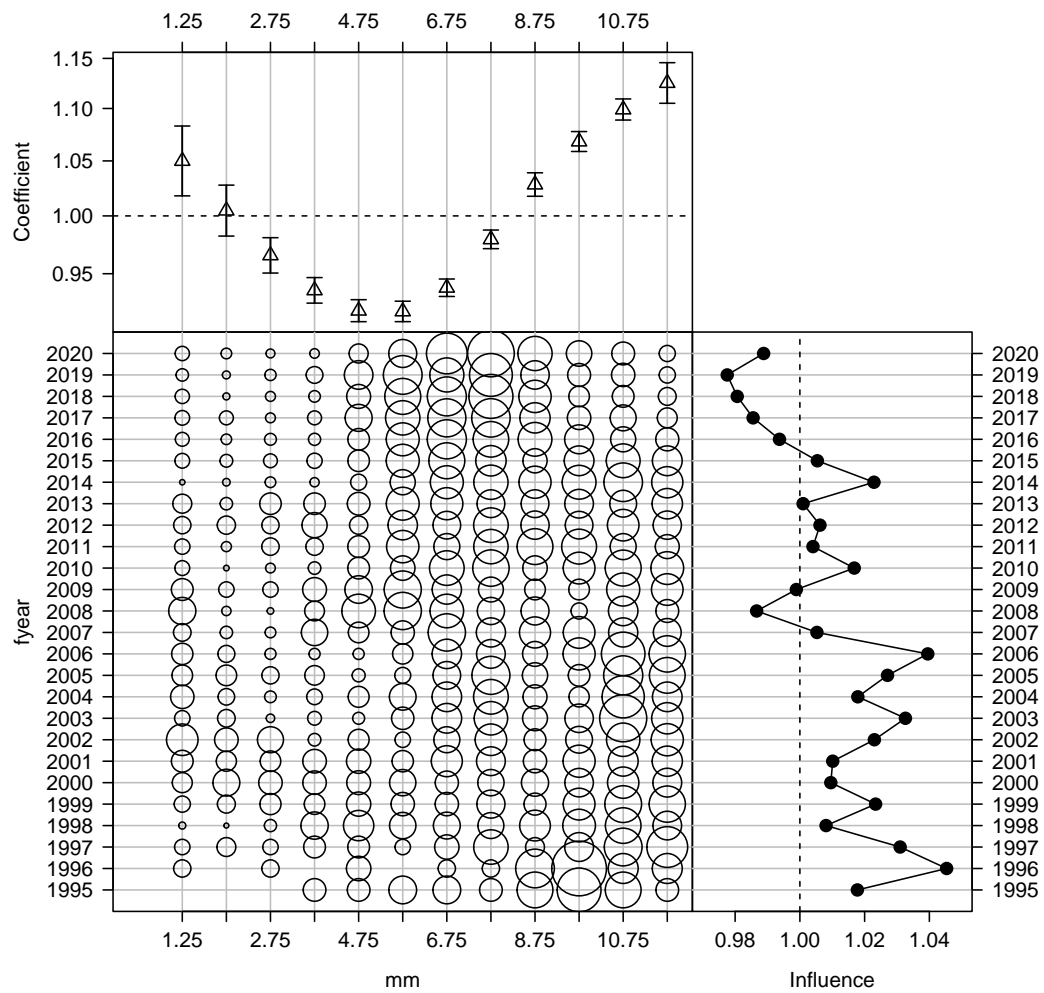


Figure B-107: Influence of month for the combined DW low-latitudes (<35 degree South) fleet (bubble plot; bubbles scales by effort) on CPUE; influence (right hand plot) shows the standardising effect (a positive effect reduces the standardised CPUE by the equivalent amount). Estimated coefficients are given in the top panel.

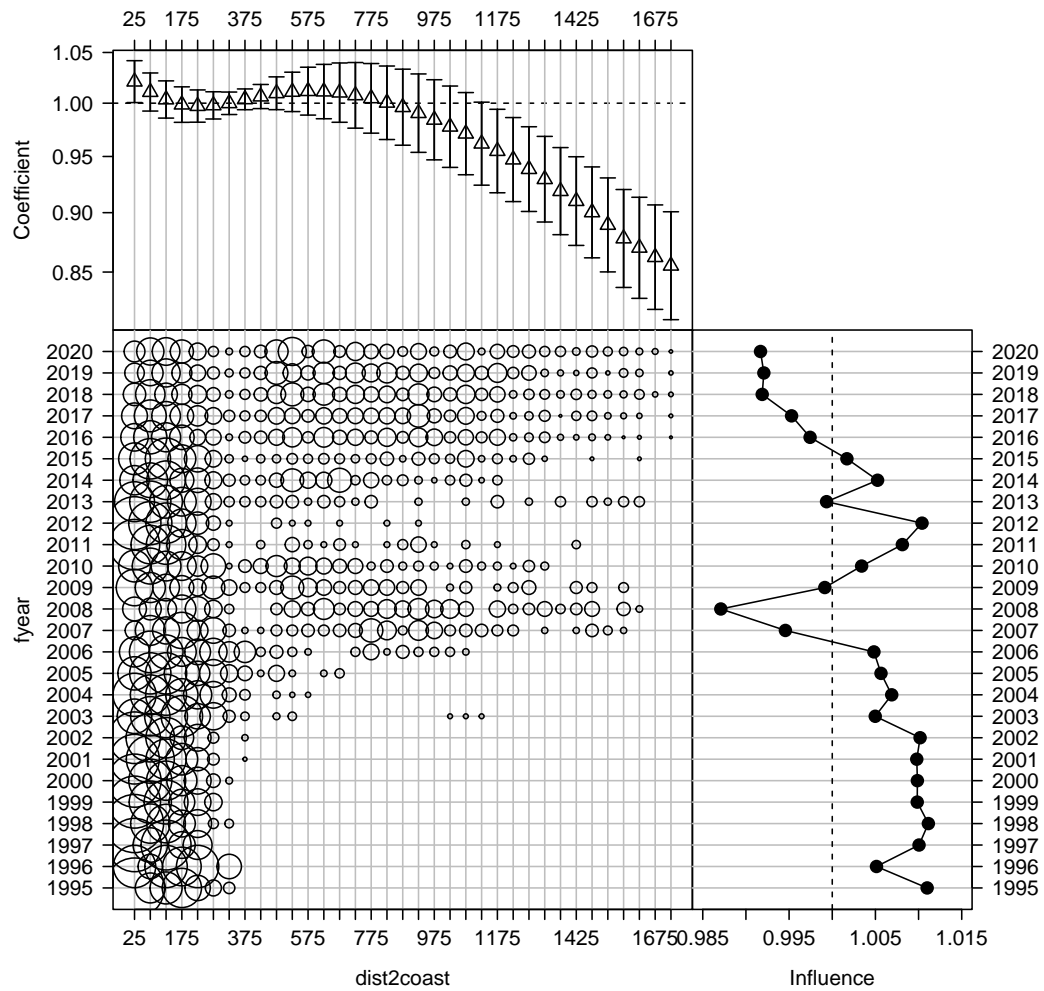


Figure B-108: Influence of distance to coast composition for the combined DW low-latitudes (<35 degree South) fleet (bubble plot; bubbles scales by effort) on CPUE; influence (right hand plot) shows the standardising effect (a positive effect reduces the standardised CPUE by the equivalent amount). Estimated coefficients are given in the top panel.

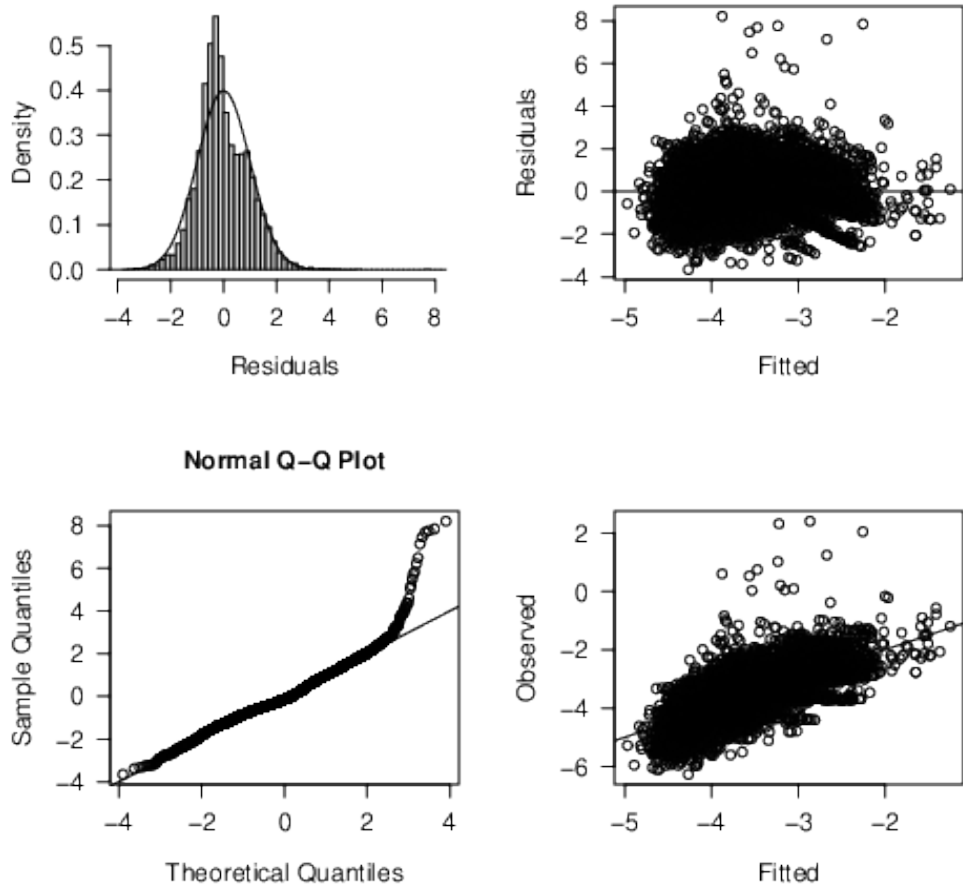


Figure B-109: Diagnostics for the log-normal CPUE standardisation model for the combined DW low-latitudes (<35 degree South) fleet strata with positive catch.

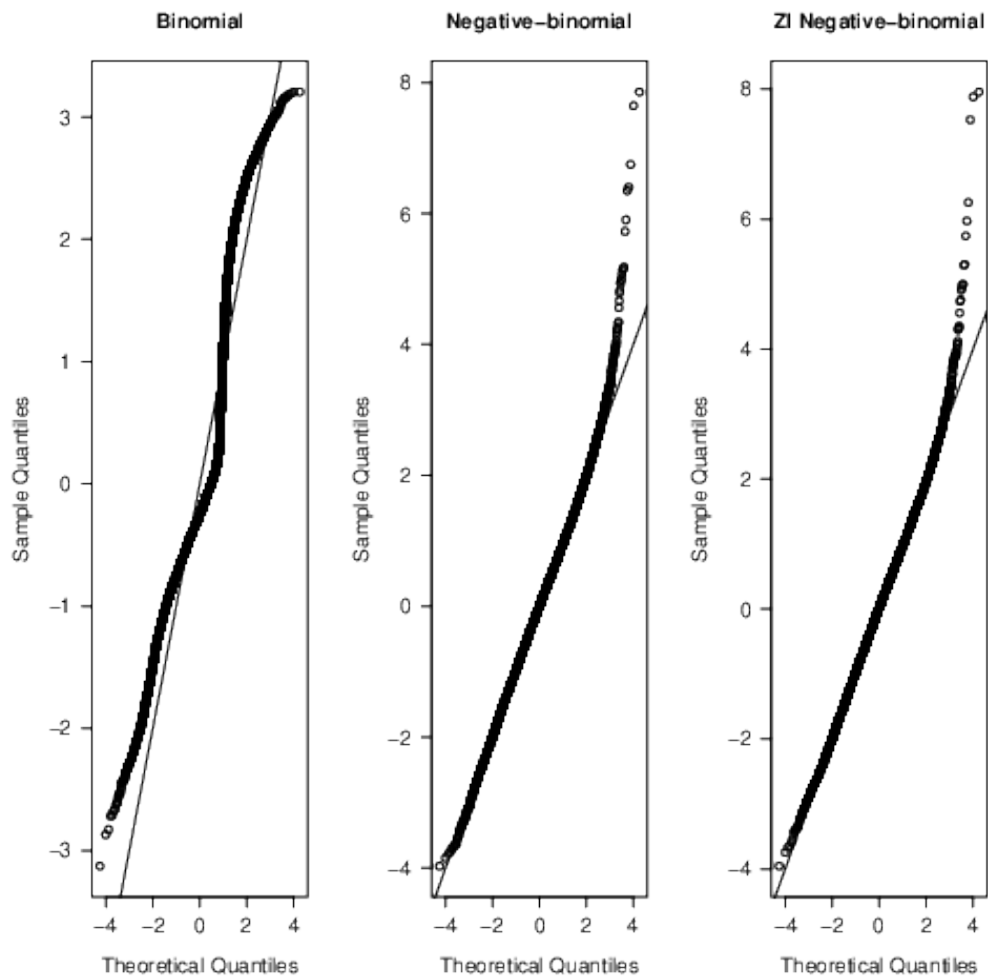


Figure B-110: Quantile residual diagnostics for the binomial component, as well as alternative CPUE standardisation models for the combined DW low-latitudes (<35 degree South) fleet strata with positive catch.